

ABSTRACT

JIANG, JIANBING. Light-harvesting Architectures with Natural Protein Scaffolds and Synthetic Chromophores. (Under the direction of Professor Jonathan S. Lindsey).

The challenge of creating both pigment building blocks and scaffolding to organize a large number of such pigments has long constituted the central impediment to the construction of artificial light-harvesting architectures. While light-harvesting (LH) antenna systems generally have near-quantitative transfer of excitation energy among pigments, only a fraction of the solar spectrum is typically absorbed. A platform architecture for study of light-harvesting phenomena has been developed that employs native peptide analogs, native bacteriochlorophyll *a* (BChl *a*), and synthetic chromophores. Solar coverage can be extended beyond that in the natural systems by covalent attachment of chromophores with complementary spectral properties, and the cross-section of absorption at particular wavelengths can be enhanced by multiple copies of the same chromophore.

Bacteriochlorins absorb strongly in the near-infrared (NIR) spectral region and hence may be well suited for applications on light-harvesting materials. In one set of bacteriochlorins, nine lipophilic, wavelength-tunable (730–820 nm) bacteriochlorins have been prepared that bear a single bioconjugatable group. Three synthetic bacteriochlorin building blocks were used to construct the set of bacteriochlorins that contain an azido group for Cu(I)-catalyzed click chemistry, an ester group for non-traceless Staudinger ligation, a thioester for traceless Staudinger ligation, an aldehyde for oxime formation, and a maleimido group for thioether formation. NIR wavelength tuning was achieved by installation of auxochromes at β -pyrrole positions, incorporation of an exocyclic 6-membered imide moiety, or conversion of the free base macrocycle to the zinc chelate.

Bioconjugatability of target bacteriochlorins was established on small molecules as well as with two tetrapeptides (each containing one non-natural amino acid residue). Studies of orthogonal couplings also were carried out and showed desirable experimental results.

Further applications of bacteriochlorins have been largely limited by the intrinsic lipophilicity of the bacteriochlorin macrocycle. In another set of bacteriochlorins, a new molecular design is investigated wherein 3,5-dicarboxyphenyl units are appended to the β -pyrrolic positions of the bacteriochlorin. Aqueous solubility was examined by absorption spectral interrogation of samples over a 1000-fold concentration range with reciprocal change in pathlength ($\sim 0.5, 5, 50, \text{ and } 500 \mu\text{M}$; 10, 1, 0.1, and 0.01-cm pathlength cuvettes). As the third set, bacteriochlorins bearing distinct water-solubilizing motifs is studied. Water-solubility was assessed by examination of the absorption spectra across a 1000-fold concentration range. Each of the water-soluble bacteriochlorins was prepared in reasonable yield (51–73%) from the building block and displayed good aqueous solubility, desired photophysical properties and potential for further modification at the 15-position. All of these features open the door for studies with bacteriochlorins in aqueous media.

Three new biohybrid designs, each of which employs analogues of the β -peptide from *Rhodobacter sphaeroides*, have been investigated. In the first design, amino acids at seven different positions on the peptide were individually substituted with cysteine, to which a synthetic chromophore was covalently attached. All chromophore-peptides readily formed LH1-type complexes upon combination with the α -peptide and BChl *a*. Efficient energy transfer occurs from the attached chromophore to the circular array of 875-nm absorbing BChl *a* molecules (denoted B875). In the second design, use of two attachment sites (positions -10 and -21) on the peptide affords. In the third design, three spectrally distinct

bacteriochlorin–peptides were prepared (each attached to cysteine at the –14 position) and combined in an ~1:1:1 mixture to form a heterogeneous mixture of LH1-type complexes with increased solar coverage and nearly quantitative energy transfer from each bacteriochlorin to B875. Collectively, the results illustrate the great latitude of the biohybrid approach for the design of diverse light-harvesting systems.

© Copyright 2015 Jianbing Jiang

All Rights Reserved

Light-Harvesting Architectures with Natural Protein Scaffolds and Synthetic Chromophores

by
Jianbing Jiang

A dissertation submitted to the Graduate Faculty of
North Carolina State University
in partial fulfillment of the
requirements for the degree of
Doctor of Philosophy

Chemistry

Raleigh, North Carolina

2015

APPROVED BY:

Jonathan S. Lindsey
Committee Chair

Christian Melander

Reza A. Ghiladi

Gavin Williams

DEDICATION

This work is dedicated to my parents, wife and daughter.

BIOGRAPHY

Jianbing Jiang was born in Taizhou, Jiangsu province in China on August 5, 1984 to Guocai Jiang and Yihua Cao. Jianbing earned his Bachelor's degree in applied chemistry from Jiangnan University in 2007. His advisor is professor Changge Zheng, and the thesis title is "synthesis of ligands with fluorine for metal-organic frameworks (MOFs)".

After graduation, Jianbing joined professor He Tian's research group in Eastern China University and Science and Technology, Shanghai, China, and focus on the polymeric sensing materials for ion detection in aqueous solution. The thesis title is "properties of chemosensors polymerized by reversible addition-fragmentation chain transfer (RAFT) method". Jianbing obtained the Master's degree in applied chemistry in 2010.

In summer 2010, Jianbing came to US to pursue his PhD degree at North Carolina State University. He joined in professor Bruce Novak's group for polymer chemistry and worked there for one year until professor Novak moved to another institute. In summer 2011, Jianbing joined in professor's Jonathan Lindsey's group and focused on the synthesis of property-tunable chromophores with applications on light-harvesting biohybrid antennas.

ACKNOWLEDGMENTS

My deepest gratitude to those who never stop helping me in work and life.

Advisor

Jonathan S. Lindsey

Committee members

Dr. Ghiladi, Dr. Melander, Dr. Williams

Graduate school representative

Dr. Argyropoulos

Collaborators

The Bocian lab at University of California at Riverside

The Holten lab at Washington University in St. Louis

The Loach lab at Northwestern University

Family

Guocai Jiang, Yihua Cao, Guoxiang Gu, Zhongqiu Qu, Wei Gu, Yanlin Elaine Jiang

TABLE OF CONTENTS

	Page #
LIST OF FIGURES	xii
LIST OF SCHEMES	xvii
LIST OF CHARTS	xix
LIST OF TABLES	xx
LIST OF EQUATIONS	xxi
CHAPTER 1 General Introduction: Tetrapyrroles and Photosynthesis	
Background	1
References	8
CHAPTER 2 Near-Infrared Tunable Bacteriochlorins for Bioorthogonal Labeling	
Introduction	10
Results and discussion	16
(I) Molecular design	16
(A) Synthesis	16
(B) Wavelength tuning	17
(C) Bioconjugation motifs	19
(II) Synthesis of bacteriochlorins	20
(A) Bacteriochlorins for oxime formation	20
(B) Bacteriochlorins for cysteinyl ligation	23

(C) Bacteriochlorins for Staudinger ligation.....	24
(D) Bacteriochlorins for click chemistry	27
(III) Photophysical properties	30
(IV) Bioconjugation tests.....	32
(A) Copper metalation experiments.....	33
(B) Model studies with small molecules.....	35
(C) Studies with peptides	36
(D) Model studies of bioorthogonal coupling.....	38
Conclusion and outlook	40
Experimental section.....	41
(I) General methods	41
(II) Syntheses	41
(III) Protocols.....	51
(IV) Bioconjugation reactions.....	52
Acknowledgement	56
References.....	56
CHAPTER 3 Hydrophilic Tetracarboxy Bacteriochlorins for Photonics Applications	
Introduction.....	64
Results and discussion	72
(I) Reconnaissance.....	72
(II) Synthesis.....	75

(A) Suzuki coupling partner.....	75
(B) Bacteriochlorin building blocks.....	75
(C) Hydrophilic bacteriochlorins	80
(D) Bioconjugatable hydrophilic bacteriochlorin	82
(III) Photophysical properties	84
(A) Absorption and emission spectra.....	84
(B) Effect of concentration on spectral properties	87
(IV) Bioconjugation	88
Conclusions.....	90
Experimental section.....	91
(I) General methods	91
(II) Recovery of 2,6-di- <i>tert</i> -butylpyridine (DTBP)	92
(III) Absorption versus concentration study	92
(IV) Fluorescence yield determinations.....	93
(V) Synthesis.....	94
(VI) Preparation of β (-14Cys)BC-16.....	110
Notes and references.....	112
CHAPTER 4 Evaluation of Motifs (Carboxylate, Phosphonate, Ammonium and PEG)	
for Water-Solubilization of Synthetic Bacteriochlorins	
Introduction.....	120
Results and discussion	124

(I) Synthesis	124
(A) Suzuki coupling partner.....	124
(B) Hydrophilic bacteriochlorins	127
(II) Photophysical properties.....	131
(A) Absorption and emission spectra.....	131
(B) Effect of concentration on spectral properties	133
(III) 15-Bromination study.....	136
(IV) Comparison	138
Experimental section.....	141
(I) General methods	141
(II) Synthesis.....	141
(III) Absorption versus concentration study	153
(IV) Fluorescence yield determinations.....	154
References.....	154

CHAPTER 5 Polarity-Tunable and Wavelength-Tunable Bacteriochlorins Bearing a Single Carboxylic Acid or NHS Ester. Use in a Protein Bioconjugation Model System

Introduction.....	158
Results and discussion	165
(I) Synthesis.....	165
(A) Lipophilic bacteriochlorins.....	165
(B) Hydrophilic bacteriochlorin.....	171

(II) Photophysical properties.....	175
(III) Bioconjugation study.....	179
Outlook	187
Experimental section.....	188
(I) General methods	188
(II) Synthesis.....	188
(III) Protocol for preparation of Mb conjugate	205
(IV) Heme-removal protocol	206
(V) Fluorescence quantum yield measurements.....	206
(VI) Förster energy-transfer calculations.....	207
References.....	207

CHAPTER 6 Amphiphilic, Hydrophilic, or Hydrophobic Synthetic Bacteriochlorins in Biohybrid Light-Harvesting Architectures. Consideration of Molecular Designs

Introduction.....	215
Results and discussion	220
(I) Synthetic bioconjugatable bacteriochlorins	220
(A) Reconnaissance	220
(B) Synthesis of amphiphilic bacteriochlorin B1.....	222
(II) Bacteriochlorin–peptide conjugate.....	224
(A) Peptide choice.....	224
(B) Bioconjugate formation and characterization.....	224

(C) Comparison of hydrophilic, hydrophobic or amphiphilic bacteriochlorins	226
(III) $\beta\beta$ -Dyads	227
(A) Formation	227
(B) Quantitation of assembly	231
(C) Equilibrium study	232
(D) Energy-transfer studies	233
(E) Studies of multi-exponential decays in dyads	240
Outlook	243
Experimental section	244
(I) General methods	244
(II) Synthesis	245
(III) Preparation of β -B1	248
(IV) Dyad formation from β -B1	250
References	251

CHAPTER 7 Versatile Design of Biohybrid Light-Harvesting Architectures to Tune

Location, Density and Spectral Coverage of Attached Synthetic Chromophores for Enhanced Energy Capture

Introduction	258
Methods and materials	264
(I) Peptides	264

(II) Chromophores	266
(III) Chromophore–peptide conjugates.....	266
(IV) Formation of subunits and LH1-type complexes.....	267
(V) Photophysical and infrared characterization studies	267
Results and discussion	268
(I) Multiple sites of attachment to the β -peptide.....	268
(II) Two chromophores attached to the β -peptide	278
(III) Combining three distinct chromophore–peptide conjugates.....	281
References.....	286

LIST OF FIGURES

Figure 1.1.	Cartoon of (a) reaction center surrounded by LH 1 and LH2; (b) LH1 complex and reaction center; (c) LH2 complex; (d) heterodimer composed of α peptide, β peptide and BChl <i>a</i>	2
Figure 1.2.	Magnesium coordination with His residue and hydrogen bonding between Trp residues and carbonyl groups on BChl <i>a</i> . At the bottom are the α and β peptides sequences.....	4
Figure 1.3.	(a) Arrangement of bacteriochlorophylls in the LH2 of <i>Rhodospirillum molischianum</i> . (b) Arrangement of the BChl <i>a</i> molecules within the B850 ring of LH2 from <i>Rhodopseudomonas acidophila</i>	5
Figure 1.4.	Sequence of α peptide, β peptide and truncated 31mer (from top to bottom) of <i>Rhodobacter sphaeroides</i> LH1.	6
Figure 1.5.	(A) Photon flux density spectrum of AM1.5 solar radiation. (B) Absorption spectra of native LH2 (blue) and LH1 plus reaction center (RC) (red) from a <i>Rhodobacter sphaeroides</i>	6
Figure 1.6.	Normalized absorption (solid) and fluorescence (dashed) spectra of bioconjugatable dyes (colored) and of BChl <i>a</i> dimer B820 in subunit complex [31mer(-14Cys)BChl]₂ (black)... ..	7
Figure 2.1.	Nexus of design issues for NIR chromophores	11
Figure 2.2.	Absorption spectra (normalized) of NIR-active chromophores.....	13
Figure 2.3.	Absorption and emission spectra of target bacteriochlorins at room temperature in CH ₂ Cl ₂	31

Figure 3.1.	Normalized absorption spectra (solid) and emission spectra (dashed) of BC-6 and BC-7 in aqueous potassium phosphate buffer (0.5 M, pH 7.0) at room temperature.	85
Figure 3.2.	Absorption versus concentration of BC-6 over a range of 1000-fold.	87
Figure 3.3.	Preparation of β -(-14Cys) BC-16 conjugate.	89
Figure 4.1.	Normalized absorption spectra (solid) and emission spectra (dashed) of BC3 in aqueous potassium phosphate buffer (0.5 M, pH 7.0) at room temperature.	132
Figure 4.2.	Flowchart for absorption versus concentration study (panel A), and Absorption versus concentration of BC1–BC5 each over a range of 1000-fold (panels B–F).	135
Figure 5.1.	Molecular design features of synthetic bacteriochlorins.	162
Figure 5.2.	Normalized absorption spectra in DMF at room temperature.	176
Figure 5.3.	Normalized absorption and fluorescent spectra in potassium phosphate buffer (0.5 M, pH 7, for BC7-9) and DMF (for BC10) at room temperature.	177
Figure 5.4.	(A). Absorption spectra of Mb, BC7 and conjugate Mb-BC7 in potassium phosphate buffer (0.5 M, pH 7.0). (B). The normalized experimental (blue), reconstructed (cyan) absorption, and emission (magenta, dashed) spectra of conjugate Mb-BC7	182
Figure 5.5.	The MALDI spectra of the conjugate samples of Mb to (A) 0, (B) 2, (C) 10, and (D) 50 equiv of BC7	185

Figure 5.6.	Fluorescence quantum yield values as a function of loading and \pm heme.....	186
Figure 6.1.	(A) $\alpha\beta$ -subunit of the LH2 (B800–850) antenna of <i>Phaeospirillum</i> (<i>Phs.</i>) <i>molischianum</i> . (B) Absorption spectra of light-harvesting architectures and individual components.....	217
Figure 6.2.	Dyad formation as a function of concentration of octG and temperature.....	228
Figure 6.3.	Absorption spectra for formation of dyads from β-B2 signaled by the peak at 823 nm.	230
Figure 6.4.	Variable-temperature study of (β-B2/BChl) ₂ dyad assembly/disassembly at 22.6 mM octG in aqueous phosphate buffer.	233
Figure 6.5.	Absorptance (1 – transmittance) spectrum (red) versus fluorescence excitation spectrum (blue) at 10 °C using ($\lambda_{\text{det}} = 835\text{--}840$ nm for $\beta\beta$ -dyads (β-B1/BChl) ₂ (A), (β-B2/BChl) ₂ (B), (β-B3/BChl) ₂ (C) and (β-OGR/BChl) ₂ (D).	234
Figure 6.6.	Representative transient absorption kinetics obtained at 10 °C for chromophore–peptide conjugates or dyads.	236
Figure 6.7.	(A) Representative time profile for decay of B820 bleaching. (B) The decay profile obtained using 1 μ J per pulse along with a fit to a function consisting of the convolution of the instrument response and two-exponentials plus a constant.	242
Figure 6.8.	Absorption spectra for formation of dyads signaled by the peak at 822 nm.	251

Figure 7.1.	(a) $\alpha\beta$ -subunit of the LH2 (B800–850) complex of <i>Phaeospirillum</i> (<i>Phs.</i>) <i>molischianum</i> . Coordinating histidines are illustrated (black). (b and c) Side and top view of a model of the <i>Rb. sphaeroides</i> LH1 oligomer. (d) Absorption spectra of BChl <i>a</i> in 0.90% octyl glucoside (mauve), $\alpha\beta$ -dyad (B820) reconstituted from native <i>Rb. sphaeroides</i> α - and β -peptides and BChl <i>a</i> (gold).	261
Figure 7.2.	(a) Normalized absorption (solid) and fluorescence (dashed) spectra of the commercial dye Oregon Green 488 maleimide (OGR), bacteriochlorins BC1 , BC2 and BC3 , and BChl <i>a</i> ring B875 in LH1-type antenna. (b) Structures of BC1 , BC2 , BC3 , OGR , and BChl <i>a</i>	263
Figure 7.3.	Single-reflection FTIR spectra of synthetic native-length peptides, Cys-mutants, and chromophore–peptide conjugates in films on gold.	270
Figure 7.4.	(a) $\alpha\beta$ -subunit of the LH2 (B800–850) complex of <i>Phs. molischianum</i> . (b) Absorption spectra of the LH1-type complex prepared from the native α -peptide, BChl <i>a</i> and $\beta(-14)$ (grey) or $\beta(-14)$ BC2 (red).	272
Figure 7.5.	(a) Fluorescence emission for $\beta(-14)$ BC2 chromophore–peptide conjugate (mauve) and $\beta(-14)$ BC2 plus native α -peptide and BChl <i>a</i> to form the LH1-type oligomer (blue). (b) Absorbance (1-T) (coral) versus fluorescence excitation (grey) ($\lambda_{\text{det}} = 890$ nm) for LH1-type oligomer. (c) Time profiles for combined B875 bleaching and B875* stimulated emission for LH1-type oligomer containing $\beta(-14)$	276

Figure 7.6. (a) Absorption spectra of **BC2** (burgundy), and oligomer antenna formed by combining BChl *a*, native α -peptide, and conjugates. (b) Addition of BChl *a* to $\beta(-6)$ BC2 and the native α -peptide at 0.90% octyl glucoside.279

Figure 7.7. (a) Schematic structures of $\alpha\beta$ -dyads with bacteriochlorins BC1 (mauve) or BC2 (gold) or BC3 (teal) attached to the -14 position of the β -peptide. (b) Cartoon showing one of a large number of possible arrangements of BC1 (mauve triangle) and BC2 (gold triangle) and BC3 (teal circle) around an $(\alpha\beta)_n$ cyclic oligomer. (c) Absorption spectra for LH1-type complexes prepared by individually combining chromophore-peptide conjugates with the native LH1 α -peptide and BChl *a*. (d) Absorption spectra for heterogeneous LH1-type complexes prepared with native α -peptide, BChl *a* and an approximately 1:1:1 ratio of $\beta(-14)$ BC1, $\beta(-14)$ BC2, and $\beta(-14)$ BC3 (violet), and the calculated sum of the spectra of the three individual homogeneous oligomers pictured in panel c (dashed purple).282

LIST OF SCHEMES

Scheme 2.1.	Synthesis route and design features of stable bacteriochlorins.....	18
Scheme 2.2.	Molecular design of bacteriochlorins and ligation motifs	20
Scheme 2.3.	Synthesis of a formylbacteriochlorin for oxime formation.....	22
Scheme 2.4.	Synthesis of a maleimido-bacteriochlorin.	23
Scheme 2.5.	Synthesis of bacteriochlorins for Staudinger ligation.....	25
Scheme 2.6.	Synthesis of bacteriochlorins for Staudinger ligation.....	26
Scheme 2.7	Approaches toward an azido-bacteriochlorin	28
Scheme 2.8.	Synthesis of an azidobacteriochlorin.	29
Scheme 2.9.	Investigation of copper insertion with bacteriochlorins.....	34
Scheme 2.10.	Proof-of-principle ligation reactions.....	36
Scheme 2.11.	Preparation of peptidyl-bacteriochlorin conjugates	37
Scheme 3.1.	Synthesis of bacteriochlorins and molecular design features	67
Scheme 3.2.	15-Bromination of a 3,13-diphenylbacteriochlorin.	74
Scheme 3.3.	Synthesis of dicarboxy Suzuki coupling partner.	75
Scheme 3.4.	Synthesis of a dibromo-diester bacteriochlorin.	78
Scheme 3.5.	Synthesis of a 2,12-dibromobacteriochlorin.	80
Scheme 3.6.	Suzuki coupling to give diarylbacteriochlorins	81
Scheme 3.7	Hydrophilic bioconjugatable bacteriochlorin.	83
Scheme 4.1.	Synthesis of diphosphono Suzuki coupling partner 1	125
Scheme 4.2.	Synthesis of bis(aminomethyl)phenyl Suzuki coupling partner 2	126
Scheme 4.3.	Synthesis of Suzuki coupling partner 3	127

Scheme 4.4.	Synthesis of phosphono bacteriochlorin BC1	128
Scheme 4.5.	Synthesis of bacteriochlorins BC3 and BC5	129
Scheme 4.6.	Synthesis of bacteriochlorin BC4	130
Scheme 4.7	15-Bromination of bacteriochlorin precursors BC1a–BC4a	137
Scheme 5.1.	Synthesis of monocarboxy-bacteriochlorins BC1 , BC4 and BC5	167
Scheme 5.2.	Synthesis of monocarboxy-bacteriochlorin BC2	168
Scheme 5.3.	Synthesis of monocarboxy-bacteriochlorin BC3	169
Scheme 5.4.	Demethoxylation upon imide formation.	170
Scheme 5.5.	Synthesis of monocarboxy-bacteriochlorin BC6	171
Scheme 5.6.	Synthesis of tetracarboxy-bacteriochlorin-NHS esters BC7 and BC8	172
Scheme 5.7	Synthesis of tetracarboxy-bacteriochlorin-NHS ester BC9	174
Scheme 5.8.	Synthesis of the tetracarboxy-bacteriochlorin–imide.	175
Scheme 6.1.	Synthesis of amphiphilic bioconjugatable bacteriochlorin B1	221

LIST OF CHARTS

Chart 1.1.	Structure of BChl <i>a</i> .	3
Chart 2.1.	Naturally occurring bacteriochlorins.	12
Chart 2.2.	Synthetic NIR chromophores.	14
Chart 3.1.	Bacteriochlorophylls.	65
Chart 3.2.	Hydrophilic bacteriochlorins.	68
Chart 3.3.	Hydrophilic tetrapyrroles I-V .	70
Chart 3.4.	New designs of candidate hydrophilic bacteriochlorins.	71
Chart 3.5.	Bacteriochlorin building blocks.	76
Chart 4.1.	Representative hydrophilic bacteriochlorins I-XII .	121
Chart 4.2.	Bacteriochlorin scaffold and distinct water-solubilizing groups.	123
Chart 5.1.	Representative bacteriochlorophylls and tolyporphins.	159
Chart 5.2.	Representative bioconjugatable synthetic bacteriochlorins.	161
Chart 5.3.	Structures of six lipophilic monocarboxy-bacteriochlorins and four hydrophilic tetracarboxy-bacteriochlorins bearing an NHS ester.	164
Chart 5.4.	Three known bacteriochlorin building blocks.	166
Chart 5.5.	Parent bacteriochlorins lacking bioconjugatable tethers.	178
Chart 6.1.	Amphiphilic, hydrophilic and hydrophobic bacteriochlorins.	221

LIST OF TABLES

Table 1.1.	Dyad and oligomer formation from 31mer, β peptide, α peptide and BChl <i>a</i>	6
Table 2.1.	Comparison of spectral properties of targets versus benchmark bacteriochlorins.	32
Table 2.2.	Anticipated reactions for successive bioconjugation.	39
Table 3.1.	Effects of β -pyrrole substituents on 15-bromination.	73
Table 3.2.	Absorption and fluorescence properties of bacteriochlorins.	86
Table 4.1.	Detected charge states of BC1–BC5 upon MS analysis.	131
Table 4.2.	Absorption and fluorescence properties of bacteriochlorins.	134
Table 4.3.	Properties of hydrophilic bacteriochlorins BC1–BC5	140
Table 5.1.	Absorption and fluorescence properties of lipophilic bacteriochlorins.	177
Table 5.2.	Absorption and fluorescence properties of bacteriochlorins.	178
Table 5.3.	Absorption and fluorescence properties of conjugate Mb-BC7 with different equivalents of BC7 input.	183
Table 6.1.	Energy-Transfer Parameters for Dyads.	226
Table 7.1.	Synthetic peptides, conjugates, and oligomer antenna.	265
Table 7.2.	Efficiency of excitation-energy transfer in LH1-type complexes.....	275

LIST OF EQUATIONS

Equation 6.1	231
Equation 6.2	231
Equation 6.3	231

CHAPTER 1

General Introduction: Tetrapyrroles and Photosynthesis

Background

Photosynthesis is a process in which light energy from the sun is captured by an antenna complex, and then transferred to the reaction center to ultimately drive a series of chemical reactions. Among the solar output range, the entire visible and near infrared (NIR) spectral regions (400 nm to 1000 nm) are highly active in driving the photosynthesis process. However, in the past few decades, efforts toward photosynthetic mimicry have chiefly been focused on chromophores with absorption in the visible region (e.g., porphyrins), and there has been little access to chromophores with (1) absorption in the NIR region and, (2) suitably malleable synthetic chemistry for use in artificial constructs. Recent access to synthetic bacteriochlorins has, in principle, enabled utilization of the NIR region.¹ The synthetic bacteriochlorins are distinguished by wavelength tunability of a sharp and intense absorption band in the NIR region, a reasonable degree of synthetic tailorability (for solubility, bioconjugation, etc.), and stability to the medium and environmental conditions typical for bioconjugation and photosynthesis studies.²

In nature, two major types of light-harvesting complexes are found in purple photosynthetic bacteria (Figure 1.1a). The first kind is the core light-harvesting complex (LH1), which is in close proximity to the photochemical reaction center and in a fixed stoichiometric ratio with the reaction center (Figure 1.1b). The second kind has an accessory form of light-harvesting complex (LH2), which is more distant from the reaction center, and whose ratio to the reaction center varies depending on the environmental conditions such as

light intensity, oxygen partial pressure and temperature (Figure 1.1c).³ Biochemical and spectroscopic results have shown that both LH1 and LH2 are composed of associated heterodimers consisting of BChl *a*, an α peptide and a β peptide (Figure 1.1d). In the cartoon, the α peptide is shown in blue, the β is shown in green, and BChl *a* is displayed in magenta. Both peptides have a hydrophobic membrane-spanning domain flanked by relatively polar N-terminal and C-terminal domains.⁴ The LH and $\alpha\beta$ complexes can be separated from the bacteria, and the α peptide, β peptide and BChl *a* can be further separated from the heterodimers and can be reconstituted to give the same photosynthetic properties.^{5,6}

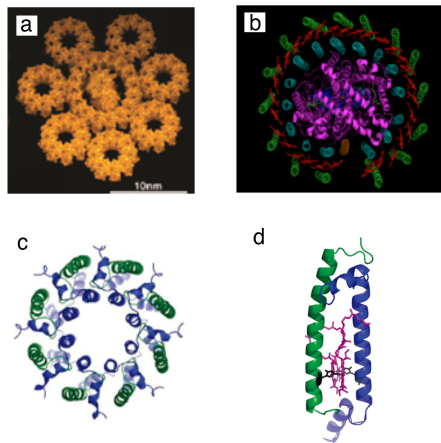


Figure 1.1. Cartoon of (a) reaction center surrounded by LH 1 (bigger ring in the center) and LH2 (peripheral smaller rings); (b) LH1 complex (outside ring) and reaction center (in the middle); (c) LH2 complex; (d) heterodimer composed of α peptide (blue), β peptide (green) and BChl *a* (magenta). Diagrams adapted from Professors Neil Hunter and Richard Cogdell.

Great effort had been made to explore the relationship between the structures and functions of the light-harvesting complexes. Three factors are considered to attribute to the formation of the dyads and the oligomers.

First, BChl *a* – peptide interaction. Coordination between the magnesium of BChl *a* with the His residue was suggested to contribute at least half of the total energy for complex stabilization (Figure 1.2).⁷ To evaluate the importance of this His residue, His0 of β peptide of *Rhodobacter sphaeroides* was mutated to Asn, Tyr, or Leu, and only H0A exhibited a slight LH1 complex formation, all the other two mutants totally lost the ability for complex formation. This unsuccessful formation of the complex meant that the stabilization of this complex is expected to occur with 4.5-5.5 kcal/mol binding energy.⁷ Hydrogen bonding is another form of BChl *a*-peptide interaction. Reconstitution experiments using analogs of BChl *a* indicated that the C3¹ and C13¹ groups were important for formation of dyads and oligomers (Chart 1.1 and Figure 1.2) because these groups would be very good hydrogen bond acceptors, and the α Trp+11 and β Trp+9 were proven to be good hydrogen bonding donors (Figure 1.2). His0 was proven to form a hydrogen bond with the C13¹ carbonyl group of BChl *a* which is coordinated to the partner peptide, thus, a kind of cross hydrogen bonding occurs which would help stabilize the dyads (Figure 1.2).

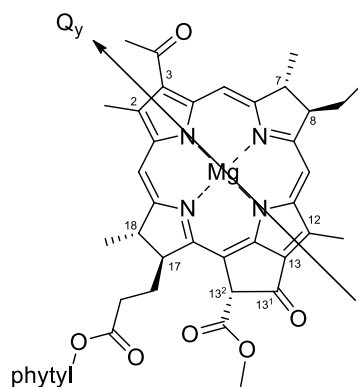


Chart 1.1. Structure of BChl *a*.

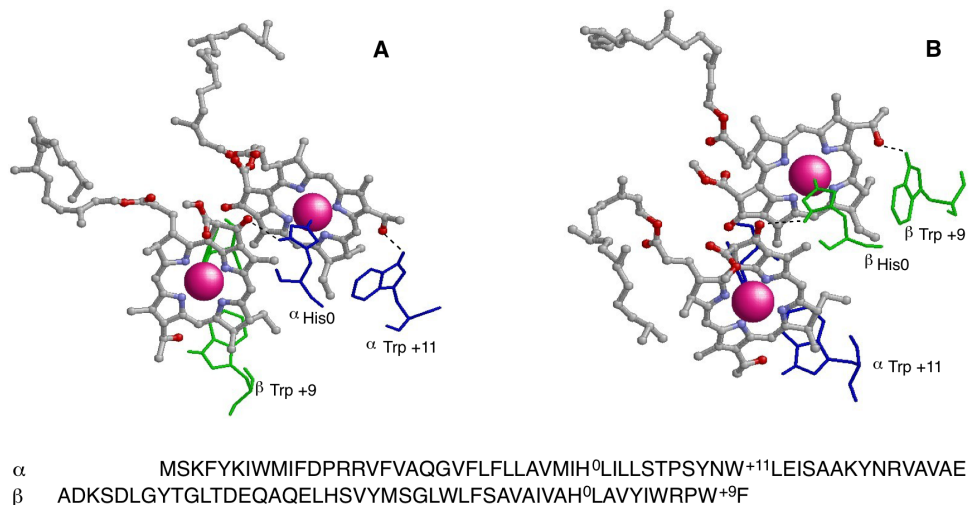


Figure 1.2. Magnesium coordination with His residue and hydrogen bonding between Trp residues and carbonyl groups on BChl *a*. At the bottom are the α and β peptides sequences.

Second, BChl *a* – BChl *a* interactions. The crystal structure of *Rhodospirillum molischianum* indicates that the distance between Mg atom in the $\alpha\beta$ heterodimer was 9.2 Å, and the Q_y axes of the BChl *a* are antiparallel to each other (Figure 1.3a).⁸ In the structure of LH2 of *Rhodospirillum molischianum*, the BChl *a* molecules in the oligomer overlap at ring I and the two BChl *a* molecules in the dyads overlap at rings III and V (Figure 1.3b).⁷ Thus, an extensive array of BChl *a* molecules is formed so that the energy is absorbed in the NIR region and the excited-state energy is quickly delocalized among the excitonically coupled molecules.

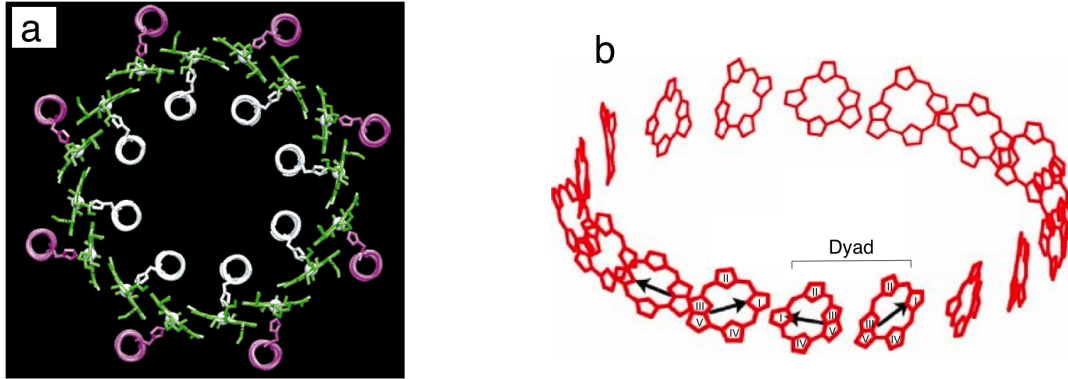


Figure 1.3. (a) Arrangement of bacteriochlorophylls in the LH2 of *Rhodospirillum rubrum*. BChl *a* molecules are in green, the α peptides are in white and β peptides are in magenta. (b) Arrangement of the BChl *a* molecules within the B850 ring of LH2 from *Rhodospseudomonas acidophila*. Cartoon pictures are adopted from reference 8.

The ability of separated native α and β peptides to form dyads and oligomers in the presence of BChl *a* prompted scientists to ponder the minimum structural requirements of the peptides for this reconstitution. Years ago, the Loach lab revealed that the 31mer derived from the β peptide (removal of the 17 residues from the N terminus) (Figure 1.4) possessed ability similar to that of the full β for reconstitution.⁴ One advantage of 31mer over the β peptide is that the 31mer can not only form the $\beta\beta$ dimer, but also can form the oligomers in the absence of the α peptide. In contrast, the β peptide can only form the $\beta\beta$ dimer, but can not form the oligomers in the absence of native α (Table 1.1 and Figure 1.5).⁴ Thus, both the 31mer and β peptide can readily associate with BChl *a* by apical histidine ligation to form a $\beta\beta$ -subunit dimer that contains two BChl *a* molecules.^{9,10,11,12}

α MSKFYKIWMIFDPRRVFVAQGVFLFLAVMIH⁰LILLSTPSYNWLEISAAKYNRVAVAE
 β ADKSDLGYTGTLTDEQAQELHSVYMSGLW-10LFSAVAIVAH⁰LAVYIWRPWF
 31mer ELHSVYMSGLW-10LFSAVAIVAH⁰LAVYIWRPWF

Figure 1.4. Sequence of α peptide, β peptide and truncated 31mer (from top to bottom) of *Rhodobacter sphaeroides* LH1.

Table 1.1. Dyad and oligomer formation from 31mer, β peptide, α peptide and BChl *a*.

Precursors	Dyad absorption	Oligomer absorption
$\alpha + \beta + \text{BChl } a$	820 nm	870 nm
$\beta + \beta + \text{BChl } a$	820 nm	No formation
31mer + 31mer + BChl <i>a</i>	820 nm	850 nm

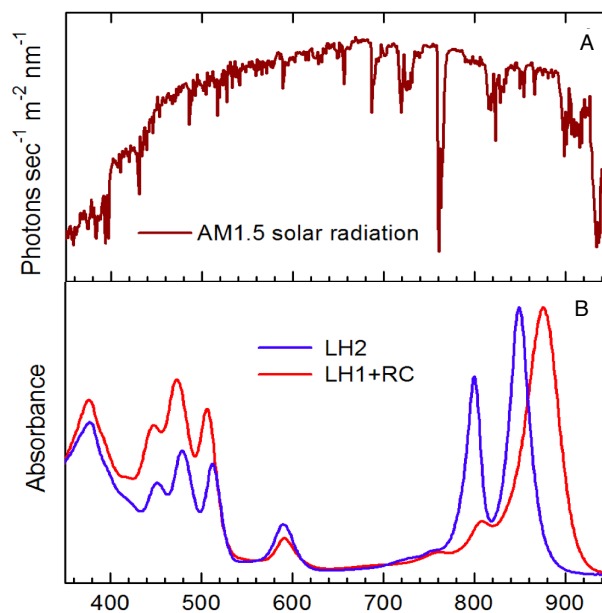


Figure 1.5. (A) Photon flux density spectrum of AM1.5 solar radiation. (B) Absorption spectra of native LH2 (blue) and LH1 plus reaction center (RC) (red) from a *Rhodobacter sphaeroides* mutant that has sphaeroidene as the only carotenoid, which gives rise to the 440–540 nm absorption.

A lot of effort over the past few decades has been made to build synthetic light-harvesting systems, which required constructing both the chromophores and scaffolding.^{13,14} The ability of separated native α and β peptides to form the dyads and oligomers in the presence of BChl *a* prompted groups to consider the formation of biohybrid light-harvesting systems, in which synthetic chromophores are incorporated onto native peptides and reconstituted to form the photosynthetic antenna complexes in a natural manner.

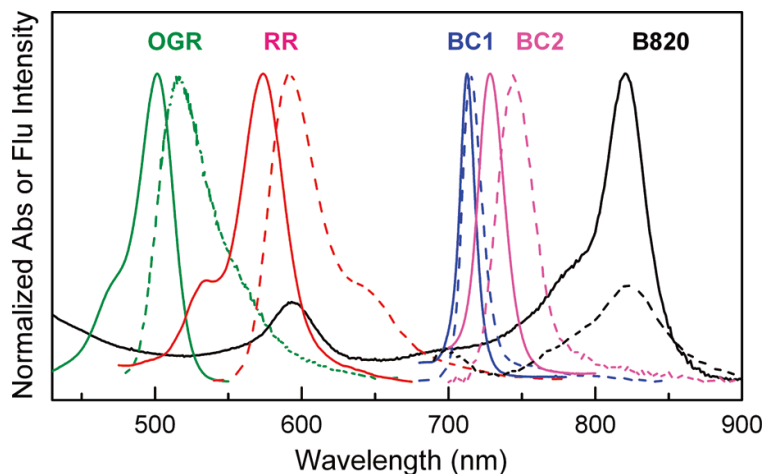


Figure 1.6. Normalized absorption (solid) and fluorescence (dashed) spectra of bioconjugatable dyes (colored) and of BChl *a* dimer B820 in subunit complex $[31\text{mer}(-14\text{Cys})\text{BChl}]_2$ (black). The B820 fluorescence is scaled arbitrarily for clarity. (Figure is retrieved from ref 14)

Based on the rationale above, some work has been done and published,¹⁴ in which a truncated 31mer of β peptide of *Rhodobacter sphaeroides* LH1 complex was used. The 31mer peptide was engineered with a Cys site (-10 position) for bioconjugation with maleimide-terminated chromophores, which include synthetic bacteriochlorins (**BC1** and

BC2, structures not shown here) and two commercial dyes (Oregon Green **ORG** and Rhodamine Red **RR**, structures not shown here) (Figure 1.6). Upon appropriate placement, energy transfer from the synthetic bacteriochlorin to the BChl *a* dimer was almost quantitative.¹⁴

As an extension to this light-harvesting biohybrid work, two major work was pursued: (1) synthesis of novel chromophores that are wavelength-tunable, polarity-tunable, highly fluorescent and bioconjugatable; and (2) different strategies for construction of light-harvesting architectures to make better use of the solar energy.

References

1. H.-J. Kim and J. S. Lindsey, *J. Org. Chem.*, 2005, **70**, 5475–5486.
2. E. Yang, C. Kirmaier, M. Krayner, M. Taniguchi, H.-J. Kim, J. R. Diers, D. F. Bocian, J. S. Lindsey and D. Holten *J. Phys. Chem. B*, 2011, **115**, 10801–10816.
3. J. B. Todd, P. S. Parkes-Loach, J. F. Leykam and P. A. Loach, *Biochemistry*, 1998, **37**, 17458–17468.
4. K. A. Meadows, P. S. Parkes-Loach, J. W. Kehoe and P. A. Loach, *Biochemistry*, 1998, **37**, 3411–3417.
5. P. S. Parkes-Loach, J. R. Sprinkle and P. A. Loach, *Biochemistry*, 1988, **27**, 2718–2727.
6. A. F. Mironov and M. A. Grin, *J. Porphyrins Phthalocyanines*, 2008, **12**, 1163–1172.
7. P. A. Loach and P. S. Parkes-Loach, In *The Purple Phototrophic Bacteria*, ed N. C. Hunter, F. Daldal, M. C. Thurnauer and T. J. Beatty, Springer Science, 2010, pp. 181–198.

8. J. Koepke, X. Hu, C. Muenke, K. Schulten, H. Michel, *Structure*, 1996, **4**, 581–597.
9. P. S. Parkes-Loach, A. P. Majeed, C. J. Law and P. A. Loach, *Biochemistry*, 2004, **43**, 7003–7016.
10. P. A. Loach and P. S. Parkes-Loach, In *Advances in Photosynthesis and Respiration*, ed. C. N. Hunter, F. Daldal, M. C. Thurnauer and J. T. Beatty, Springer, Dordrecht, The Netherlands, 2009, pp. 181–198.
11. C. J. Law, J. Chen, P. S. Parkes-Loach and P. A. Loach, *Photosynth. Res.* 2003, **75**, 193–210.
12. H. Paulsen, In *Chlorophylls and Bacteriochlorophylls: Biochemistry, Biophysics, Functions and Applications*, ed. B. Grimm, R. J. Porra, W. Rüdiger and H. Scheer, Springer, Dordrecht, The Netherlands, 2006, pp. 375–385.
13. T. A. Moore, A. L. Moore and D. Gust, *Philos. Trans. R. Soc. London B*, 2002, **357**, 1481–1498.
14. J. W. Springer, P. S. Parkes-Loach, K. R. Reddy, M. Krayner, J. Jiao, G. M. Lee, D. M. Niedzwiedzki, M. A. Harris, C. Kirmaier, D. F. Bocian, J. S. Lindsey, D. Holten and P. A. *J. Am. Chem. Soc.* 2012, **134**, 4589–4599.

CHAPTER 2

Near-Infrared Tunable Bacteriochlorins for Bioorthogonal Labeling

Preamble. The contents in this chapter have been submitted, reviewed and recommended for publication after minor revision⁹⁴ with contributions from Masahiko Taniguchi (associate research professor in the Lindsey group) for the spectra in the introduction section.

Introduction

Molecules or materials with near-infrared (NIR) spectral features, namely absorption and emission, offer abundant opportunities in photochemistry, but such substances have been far less developed than those for use in the ultraviolet or visible spectrum.¹⁻⁸ For many applications, the ideal features of a NIR chromophore include the ability to (1) control overall molecular polarity (hydrophilic, amphiphilic, or hydrophobic), (2) install a single bioconjugatable tether, (3) tune the position of the long-wavelength absorption band, (4) exert control over the nature of the excited state (e.g., lifetime, decay pathways), and (5) prepare the chromophore via a robust synthesis (Figure 2.1). Few if any chromophores satisfy all five criteria. A commonly desired excited-state property is well-defined fluorescence, which encompasses a controllable Stokes' shift, defined full-width-at-half-maximum, and high Φ_f value. Other applications may seek a quantitative yield of intersystem crossing. The bioconjugatable tether enables attachment of the chromophore to a biomolecule, surface, particle, or cell. The synthesis criterion, which does not concern performance characteristics but does concern availability and tailorability, is best satisfied by simple procedures beginning with readily available starting materials.

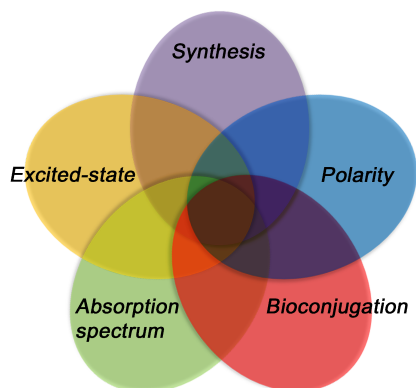


Figure 2.1. Nexus of design issues for NIR chromophores.

The NIR-active molecules of bacterial photosynthesis are bacteriochlorophylls, which function in light-harvesting and charge-separation processes.⁹ The structures of bacteriochlorophyll *a* and bacteriochlorophyll *b* are shown in Chart 2.1. The bacteriochlorophylls contain the bacteriochlorin (i.e., tetrahydroporphyrin) chromophore. An additional family of naturally occurring bacteriochlorins, albeit apparently non-photosynthetic, are the tolyporphins, exemplified by tolyporphin A from a soil cyanophyte.¹⁰⁻
¹⁶ The absorption spectra of bacteriochlorophylls *a* and *b* as well as that of tolyporphin A (and its copper chelate) are shown in Figure 2.2.¹⁷⁻²⁰ The features of bacteriochlorophylls can be compared with those of synthetic NIR-active chromophores.

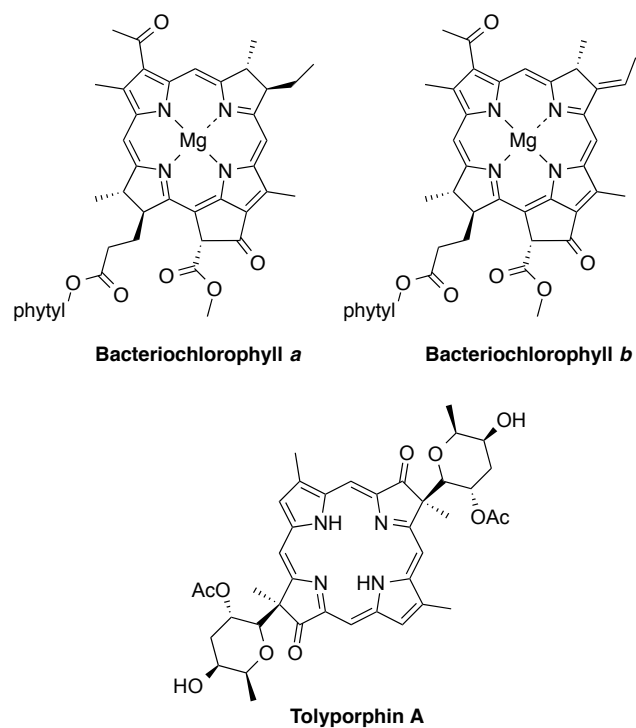


Chart 2.1. Naturally occurring bacteriochlorins.

Synthetic, non-natural chromophores that absorb and/or emit in the NIR region include members of the phthalocyanine, cyanine dye, boron-dipyrin, and quantum dot families.^{18,21-25} Representative examples are shown in Chart 2.2 along with absorption spectra in Figure 2.2. Each class has attractive features as well as limitations, as described as follows.

- (1) Phthalocyanines typically have a very high fluorescence quantum yield (Φ_f) but are poorly soluble in organic solvents; moreover, while phthalocyanines that have D_{2h} or D_{4h} symmetry are readily prepared via robust routes, the ability to rationally tailor phthalocyanines is quite limited in comparison with that of many other chromophores.²⁶

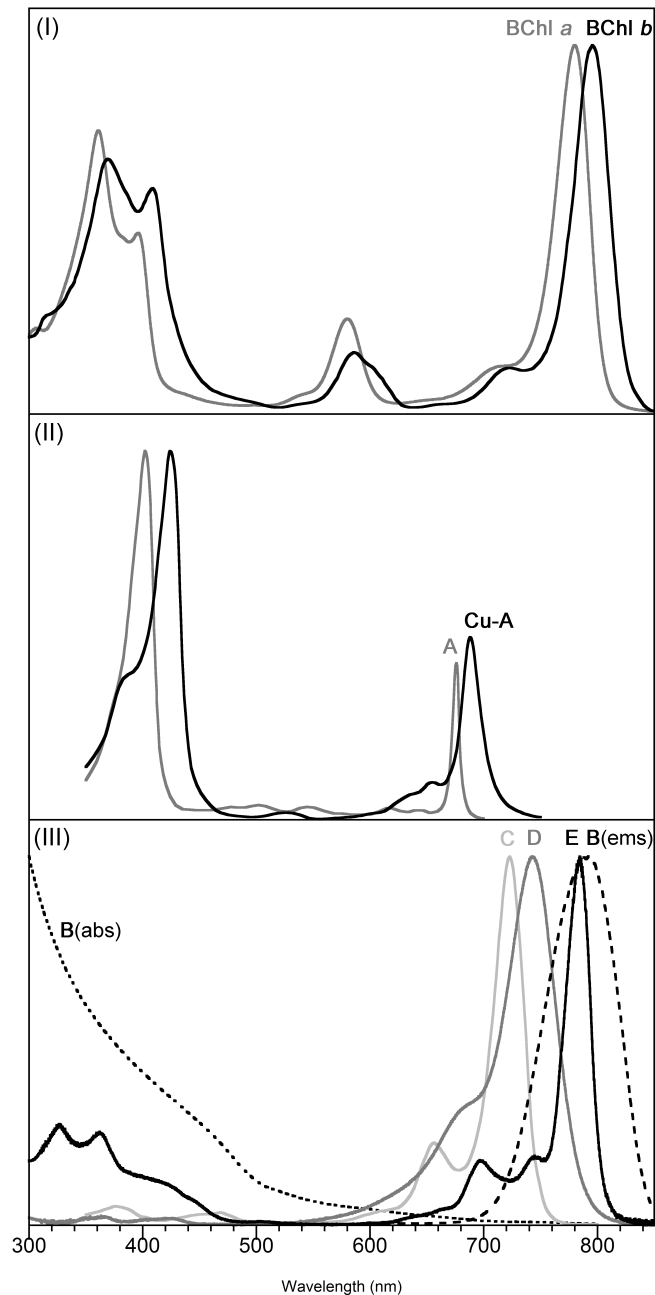


Figure 2.2. Absorption spectra (normalized) of NIR-active chromophores. Panel I: Bacteriochlorophylls *a* (toluene)^{17,18} and *b* (diethyl ether).¹⁹ Panel II: Tolyporphin A (**A**) and copper(II)-tolyporphin A (**Cu-A**) (methanol).²⁰ Panel III: selected synthetic chromophores – Qdot 800 (**B**) absorption in dotted line; emission in dashed line (pH 7.2 buffer),²¹ boron-dipyrin (**C**, CHCl₃),²² indotricarboyanine dye (**D**, ethanol),^{18,23} and tetra-*tert*-butyl-2,3-naphthalocyanine (**E**, chlorobenzene).^{18,24}

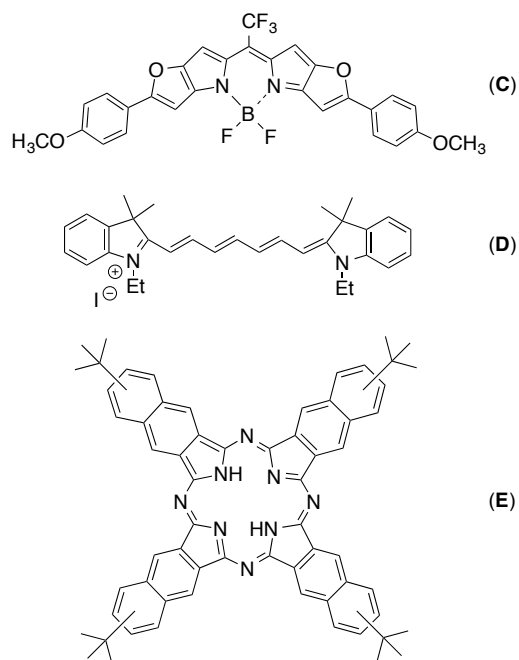


Chart 2.2. Synthetic NIR chromophores.

- (2) Cyanine dyes exhibit wavelength tunability by virtue of changes in the length of the polyene chain as well as changes in the nature of the “heterocyclic nuclei” at the termini of the polyene.²⁷ The synthetic chemistry has received intense attention over the years.²⁸ Cyanines are intrinsically charged, however, frequently causing aggregation and thereby limiting approaches for purification and handling. Moreover, cyanine dyes tend to have broad absorption spectra, and are known to form photoisomers upon illumination, which can impede some photochemical applications.^{2,4,6,29}
- (3) Boron-dipyrins with few or no conjugated substituents typically absorb in the ~500–600 nm region.³⁰ Quite recently, boron-dipyrins that bear more

extensively conjugated substituents have been developed that absorb on the high-energy edge of the NIR region (i.e., 700 nm).^{7,22} It remains to be seen how deeply the absorption can be pushed into the NIR while retaining desirable photochemical features.

- (4) Quantum dots have been prepared that emit in the NIR region.⁸ An attraction of quantum dots is the strong resistance to photobleaching even upon long-term illumination; limitations include the very broad absorption spectra and the lack of synthetic tailorability.

Viewed in the context of available synthetic NIR-active chromophores, bacteriochlorophylls – Nature’s chosen NIR-active chromophores – are not very amenable to synthetic manipulation for wavelength tuning given the nearly full complement of substituents arrayed about the perimeter of the macrocycle. Total syntheses of the bacteriochlorophylls have not been reported. The synthesis of tolyporphin A has been accomplished, but the daunting and lengthy nature of the synthesis would appear to impede most applications.³¹⁻³³ Bioconjugation of synthetically accessible porphyrins has been studied quite extensively,³⁴ but porphyrins lack the NIR absorption characteristic of bacteriochlorins.

A decade ago, we reported a *de novo* route to bacteriochlorins.³⁵ Since then, we and others have exploited the synthesis to gain access to bacteriochlorins that are (1) lipophilic and wavelength tunable (ranging from ~690 nm to ~900 nm;³⁶⁻⁴⁰ (2) lipophilic and bioconjugatable,^{38,41-45} (3) lipophilic, wavelength-tunable, and bioconjugatable;^{38,45,46} (4) hydrophilic;^{36,45,47} (5) hydrophilic and bioconjugatable;^{45,48} and (6) amphiphilic and

bioconjugatable.⁴⁹ In each case, the bioconjugatable group was a carboxylic acid or *N*-hydroxysuccinimido ester (for reaction with an amine to give an amide), or a maleimide (for reaction with a thiol to give a thioether). Other bacteriochlorins bearing a single bioconjugatable tether also have been prepared by derivatization of synthetic porphyrins or by modification of bacteriochlorophylls,⁵⁰⁻⁵⁵ but wavelength tuning has necessarily been limited.

In this paper, we explore an expanded range of functional groups for bioconjugation with a palette of wavelength-tunable synthetic bacteriochlorins. The bioconjugation motifs include an aldehyde group (for reaction with a hydroxamine to give an oxime), a maleimide group (for reaction with a thiol to form a thioether), an ester or thioester group (for reaction with an azide via Staudinger ligation to give an amide), or an azide group (for click chemistry with an ethyne to give a triazole). Altogether, nine new bacteriochlorins have been prepared. The bacteriochlorins are lipophilic, exhibit a long-wavelength absorption band that ranges from 729 nm to 820 nm, and have been examined in prototype bioconjugation reactions. The prototype reactions in conjunction with literature considerations have led to a 4 x 4 matrix for successive bioorthogonal coupling reactions.

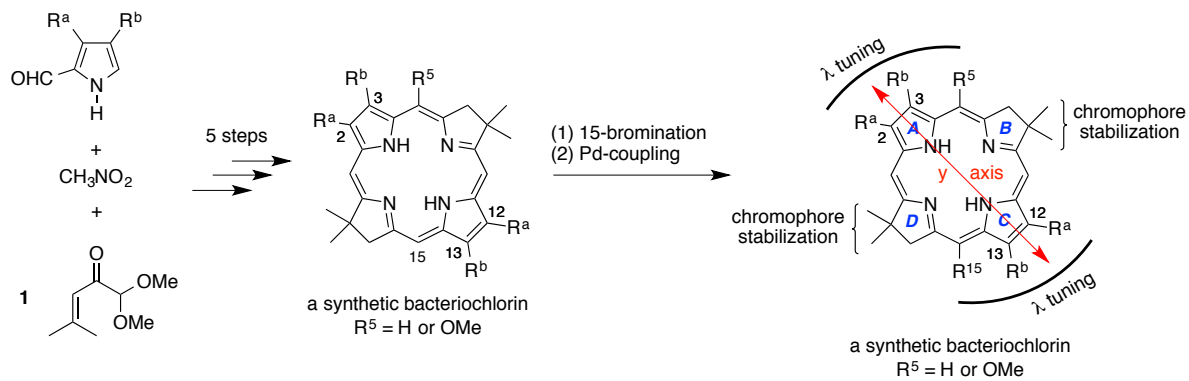
Results and discussion

(I) Molecular design

(A) Synthesis. Methods for bacteriochlorin synthesis include the following: (i) modification of the natural bacteriochlorophylls,^{56,57} (2) hydrogenation or reductive addition of natural or synthetic porphyrins or chlorophylls,^{58,59} and (3) *de novo* synthesis.^{32-35,37,60-62} The *de novo* synthesis methods entail considerable investment in laboratory work but afford

commensurate control over molecular tailorability. The *de novo* route developed in our group employs three organic starting materials (a pyrrole-2-carboxaldehyde, nitromethane, and α,β -unsaturated ketone **1**⁶²), which can be smoothly converted in a 5-step synthesis to the corresponding bacteriochlorin, as shown in Scheme 2.1. The geminal dimethyl group in each pyrroline ring blocks potential oxidative pathways leading to chlorins or porphyrins. The bacteriochlorin can be the substrate for further derivatization. For the work described herein, regioselective 15-bromination⁶⁰ of a 5-methoxybacteriochlorin followed by Pd-coupling has provided a facile means for introduction of a single bioconjugatable group.

(B) Wavelength tuning. The position of the long-wavelength absorption band of the bacteriochlorin (Q_y band) sets an upper limit on the energy of the excited single state as well as the ensuing fluorescence spectrum. Hence, the ability to tune the position of the Q_y band is of utmost importance. To date, wavelength tunability of the bacteriochlorins of the architecture shown in Scheme 2.1 can be achieved by (i) installation of auxochromes at the β -pyrrole positions,^{63,64} which lie more or less coincident with the transition dipole moment of the Q_y transition (parallel to the y-axis);⁶⁵ (ii) incorporation of a fifth (or exocyclic) ring spanning the 13- and 15-positions;⁶¹ (iii) the presence or absence of a 5-methoxy group;^{35,45} (iv) conversion of the free base macrocycle to the corresponding metal chelate;⁶⁶ (v) formation of strongly coupled dyads;³⁹ and/or (vi) oxidation of the β -pyrroline methylene unit to give an oxo- or dioxobacteriochlorin.⁴⁰ In the latter regard, note that tolyporphin A is a dioxobacteriochlorin.

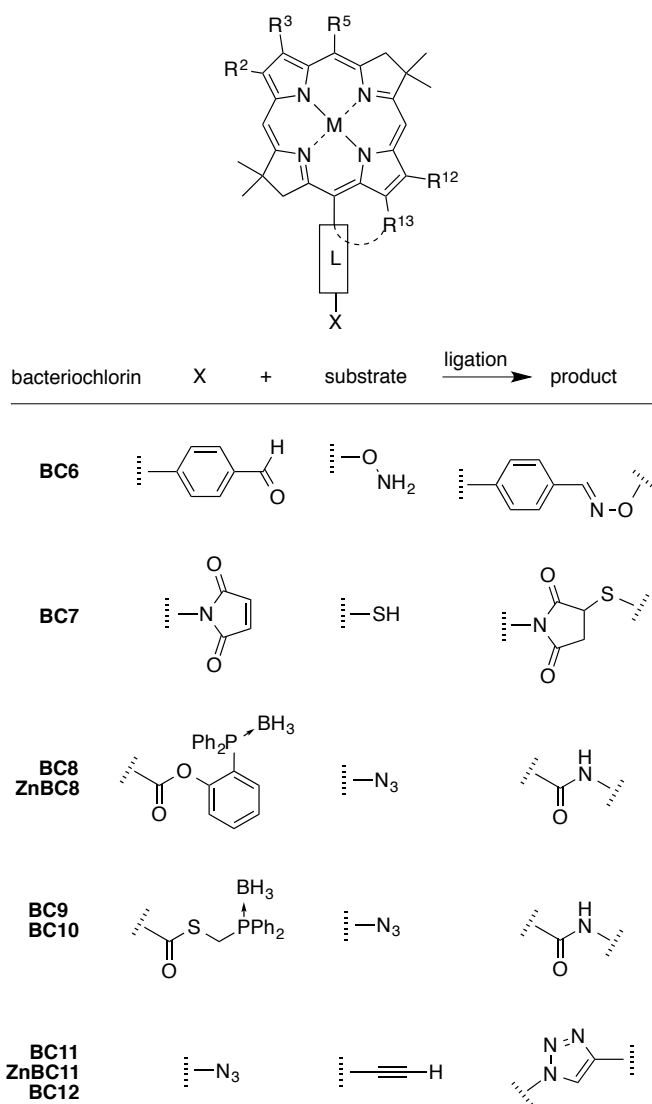


Scheme 2.1. Synthesis route and design features of stable bacteriochlorins (top). Relevant bacteriochlorin benchmarks (**BC1**,³⁸ **BC2**,³⁸ **ZnBC2**,⁴⁵ **BC3**,⁴⁴ **BC4**,⁶⁶ **BC5**⁶¹) and position of the Q_y absorption band (bottom).

Herein, six known bacteriochlorins (free base **BC1**, **BC2**, **BC3–BC5**; zinc **ZnBC2**) served as benchmarks for the design of target bacteriochlorins with a particular Q_y band position (Scheme 2.1). Compound **ZnBC4** is fictive; the spectrum was predicted to be 805 nm on the basis of the following: (1) the corresponding free base bacteriochlorin is known

and has $\lambda_{Q_y} = 793$ nm; and (2) the insertion of zinc into the free base bacteriochlorin-imide **BC5** shifts the Q_y band from 818 to 830 nm.^{61,66} Note that the use of band positions in wavenumbers (linear on the energy scale) rather than wavelength in this case affords essentially the same prediction. The expected Q_y band position of the target bacteriochlorins thus ranges from 712 nm to 818 nm.

(C) Bioconjugation motifs. A range of bioconjugatable groups is available for bioorthogonal labeling^{2,67-75} as illustrated in Scheme 2.2. In principle, a given bioconjugatable motif could be installed on a bacteriochlorin with a given Q_y band position. Here, the choice of bioconjugatable motif was not matched to any particular range of the Q_y band. The expected wavelength ranges (for given compounds and bioconjugation motifs) include 712, 793 and 805 nm (**BC1**, **BC4**, **ZnBC4**; an azide for click chemistry), 729 or 738 nm (**BC2**, **ZnBC2**; an ester or thioester for traceless Staudinger ligations), 756 nm (**BC3**; an aldehyde for oxime formation), and 818 nm (**BC5**; a maleimide for thioether formation). Thus, the particular bacteriochlorins prepared were chosen to be illustrative of the various combinations of bioconjugatable motif and wavelength of absorption.



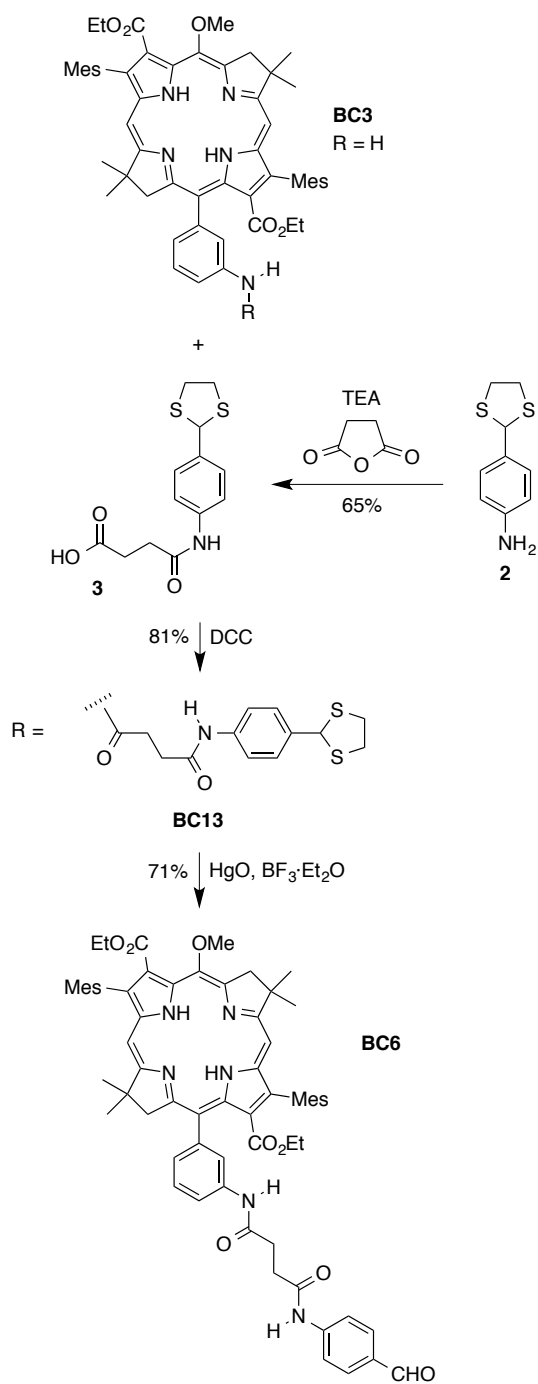
Scheme 2.2. Molecular design of bacteriochlorins and ligation motifs.

(II) Synthesis of bacteriochlorins

(A) Bacteriochlorins for oxime formation. The installation of a formyl group on a bacteriochlorin, as required for oxime formation, can be accomplished in a number of ways. The present method of bacteriochlorin formation is such that the substituents on ring A and

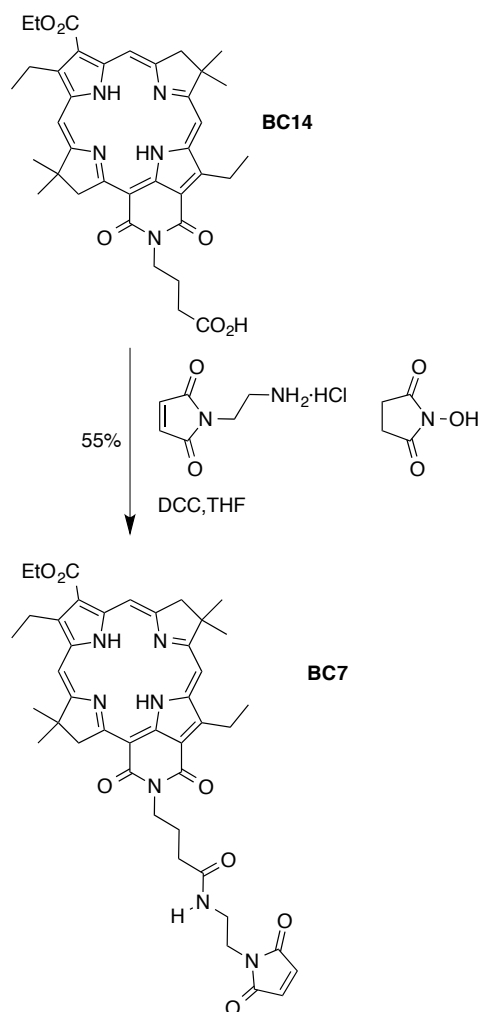
ring C are identical (Scheme 2.1). A 3,13-dibromobacteriochlorin so-prepared has been subjected to Pd-mediated carbonylation to give the corresponding 3,13-diformylbacteriochlorin accompanied by a monoformylbacteriochlorin due to dehalogenation.³⁶ The monoformylbacteriochlorin has been used in reductive amination procedures and to form a semicarbazone and an oxime.³⁸ While demonstrating capability, the approach was hamstrung by the difficulty of preparing the monoformylbacteriochlorin.

The rational installation of a single formyl group is best done by attachment to the 15-position, given that a 15-bromobacteriochlorin can be prepared quite smoothly. Given the availability of a bacteriochlorin bearing a 3-aminophenyl group at the 15-position, a bifunctional spacer thus was prepared to install the formyl group at a distance from the bacteriochlorin nucleus. Reaction of a dithiolane-protected analogue of *p*-aminobenzaldehyde (**2**)⁷⁶ with succinic anhydride gave the dithiolane-protected succinamic acid (**3**) as shown in Scheme 2.3. The coupling of **3** with aminobacteriochlorin **BC3**⁴⁴ in the presence of *N,N*-dicyclohexylcarbodiimide (DCC) afforded the dithiolane-protected bacteriochlorin **BC13**. Standard treatment⁷⁶ of the latter to remove the dithiolane afforded monoformyl-bacteriochlorin **BC6**.



Scheme 2.3. Synthesis of a formylbacteriochlorin for oxime formation.

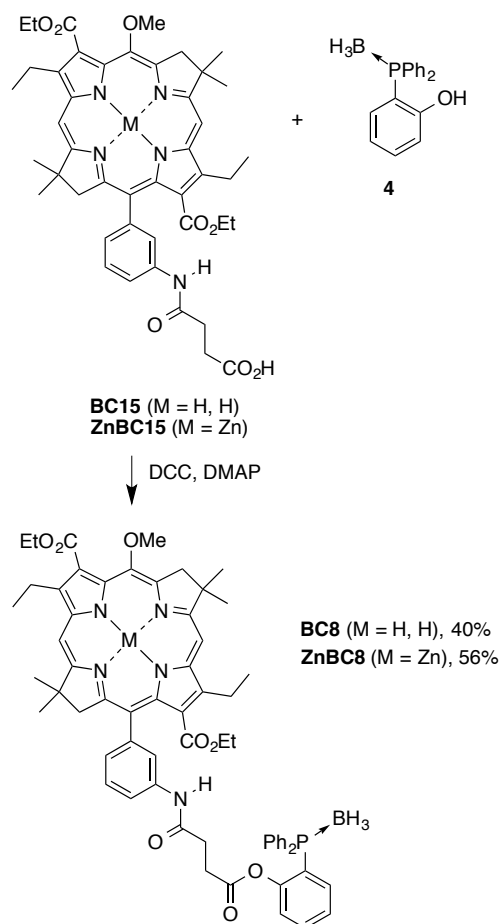
(B) Bacteriochlorins for cysteinyl ligation. A bacteriochlorin-imide bearing an alkyl tether terminated with a maleimido group was prepared as shown in Scheme 2.4. Thus, coupling of bacteriochlorin-imide **BC14**⁴⁵ and *N*-(2-aminoethyl)maleimide in the presence of DCC and *N*-hydroxysuccinimide⁷⁷ afforded the maleimido-bacteriochlorin-imide **BC7**. Bacteriochlorin **BC7** is analogous to a prior maleimido-bacteriochlorin-imide that bears an aryl-containing tether.³⁸



Scheme 2.4. Synthesis of a maleimido-bacteriochlorin.

(C) Bacteriochlorins for Staudinger ligation. Staudinger ligation involves the nucleophilic attack of phosphorus on an azide to form an iminophosphorane intermediate after loss of N₂.^{69,78} When a neighboring electrophile (such as an ortho ester group) traps the reactive iminophosphorane intermediate, the phosphine oxide unit is ultimately retained on the final amido product, which is referred to as non-traceless Staudinger ligation. An attractive alternative is traceless Staudinger ligation wherein the triarylphosphine oxide unit is liberated by virtue of a cleavable linker.^{69,78} The bacteriochlorins described here were designed for traceless Staudinger ligation, with a first set containing an ester unit and the second set a thioester unit.

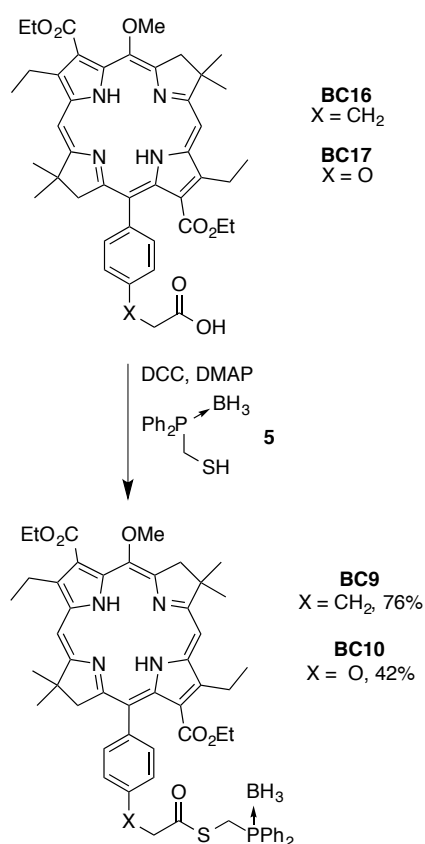
The first set of bacteriochlorins for Staudinger ligation required the presence of a 2-(diphenylphosphanyl)phenyl alkanoate attached to the bacteriochlorin. We initially examined the use of (2-hydroxyphenyl)diphenylphosphine⁹⁴ but then turned to the use of the borane complex thereof (**4**). The reaction of phenol **4** [derived from (2-hydroxyphenyl)diphenylphosphine and BH₃·SMe₂]⁷⁹ with bacteriochlorin **BC15**⁴⁵ to form the ester was carried out in the presence of DCC and 4-(*N,N*-dimethylamino)pyridine (DMAP) (Scheme 2.5). The resulting **BC8** can be used directly for Staudinger ligations.



Scheme 2.5. Synthesis of bacteriochlorins for Staudinger ligation.

In anticipation of the use of bacteriochlorins such as **BC8** in the presence of click-chemistry reactions, which typically requires the presence of a copper reagent, a zinc bacteriochlorin was prepared to avoid undesired metal scavenging during any orthogonal bioconjugation process. Copper(II) bacteriochlorins are unsuitable candidates for many photochemical applications due to the short excited-state lifetime.⁶⁶ Thus, **ZnBC15**⁴⁵ was also coupled with **4** via DCC and DMAP to give the corresponding zinc bacteriochlorin **ZnBC8** for Staudinger ligation (Scheme 2.5).

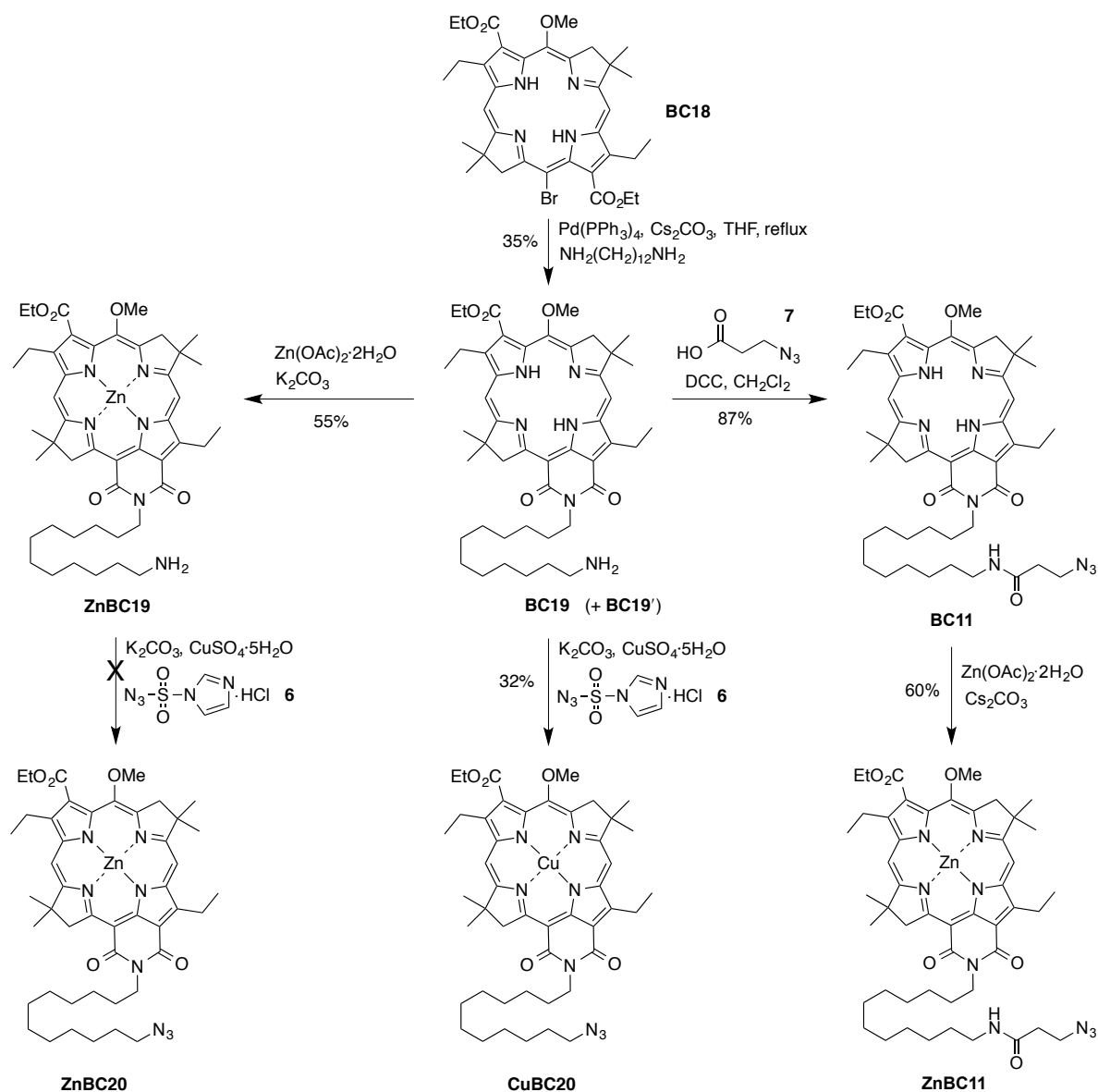
The second set of bacteriochlorins for Staudinger ligation contain a thioester unit to facilitate displacement as part of the traceless design. Bacteriochlorin **BC16**⁴⁵ was coupled with *P*-borane (diphenylphosphino)methylthiol (**5**) mediated by DCC and DMAP to afford the target bacteriochlorin bearing a thioester (**BC9**) in 76% yield (Scheme 2.6). Similarly, bacteriochlorin **BC17**⁴⁵ was coupled with **5** to afford the target bacteriochlorin bearing a thioester (**BC10**) in 42% yield. The phenoxyacetyl linker of the type present in **BC10** has been reported to be somewhat labile depending on the nature of the leaving group attached to the carbonyl moiety.⁸⁰



Scheme 2.6. Synthesis of bacteriochlorins for Staudinger ligation.

(D) Bacteriochlorins for click chemistry. Installation of an azido group was first examined by reaction of an aminobacteriochlorin with a diazo transfer reagent. Thus, carbonylation of **BC18** with 1,12-dodecandiamine afforded bacteriochlorin-imide **BC19** in 35% yield (Scheme 2.7). A side product removed by column chromatography was presumably the bacteriochlorin-15-monocarboximide (**BC19'**) upon analysis by matrix-assisted laser-desorption ionization mass spectrometry (MALDI-MS, obsd $m/z = 826.8$) and absorption spectroscopy (Q_y band at 736 nm). The bacteriochlorin **BC19** was then treated with the diazo transfer reagent,⁸¹ imidazole-1-sulfonyl azide hydrochloride (**6**), for conversion of the primary amine to the azido group. The azido group was detected by IR spectroscopy (2094 cm^{-1}) in the purified product. However, the bacteriochlorin Q_y band was bathochromically shifted by 21 nm (to 815 nm) compared with that of **BC19** ($Q_y = 794\text{ nm}$), and electrospray ionization mass spectrometry (ESI-MS) data were consistent with formation of the copper bacteriochlorin **CuBC20**.

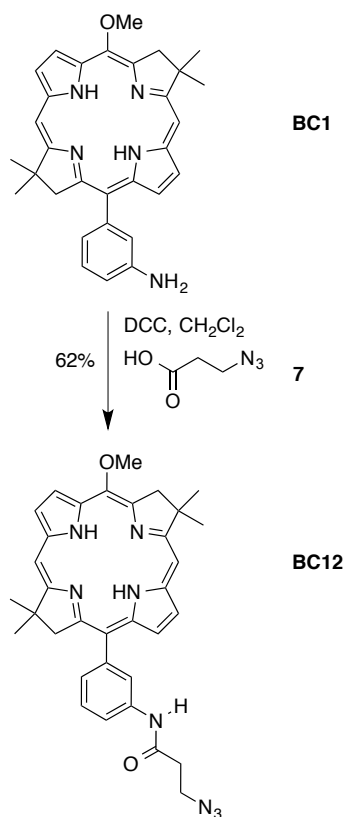
To avoid copper metalation, the free base bacteriochlorin **BC19** was treated with a mild base (K_2CO_3 or Cs_2CO_3) and zinc acetate dihydrate to afford the corresponding zinc bacteriochlorin **ZnBC19** (Scheme 2.7). The latter was treated to azide formation by reaction with **6** but the desired product **ZnBC20** was not observed, perhaps due to aggregation prompted by interaction of the alkylamine and the zinc bacteriochlorin.



Scheme 2.7. Approaches toward an azido-bacteriochlorin.

An alternative, copper-free approach to install an azido group on the bacteriochlorin relied on attachment of a preformed azido-containing reactant. Thus, free base bacteriochlorin **BC19** was coupled with 3-azidopropionic acid (**7**)⁸² in the presence of DCC

to form the amide (Scheme 2.7). The resulting azido-bacteriochlorin (**BC11**) was then metalated with zinc as desired for use in click-chemistry procedures. The target bacteriochlorin (**ZnBC11**) gave the expected bands upon examination by IR (azido group, 2098 cm^{-1}) and absorption (Q_y band at 806 nm) spectroscopy.



Scheme 2.8. Synthesis of an azidobacteriochlorin.

The success of the approach with the preformed azidopropionic acid was applied with an aminobacteriochlorin that absorbs at shorter wavelength. Thus, coupling of bacteriochlorin **BC1**³⁸ with 3-azidopropionic acid (**7**) in the presence of DCC afforded

amide-bacteriochlorin **BC12** (Scheme 2.8). To assess whether **BC12** could be used for copper-catalyzed click reactions, a set of control experiments concerning copper scavenging was carried out (*vide infra*).

(III) Characterization and photophysical properties

The bacteriochlorins were readily soluble in organic solvents as expected given the hydrophobic nature of the macrocycle and the appended substituents. Each target bacteriochlorin was examined for homogeneity by thin-layer chromatography and was characterized by ¹H NMR spectroscopy, mass spectrometry (MALDI-MS, ESI-MS), absorption spectroscopy, and fluorescence spectroscopy (except for **BC8** and **ZnBC8**). The bacteriochlorins (as expected) were quite stable on routine handling on the open benchtop and also were stable for at least 3 years upon storage in the dark at -20 °C.

Absorption spectra were collected in CH₂Cl₂. Each bacteriochlorin exhibited an absorption spectrum characteristic of the bacteriochlorin chromophore.¹⁹ The spectra for five free base bacteriochlorins and two zinc bacteriochlorins are shown in Figure 2.3. Bacteriochlorins **BC9** and **BC10** exhibited identical spectra with that of **BC8** and are not shown in the figure. The position of the respective Q_y band among the members of the series ranges from 713 nm to 820 nm. A comparison of predicted Q_y band position on the basis of the benchmark bacteriochlorins with that of the target bioconjugatable bacteriochlorins is shown in Table 2.1. The variation was at most 2 nm, which is not surprising given that the bioconjugatable motifs are positioned at sites removed from the bacteriochlorin chromophore.

The fluorescence emission spectra also were recorded for the bioconjugatable bacteriochlorins. The spectra are displayed in Figure 2.3 and listed in Table 2.1. One

exception was for bacteriochlorins containing the phosphine moiety for Staudinger ligation (**BC8** and **ZnBC8**), where the values for the immediate precursors, **BC15** and **ZnBC15**, are provided. In each case the Stokes' shift was ≤ 8 nm, which is typical for members of this family of gem-dimethyl-substituted bacteriochlorins. A further characteristic feature of the bacteriochlorins is the narrow absorption and emission band. The full-width-at-half maximum (fwhm) of the Q_y absorption band and the corresponding emission band is listed for each of the bacteriochlorins (Table 2.1). In each case, the absorption fwhm is ≤ 30 nm, and the emission fwhm is ≤ 39 nm.

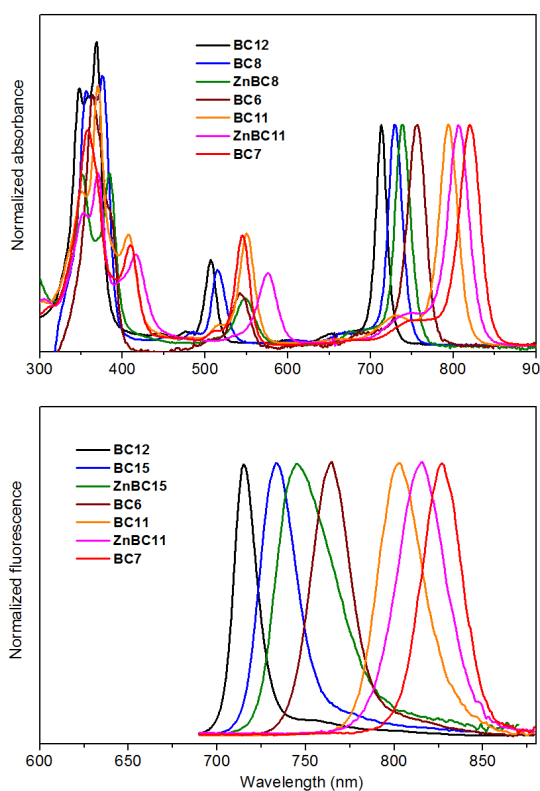


Figure 2.3. Absorption (top) and fluorescence emission (bottom) spectra of target bacteriochlorins at room temperature in CH_2Cl_2 , except emission of **BC15** and **ZnBC15** (precursors of **BC8** and **ZnBC8**, respectively) in DMF.

Table 2.1. Comparison of spectral properties of target versus benchmark bacteriochlorins.^a

Benchmark BC	λ_{abs} (nm)	Bioconj BC	λ_{abs} (nm) ^c	$\Delta\lambda$ (nm) ^d	λ_{em} (nm) ^c	Abs fwhm, nm ^c	Em fwhm, nm ^c
BC1	712	BC12	713	1	715	16	15
BC2	729	BC8 (BC15)^e	730 (727) ^e	1	(733) ^e	(21) ^e	(24) ^e
BC2	729	BC9	729	0	735	20	24
BC2	729	BC10	729	0	734	19	24
ZnBC2	738	ZnBC8 (ZnBC15)^e	739 (737) ^e	1	(745) ^e	(24) ^e	(39) ^e
BC3	756	BC6	756	1	763	26	26
BC4	793	BC11	795	1	803	26	30
ZnBC4	805 ^b	ZnBC11	806	1	813	30	32
BC5	818	BC7	820	2	825	30	26

^aAll data were collected in CH₂Cl₂, except **BC15** and **ZnBC15** in DMF. ^bPredicted on the basis of data from similar compounds (*vide supra*). ^cData pertain to the bioconjugatable bacteriochlorins in column 3. ^dDifference between Q_y absorption band positions of the bioconjugatable bacteriochlorins (column 4) versus the benchmark bacteriochlorins (column 2). ^eAbsorption and fluorescence emission data of **BC15** and **ZnBC15** are from ref 45.

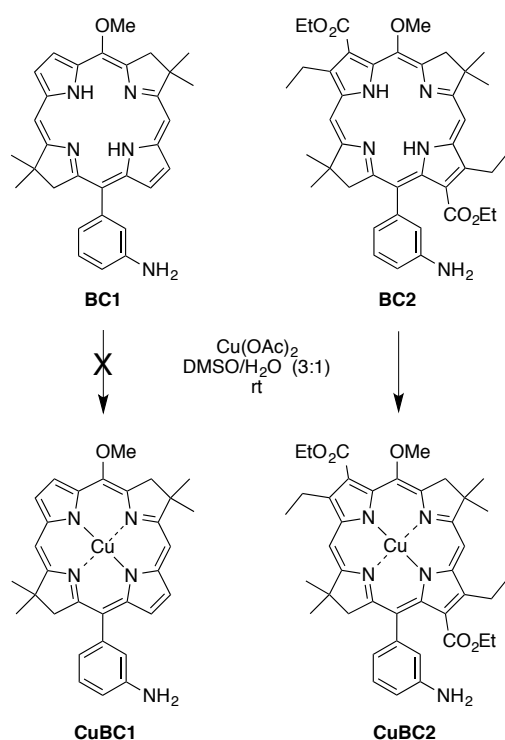
(IV) Bioconjugation tests

Four studies were carried out to assess suitability of the various bacteriochlorins for bioconjugation processes. The studies include (1) the susceptibility of free base bacteriochlorins to the presence of copper in click-chemistry reactions; (2) reaction of each of the respective bioconjugation motifs with small molecules; (3) analogous reactions with tetrapeptides; and (4) examination of the preferred sequence of bioconjugation for use with the bacteriochlorins in series. The studies are described as follows.

(A) Copper metalation experiments. A control experiment was carried out to establish the susceptibility of selected bacteriochlorins to copper insertion. Bacteriochlorins undergo metalation with far greater difficulty than that of chlorins or porphyrins, and among bacteriochlorins, the presence of electron-withdrawing groups facilitates metalation.⁶⁶ Bacteriochlorins **BC1** and **BC2** were treated with copper(II) acetate under dilute-solution, room-temperature conditions typical of bioconjugation reactions (Scheme 2.9). The concentrations of bacteriochlorin were 0.2, 1.0 and 5.0 mM each with 5 equiv of copper(II) acetate. [While Cu(I) is regarded as catalytic, the typical usage in the field appears to employ 5–10 equiv relative to the substrates.^{83,84}] The reactions were monitored by absorption spectroscopy, given that the Q_y band of the copper bacteriochlorin is bathochromically shifted by ~20 nm versus the free base bacteriochlorin⁶⁶ (e.g., 729 nm for **BC2**; 749 nm for **CuBC2**). The bacteriochlorin with two ester groups (**BC2**) at the lowest concentration readily underwent metalation, with ~50% completion after 4 h and apparent completion after 21 h. By contrast, the bacteriochlorin lacking such ester substituents (**BC1**) reacted far more slowly, with only a limited amount of metalation at the 21 h timepoint. Confirmation of copper insertion or lack thereof was provided by MALDI-MS analysis of the crude reaction mixtures.⁹⁴

While click chemistry employs a Cu(I) reagent, which is not expected to readily insert to a bacteriochlorin, the *in situ* formation of Cu(II) species would seem inevitable on routine handling. Indeed, treatment of **BC2** to the conditions for click chemistry [i.e., with a Cu(I) reagent and tris[(1-benzyl-1*H*-1,2,3-triazol-4-yl)methyl]amine (TBTA)⁸⁵ as stabilizing ligand] also resulted in copper insertion. Taken together, bacteriochlorins such as **BC1** for click

chemistry (e.g., **BC12**) should be amenable to direct use in click chemistry reactions over short timeframes, and analogous bacteriochlorins can be used in the presence of copper reagents without risk of metalation. On the other hand, bacteriochlorins such as **BC2** with two ester groups (e.g., **BC8-BC10**) would require protection as the zinc chelate (e.g., **ZnBC8**). The same analysis applies to bacteriochlorins with more than two carbonyl groups (e.g., bacteriochlorin-imide **BC11**) where the zinc chelate (**ZnBC11**) would be required. Following the completion of this work, a report appeared concerning ligands for copper that enable click chemistry (albeit at high concentration) yet preclude metalation of porphyrin substrates.⁸⁶



Scheme 2.9. Investigation of copper insertion with bacteriochlorins.

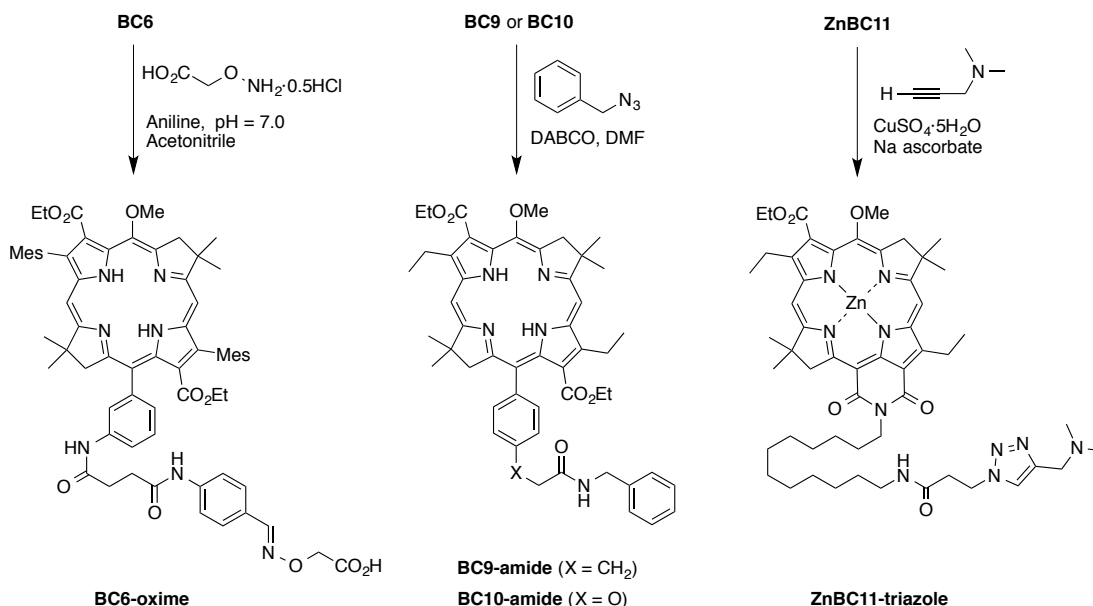
(B) Model studies with small molecules. To determine suitable conditions for each reaction pair and the preferred order for successive bioconjugation, model reactions of bacteriochlorins and small molecules were conducted before progressing to use with peptides. Each conjugate was isolated and characterized by MALDI-MS, ESI-MS, and absorption spectroscopy; also, the absence of the parent bacteriochlorin was confirmed by TLC analysis.

The reaction of **BC6** with oxyamine-containing *o*-(carboxymethyl)hydroxylamine hemihydrochloride was carried out in a mixed solution of aqueous phosphate (pH = 7.0) and acetonitrile (Scheme 2.10). Excess aniline^{87,88} (1000 equiv) was added to activate the aldehyde group of **BC6**. The reaction reached completion within 3 h to give the resulting oxime-containing product **BC6-oxime**.

The Staudinger reaction of **BC8** or **ZnBC8** was carried out under a variety of conditions. In each case, a side product was observed and little target product was detected.⁹⁴ Spectral data suggested the side reaction stemmed from the aromatic amide hydrogen attacking the iminophosphorane intermediate. This observation prompted development of thioester bacteriochlorins (**BC9** and **BC10**) for Staudinger ligation (Scheme 2.10). Indeed, the reaction of bacteriochlorin **BC9** or **BC10** with benzyl azide in DMF containing 1,4-diazabicyclo[2.2.2]octane (DABCO) at 45 °C gave the expected product (**BC9-amide**, 61%; **BC10-amide**, 42%).

The reaction of azido-bacteriochlorin **ZnBC11** with the alkyne 3-dimethylamino-1-propyne was conducted (Scheme 2.10). The catalyst Cu(I) was generated by reacting CuSO₄·5H₂O with the reducing agent sodium ascorbate. The reaction reached completion within 5 h to give the resulting triazole-containing product **ZnBC11-triazole**. The integrity

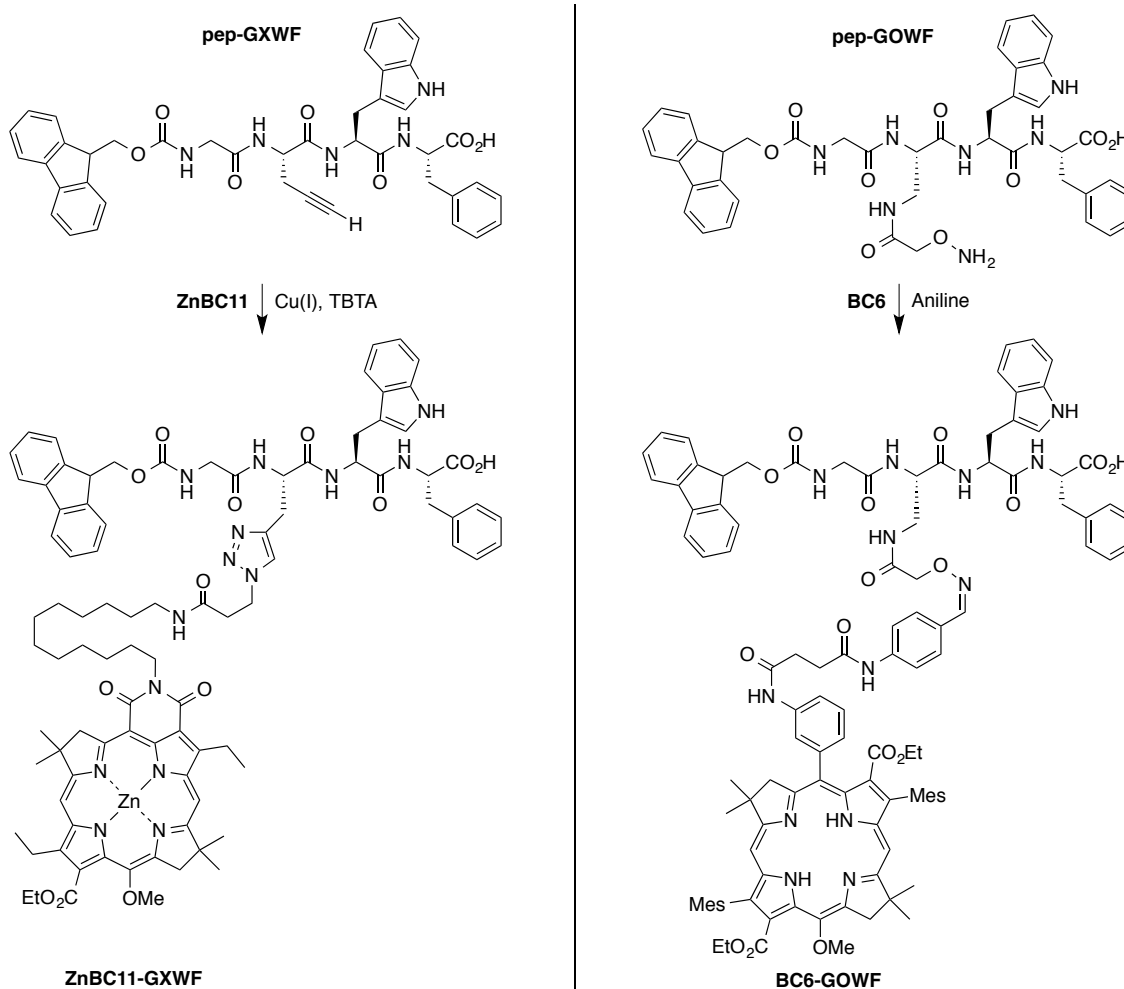
of the zinc bacteriochlorin was manifested upon inspection of (1) the Q_y band in the absorption spectrum (at 806 nm, not 815 nm typical of the corresponding copper bacteriochlorin; e.g., **CuBC20**), and (2) the molecular ion peak manifold in the ESI-MS spectrum. Neither showed the features characteristic of the copper bacteriochlorin.



Scheme 2.10. Proof-of-principle ligation reactions.

(C) Studies with peptides. Bioconjugations were carried out with two model tetrapeptides that contain an alkyne (**pep-GXWF**) or an oxyamine (**pep-GOWF**) group. The bioconjugations were performed with azido-bacteriochlorin **ZnBC11** and formyl-bacteriochlorin **BC6**, respectively. The two tetrapeptides were prepared by solid-phase peptide synthesis (see Experimental Section). Each peptide upon release from the resin was

purified by three ‘cocktail dissolution – precipitation cycles’, and used as such for model bioconjugations.



Scheme 2.11. Preparation of peptidyl-bacteriochlorin conjugates.

The reaction of **ZnBC11** and peptide **pep-GXWF** in DMSO containing TBTA and freshly prepared Cu(I) reached completion at room temperature over 5.5 h (Scheme 2.11, left panel). Removal of the solvent by lyophilization, the copper and sodium salts by washing

with deionized water, and the residual **ZnBC11** by washing with diethyl ether gave the bacteriochlorin-peptide conjugate **ZnBC11-GXWF**. The reaction of **BC6** and peptide **pep-GOWF** was conducted in a mixed solvent of DMSO and aqueous phosphate buffer (3:1) with excess aniline as catalyst for 16 h (Scheme 2.11, right panel). Removal of the solvent under high vacuum followed by excess **BC6** by washing with diethyl ether (confirmed by TLC analysis) gave the bacteriochlorin-peptide conjugate **BC6-GOWF**.

(D) Model studies of bioorthogonal coupling. Bioorthogonal coupling has been the subject of considerable investigation.^{2,70-75} To determine the preferred order of successive bioconjugation, the possibility of cross-reactions among the various functional groups that would thwart orthogonal coupling was considered. The array of known and expected reactions under bioconjugation conditions for the bacteriochlorins prepared herein is provided in Table 2.2; during the course of this work more expansive tables of general relevance were reported.^{74,75} The ‘bioconjugation conditions’ refer to dilute solution (e.g., mM) typically in mixed aqueous-organic media. Two control experiments were carried out to complete the entries in the array.⁹⁴ In this array, couplings for a given bioconjugation pair are positioned along the diagonal; cross-reactions appear as off-diagonal entries. For purely orthogonal couplings among the set, if all off-diagonal combinations resulted in no reaction, then the four pairs of bioconjugation reactions could be implemented in any order.

The existence of several cross-reactions raises immediate problems for successive bioconjugation. The chief problems are that (1) maleimide can also react with an azide⁸⁹ or oxyamine group; and (2) the azide is used both in click chemistry and in Staudinger ligation, and hence appears both as the reacting motif in the chromophore and in the substrate for the

respective reactions. Further cross-reactions can occur under forcing conditions.^{90,91}

Given such possible cross-reactions, it still appears possible to carry out successive bioconjugations: a multifunctional substrate bearing a thiol, oxyamine, azide and alkyne group (Row 1 in Table 2.2) could be targeted with a series of bioconjugatable bacteriochlorins that bear maleimide, aldehyde, phosphine and azide units (Column 1 in Table 2.2). The preferred reaction sequence is as follows: (1) phosphine + azide, (2) azide + alkyne [Cu(I)], (3) aldehyde + oxyamine, and (4) maleimide + thiol. In other words, Staudinger ligation first, then click chemistry, then oxime formation, and finally maleimido-thiol ligation. Implementation of Staudinger ligation first (which occurs in the absence of any copper reagent) to react the azide on the substrate opens the door to use of click chemistry second [in the presence of Cu(I)] to react a bacteriochlorin containing an azide. Use of oxime formation next consumes the oxyamine functional group, in which case the final reaction of maleimide is not expected to suffer cross-reaction with the oxyamine group.

Table 2.2. Matrix of reactions for successive bioconjugation.^a

Bacteriochlorin	Substrate functional groups			
	Thiol	Oxyamine	Azide	Alkyne
Maleimide	√ ^{b,c}	√ ^c	√ ^b	X ^e
Aldehyde	X ^{c,d}	√ ^{b,c}	X ^f	X ^{b,f}
Phosphine	X ^e	X ^e	√ ^{b,c}	X ^e
Azide	X ^e	X ^e	--- ^g	√ ^{b,c,h}

^a√ = reactive; X = not reactive. ^bLiterature results. ^cResults obtained here.⁹⁴ ^dKnown to reversibly form a hemithioacetal or dithioacetal at high concentration. ^eExpected result. ^fReaction occurs under forcing conditions. ^gNo self-reaction. ^hOnly in the presence of Cu(I).

Conclusions and outlook

To gain access to bacteriochlorins that satisfy the criteria shown in Figure 2.1 requires extensive development. The work to date generally has demonstrated attainment of three to four combinations together, but all five criteria have not yet been met simultaneously. The work described herein demonstrates considerable expansion of the capabilities for bioconjugation in the context of wavelength-tunable NIR-active chromophores. Such proof-of-principle has been achieved while employing relatively small quantities of lipophilic bacteriochlorins. The largest impact of a palette of bioconjugatable bacteriochlorins will likely accrue in studies in aqueous solution. Strategies for aqueous solubilization of bacteriochlorins have been investigated and initial designs validated.^{45,48,49} Methods for the preparation of bacteriochlorins in >100-mg quantities also have been demonstrated.³⁷ A next objective is to combine these various features to achieve a palette of water-soluble, bioconjugatable, NIR wavelength-tunable bacteriochlorins for photochemical studies in the 700–900 nm region. Examination of successive bioconjugations with a palette of chromophores including bacteriochlorins identical or similar to those prepared herein is an integral goal, including use of such bacteriochlorins in successive bioconjugations according to the 4 x 4 matrix shown in Table 2.2. Such a palette of NIR-active chromophores may prove valuable for applications in energy sciences and life sciences.

Experimental section

(I) General methods

^1H NMR (300 MHz) spectra, ^{13}C NMR spectra (100 MHz), and ^{31}P NMR (121 MHz) were collected at room temperature in CDCl_3 (with tetramethylsilane as internal reference) unless noted otherwise. Absorption spectra were collected in CH_2Cl_2 at room temperature. Bacteriochlorins were analyzed by matrix-assisted laser desorption mass spectrometry (MALDI-MS) in the presence of the matrix 1,4-bis(5-phenyl-2-oxazolyl)benzene (POPOP).⁹² Silica gel (40 μm average particle size) was used for column chromatography. All solvents were reagent grade and were used as received unless noted otherwise. THF was freshly distilled from sodium/benzophenone ketyl. Sonication of suspensions was carried out in a benchtop sonication bath. Compounds **2**,⁷⁶ **4**,⁷⁹ **5**,⁷⁹ **7**,⁸² **BC1**,³⁸ **BC2**,³⁸ **BC3**,⁴⁴ **BC14**,⁴⁵ **BC15**,⁴⁵ **ZnBC15**,⁴⁵ **BC16**,⁴⁵ **BC17**,⁴⁵ and **BC18**³⁷ were synthesized according to the literature.

(II) Syntheses

***N*-[4-(1,3-Dithiolan-2-yl)phenyl]succinamic acid (3)**. A solution of **2** (444 mg, 2.30 mmol) and succinic anhydride (225 mg, 2.30 mmol) in CH_2Cl_2 (11.0 mL) was treated with triethylamine (470 μL , 3.50 mmol, 1.50 equiv) and stirred for 16 h at room temperature. 2 N HCl solution was added to the reaction mixture. The resulting precipitate was extracted twice with CH_2Cl_2 . The organic extract was dried (Na_2SO_4) and concentrated to afford a yellowish solid (435 mg, 65%): mp 175–177 $^\circ\text{C}$; ^1H NMR (300 MHz, $\text{DMSO}-d_6$) δ 2.47–2.52 (m, 4H), 3.27–3.58 (m, 2H), 3.44–3.52 (m, 2H), 5.67 (s, 1H), 7.40 (d, $J = 9.0$ Hz, 2H), 7.50 (d, $J = 9.0$ Hz, 2H); ^{13}C NMR (75 MHz, $\text{DMSO}-d_6$) δ 29.4, 31.7, 55.5, 119.4, 128.9,

135.5, 139.6, 170.8, 174.5; ESI-MS obsd 298.0563, calcd 298.0521 [(M + H)⁺, M = C₁₃H₁₅NO₃S₂].

15-{3-[4-((4-Formylphenyl)amino)-4-oxobutanamido]phenyl}-3,13-bis(ethoxycarbonyl)-2,12-dimesityl-5-methoxy-8,8,18,18-tetramethylbacteriochlorin (BC6). Following a standard procedure,⁷⁶ a mixture of HgO (1.5 mg, 6.9 μmol) and BF₃·Et₂O (1.0 μL, 6.9 μmol) in THF and water (0.2 mL, 1:1) was stirred at room temperature for 5 min, followed by addition of **BC13** (1.5 mg, 1.3 μmol). The slurry was stirred at room temperature for 30 min. The reaction mixture was diluted with CH₂Cl₂ and washed with saturated aqueous NaHCO₃. The organic layer was dried (Na₂SO₄), concentrated and chromatographed [silica, CH₂Cl₂/ethyl acetate (9:1)]. The resulting solid was treated with hexanes, sonicated, and centrifuged. The supernatant was discarded to afford a reddish solid (1.0 mg, 71%): ¹H NMR (300 MHz, CDCl₃) δ -0.86 (s, 1H), -0.52 (s, 1H), 1.06 (t, *J* = 7.2 Hz, 3H), 1.19 (t, *J* = 7.2 Hz, 3H), 1.78 (d, *J* = 5.1 Hz, 6H), 1.82 (s, 6H), 1.94 (d, *J* = 5.1 Hz, 6H), 2.09 (d, *J* = 3.3 Hz, 6H), 2.21 (s, 3H), 2.49 (s, 3H), 2.87 (m, 4H), 3.65 (s, 3H), 3.68 (s, 2H), 4.24 (d, *J* = 2.4 Hz, 2H), 4.32 (q, *J* = 7.2 Hz, 2H), 4.42 (q, *J* = 7.2 Hz, 2H), 6.56 (s, 1H), 6.64 (s, 1H), 7.08–7.15 (m, 4H), 7.34 (s, 1H), 7.39 (s, 1H), 7.47 (d, *J* = 7.2 Hz, 1H), 7.70 (d, *J* = 8.4 Hz, 2H), 7.79 (d, *J* = 8.4 Hz, 2H), 8.58 (br, 1H), 9.61 (s, 1H), 9.63 (s, 1H), 9.87 (s, 1H); ESI-MS obsd 1075.5322, calcd 1075.5328 [(M + H)⁺, M = C₆₆H₇₀N₆O₈]; MALDI-MS obsd 1074.9; λ_{abs} (CH₂Cl₂) 364, 542, 757 nm.

15²-N-[4-(2-(Maleimido)ethylamino)-4-oxobutyl]-3-ethoxycarbonyl-2,12-diethyl-8,8,18,18-tetramethylbacteriochlorin-13,15-dicarboximide (BC7). Following a reported procedure,⁷⁷ a mixture of **BC14** (6.6 mg, 10 μmol), *N*-(2-aminoethyl)maleimide

hydrochloride (3.5 mg, 20 μmol), *N*-hydroxysuccinimide (2.3 mg, 20 μmol) and triethylamine (3.0 mL, 20 μmol) in THF (0.40 mL) was stirred for 5 min, followed by addition of DCC (4.1 mg, 20 μmol) in THF (0.10 mL). The reaction was stirred at room temperature for 16 h. The resulting mixture was filtered to remove insoluble material. The filtrate was washed with 1 N HCl and extracted with CH_2Cl_2 . The organic extract was dried (MgSO_4), concentrated, and chromatographed [silica, CH_2Cl_2 /ethyl acetate (3:2)] to afford a reddish solid (4.3 mg, 55%): ^1H NMR (300 MHz, CDCl_3) δ -0.63 (s, 1H), -0.41 (s, 1H), 1.67–1.76 (m, 12H), 1.92 (s, 9H), 2.22–2.32 (m, 2H), 2.44 (t, J = 6.9 Hz, 2H), 3.58–3.64 (m, 2H), 3.79–3.83 (m, 4H), 4.04–4.22 (m, 4H), 4.32 (s, 2H), 4.69 (s, 2H), 4.77 (q, J = 3.9 Hz, 2H), 6.72 (s, 2H), 7.05 (t, J = 5.7 Hz, 1H), 8.56 (s, 1H), 8.68 (s, 1H), 9.54 (s, 1H); ESI-MS obsd 775.3677, calcd 775.3688 (M^+ , $\text{M} = \text{C}_{43}\text{H}_{49}\text{N}_7\text{O}_7$); MALDI-MS obsd 774.8; λ_{abs} (CH_2Cl_2) 358, 409, 545, 820 nm.

***P*-Borane 15-[3-(2-(diphenylphosphino)phenoxy)-3-oxobutanamido]phenyl]-3,13-bis(ethoxycarbonyl)-2,12-diethyl-8,8,18,18-tetramethylbacteriochlorin (BC8).** A mixture of **BC15** (3.7 mg, 4.7 μmol), DCC (1.2 mg, 5.8 μmol) and DMAP (0.1 mg, 0.82 μmol) in CH_2Cl_2 (0.10 mL) was treated with **4** (1.6 mg, 5.5 μmol) in CH_2Cl_2 (50 μL) and stirred under argon at room temperature for 1.2 h. The resulting mixture was filtered to remove insoluble material. The filtrate was concentrated and chromatographed [silica, CH_2Cl_2 /ethyl acetate (9:1)] to yield a greenish solid (2.0 mg, 40%): ^1H NMR (300 MHz, CDCl_3) δ -1.84 (s, 1H), -1.53 (s, 1H), 1.21–1.26 (m, 6H), 1.61–1.78 (m, 9H), 1.81 (s, 3H), 1.83 (s, 3H), 1.94 (s, 6H), 2.42–2.48 (m, 4H), 3.74–3.94 (m, 8H), 4.25 (s, 3H), 4.36 (s, 2H),

4.78 (q, $J = 7.2$ Hz, 2H), 7.15–7.32 (m, 3H), 7.41–7.67 (m, 15H), 8.05–8.06 (br, 1H), 8.56 (s, 1H), 8.60 (s, 1H); ^{31}P NMR (CDCl_3) 19.3; ESI-MS obsd 1066.5067, calcd 1066.5060 [(M + H) $^+$, M = $\text{C}_{63}\text{H}_{69}\text{BN}_5\text{O}_8\text{P}$]; MALDI-MS obsd 1051.7 (M – BH_3); IR (solid film) 3355, 2962, 2929, 2251, 1720, 1608, 1437 cm^{-1} ; λ_{abs} (CH_2Cl_2) 356, 376, 515, 730 nm.

***P*-Borane Zn(II)-15-[3-(2-(diphenylphosphino)phenoxy)-3-oxobutanamido]phenyl]-3,13-bis(ethoxycarbonyl)-2,12-diethyl-8,8,18,18-tetramethylbacteriochlorin (ZnBC15).** A mixture of **ZnBC15** (7.5 mg, 8.8 μmol), DCC (2.2 mg, 10.5 μmol) and DMAP (0.1 mg, 0.82 μmol) in CH_2Cl_2 (800 μL) was treated with **4** (3.1 mg, 10.5 μmol) in CH_2Cl_2 (50 μL) and stirred under argon at room temperature for 1.5 h. The resulting mixture was filtered to remove insoluble material. The filtrate was concentrated and chromatographed [silica, CH_2Cl_2 /ethyl acetate (7:1)] to yield a reddish solid (5.6 mg, 56%): ^1H NMR (300 MHz, $\text{THF-}d_8$) δ 1.00–1.35 (m, 6H), 1.51–1.69 (m, 9H), 1.82 (s, 3H), 1.83 (s, 3H), 1.95 (s, 6H), 2.49 (s, 4H) 3.64–3.82 (m, 8H), 3.96 (s, 2H), 4.14 (s, 3H), 4.38 (s, 2H), 4.61 (q, $J = 6.9$ Hz, 2H), 4.83 (d, $J = 7.8$ Hz, 2H), 7.21–7.70 (m, 13H), 8.12–8.14 (m, 1H), 8.46 (s, 1H), 8.51 (s, 1H), 9.20 (s, 1H); ^{31}P NMR ($\text{THF-}d_6$) 19.5; ESI-MS obsd 1128.4099, calcd 1128.4190 [(M + H) $^+$, M = $\text{C}_{63}\text{H}_{67}\text{BN}_5\text{O}_8\text{PZn}$]; MALDI-MS obsd 1129.5; λ_{abs} (CH_2Cl_2) 355, 385, 553, 739 nm.

***P*-Borane 15-{4-[3-(((diphenylphosphanyl)methyl)thio)-3-oxopropyl]phenyl}-3,13-bis(ethoxycarbonyl)-2,12-diethyl-8,8,18,18-tetramethylbacteriochlorin (BC9).** A mixture of **BC16** (6.2 mg, 8.3 μmol), DCC (5.2 mg, 25 μmol) and DMAP (0.2 mg, 1.6 μmol) in CH_2Cl_2 (0.60 mL) was treated with *P*-borane (diphenylphosphino)methylthiol (**5**, 8.9 mg,

36 μmol) and stirred under argon at room temperature for 1.5 h. The resulting mixture was filtered to remove insoluble material. The filtrate was concentrated and chromatographed [silica, CH_2Cl_2 /ethyl acetate (49:1)] to yield a greenish solid (6.2 mg, 76%): ^1H NMR (300 MHz, CDCl_3) δ -1.85 (brs, 1H), -1.54 (brs, 1H), 0.8–1.2 (m, 3H), 1.26 (t, $J = 7.6$ Hz, 3H), 1.61–1.67 (m, 6H), 1.75 (t, $J = 7.6$ Hz, 3H), 1.81 (s, 6H), 1.93 (s, 6H), 2.99–3.10 (m, 4H), 3.76–3.85 (m, 10H), 4.25 (s, 3H), 4.36 (s, 2H), 4.77 (q, $J = 7.6$ Hz, 2H), 7.34 (d, $J = 7.6$ Hz, 2H), 7.49–7.56 (m, 6H), 7.58 (d, $J = 7.6$ Hz, 2H), 7.75–7.80 (m, 4H), 8.55 (s, 1H), 8.59 (s, 1H); ^{31}P NMR ($\text{THF-}d_8$) 19.5; ESI-MS obsd 976.4615, calcd 976.4643 [(M + H) $^+$, M = $\text{C}_{57}\text{H}_{66}\text{BN}_4\text{O}_6\text{PS}$]; MALDI-MS obsd 962.9 (M – BH_3); λ_{abs} (CH_2Cl_2) 356, 365, 376, 515, 729 nm.

***P*-Borane 15-{4-[2-(((diphenylphosphanyl)methyl)thio)-2-oxoethoxy]phenyl}-3,13-bis(ethoxycarbonyl)-2,12-diethyl-8,8,18,18-tetramethylbacteriochlorin (BC10).** A mixture of **BC17** (9.2 mg, 12 μmol), DCC (7.6 mg, 37 μmol) and DMAP (0.30 mg, 2.5 μmol) in CH_2Cl_2 (0.8 mL) was treated with **5** (11 mg, 45 μmol) and stirred under argon at room temperature for 1.5 h. The resulting mixture was filtered to remove insoluble material. The filtrate was concentrated and chromatographed [silica, CH_2Cl_2 /ethyl acetate (49:1)] to yield a greenish solid (5.0 mg, 42%): ^1H NMR (300 MHz, CDCl_3) δ -1.85 (brs, 1H), -1.55 (brs, 1H), 0.8–1.2 (m, 3H), 1.26 (t, $J = 7.6$ Hz, 3H), 1.62–1.68 (m, 6H), 1.75 (t, $J = 7.6$ Hz, 3H), 1.82 (s, 6H), 1.93 (s, 6H), 3.75 (t, $J = 7.6$ Hz, 2H), 3.81–3.93 (m, 8H), 4.25 (s, 3H), 4.36 (s, 2H), 4.75–4.81 (m, 4H), 7.04 (d, $J = 9.2$ Hz, 2H), 7.49–7.56 (m, 6H), 7.68 (d, $J = 9.2$ Hz, 2H), 7.75–7.80 (m, 4H), 8.56 (s, 1H), 8.60 (s, 1H); ^{31}P NMR ($\text{THF-}d_8$) 20.1; ESI-MS obsd

1000.4261, calcd 1000.4255 [(M + Na)⁺, M = C₅₆H₆₄BN₄O₇PS]; MALDI-MS obsd 965.5 (M – BH₃); λ_{abs} (CH₂Cl₂) 357, 365, 376, 515, 729 nm.

15²-[12-(3-Azidopropionamido)dodecyl]-3-ethoxycarbonyl-2,12-diethyl-5-methoxy-8,8,18,18-tetramethylbacteriochlorin-13,15-dicarboximide (BC11). A mixture of **BC19** (2.4 mg, 3.1 μmol), 3-azidopropionic acid (**7**, 3.6 mg, 31 μmol, 10 equiv) and DCC (6.3 mg, 31 μmol, 9.9 equiv) in CH₂Cl₂ (0.10 mL) was stirred at room temperature for 16 h. The reaction mixture was filtered to remove insoluble material. The filtrate was concentrated and chromatographed [silica, CH₂Cl₂/ethyl acetate (19:1)]. The resulting purple solid was treated with hexanes (3.0 mL) and sonicated to give a clear solution. The solvent was partially removed by purging with argon. The resulting solid was isolated by filtration and dried to obtain a purple solid (2.4 mg, 87%): ¹H NMR (300 MHz, CDCl₃) δ –0.95 (s, 1H), –0.48 (s, 1H), 1.24–1.78 (m, 29H), 1.89 (s, 6H), 1.91 (s, 6H), 2.39 (t, *J* = 6.6 Hz, 2H), 3.26 (q, *J* = 6.6 Hz, 2H), 3.62 (t, *J* = 6.6 Hz, 2H), 3.74 (q, *J* = 7.8 Hz, 2H), 4.17–4.26 (m, 7H), 4.43 (t, *J* = 7.8 Hz, 2H), 4.71 (s, 2H), 4.76 (q, *J* = 7.8 Hz, 2H), 5.59 (s, 1H), 8.41 (s, 1H), 8.68 (s, 1H); ESI-MS obsd 878.5254, calcd 878.5287 [(M + H)⁺, M = C₄₉H₆₇N₉O₆]; IR (solid film) 3321, 2925, 2852, 2098, 1681, 1537 cm^{–1}; λ_{abs} (CH₂Cl₂) 350, 370, 408, 550, 794 nm.

Zn(II)-15²-[12-(3-Azidopropionamido)dodecyl]-3-ethoxycarbonyl-2,12-diethyl-5-methoxy-8,8,18,18-tetramethylbacteriochlorin-13,15-dicarboximide (ZnBC11). A mixture of free base bacteriochlorin **BC11** (2.4 mg, 2.7 μmol), Zn(OAc)₂·2H₂O (18 mg, 82 μmol, 31 equiv) and Cs₂CO₃ (27 mg, 82 μmol, 31 equiv) in CH₂Cl₂ and methanol (0.4 mL, 1:1) was stirred for 4 h in an oil bath at 50 °C. The solvent was then removed by evaporation, and the resulting solid was washed with water. The mixture was extracted with CH₂Cl₂. The

combined CH₂Cl₂ extract was dried (Na₂SO₄), concentrated and chromatographed [silica, CH₂Cl₂/ethyl acetate (5:1)]. The resulting solid was treated with hexanes, sonicated, and centrifuged. The supernatant was discarded leaving a green solid (1.5 mg, 60%): ¹H NMR (300 MHz, CDCl₃) δ 1.29–1.69 (m, 29H), 1.88 (s, 6H), 1.91 (s, 6H), 2.30 (t, *J* = 6.3 Hz, 2H), 3.14 (q, *J* = 6.3 Hz, 2H), 3.48 (t, *J* = 6.3 Hz, 2H), 3.62 (q, *J* = 7.8 Hz, 2H), 4.07–4.14 (m, 5H), 4.26 (s, 2H), 4.34 (t, *J* = 7.8 Hz, 2H), 4.60 (q, *J* = 7.8 Hz, 2H), 4.71 (s, 2H), 7.05 (s, 1H), 8.32 (s, 1H), 8.59 (s, 1H); ESI-MS obsd 940.4399, calcd 940.4422 [(M + H)⁺, M = C₄₉H₆₅N₉O₆]; IR (solid film) 3327, 2923, 2850, 2098, 1668, 1548, 1037 cm⁻¹; λ_{abs} (CH₂Cl₂) 353, 370, 416, 576, 806 nm.

15-[3-(3-Azidopropionamido)phenyl]-5-methoxy-8,8,18,18-

tetramethylbacteriochlorin (BC12). A mixture of **BC1** (6.0 mg, 12 μmol), 3-azidopropionic acid (**7**, 7.0 mg, 61 μmol) and DCC (13 mg, 61 μmol) in CH₂Cl₂ (0.61 mL) was stirred for 16 h. The mixture was filtered to remove insoluble material. The filtrate was concentrated and chromatographed [silica, CH₂Cl₂/ethyl acetate (9:1)] to afford a reddish solid (4.5 mg, 62%): ¹H NMR (300 MHz, CDCl₃) δ -2.22 (s, 1H), -1.97 (s, 1H), 1.87 (d, *J* = 6.3 Hz, 6H), 1.97 (d, *J* = 6.3 Hz, 6H), 2.62 (t, *J* = 4.8 Hz, 2H), 3.73 (t, *J* = 4.8 Hz, 2H), 4.04 (s, 2H), 4.42 (s, 2H), 4.50 (s, 3H), 7.50 (s, 1H), 7.60–7.66 (m, 2H), 7.81 (s, 1H), 7.98–8.01 (m, 1H), 8.17–8.18 (m, 1H), 8.62–8.64 (m, 1H), 8.68–8.71 (m, 3H), 8.94–8.95 (m, 1H); ¹³C NMR (100 MHz, CDCl₃) δ 31.30, 31.46, 37.2, 45.5, 46.0, 47.5, 47.7, 51.9, 65.5, 97.2, 97.7, 112.6, 117.8, 119.3, 121.2, 122.5, 123.1, 123.8, 128.86, 128.93, 131.7, 135.2, 135.8, 136.4,

137.2, 143.9, 153.7, 158.7, 168.5, 168.8, 169.2; ESI-MS obsd 588.2951, calcd 588.2956 (M^+ , $M = C_{34}H_{36}N_8O_2$); MALDI-MS obsd 589.3; λ_{abs} (CH_2Cl_2) 348, 368, 507, 713 nm.

15-{3-[4-(4-(1,3-Dithiolan-2-yl)phenylamino)-4-oxobutanamido]phenyl}-3,13-bis(ethoxycarbonyl)-2,12-dimesityl-5-methoxy-8,8,18,18-tetramethylbacteriochlorin (BC13). A mixture of **3** (2.6 mg, 8.6 μmol) and DCC (1.8 mg, 8.6 μmol) in CH_2Cl_2 (0.20 mL) was treated with **BC3** (1.5 mg, 1.7 μmol) and stirred for 16 h. The resulting mixture was filtered to remove insoluble material. The filtrate was concentrated and chromatographed [silica, CH_2Cl_2 /ethyl acetate (9:1)]. The resulting solid was treated with hexanes, sonicated, and centrifuged. The supernatant was discarded leaving a reddish solid (1.6 mg, 81%): $^1\text{H NMR}$ (300 MHz, CDCl_3) δ -0.84 (s, 1H), -0.51 (s, 1H), 1.06 (t, $J = 6.9$ Hz, 3H), 1.20 (t, $J = 6.9$ Hz, 3H), 1.79 (s, 6H), 1.82 (d, $J = 3.9$ Hz, 6H), 1.94 (d, $J = 2.7$ Hz, 6H), 2.09 (s, 6H), 2.21 (s, 3H), 2.49 (s, 3H), 2.83 (m, 4H), 3.26–3.34 (m, 2H), 3.57–3.47 (m, 2H), 3.64 (s, 3H), 3.68 (s, 2H), 4.24 (d, $J = 2.7$ Hz, 2H), 4.32 (q, $J = 6.9$ Hz, 2H), 4.42 (q, $J = 6.9$ Hz, 2H), 5.58 (s, 1H), 6.54 (s, 1H), 6.65 (s, 1H), 7.04–7.12 (m, 4H), 7.37–7.50 (m, 6H), 7.64 (s, 1H), 7.93 (s, 1H), 9.60 (s, 1H), 9.63 (s, 1H); ESI-MS obsd 1151.5130, calcd 1151.5133 [$(M + H)^+$, $M = C_{68}H_{74}N_6O_7S_2$]; MALDI-MS obsd 1151.0; λ_{abs} (CH_2Cl_2) 364, 542, 756 nm.

15²-N-(12-Aminododecyl)-3-ethoxycarbonyl-2,12-diethyl-5-methoxy-8,8,18,18-tetramethylbacteriochlorin-13,15-dicarboximide (BC19). Following a reported carbamoylation procedure to install the imide ring,⁶¹ a mixture of bromo-bacteriochlorin **BC18** (57 mg, 0.084 mmol), $\text{Pd}(\text{PPh}_3)_4$ (97 mg, 0.084 mmol), Cs_2CO_3 (85 mg, 0.26 mmol, 3.0 equiv) and 1,12-dodecandiamine (76 mg, 0.38 mmol, 4.5 equiv) was dried under high vacuum in a Schlenk flask for 1 h. The flask was then filled with CO and THF (11 mL),

which had been degassed by argon for 25 min and flushed with CO for 25 min. The reaction mixture was stirred at 80 °C for 18 h under a CO atmosphere at ambient pressure. The reaction mixture was cooled to room temperature and washed with water. The organic layer was dried (Na₂SO₄), concentrated and chromatographed [silica, CH₂Cl₂/methanol (4:1)]. The resulting solid was treated with hexanes, sonicated, and centrifuged. The supernatant was discarded leaving a reddish solid (23 mg, 35%): ¹H NMR (300 MHz, CDCl₃) δ -0.96 (s, 1H), -0.48 (s, 1H), 1.20–1.78 (m, 29H), 1.89 (s, 6H), 1.91 (s, 6H), 2.68 (t, *J* = 4.5 Hz, 2H), 3.73 (t, *J* = 7.8 Hz, 2H), 4.16–4.28 (m, 7H), 4.43 (t, *J* = 7.8 Hz, 2H), 4.76 (s, 2H), 4.76 (q, *J* = 7.8 Hz, 2H), 5.38 (s, 2H), 8.41 (s, 1H), 8.68 (s, 1H); ESI-MS obsd 781.5011, calcd 781.5006 [(M + H)⁺, M = C₄₆H₆₄N₆O₅]; MALDI-MS obsd 780.3; IR (solid film) 3386, 2927, 1729, 1682, 1645, 1537 cm⁻¹; λ_{abs} (CH₂Cl₂) 351, 370, 407, 550, 794 nm.

Zn(II)-15²-N-(12-Azidododecyl)-3-ethoxycarbonyl-2,12-diethyl-5-methoxy-8,8,18,18-tetramethylbacteriochlorin-13,15-dicarboximide (ZnBC19). A mixture of free base bacteriochlorin **BC19** (10 mg, 13 μmol), Zn(OAc)₂·2H₂O (84 mg, 0.38 mmol, 30 equiv) and K₂CO₃ (53 mg, 0.38 mmol, 30 equiv) in CH₂Cl₂ and methanol (1.4 mL, 1:1) was stirred for 4 h in an oil bath at 50 °C. The reaction mixture was washed with water. The organic layer was dried (Na₂SO₄), concentrated and chromatographed [silica, CH₂Cl₂/methanol (19:1)] to afford a green solid (6.0 mg, 55%): ¹H NMR (300 MHz, THF-*d*₈) δ 1.30–1.70 (m, 31H), 1.89 (s, 6H), 1.91 (s, 6H), 3.57–3.67 (m, 4H), 4.08–4.16 (m, 5H), 4.26 (s, 2H), 4.37 (t, *J* = 7.2 Hz, 2H), 4.61 (q, *J* = 7.2 Hz, 2H), 4.72 (s, 2H), 8.31 (s, 1H), 8.60 (s, 1H); ESI-MS obsd 843.4124, calcd 843.4146 [(M + H)⁺, M = C₄₆H₆₂N₆O₅Zn]; MALDI-MS obsd 842.6; λ_{abs} (CH₂Cl₂) 356, 374, 415, 585, 807 nm.

Cu(II)-15²-N-(12-Azidododecyl)-3-ethoxycarbonyl-2,12-diethyl-5-methoxy-8,8,18,18-tetramethylbacteriochlorin-13,15-dicarboximide (CuBC20). Following a reported procedure azide formation,⁸¹ a mixture of **BC19** (23 mg, 30 μ mol), K₂CO₃ (0.11 g, 0.77 mmol, 26 equiv), CuSO₄·5H₂O (6.0 mg, 24 μ mol, 0.80 equiv) and imidazole-1-sulfonyl azide hydrochloride (**6**, 6.2 mg, 30 μ mol, 1.0 equiv) in CH₂Cl₂ and methanol (2.0 mL, 1:1) was stirred under argon at room temperature for 16 h. The mixture was dried under vacuum and washed with water. The organic layer was dried (Na₂SO₄), concentrated and chromatographed (silica, CH₂Cl₂) to afford a dark reddish solid (8.2 mg, 32%): ESI-MS obsd 867.3961, calcd 867.3977 [(M + H)⁺, M = C₄₆H₆₀CuN₈O₅]; IR (solid film) 3387, 2925, 2852, 2094, 1725, 1678, 1599, 1384, 1041 cm⁻¹; λ_{abs} (CH₂Cl₂) 363, 419, 555, 815 nm.

Peptides. The peptides **pep-GXWF** and **pep-GOWF** were synthesized on a fully automated Syro Wave peptide synthesizer (Biotage) via standard *solid-phase peptide synthesis* method using Fmoc-Phe-Wang resin (0.802 mmol/g). Amino acids were Fmoc protected: Fmoc-L-Trp(Boc)-OH (one letter code, W), Fmoc-Gly-OH (one letter code, G), Fmoc-L-Dap(Boc-Aoa)-OH (one letter code, O), Fmoc-L-propargyl-Gly-OH (one letter code, X). Preloaded Wang-Phe resin (200 mg, 160.4 μ mol; one letter code, F) was used as the solid phase. Fmoc deprotection was performed in two stages using solutions: (1) 40% piperidine in DMF for 3 min and (2) 20% piperidine in DMF for 10 min. The coupling reaction was performed using Fmoc-protected amino acids (5 equiv, 0.5 M in DMF) activated by *N,N,N',N'*-tetramethyl-*O*-(1*H*-benzotriazol-1-yl)uronium hexafluorophosphate [HBTU, 5 equiv, 1.0 M in DMF/NMP (1:1)] and *N,N*-diisopropylethylamine (10 equiv). After completing the synthesis of the peptide, the resin was successively washed with DMF

(2 mL, three times) and CH₂Cl₂ (2 mL, three times), and then dried thoroughly overnight under high vacuum. Peptide release was performed using a cocktail of TFA/*m*-cresol/H₂O/triisopropylsilane (93: 2.5: 2.5: 2) for 2 h at room temperature. After filtration to remove resin, the filtrate was treated with cold diethyl ether to precipitate the crude product. The peptide was then dissolved in the same cocktail and then precipitated by addition of diethyl ether. This procedure (cocktail dissolution – precipitation cycle) was repeated three times to afford the final peptide (no further purification, no amounts recorded). Data for **pep-GXWF**: ESI-MS obsd 726.2919, calcd 726.2922 [(M + H)⁺, M = C₄₂H₃₉N₅O₇]; MALDI-MS obsd 748.5 (M + Na⁺). Data for **pep-GOWF**: ESI-MS obsd 790.3188, calcd 790.3195 [(M + H)⁺, M = C₄₂H₄₃N₇O₉].

(III) Protocols

Procedure for copper insertion with Cu(II). A stock solution (10 mM) of bacteriochlorin was prepared by dissolving **BC1** (4.3 mg, 8.7 μmol) of in DMSO (0.87 mL) or **BC2** (5.5 mg, 7.9 μmol) in DMSO (0.79 mL). A stock solution of Cu(OAc)₂ (50 mM) was prepared by dissolving Cu(OAc)₂ (18.7 mg, 0.10 mmol) of in a mixed solvent of DMSO (1.0 mL) and deionized water (1.0 mL). For a reaction with bacteriochlorin at 5.0 mM and 5.0 equiv of copper, the copper solution (0.50 mL) was transferred to the bacteriochlorin solution (0.50 mL) to give a mixed solvent of DMSO (0.75 mL) and water (0.25 mL). For a reaction with bacteriochlorin at 0.20 mM and 5.0 equiv of copper, the copper stock solution (20 μL) was diluted by addition to a mixed solvent of DMSO (0.24 mL) and water (0.24 mL). The bacteriochlorin stock solution (20 μL) also was diluted by addition of DMSO (0.48 mL). The diluted copper solution (0.50 mL) was then transferred to the diluted bacteriochlorin

solution (0.50 mL) to give a mixed solvent of DMSO (0.75 mL) and water (0.25 mL). These reaction mixtures were stirred in the dark at room temperature.

Procedure for copper insertion with Cu(I). The experiments for copper insertion in the presence of Cu(I) were conducted using bacteriochlorin (1.9 – 3.0 mg, 2.7 – 4.3 μmol , 0.10 – 3.0 mM), $\text{CuSO}_4 \cdot 5\text{H}_2\text{O}$ (5 equiv), sodium ascorbate (10 equiv) and TBTA (5 equiv) in a mixed solvent of DMSO and deionized water (1:1). The experimental procedures for these four model studies (0.10, 0.25, 0.90 and 3.0 mM) are almost identical. An exemplary procedure for bacteriochlorin at 0.1 mM is as follows: The catalyst Cu(I) was generated by reacting $\text{CuSO}_4 \cdot 5\text{H}_2\text{O}$ (5.3 mg, 21 μmol , 5.0 equiv relative to the bacteriochlorin) with sodium ascorbate (8.6 mg, 0.43 μmol , 10 equiv relative to the bacteriochlorin) in water (21 mL) at room temperature. The catalyst solution was added to a solution of TBTA (11 mg, 21 μmol , 5.0 equiv relative to the bacteriochlorin) in DMSO (10 mL) under an atmosphere of argon, and the combined Cu(I)-TBTA solution (31 mL) was then transferred to the bacteriochlorin (3.0 mg, 4.3 μmol) solution in DMSO (11 mL). The resultant mixture was stirred in the dark at room temperature for 16 h, and analyzed MALDI-MS.

(IV) Bioconjugation reactions

15-{3-[4-((4-((Carboxymethoxyimino)methyl)phenyl)amino)-4-oxobutanamido]phenyl}-3,13-bis(ethoxycarbonyl)-2,12-dimesityl-5-methoxy-8,8,18,18-tetramethylbacteriochlorin (BC6-oxime). A solution of **BC6** (2.6 mg, 2.4 μmol) and *o*-(carboxymethyl)hydroxylamine hemihydrochloride (1.3 mg, 12 μmol , 5.0 equiv relative to bacteriochlorin) in a mixed solvent of aqueous phosphate buffer (0.39 mL, 0.3 M, pH = 7.0)

and acetonitrile (0.39 mL, 1:1) at room temperature was treated with excess aniline (0.21 mmol, 1000 equiv relative to bacteriochlorin) to activate the aldehyde group. TLC analysis [silica, ethyl acetate, R_f (**BC6**) = 0.8, R_f (**BC6-oxime**) = 0] showed the reaction to be complete within 3.0 h. Purification by column chromatography (silica, ethyl acetate) followed by MALDI-MS and ESI-MS confirmed the identity of the product **BC6-oxime** (no amount recorded). Absorption values indicated that the chromophore remained intact: ESI-MS obsd 1148.5491, calcd 1148.5492 [(M + H)⁺, M = C₆₈H₇₃N₇O₁₀]; MALDI-MS 1146.0; λ_{abs} (CH₂Cl₂) 364, 543, 757 nm.

15-{4-[4-(3-(Benzylamino)-3-oxopropyl)phenyl]-3,13-bis(ethoxycarbonyl)-2,12-diethyl-8,8,18,18-tetramethylbacteriochlorin (BC9-amide) and 15-{4-[2-(Benzylamino)-2-oxoethoxy]phenyl}-3,13-bis(ethoxycarbonyl)-2,12-diethyl-8,8,18,18-tetramethylbacteriochlorin (BC10-amide). Bacteriochlorin **BC9** or **BC10** (2.2–2.5 mg) in DMF (4.0 mM) was treated with DABCO (4.0 equiv) at 45 °C and stirred under argon for 5 min. Benzyl azide (4 equiv) was added, and the resulting mixture was stirred in the dark for 5.5 h. DMF was removed in vacuo. The resulting greenish crude solid was dissolved in ethyl acetate and washed with water. The organic layer was separated, dried (Na₂SO₄) and concentrated. Column chromatography [silica, CH₂Cl₂/ethyl acetate (17:3)] provided a greenish solid (1.1 mg, 61% for **BC9-amide**; 0.9 mg, 42% for **BC10-amide**).

Zn(II)-15²-[12-(3-(4-((Dimethylamino)methyl)-1*H*-1,2,3-triazol-1-yl)propanamido)dodecyl]-3-ethoxycarbonyl-2,12-diethyl-5-methoxy-8,8,18,18-tetramethylbacteriochlorin-13,15-dicarboximide (ZnBC11-triazole). The catalyst Cu(I) was generated by reacting CuSO₄·5H₂O (1.8 mg, 7.0 μmol, 5.0 equiv relative to the

bacteriochlorin) with the reducing agent sodium ascorbate (2.9 mg, 14 μmol , 10 equiv relative to the bacteriochlorin) in water (0.35 mL) at room temperature. The catalyst solution was added to a solution of **ZnBC11** (1.4 mg, 1.4 μmol) and 3-dimethylamino-1-propyne (0.60 mg, 7.0 μmol) in DMSO (0.35 mL) at room temperature. TLC analysis [silica, CH_2Cl_2 /ethyl acetate (4:1), R_f (**ZnBC11**) = 0.4, R_f (**ZnBC11-triazole**) = 0] showed the reaction to be complete within 5 h. Purification by column chromatography (silica, methanol) followed by MALDI-MS and ESI-MS confirmed the identity of the product **ZnBC11-triazole** (no amount recorded). The absorption spectrum confirmed the integrity of the chromophore containing zinc and lack of displacement by copper during the reaction (copper bacteriochlorins typically give a broader Q_y band that is shifted to longer wavelength by ~ 20 nm⁶⁶): ESI-MS obsd 1023.5144, calcd 1023.5163 [(M + H)⁺, M = C₅₄H₇₄N₁₀O₆Zn]; MALDI-MS obsd 1022.3; λ_{abs} (CH_2Cl_2) 356, 373, 417, 581, 806 nm.

ZnBC11-GXWF. Peptide **pep-GXWF** (1.2 mg, 1.6 μmol) and **ZnBC11** (1.5 mg, 1.6 μmol) were placed in a small reaction vial, whereupon 0.30 mL of DMSO was added under argon. A solution of Cu(I) was freshly prepared in advance by mixing $\text{CuSO}_4 \cdot 5\text{H}_2\text{O}$ (2.0 mg, 5.0 equiv) in 0.20 mL of deionized water and sodium ascorbate (3.2 mg, 10 equiv) in 0.20 mL of deionized water under argon. This solution quickly turned dark and further changed to a bright yellow color within a few seconds. TBTA (4.2 mg, 5.0 equiv) in 0.10 mL of DMSO was also prepared and added to the fresh Cu(I) solution, and the resulting solution was quickly transferred in entirety to the peptide/bacteriochlorin solution under argon. The reaction vial was quickly capped and stirred at room temperature for 5.5 h. The solvent was removed overnight with a lyophilizer. Then 1 mL of deionized water was added

to the crude product followed by sonication for 5 min. The suspension was then centrifuged, and the resulting supernatant was decanted. This procedure was repeated three times (performed four times in total) to thoroughly remove copper and sodium salts. Then, 1 mL of diethyl ether was added to the crude product followed by sonication. The suspension was then centrifuged and the resulting supernatant was decanted. This procedure was repeated three times (performed four times in total) to thoroughly remove residual **ZnBC11**. The bacteriochlorin-peptide conjugate was dried under high vacuum: ESI-MS obsd 1664.7174, calcd 1664.7193 [(M + H)⁺, M = C₉₁H₁₀₄N₁₄O₁₃Zn]; MALDI-MS 1664.8; λ_{abs} (CH₂Cl₂) 354, 372, 417, 580, 811 nm.

BC6-GOWF. Peptide **pep-GOWF** (2.1 mg, 2.6 μmol) and **BC6** (1.4 mg, 1.3 μmol) were placed in a small reaction vial, and 0.15 mL of DMSO was added under argon. Aniline (0.12 mL, 1000 eq) was then added under argon, followed by addition of 300 mM aqueous phosphate buffer (50 μL). The reaction vial was quickly capped and stirred at room temperature for 16 h. The solvent was removed under high vacuum, and the resulting crude product was dried for 4.0 h. Then, 1 mL of diethyl ether was added to the crude product followed by sonication. The suspension was then centrifuged, and the resulting supernatant was decanted. This procedure was repeated three times (performed four times in total) to thoroughly remove residual **BC6** and aniline. TLC was used to confirm the complete removal of **BC6** [eluant: CH₂Cl₂/ethyl acetate (4:1), R_f (**BC6**) = 0.4, R_f (**BC6-GOWF**) = 0]. The bacteriochlorin-peptide conjugate was dried under high vacuum: ESI-MS obsd 1846.8331, calcd 1846.8345 [(M + H)⁺, M = C₁₀₈H₁₁₁N₁₃O₁₆]; MALDI-MS 1844.8; λ_{abs} (CH₂Cl₂) 364, 542, 757 nm.

Acknowledgments

Absorption spectra of several natural or synthetic tolyporphin samples were graciously provided by Prof. Yoshito Kishi (Harvard University), Dr. Thomas Minehan (California State University, Northridge),⁹³ and Dr. Michele Prinsep (University of Waikato). The data displayed in Figure 2.1 are of tolyporphin A from Dr. Prinsep.²⁰

References

- 1 J. Fabian, H. Nakazumi and M. Matsuoka, *Chem. Rev.*, 1992, **92**, 1197–1226.
- 2 M. S. T. Gonçalves, *Chem. Rev.*, 2009, **109**, 190–212.
- 3 Q. Ma and X. Su, *Analyst*, 2010, **135**, 1867–1877.
- 4 A. S. Tatikolov, *J. Photochem. Photobiol. C: Photochem. Rev.*, 2012, **13**, 55–90.
- 5 V. J. Pansare, S. Hejazi, W. J. Faenza and R. K. Prud'homme, *Chem. Mater.*, 2012, **24**, 812–827.
- 6 M. Ptaszek, In *Progress in Molecular Biology and Translational Science*, ed. M. C. Morris, Burlington, Academic Press, 2013, Vol. 113, pp. 59–108.
- 7 K. Umezawa, D. Citterio and K. Suzuki, *Anal. Sci.*, 2014, **30**, 327–349.
- 8 J. Pichaandi and F. C. J. M. van Veggel, *Coord. Chem. Rev.*, 2014, **263–264**, 138–150.
- 9 H. Scheer, In *Advances in Photosynthesis and Respiration*, ed. B. Grimm, R. J. Porra, W. Rüdiger and H. Scheer, Springer, Dordrecht, The Netherlands, 2006, Vol. 25, pp. 1–26.
- 10 M. R. Prinsep, F. R. Caplan, R. E. Moore, G. M. L. Patterson and C. D. Smith, *J. Am. Chem. Soc.*, 1992, **114**, 385–387.

- 11 C. D. Smith, M. R. Prinsep, F. R. Caplan, R. E. Moore and G. M. L. Patterson, *Oncol. Res.*, 1994, **6**, 211–218.
- 12 M. R. Prinsep, G. M. L. Patterson, L. K. Larsen and C. D. Smith, *Tetrahedron*, 1995, **51**, 10523–10530.
- 13 P. Morlière, J.-C. Mazière, R. Santus, C. D. Smith, M. R. Prinsep, C. C. Stobbe, M. C. Fenning, J. L. Golberg, J. D. Chapman, *Cancer Res.*, 1998, **58**, 3571–3578.
- 14 M. R. Prinsep, G. M. L. Patterson, L. K. Larsen and C. D. Smith, *J. Nat. Prod.*, 1998, **61**, 1133–1136.
- 15 T. G. Minehan, L. Cook-Blumberg, Y. Kishi, M. R. Prinsep and R. E. Moore, *Angew. Chem. Int. Ed.*, 1999, **38**, 926–928.
- 16 M. R. Prinsep and J. Puddick, *Phytochem. Anal.*, 2011, **22**, 285–290.
- 17 J. S. Connolly, E. B. Samuel and A. F. Janzen, *Photochem. Photobiol.*, 1982, **36**, 565–574.
- 18 J. M. Dixon, M. Taniguchi and J. S. Lindsey, *Photochem. Photobiol.*, 2005, **81**, 212–213.
- 19 M. Kobayashi, M. Akiyama, H. Kano and H. Kise, in *Advances in Photosynthesis and Respiration*, ed. B. Grimm, R. J. Porra, W. Rüdiger and H. Scheer, Springer, Dordrecht, The Netherlands, 2006, Vol. 25, pp. 79–94.
- 20 M. R. Prinsep and T. G. Appleton, unpublished data.
- 21 www.Lifetechnologies.com, accession date 01/14/2015.
- 22 K. Umezawa, Y. Nakamura, H. Makino, D. Citterio and K. Suzuki, *J. Am. Chem. Soc.*, 2008, **130**, 1550–1551.

- 23 P. J. Sims, A. S. Waggoner, C.-H. Wang and J. F. Hoffman, *Biochem.*, 1974, **13**, 3315–3330.
- 24 A. Muranaka, M. Yonehara and M. Uchiyama, *J. Am. Chem. Soc.*, 2010, **132**, 7844–7845.
- 25 R. W. Wagner and J. S. Lindsey, *Pure Appl. Chem.*, 1996, **68**, 1373–1380.
Corrigendum: R. W. Wagner and J. S. Lindsey, *Pure Appl. Chem.*, 1998, **70** (8), p. i.
- 26 V. N. Nemykin and E. A. Lukyanets, *Arkivoc*, 2010, 136–208.
- 27 D. M. Sturmer and D. W. Heseltine, In *The Theory of the Photographic Process*, ed. T. H. James, Macmillan Publishing Co., Inc., New York, 4th Ed., 1977, pp. 194–234.
- 28 K. Venkataraman, *The Chemistry of Synthetic Dyes*, Academic Press, New York, 1952, Vol. 2, pp. 1143–1186.
- 29 K. Rurack and M. Spieles, *Anal. Chem.*, 2011, **83**, 1232–1242.
- 30 A. Loudet and K. Burgess, *Chem. Rev.*, 2007, **107**, 4891–4932.
- 31 T. G. Minehan and Y. Kishi, *Tetrahedron Lett.*, 1997, **38**, 6811–6814.
- 32 T. G. Minehan and Y. Kishi, *Angew. Chem. Int. Ed.*, 1999, **38**, 923–925.
- 33 W. Wang and Y. Kishi, *Org. Lett.*, 1999, **1**, 1129–1132.
- 34 F. Guintini, C. M. A. Alonso and R. W. Boyle, *Photochem. Photobiol. Sci.*, 2011, **10**, 759–791.
- 35 H.-J. Kim and J. S. Lindsey, *J. Org. Chem.*, 2005, **70**, 5475–5486.
- 36 C. Ruzié, M. Krayner, T. Balasubramanian and J. S. Lindsey, *J. Org. Chem.*, 2008, **73**, 5806–5820.
- 37 M. Krayner, M. Ptaszek, H.-J. Kim, K. R. Meneely, D. Fan, K. Secor and J. S. Lindsey,

- J. Org. Chem.*, 2010, **75**, 1016–1039.
- 38 K. R. Reddy, J. Jiang, M. Krayner, M. A. Harris, J. W. Springer, E. Yang, J. Jiao, D. M. Niedzwiedzki, D. Pandithavidana, P. S. Parkes-Loach, C. Kirmaier, P. A. Loach, D. F. Bocian, D. Holten and J. S. Lindsey, *Chem. Sci.*, 2013, **4**, 2036–2053.
- 39 Z. Yu, C. Pancholi, G. V. Bhagavathy, H. S. Kang, J. K. Nguyen and M. Ptaszek, *J. Org. Chem.*, 2014, **79**, 7910–7925.
- 40 P. Vairaprakash, E. Yang, T. Sahin, M. Taniguchi, M. Krayner, J. R. Diers, A. Wang, D. M. Niedzwiedzki, J. S. Lindsey, D. F. Bocian and D. Holten, *J. Phys. Chem. B*, 2015, *submitted*.
- 41 Z. Yu and M. Ptaszek, *Org. Lett.*, 2012, **14**, 3708–3711.
- 42 V. M. Alexander, K. Sano, Z. Yu, T. Nakajima, P. L. Choyke, M. Ptaszek and H. Kobayashi, *Bioconjugate Chem.*, 2012, **23**, 1671–1679.
- 43 Z. Yu and M. Ptaszek, *J. Org. Chem.*, 2013, **78**, 10678–10691.
- 44 M. A. Harris, J. Jiang, D. M. Niedzwiedzki, J. Jiao, M. Taniguchi, C. Kirmaier, P. A. Loach, D. F. Bocian, J. S. Lindsey, D. Holten and P. S. Parkes-Loach, *Photosynth. Res.*, 2014, **121**, 35–48.
- 45 J. Jiang, C.-Y. Chen, N. Zhang, P. Vairaprakash and J. S. Lindsey, *New J. Chem.*, 2015, **39**, 403–419.
- 46 T. Harada, K. Sano, K. Sato, R. Watanabe, Z. Yu, H. Hanaoka, T. Nakajima, P. L. Choyke, M. Ptaszek and H. Kobayashi, *Bioconjugate Chem.*, 2014, **25**, 362–369.
- 47 K. R. Reddy, E. Lubian, M. P. Pavan, H.-J. Kim, E. Yang, D. Holten and J. S. Lindsey, *New J. Chem.*, 2013, **37**, 1157–1173.

- 48 J. Jiang, P. Vairaprakash, K. R. Reddy, T. Sahin, M. P. Pavan, E. Lubian and J. S. Lindsey, *Org. Biomol. Chem.*, 2014, **12**, 86–103.
- 49 J. Jiang, K. R. Reddy, M. P. Pavan, E. Lubian, M. A. Harris, J. Jiao, D. M. Niedzwiedzki, C. Kirmaier, P. S. Parkes-Loach, P. A. Loach, D. F. Bocian, D. Holten and J. S. Lindsey, *Photosyn. Res.*, 2014, **122**, 187–202.
- 50 S. Gross, A. Brandis, L. Chen, V. Rosenbach-Belkin, S. Roehrs, A. Scherz and Y. Salomon, *Photochem. Photobiol.*, 1997, **66**, 872–878.
- 51 J. M. Sutton, N. Fernandez and R. W. Boyle, *J. Porphyrins Phthalocyanines*, 2000, **4**, 655–658.
- 52 J. M. Sutton, O. J. Clarke, N. Fernandez and R. W. Boyle, *Bioconjugate Chem.*, 2002, **13**, 249–263.
- 53 A. A. Rosenkranz, V. G. Lunin, P. V. Gulak, O. V. Sergienko, M. A. Shumiantseva, O. L. Voronina, D. G. Gilyazova, A. P. John, A. A. Kofner, A. F. Mironov, D. A. Jans and A. S. Sobolev, *FASEB J.*, 2003, **17**, 1121–1123.
- 54 J. R. McCarthy, J. Bhaumik, N. Merbouh and R. Weissleder, *Org. Biomol. Chem.*, 2009, **7**, 3430–3436.
- 55 M. A. Grin, I. S. Lonin, L. M. Likhosherstov, O. S. Novikova, A. D. Plyutinskaya, E. A. Plotnikova, V. V. Kachala, R. I. Yakubovskaya and A. F. Mironov, *J. Porphyrins Phthalocyanines*, 2012, **16**, 1094–1109.
- 56 Y. Chen, G. Li and R. K. Pandey, *Curr. Org. Chem.*, 2004, **8**, 1105–1134.
- 57 M. A. Grin, A. F. Mironov and A. A. Shtil, *Anti-Cancer Agents Med. Chem.*, 2008, **8**, 683–697.

- 58 M. Galezowski and D. T. Gryko, *Curr. Org. Chem.*, 2007, **11**, 1310–1338.
- 59 C. Brückner, L. Samankumara and J. Ogikubo, in *Handbook of Porphyrin Science*, ed. K. M. Kadish, K. M. Smith and R. Guilard, World Scientific Publishing Co., Singapore, 2012, vol. 17, pp. 1–112.
- 60 D. Fan, M. Taniguchi and J. S. Lindsey, *J. Org. Chem.*, 2007, **72**, 5350–5357.
- 61 M. Krayner, E. Yang, J. R. Diers, D. F. Bocian, D. Holten and J. S. Lindsey, *New J. Chem.*, 2011, **35**, 587–601.
- 62 O. Mass and J. S. Lindsey, *J. Org. Chem.*, 2011, **76**, 9478–9487.
- 63 M. Taniguchi, D. L. Cramer, A. D. Bhise, H. L. Kee, D. F. Bocian, D. Holten and J. S. Lindsey, *New J. Chem.*, 2008, **32**, 947–958.
- 64 E. Yang, C. Ruzié, M. Krayner, J. R. Diers, D. M. Niedzwiedzki, C. Kirmaier, J. S. Lindsey, D. F. Bocian and D. Holten, *Photochem. Photobiol.*, 2013, **89**, 586–604.
- 65 M. Gouterman, In *The Porphyrins. Physical Chemistry, Part A*, ed. D. Dolphin, Academic Press, New York, 1978, Vol. 3, pp. 1–165.
- 66 C.-Y. Chen, E. Sun, D. Fan, M. Taniguchi, B. E. McDowell, E. Yang, J. R. Diers, D. F. Bocian, D. Holten and J. S. Lindsey, *Inorg. Chem.*, 2012, **51**, 9443–9464.
- 67 H. C. Kolb, M. G. Finn and K. B. Sharpless, *Angew. Chem. Int. Ed.*, 2001, **40**, 2004–2021.
- 68 V. Rostovtsev, L. G. Green, V. V. Fokin and K. B. Sharpless, *Angew. Chem. Int. Ed.*, 2002, **41**, 2596–2599.
- 69 M. Köhn and R. Breinbauer, *Angew. Chem. Int. Ed.*, 2004, **43**, 3106–3116.
- 70 M. D. Best, *Biochemistry*, 2009, **48**, 6571–6584.

- 71 L. I. Willems, W. A. van der Linden, N. Li, K.-Y. Li, N. Liu, S. Hoogendoorn, G. A. van der Marel, B. I. Florea and H. S. Overkleeft, *Acc. Chem. Res.*, 2011, **44**, 718–729.
- 72 E. M. Sletten and C. R. Bertozzi, *Acc. Chem. Res.*, 2011, **44**, 666–676.
- 73 Y.-X. Chen, G. Triola and H. Waldmann, *Acc. Chem. Res.*, 2011, **44**, 762–773.
- 74 M. F. Debets, J. C. M. van Hest and F. P. J. T. Rutjes, *Org. Biomol. Chem.*, 2013, **11**, 6439–6455.
- 75 D. M. Patterson, L. A. Nazarova and J. A. Prescher, *ACS Chem. Biol.*, 2014, **9**, 592–605.
- 76 J. S. Lindsey, S. Prathapan, T. E. Johnson and R. W. Wagner, *Tetrahedron*, 1994, **50**, 8941–8968.
- 77 H. Akizawa, M. Imajima, H. Hanaoka, T. Uehara, S. Satake and Y. Arano, *Bioconjugate Chem.*, 2013, **24**, 291–299.
- 78 S. S. van Berkel, M. B. van Eldijk and J. C. M. van Hest, *Angew. Chem. Int. Ed.*, 2011, **50**, 8806–8827.
- 79 R. Pöttsch, S. Fleischmann, C. Tock, H. Komber and B. I. Voit, *Macromolecules*, 2011, **44**, 3260–3269.
- 80 <http://laysanbio.com/> accession date 01/17/2015
- 81 E. D. Goddard-Borger and R. V. Stick, *Org. Lett.*, 2007, **9**, 3797–3800.
- 82 C. Grandjean, A. Boutonnier, C. Guerreiro, J.-M. Fournier and L. A. Mulard, *J. Org. Chem.*, 2005, **70**, 7123–7132.
- 83 T. Fricke, R. J. Mart, C. L. Watkins, M. Wiltshire, R. J. Errington, P. J. Smith, A. T. Jones and R. K. Allemann, *Bioconjugate Chem.*, 2011, **22**, 1763–1767.

- 84 X. Chen, K. Muthoosamy, A. Pfisterer, B. Neumann and T. Weil, *Bioconjugate Chem.*, 2012, **23**, 500–508.
- 85 T. R. Chan, R. Hilgraf, K. B. Sharpless and V. V. Fokin, *Org. Lett.*, 2004, **6**, 2853–2855.
- 86 M. Chrominski, A. Zieleniewska, M. Karczewski and D. Gryko, *J. Porphyrins Phthalocyanines*, 2014, **18**, 267–281.
- 87 A. Dirksen and P. E. Dawson, *Bioconjugate Chem.*, 2008, **19**, 2543–2548.
- 88 E. H. M. Lempens, B. A. Helms, M. Merckx and E. W. Meijer, *ChemBioChem*, 2009, **10**, 658–662.
- 89 P. Garner, K. Sunitha and T. Shanthilal, *Tetrahedron Lett.*, 1988, **29**, 3525–3528.
- 90 Z. Zhu and J. H. Espenson, *J. Am. Chem. Soc.*, 1996, **118**, 9901–9907.
- 91 S. J. Pridmore, P. A. Slatford, J. E. Taylor, M. K. Whittlesey and J. M. J. Williams, *Tetrahedron*, 2009, **65**, 8981–8986.
- 92 N. Srinivasan, C. A. Haney, J. S. Lindsey, W. Zhang and B. T. Chait, *J. Porphyrins Phthalocyanines*, 1999, **3**, 283–291.
- 93 T. G. Minehan, Ph.D. thesis, p. 147, Harvard University 1998.
- 94 J. Jiang, M. Maniguchi and J. S. Lindsey, *New J Chem* 2015, accepted.

CHAPTER 3

Hydrophilic Tetracarboxy Bacteriochlorins for Photonics Applications

Preamble. The contents in this chapter have been published⁷⁶ with contributions from the following individuals. Pothiappan Vairaprakash: synthesis of **BC-13**, **BC-12**, **BC-8** and corresponding precursors. Kanumuri Ramesh Reddy: synthesis of **BC-11** and corresponding precursors. Tuba Sahin: synthesis of **BC-7** from **BC-12**. M. Phani Pavan and Elisa Lubian, together with all individuals above, are involved for the molecular designs.

Introduction

Bacteriochlorins (tetrahydroporphyrins) are attractive candidates in a wide variety of photochemical studies due to their strong absorption in the near-infrared (NIR) region (700–900 nm).¹ Bacteriochlorophylls *a*, *b* and *g* contain the bacteriochlorin chromophore and provide the basis for light-harvesting processes and electron-transfer reactions in bacterial photosynthesis (Chart 3.1). Bacteriochlorophylls contain a full complement of substituents about the perimeter of the macrocycle and hence are only partially amenable toward semisynthetic tailoring^{2,3} as required for diverse studies such as cellular imaging, photodynamic therapy, clinical diagnostics, and artificial photosynthesis. The tailoring can include introduction of (i) auxochromes to tune the position of the long-wavelength absorption band, (ii) hydrophobic or hydrophilic groups to alter polarity, and (iii) one or more derivatizable groups for attachment to surfaces, macromolecules, or other entities.

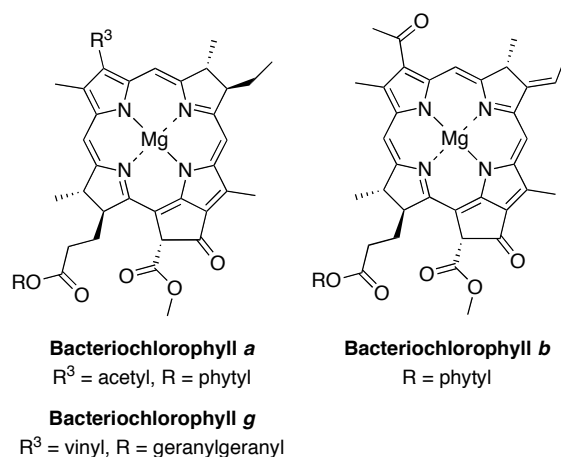
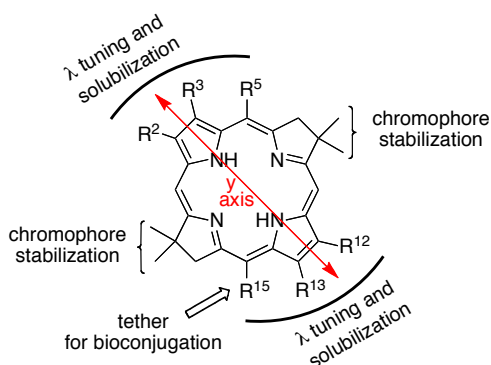
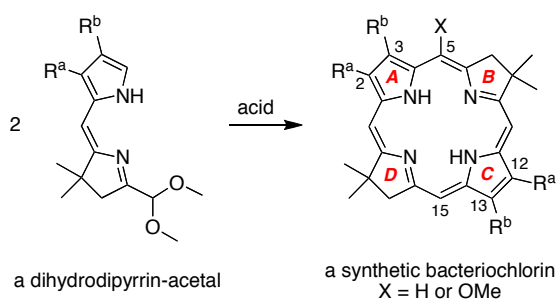


Chart 3.1. Bacteriochlorophylls.

Methods for the synthesis of bacteriochlorins are under active development by a number of groups.⁴⁻¹⁸ The methods range from the modification of native bacteriochlorophylls, hydrogenation or reductive addition to synthetic or native porphyrins or chlorins, and *de novo* synthesis.^{2,3,19,20} In the *de novo* synthesis of bacteriochlorins developed in our laboratory,^{21,22} the geminal dimethyl group in each reduced pyrrole ring increases the stability by blocking adventitious oxidative pathways. The synthesis of bacteriochlorins relies on the self-condensation of a dihydrodipyrin–acetal as shown in Scheme 3.1. The use of two identical dihydrodipyrin–acetal molecules to form the bacteriochlorin affords synthetic expediency but has the drawback that the substituents at positions 2 and 12 are identical to each other, as are those at positions 3 and 13. A single group can be introduced at the 15-position of the bacteriochlorin by regioselective bromination of the 5-methoxybacteriochlorin.²³ Wavelength tunability is achieved by installation of auxochromes at positions along the y-axis (e.g., 2, 3, 5, 12, 13, 15) as shown in Scheme 3.1.

Using the approach in Scheme 3.1, families of bacteriochlorins have been created that are lipophilic,^{13,22,24,25} amphiphilic,²⁶⁻²⁸ or hydrophilic,^{25,29,30} lipophilic and wavelength-tunable,^{13,31} as well as lipophilic, bioconjugatable, and wavelength-tunable.^{13,14,32} The nexus of “hydrophilic and bioconjugatable” has heretofore not been attained with the approach shown in Scheme 3.1 although several hydrophilic, bioconjugatable bacteriochlorins based on other synthetic approaches have been prepared.^{4,5,7,9} Regardless, a general solution that opens the door to “hydrophilic, bioconjugatable, and wavelength-tunable” bacteriochlorins of *de novo* design has not been described. An excellent review of bioconjugatable tetrapyrrole macrocycles (chiefly porphyrins and chlorins) has been prepared by Boyle and coworkers.³³ Recent reports describe semisynthetic routes to bacteriochlorins that are “lipophilic and wavelength-tunable,”³⁴ “hydrophilic and wavelength-tunable,”³⁵ or “lipophilic and bioconjugatable,”³⁶ but again, routes to the nexus of all three features have not yet been developed.



Scheme 3.1. Synthesis of bacteriochlorins (top) and molecular design features (bottom).

The structures of representative hydrophilic bacteriochlorins that we prepared previously are shown in Chart 3.2. Compound **BC-1** is compact and also was a precursor in the synthesis of **BC-3** and analogues.²⁵ Compounds **BC-2** and **BC-3** were prepared²⁵ for studies in antimicrobial photodynamic therapy. Among several analogues prepared, **BC-3** exhibited a negative logP value (−1.4) indicating preferential dissolution in water versus *n*-octanol.²⁹ Compounds **BC-4** and **BC-5** represent an initial foray into hydrophilic bacteriochlorins that were thought to be compatible with subsequent elaboration with a bioconjugatable tether. Only limited photophysical studies have heretofore been carried out concerning the bacteriochlorins in Chart 3.2. Such studies employed the polar solvents DMF (**BC-4**, **BC-5**) or methanol (**BC-1**, **BC-3**), but only in one case examined water (**BC-4**).

exhibits fluorescence quantum yield (Φ_f) of 0.012 in aqueous phosphate buffer (pH 7.4).¹⁰ A chlorin-diphosphonate (**II**) contains alkyl phosphonate groups projected above and below the plane of the macrocycle.⁵⁶ Kobuke and coworkers prepared ethyne-linked porphyrin dyad (**III**), which bears carboxy-substituted swallowtail groups at the *meso* positions. The *trans*-AB-porphyrin **IV** incorporates a phosphono-substituted swallowtail group at one of the *meso* positions, is bioconjugatable due to the iodoacetamide unit, and exhibits high (>10 mM) aqueous solubility.⁴⁹ A porphyrin (**V**) that bears a single tricarboxy-substituted aryl group is soluble at 3 mM in aqueous solution.⁵⁷ All of these examples illustrate the use of facial encumbrance to impart higher solubility of tetrapyrrole macrocycles, an approach that stems from a very lengthy thread of research.⁵⁷

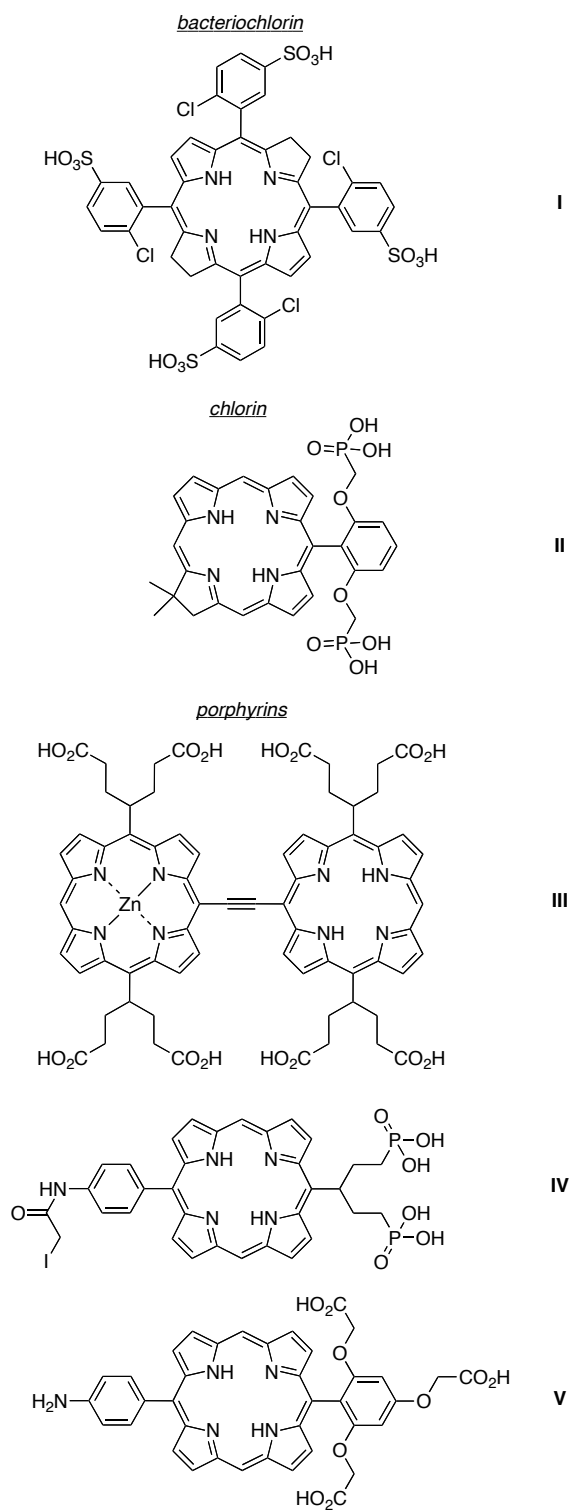


Chart 3.3. Hydrophilic tetrapyrroles **I-V**.

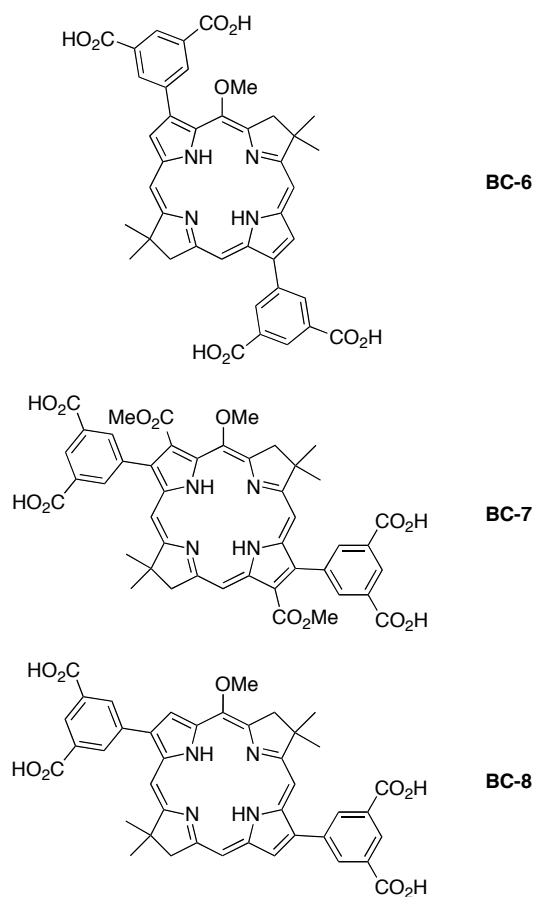


Chart 3.4. New designs of candidate hydrophilic bacteriochlorins.

In this paper, we report the synthesis of three new bacteriochlorins that bear hydrophilic motifs. The hydrophilic motif is a 3,5-dicarboxyphenyl unit attached at two β -pyrrole positions of the bacteriochlorin (Chart 3.4), a design that was chosen to support (optional) installation of a bioconjugatable tether. Bacteriochlorin **BC-6** contains 3,13-diaryl substituents, **BC-7** contains 2,12-diaryl-3,13-dicarbomethoxy substituents, and **BC-8** contains 2,12-diaryl substituents. The latter two architectures required synthesis of new dibromobacteriochlorin building blocks, which were then elaborated with the aryl groups via

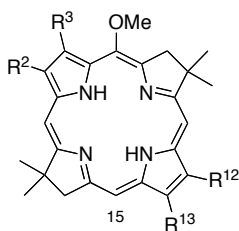
Suzuki coupling. One bioconjugatable, hydrophilic bacteriochlorin also was prepared and was reacted with a cysteine-containing 48-residue peptide analogous to a peptide from the light-harvesting antenna complex of photosynthetic bacteria. The conjugation represents as an initial step in the preparation of a biohybrid light-harvesting antenna. The work also entails photophysical characterization of the four new hydrophilic bacteriochlorins as well as those prepared previously (**BC-1 – BC-5**) that had not been examined thoroughly or at all for fluorescence properties.

Results and discussion

(I) Reconnaissance

One strategy for introduction of a single group into a synthetic bacteriochlorin relies on bromination, which often (but not always) proceeds selectively at the 15-position for structures wherein the 5-methoxy group is present. Examples of successful 15-bromination include 5-methoxybacteriochlorins with no β -pyrrole substituents (entry 1, Table 3.1) or with electroneutral, *p*-tolyl substituents at the 2,12-positions (entry 2). On the other hand, strong electron-withdrawing groups (acetyl, carboethoxy) at the 3,13-positions led to failure of 15-bromination (entries 3 and 4); by analogy, bacteriochlorins **BC-1**, the diformylbacteriochlorin precursor to **BC-2**, and **BC-3** (Chart 3.2) are unsuitable for attachment of a bioconjugatable tether. The added presence of ethyl groups at the 2,12-positions results in effective 15-bromination, whether by counterbalancing the effect of the electron-withdrawing groups or merely by blocking otherwise open β -pyrrole sites (entries 5 and 6).

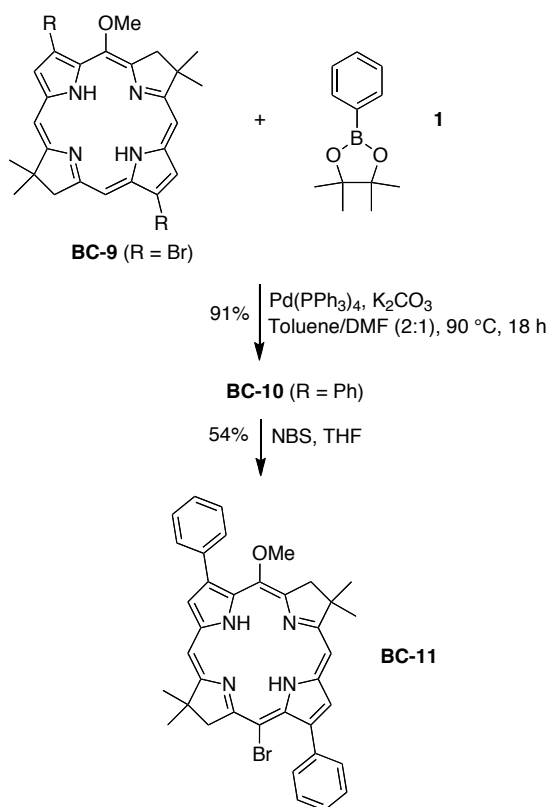
Table 3.1. Effects of β -pyrrole substituents on 15-bromination.



Entry	R ^{2,12}	R ^{3,13}	15-Br introduction	Reference
1	H	H	yes	22
2	<i>p</i> -tolyl	H	yes	23
3	H	acetyl	no	58
4	H	dioxolanyl ^a	no	58
5	Me	acetyl	yes	58
6	Et	EtO ₂ C-	yes	22,58
7	H	phenyl	yes	here

^a 2-methyl-1,3-dioxolan-2-yl.

To address the question of whether electroneutral aryl groups at the 3,13-positions would be compatible with 15-bromination, 3,13-dibromobacteriochlorin **BC-9** was treated to Suzuki coupling with 2-phenyl-4,4,5,5-tetramethyl-1,3,2-dioxaborolane (**1**) to give the corresponding 3,13-diphenylbacteriochlorin **BC-10** (Scheme 3.2). The latter was subjected to standard conditions for 15-bromination (e.g., NBS in THF) whereupon the desired 15-bromobacteriochlorin **BC-11** was smoothly formed. The result is included in Table 3.1 (entry 7) for comparison.



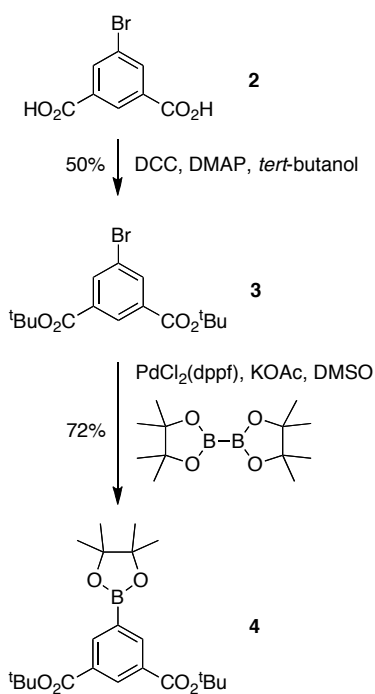
Scheme 3.2. 15-Bromination of a 3,13-diphenylbacteriochlorin.

The strategy reported by Yu and Ptaszek¹³ wherein a 3,13-dibromo-5-methoxybacteriochlorin undergoes sequential coupling at the 13- and 3-sites was found to be successful, but of little advantage here because we sought to introduce two hydrophilic aryl groups and one bioconjugatable tether. Finally, the bacteriochlorins **BC-4** and **BC-5** are reasonably polar yet *N*-protected (or unprotected) analogues thereof (inexplicably) do not undergo 15-bromination. All such considerations led to the following strategy: (1) prepare 2,12 or 3,13-dibromobacteriochlorins bearing a 5-methoxy group; (2) introduce hydrophilic aryl groups at the 2,12 or 3,13-positions by Suzuki coupling; and (3) if desired, install a

bioconjugatable handle at the 15-position (via bromination/Suzuki coupling) as the last operation of the synthesis.

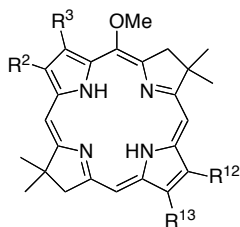
(II) Synthesis

(A) Suzuki coupling partner. The synthesis of the dicarboxy Suzuki coupling partner is shown in Scheme 3.3. Esterification of commercially available 5-bromoisophthalic acid (**2**) with *tert*-butyl alcohol was achieved with *N,N*-dicyclohexylcarbodiimide (DCC) in the presence of 4-(*N,N*-dimethylamino)pyridine (DMAP) to give **3** in 50% yield. Pd-mediated coupling⁵⁹ of the latter with bis(pinacolato)diboron gave Suzuki coupling partner **4** in 72% yield.



Scheme 3.3. Synthesis of dicarboxy Suzuki coupling partner.

(B) Bacteriochlorin building blocks. Three dibromobacteriochlorin building blocks were employed (Chart 3.5). Each contains the two bromo substituents at the β -positions of the pyrrolic rings and also contains a 5-methoxy group. The synthesis of the 3,13-dibromobacteriochlorin **BC-9** has been described previously.²²



BC-9, $R^{2,12} = H$, $R^{3,13} = Br$

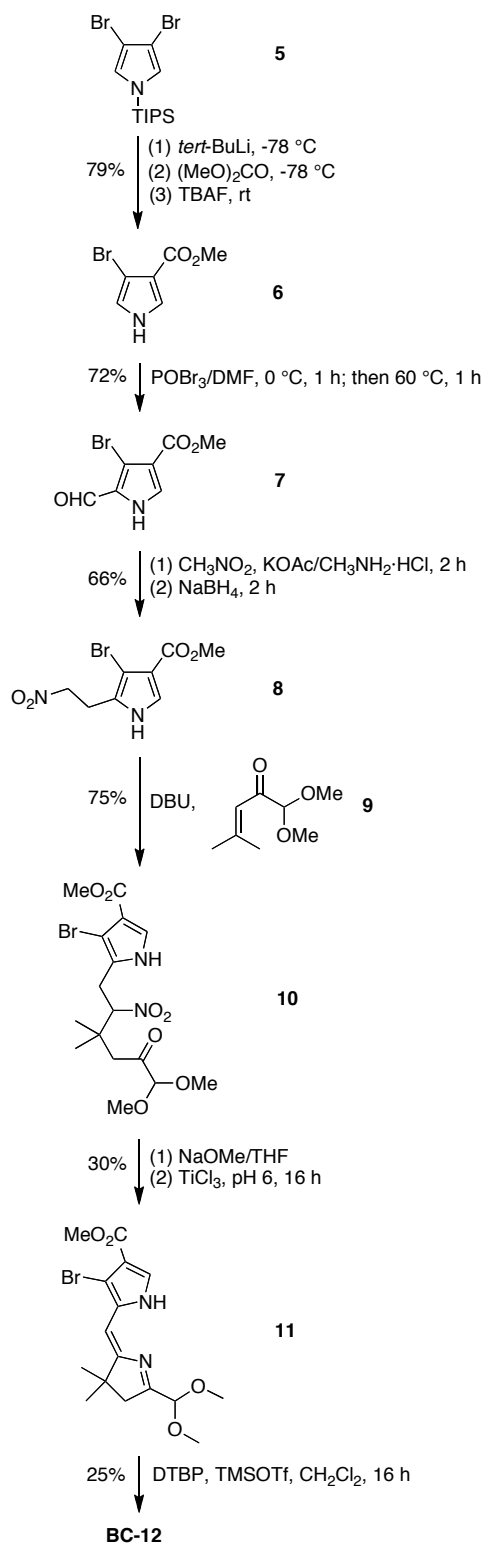
BC-12, $R^{2,12} = Br$, $R^{3,13} = CO_2Me$

BC-13, $R^{2,12} = Br$, $R^{3,13} = H$

Chart 3.5. Bacteriochlorin building blocks.

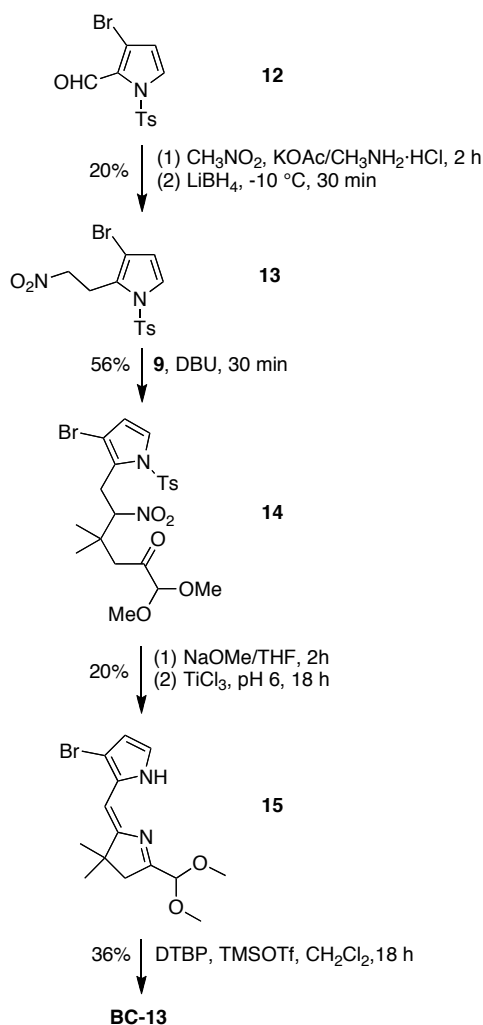
The synthesis of the 2,12-dibromo-3,13-dicarbomethoxybacteriochlorin **BC-12** began with formylation of 3-bromo-4-(methoxycarbonyl)pyrrole **6**, available from 3,4-dibromo *N*-(triisopropylsilyl)pyrrole (**5**).^{60,61} Treatment of **6** with $POCl_3/DMF$ resulted in halogen exchange, affording 3-chloro-2-formyl-4-(methoxycarbonyl)pyrrole as the major product along with a trace amount of 3-bromo-2-formyl-4-(methoxycarbonyl)pyrrole **7**. Attempts to separate the mixture failed. Although the mixture could be carried forward given that the halogen ultimately is to be displaced upon Pd-mediated coupling, we instead performed the Vilsmeier formylation using $POBr_3/DMF$, which smoothly afforded the desired pyrrolecarboxaldehyde **7** in 72% yield (Scheme 3.4). The remainder of the synthesis followed standard methods.^{22,62} conversion of **7** to the nitroethylpyrrole **8**, which upon

Michael addition with 1,1-dimethoxy-4-methyl-3-penten-2-one (**9**)^{21,63} in the presence of DBU under solvent-free conditions yielded the nitrohexanone **10** in 75% yield. Reductive cyclization in the presence of buffered TiCl₃ gave **11**, which upon treatment with TMSOTf in the presence of the proton scavenger 2,6-di-*tert*-butylpyridine (DTBP)⁶⁴ afforded the bacteriochlorin **BC-12** in 25% yield. The pattern of substituents is established at the stage of formylation, and was confirmed by single-crystal X-ray analysis of **8**.⁷⁶



Scheme 3.4. Synthesis of a dibromo-diester bacteriochlorin.

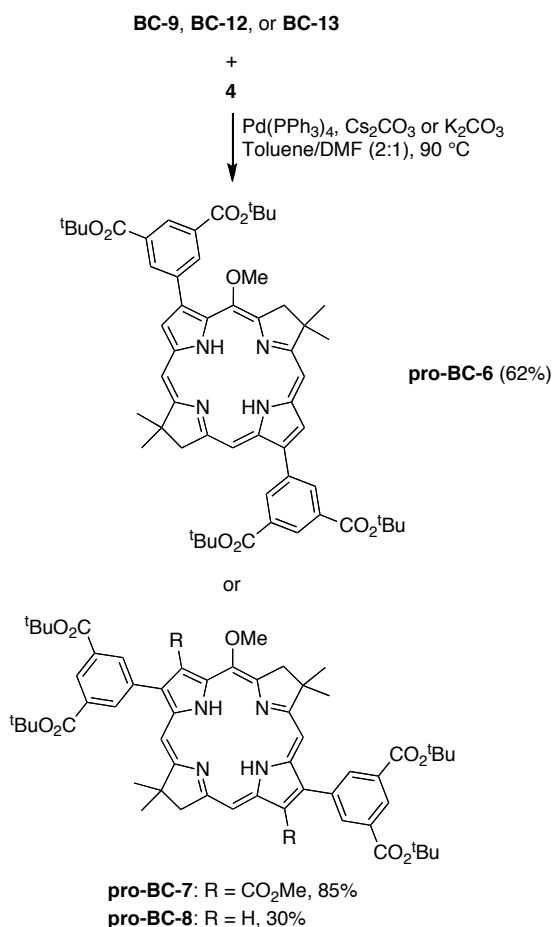
To compare the ease of functionalization in the 15-position of bacteriochlorins having hydrophilic groups at the β -pyrrolic positions, we synthesized 2,12-dibromo-5-methoxybacteriochlorin **BC-13**. The 2,12-substitution pattern presents less hindrance toward further functionalization at the 15-position. The synthesis of **BC-13** begins with 3-bromo-*N*-tosylpyrrole-2-carboxaldehyde (**12**),^{65,66} a known compound that has been prepared in 52 mg from a multistep synthesis starting with cinnamaldehyde, *p*-toluenesulfonamide and 3,3-diethoxyprop-1-yne. (The homologue 3-bromo-*N*-benzenesulfonylpyrrole-2-carboxaldehyde was recently prepared by Iwao and coworkers by direct lithiation of 3-bromo-*N*-benzenesulfonylpyrrole.^{67,68}) We carried out the synthesis at larger scale and obtained 5.5 g of **12** (Scheme 3.5). Compound **12** was treated with nitromethane followed by reduction using LiBH₄ at -10 °C to obtain the nitroethylpyrrole **13** in 20% yield. Treatment of **13** with **9** in the presence of DBU under solvent-free conditions yielded the Michael adduct **14** in 56% yield. The subsequent *N*-detosylation (5 equiv of NaOMe for 2 h) and reductive cyclization (buffered TiCl₃) were carried out in a one-flask process to give the dipyrin **15** in 20% yield. Self-condensation of **15** under standard bacteriochlorin-forming conditions (DTBP and TMSOTf in CH₂Cl₂ at room temperature) gave the corresponding 2,12-dibromo-5-methoxybacteriochlorin **BC-13** in 36% yield. A single-crystal X-ray structure of pyrrole **13** confirmed the substitution pattern of the adjacent 2-(2-nitroethyl) and 3-bromo substituents, and thereby substantiated the 2,12-dibromo substitution pattern in the corresponding bacteriochlorin target.⁷⁶



Scheme 3.5. Synthesis of a 2,12-dibromobacteriochlorin.

(C) Hydrophilic bacteriochlorins. The hydrophilic bacteriochlorins were prepared by coupling of a dibromobacteriochlorin with a Suzuki coupling partner in excess.²⁵ Each reaction was carried out in toluene/DMF (2:1) containing Pd(PPh₃)₄ and K₂CO₃ (or Cs₂CO₃) at 90 °C. The reactants and products are outlined in Scheme 3.6. Thus, the derivatization of 3,13-dibromobacteriochlorin **BC-9** with the dicarboxy coupling partner **4** gave **pro-BC-6** in 62% yield. When lesser quantities of reagents were employed, the mono-coupled mono-

bromo bacteriochlorin intermediate was isolated, and could be subjected to a second round of Suzuki coupling.⁷⁶ Yu and Ptaszek first reported selectivity in the Sonogashira coupling reaction with the same bacteriochlorin.¹³ In a similar manner, treatment of **BC-12** with **4** afforded protected bacteriochlorin **pro-BC-7** in 33% yield. Use of a lesser quantity of base (3 equiv of Cs₂CO₃ instead of 12 equiv of anhydrous K₂CO₃) afforded the protected bacteriochlorin **pro-BC-7** in considerably increased yield (85%). Finally, reaction of 2,12-dibromobacteriochlorin **BC-13** with **4** gave bacteriochlorin–tetraester **pro-BC-8** in 30% yield.

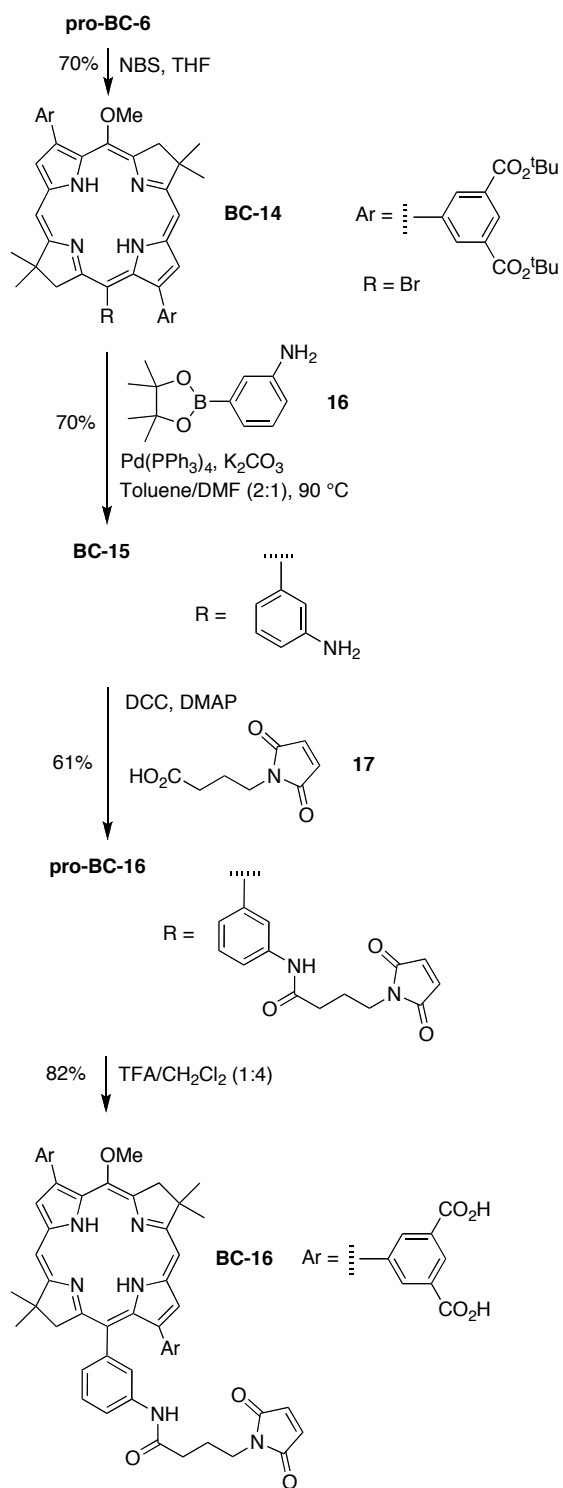


Scheme 3.6. Suzuki coupling to give diarylbacteriochlorins.

The *tert*-butyl esters were cleaved with 20% TFA in CH₂Cl₂ to give **BC-6** (88% yield), **BC-7** (89%), and **BC-8** (90%). In the case of **BC-7**, there was no sign of hydrolysis of the carbomethoxy groups. The chemoselectivity and essentially quantitative nature of the protecting group cleavage reactions enabled the resulting bacteriochlorins **BC-6 – BC-8** to be characterized and used directly without purification.

(D) Bioconjugatable hydrophilic bacteriochlorin. The 3,13-diaryl bacteriochlorin bearing four protected carboxylic acids (**pro-BC-6**) was selected for elaboration with a bioconjugatable tether (Scheme 3.7). Treatment with NBS smoothly afforded the 15-bromination product **BC-14** in 70% yield. Indeed, the presence of the 3,5-diester substituents on the neighboring 13-aryl unit did not cause an adverse effect given that the yield was slightly higher than that in a control experiment (54%) with the 3,13-diphenyl bacteriochlorin **BC-10** (Scheme 3.2). Suzuki coupling reaction under the same conditions as used for the dibromobacteriochlorins above with **BC-14** and anilino Suzuki coupling partner **16** gave the corresponding 15-anilino-bacteriochlorin (**BC-15**). DCC-mediated amidation with 4-maleimidobutyric acid (**17**) gave the bioconjugatable bacteriochlorin in protected form (**pro-BC-16**). Finally, treatment with TFA unveiled the four free carboxylic acids. The resulting bacteriochlorin (**BC-16**) is highly soluble in aqueous solution.

The bacteriochlorins typically were characterized by absorption and fluorescence spectroscopy, ¹H NMR spectroscopy, ¹³C NMR spectroscopy where quantity and solubility allowed, MALDI mass spectrometry, and ESI mass spectrometry. ¹³C NMR spectra were not collected for the compounds prepared to explore solubility features (**BC-6 – BC-8**) owing to insufficient quantities; whereas **BC-16** was characterized by ¹³C NMR spectroscopy.



Scheme 3.7. Hydrophilic bioconjugatable bacteriochlorin.

(III) Photophysical properties

(A) Absorption and emission spectra. The absorption and emission spectra were collected for each target bacteriochlorin. The bacteriochlorins that bear quaternized ammonium groups (**BC-2 – BC-5**) were examined in water, whereas those that contain ionizable groups (**BC-1, BC-6 – BC-8, BC-16**) were examined in aqueous phosphate buffer. All target bacteriochlorins and protected bacteriochlorin precursors also were examined in DMF. The parameters of interest include (i) the position of the long-wavelength absorption band (which establishes an upper limit on the energy of the excited singlet state), termed the Q_y band, (ii) the sharpness of the Q_y band, measured by the full-width-at-half-maximum (fwhm), (iii) the position and fwhm of the fluorescence emission band, which provides information about any reorganization of the excited singlet state, and (iv) the fluorescence quantum yield (Φ_f), which bears on the suitability for a host of photochemical applications. All of these parameters are listed in Table 3.2 for 18 bacteriochlorins. In addition, representative spectra are shown for **BC-6** and **BC-7** in Figure 3.1.

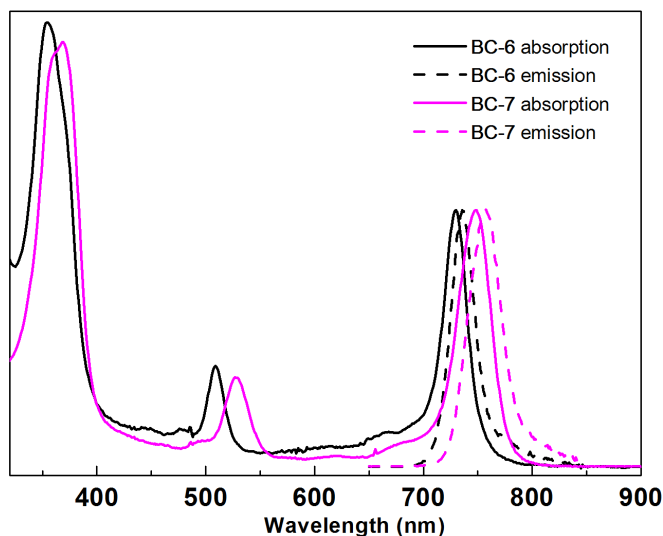


Figure 3.1. Normalized absorption spectra (solid) and emission spectra (dashed) of **BC-6** and **BC-7** in aqueous potassium phosphate buffer (0.5 M, pH 7.0) at room temperature. Spectral parameters are given in Table 3.2.

In general, the spectroscopic properties in aqueous buffer of the new hydrophilic bacteriochlorins (**BC-6 – BC-8, BC-16**) were quite similar to those of the prior hydrophilic bacteriochlorins (**BC-1 – BC-5**). Bacteriochlorin **BC-16** exhibited essentially identical properties to those of **BC-6**, indicating the absence of any adverse effects of the bioconjugatable tether. Moreover, in the one case examined (**BC-16**), the absorption spectrum was essentially unchanged when the sample was allowed to stand in aqueous buffer at room temperature over the course of 5 hours. The findings augur well for the use of the hydrophilic bacteriochlorins in photochemical applications wherein sharp absorption and fluorescence bands are required in an aqueous environment.

Table 3.2. Absorption and fluorescence properties of bacteriochlorins.

Reference	Compound	Solvent	λ_{abs} , nm	FWHM nm (Abs)	λ_{em} , nm	FWHM nm (Flu)	Φ_f
here	BC-1	DMF	728	28	735	26	0.14
here	BC-1	Pi buffer ^a	741	24	745	23	0.089
here	BC-2	DMF	724	26	727	22	0.13
here	BC-2	water ^a	732	20	734	18	0.12
here	BC-3	DMF	730	20	735	27	0.090
here	BC-3	water	733	20	739	22	0.11
30 ^b	BC-4	DMF	734	20	738	32	0.20
30 ^b	BC-4	water ^a	732	23	738	22	0.096
30 ^b	BC-5	DMF	753	30	759	29	0.065
30 ^b	BC-5	water ^a	752	31	758	33	0.010
here	pro-BC-6	DMF	731	24	738	25	0.18
here	BC-6	DMF	729	22	735	23	0.19
here	BC-6	Pi buffer	730	26	736	26	0.078
here	pro-BC-7	DMF	753	25	759	26	0.18
here	BC-7	DMF	746	31	753	23	0.16
here	BC-7	Pi buffer	749	35	758	37	0.11
here	pro-BC-8	DMF	736	22	742	23	0.20
here	BC-8	DMF	732	25	739	23	0.14
here	BC-8	Pi buffer	734	29	740	27	0.077
here	pro-BC-16	DMF	728	22	735	25	0.21
here	BC-16	DMF	726	21	732	24	0.16
here	BC-16	Pi buffer	729	23	735	25	0.074

^a Each sample contains 1% DMF to facilitate initial dissolution. Pi buffer: 0.5 M potassium phosphate at pH 7.0. ^bFluorescence yield data have not been reported previously.

(B) Effect of concentration on spectral properties. The spectral properties described in Table 3.2 and shown in Figure 3.1 were obtained at a concentration of $\sim 1 \mu\text{M}$. For many applications, however, substantially higher concentrations are required. Even if end-uses employ low (e.g., μM) concentrations, methods of fabrication such as bioconjugation may require higher concentrations. To assess the solution properties of the bacteriochlorins at higher concentrations, the absorption spectrum was measured in 10-fold increments over a 1000-fold range, encompassing $\sim 300\text{--}600 \mu\text{M}$ to $\sim 0.3\text{--}0.6 \mu\text{M}$. To maintain a constant absorbance by reciprocal variation of concentration and pathlength, assuming no concentration-dependent aggregation, a series of four cuvettes with 1000-fold range of pathlengths was employed.⁷⁶ In this manner, the absorption spectra could be directly compared without instrumental limitations on sensitivity or dynamic range, thereby affording little change in signal-to-noise ratio.⁷⁰

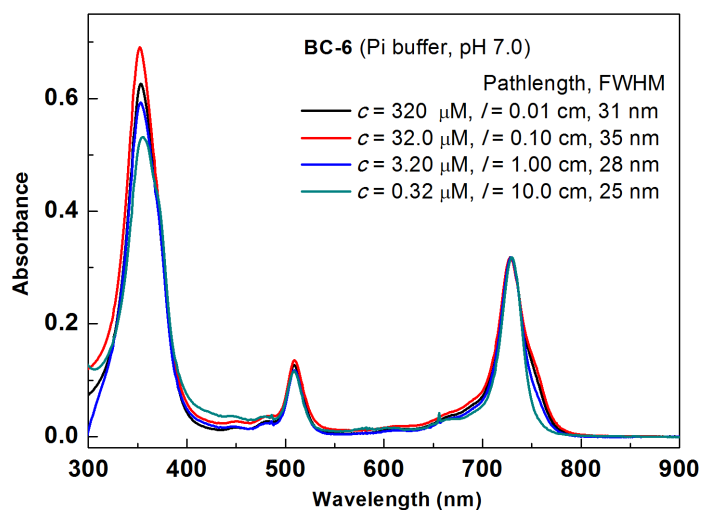


Figure 3.2. Absorption versus concentration of **BC-6** over a range of 1000-fold.

The spectral data of bacteriochlorin **BC-6** measured at four concentrations (~300, 30, 3 and 0.3 μM) were compared.⁷⁶ The concentrations reported here are based on the absorbance of the ~30 μM solution measured at the Q_y transition (assuming $\epsilon_{Q_y} = 100,000 \text{ M}^{-1} \text{ cm}^{-1}$).²¹ The slight amount of broadening in the Q_y band at higher concentration is consistent with some degree of aggregation, yet at all concentrations the general spectroscopic features indicative of bacteriochlorins were retained, and the sample remained visually clear. Similar results were observed with **BC-7** and **BC-8** (Figs. S5 and S6).

(IV) Bioconjugation

One motivation for the development of bacteriochlorin chemistry concerns the development of biohybrid light-harvesting antennas wherein synthetic chromophores or other entities are integrated with constituents (or analogues) of the natural photosynthetic systems.^{32,71,72} Like the natural antennas, the biohybrid antennas form by a multi-tiered self-assembly process, exhibit structure of ~10-nm dimensions, and incorporate up to several dozen chromophores in an integrated architecture.⁷² The design, preparation and characterization of biohybrid antennas thus touches diverse fields encompassing photosynthesis, biophysics, supramolecular chemistry, synthetic chemistry, and materials science.

We have previously employed lipophilic maleimido–bacteriochlorins for attachment to peptides analogous to those found in the natural light-harvesting antennas of bacterial photosynthesis. The resulting conjugates were then examined in aqueous detergent (micellar) solutions. A biohybrid antenna also has been prepared in detergent solution by attachment of a lipophilic maleimido–terrylene dye to a recombinant photosynthetic antenna complex.⁷³

The availability of a hydrophilic bioconjugatable bacteriochlorin (**BC-16**) holds out the possibility of examining analogous conjugates with lesser or no detergents in aqueous solution, ultimately broadening the scope of applications in materials science (such as attachment to diverse surfaces⁷⁴). Thus, the helical β -peptide (Figure 3.3) of *Rhodobacter sphaeroides* light harvesting complex I provided the inspiration for the choice of peptide to use herein. The native β -peptide has the sequence

ADKSDLGYTGLTDEQAQELHSVY**M**⁻¹⁴SGLWLFSAVAIVA**H**⁰LAVYIWRPWF, where the site of histidine ligation to noncovalently bound bacteriochlorophyll *a* is indicated in bold (**H**⁰). The peptide employed herein is identical to the native β -peptide but contains a cysteine in lieu of the methionine residue (in bold at the -14 position). The resulting synthetic peptide, denoted β (-14Cys), thus contains a single cysteine for the ligation with **BC-16**.

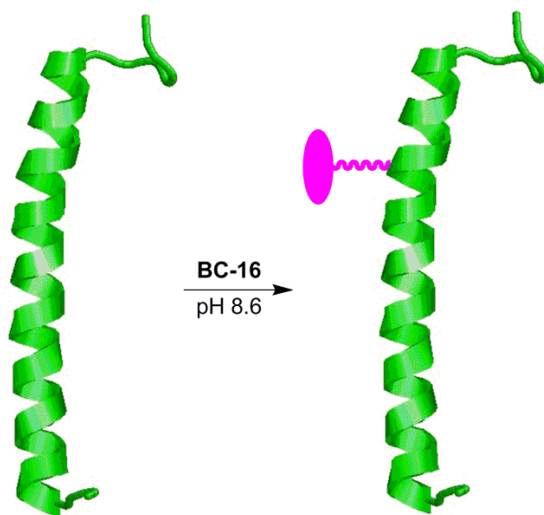


Figure 3.3. Preparation of β (-14Cys)BC-16 conjugate. The attached bacteriochlorin is illustrated in magenta.

The reaction was carried out with β -(-14Cys) at 2 mM and a 50% excess of BC-16 (3 mM) in a mixed aqueous-organic medium of Tris buffer (pH 8.6) and DMF (1:4) at room temperature for 3 hours. The starting peptide and the conjugate [denoted β -(-14Cys)BC-16] closely chromatographed on reverse-phase HPLC using a C4 column. The desired conjugate was obtained in ~50% yield by reverse-phase HPLC purification.⁷⁶ It warrants mention that the conjugate is present as a mixture of diastereomers owing to the stereocenter created upon thio-maleimido conjugation. The absorption spectrum of the purified conjugate β -(-14Cys)BC-16 clearly showed bands due to the peptide in the UV region (282 nm) and the bacteriochlorin in the near-UV (363 nm), visible (515 nm), and NIR (729 nm) region.⁷⁶ Electrospray ionization mass spectrometry (ESI-MS) also gave a strong peak upon hypermass ion reconstruction of the intact bacteriochlorin-peptide conjugate at $m/z = 6410.0550$, to be compared with that for the peptide precursor at $m/z = 5425.7052$. The conjugate β -(-14Cys)BC-16 will be employed in studies with bacteriochlorophyll *a* and the complementary native α -peptide to form self-assembled $\alpha\beta$ -dyads and light-harvesting cyclic oligomeric antennas therefrom.^{32,71,72} The facile preparation, good yield, and ease of handling of the conjugate together augur well for the overall molecular design approached described herein.

Conclusions

The new molecular designs investigated herein entail introduction of polar aryl groups at the 2,12- or 3,13-positions of the bacteriochlorin macrocycle. The aryl groups investigated bear carboxylic acid entities at the 3,5-positions, thereby achieving a degree of facial encumbrance by ionized functional groups at neutral pH. The hydrophilic

bacteriochlorins were readily prepared from the corresponding dibromobacteriochlorin building blocks. In one case examined, the presence of the hydrophilic aryl groups in protected form does not interfere with the attachment of a bioconjugatable tether. The resulting bacteriochlorins generally are soluble in polar media (aqueous or DMF) and exhibit spectroscopic properties – sharp absorption and emission bands, a small Stokes’s shift, and modest fluorescence quantum yield – that are attractive for a wide range of photochemical applications. The molecular designs described herein also may prove instructive in guiding the development of bacteriochlorins that reside at the “hydrophilic, bioconjugatable, and wavelength-tunable” nexus.

Experimental section

(I) General methods.

^1H NMR (400 MHz) or ^{13}C NMR (100 MHz) spectroscopy was performed at room temperature in CDCl_3 (with tetramethylsilane as internal reference) unless noted otherwise. Silica gel (40 μm average particle size) was used for column chromatography. All solvents were reagent grade and were used as received unless noted otherwise. THF was freshly distilled from sodium/benzophenone ketyl. Anhydrous CH_2Cl_2 was used as received. Matrix-assisted laser-desorption mass spectrometry (MALDI-MS) was performed with the matrix 1,4-bis(5-phenyl-2-oxazol-2-yl)benzene (POPOP)⁷⁵ unless noted otherwise. ESI-MS data are reported for the molecular ion or cationized molecular ion. Noncommercial compounds **5**,^{60,61} **9**,^{21,63} **12**^{65,66} and **BC-9**²² were prepared following literature procedures. The peptide **β (-14Cys)** was purchased from Bio-Synthesis, Lewisville, TX in 90% purity. All other compounds were used as received from commercial sources.

(II) Recovery of 2,6-di-*tert*-butylpyridine (DTBP)

The condensation to form bacteriochlorins requires the use of substantial quantities of the hindered base DTBP, which is quite expensive. The following protocol enables recovery of DTBP: Quench the crude bacteriochlorin-forming reaction mixture (carried out in CH₂Cl₂) with saturated aqueous NaHCO₃. Separate the CH₂Cl₂ layer and dry over Na₂SO₄. Concentrate the CH₂Cl₂ extract by rotary evaporation to afford the crude product, which typically contains bacteriochlorin, byproducts derived from the dihydrodipyrin–acetal reactants, and DTBP. Prepare a silica column with hexanes and apply the crude product to the top of the column. Elute with hexanes, whereupon DTBP elutes as a translucent band upon visualization via flashlight illumination from the backside of the column. Collect the translucent band and remove the solvent by rotary evaporation (≤ 40 °C, ~ 50 mm Hg). The DTBP has bp ~ 100 °C at 23 mm Hg.⁶⁴ The DTBP is obtained as a colorless liquid after drying under high vacuum (oil pump, ~ 0.05 mm Hg, room temperature) for 5 min, whereas the typical commercial product is light yellow. In this manner, $>95\%$ of the DTBP can be recovered (at scales of 2–25 mL of DTBP). TLC analysis (silica, hexanes, $R_f = 0.8$) shows only one spot. The DTBP obtained in this manner is stable at 4 °C for at least 6 months, and can be used in bacteriochlorin-forming reactions with no adverse effects versus that obtained from commercial sources.

(III) Absorption versus concentration study

For each bacteriochlorin, four different solutions (solution *A*, *B*, *C* and *D*) in aqueous potassium phosphate buffer (0.5 M, pH = 7.0) were prepared. The concentration of the solution *A* (~ 500 μ M) afforded absorbance (*A*) ~ 0.5 for the Q_y transition measured with a

0.01-cm pathlength cuvette. Successive serial dilution (10 times each) with buffer gave bacteriochlorin concentrations as follows: [solution *A*] = 10 x [solution *B*] = 100 x [solution *C*] = 1000 x [solution *D*].

In a typical experiment for the aggregation studies,⁷⁶ a stock solution was prepared in a small vial containing bacteriochlorin (~0.1 mg; ~0.1 μM) by adding a small amount of DMSO (12.5 μL , to facilitate dissolution) followed by aqueous potassium phosphate buffer (237.5 μL , 0.5 M, pH = 7.0). The resulting sample was sonicated for one minute and then filtered (poly-vinylidene difluoride high-volume low pressure filter, pore size 0.45 μm) to obtain solution *A* (~500 μM). The absorbance of solution *A* was measured in a 0.01-cm pathlength cuvette. Solution *B* was obtained by mixing solution *A* (100 μL) with buffer (900 μL) in a small vial. The absorbance of solution *B* was measured in a 0.1-cm pathlength cuvette. For further dilution, solution *B* (300 μL) was mixed with buffer (2.70 mL) in a 1-cm pathlength cuvette to obtain solution *C* and the absorbance was measured. Solution *C* (2.50 mL) was transferred into a 25 mL standard measuring flask and made up to the mark with buffer. The absorbance of the resulting solution *D* was measured in a 10-cm pathlength cuvette. The procedure was followed for each bacteriochlorin **BC-6 – BC-8**.

(IV) Fluorescence yield determinations

The Φ_f values (in DMF, water, or aqueous potassium phosphate buffer) were determined relative to that of 5-methoxy-8,8,18,18-tetramethyl-2,12-di-*p*-tolylbacteriochlorin in toluene ($\Phi_f = 0.18$)²¹ without correction for refractive index differences.

(V) Synthesis

Di-*tert*-butyl 5-bromoisophthalate (3). A mixture of **2** (2.45 g, 10.0 mmol), DCC (3.82 g, 18.5 mmol) and DMAP (0.244 g, 2.00 mmol) in CH₂Cl₂ (25 mL) and DMF (25 mL) was treated with *tert*-butyl alcohol (9.5 mL, 100. mmol). The mixture was stirred under argon at room temperature for 16 h. The resulting mixture was filtered to remove insoluble material. The filtrate was concentrated and chromatographed [silica, CH₂Cl₂/hexanes (1:1)] to yield a white solid (1.8 g, 50%): mp 95–96 °C; ¹H NMR δ 1.60 (s, 18H), 8.25 (d, *J* = 1.6 Hz, 2H), 8.49 (t, *J* = 1.6 Hz, 1H); ¹³C NMR δ 28.3, 82.5, 122.4, 129.2, 134.2, 136.2, 163.9; ESI-MS obsd 379.0523, calcd 379.0515 [(M + Na)⁺, M = C₁₆H₂₁BrO₄].

Di-*tert*-butyl 5-(4,4,5,5-tetramethyl-1,3,2-dioxaborolan-2-yl)isophthalate (4). Following a general procedure,⁵⁹ samples of **3** (250 mg, 0.700 mmol), bis(pinacolato)diboron (213.4 mg, 0.84 mmol), Pd(pddf)Cl₂ (15.4 mg, 21.0 μmol), KOAc (206 mg, 2.10 mmol), and DMSO (4.2 mL, deaerated by bubbling with argon) was added to a Schlenk flask. The reaction mixture was deaerated by three freeze-pump-thaw cycles with argon. The reaction mixture was stirred at 80 °C for 2 h. The reaction mixture was cooled to room temperature, diluted with ethyl acetate and washed with brine. The organic layer was separated, dried (Na₂SO₄) and concentrated. Column chromatography [silica, CH₂Cl₂/ethyl acetate (47:3)] provided a white solid (203 mg, 72%): mp 195–196 °C; ¹H NMR δ 1.36 (s, 12H), 1.62 (s, 18H), 8.54 (d, *J* = 1.6 Hz, 2H), 8.65 (t, *J* = 1.6 Hz, 1H); ¹³C NMR δ 25.1, 28.4, 81.7, 84.5, 131.9, 133.2, 139.5, 165.4; ESI-MS obsd 427.2277, calcd 427.2263 [(M + Na)⁺, M = C₂₂H₃₃BO₆].

3-Bromo-4-(methoxycarbonyl)pyrrole (6). A solution of *tert*-BuLi (25.0 mL, 1.7 M in pentane, 42.5 mmol) was slowly cannulated into a solution of **5** (10.7 g, 28.0 mmol) in THF (200 mL) at $-78\text{ }^{\circ}\text{C}$ under argon. After 30 min, dimethyl carbonate (7.58 mL, 90.0 mmol) was added and the stirring was continued for another 30 min. The reaction mixture was allowed to warm to $0\text{ }^{\circ}\text{C}$ and treated with saturated aqueous NaHCO_3 . The reaction mixture was extracted with ethyl acetate. The organic extract was washed (water, brine), dried (Na_2SO_4) and concentrated by rotary evaporation. The resulting viscous material was mixed with excess hexanes and sonicated for a few minutes. A solid settled out, whereupon the supernatant was decanted. The solid was dried under reduced pressure, dissolved in THF (100 mL) and treated at room temperature with TBAF \cdot 3H $_2$ O (11.0 g, 35.0 mmol) for 30 min under argon. The reaction mixture was diluted with diethyl ether, washed (water, brine), dried (Na_2SO_4) and concentrated by rotary evaporation. The resulting residue was dissolved in a minimum amount of CH_2Cl_2 , and then excess hexanes was added. The resulting precipitate was separated and dried under reduced pressure to afford a pale yellow solid (4.48 g, 79%): mp $96\text{--}98\text{ }^{\circ}\text{C}$; ^1H NMR δ 3.83 (s, 3H), 6.83 (d, $J = 2.4\text{ Hz}$, 1H), 7.42 (dd, $J_1 = 2.4\text{ Hz}$, $J_2 = 3.2\text{ Hz}$, 1H), 8.58 (brs, 1H); ^{13}C NMR ($\text{CDCl}_3/\text{CD}_3\text{OD}$) δ 51.1, 96.6, 113.5, 120.5, 125.1, 164.8; ESI-MS obsd 203.9655, calcd 203.9655 [(M + H) $^+$, M = $\text{C}_6\text{H}_6\text{BrNO}_2$].

3-Bromo-2-formyl-4-(methoxycarbonyl)pyrrole (7). A mixture of **6** (3.06 g, 15.0 mmol) and POBr_3 (5.16 g, 18.0 mmol) under argon was treated with DMF (50.0 mL) at $0\text{ }^{\circ}\text{C}$. The resulting mixture was stirred at $0\text{ }^{\circ}\text{C}$ for 1 h and then at $60\text{ }^{\circ}\text{C}$ for 1 h. The reaction mixture was treated with a mixture of saturated aqueous sodium acetate and CH_2Cl_2 [300 mL, 1:1 (v/v)] and stirred for 1 h. The aqueous phase was separated and extracted with CH_2Cl_2 .

The combined organic phase was washed with water (5 x 300 mL), dried (Na₂SO₄), and concentrated. The resulting solid was dissolved in a minimum amount of CH₂Cl₂, and then excess hexanes was added. The resulting precipitate was separated by filtration and dried under reduced pressure to afford a light brown solid (2.50 g, 72%): mp 187–189 °C; ¹H NMR (CDCl₃/CD₃OD) δ 3.87 (s, 3H), 4.05 (brs, 1H), 7.69 (s, 1H), 9.67 (d, *J* = 0.8 Hz, 1H); ¹³C NMR (CDCl₃/CD₃OD) δ 51.7, 110.3, 116.5, 130.7, 131.0, 163.5, 180.1; ESI-MS obsd 231.9611, calcd 231.9604 [(M + H)⁺, M = C₇H₆BrNO₃].

3-Bromo-4-(methoxycarbonyl)-2-(2-nitroethyl)pyrrole (8). Following a general procedure,⁶² a stirred mixture of **7** (1.80 g, 7.75 mmol), potassium acetate (1.47 g, 15.0 mmol), and methylamine hydrochloride (1.01 g, 15.0 mmol) in absolute ethanol (10.0 mL) was treated with nitromethane (1.20 mL, 22.0 mmol). The resulting mixture was stirred at room temperature for 2 h, whereupon water was added. The resulting precipitate was separated by filtration, washed with water and dried under reduced pressure to afford a yellow solid, which was used directly in the next step. The crude solid material was dissolved in CHCl₃/2-propanol (3:1, 100 mL). Silica (10 g) and NaBH₄ (378 mg, 10.0 mmol) were added, and the mixture was stirred at room temperature under argon for 2 h. The reaction mixture was filtered, and the filtrate was concentrated. The resulting crude material was dissolved in CH₂Cl₂. The organic solution was washed with water, dried (Na₂SO₄) and concentrated to afford a pale brown solid (1.42 g, 66% yield): mp 148–150 °C; ¹H NMR (CDCl₃/CD₃OD) δ 3.32 (t, *J* = 7.2 Hz, 2H), 3.81 (s, 3H), 4.63 (t, *J* = 7.2 Hz, 2H), 7.38 (s, 1H); ¹³C NMR (CDCl₃/CD₃OD) δ 24.5, 51.3, 73.6, 96.8, 114.1, 125.0, 126.3, 164.8; ESI-MS obsd 276.9824, calcd 276.9818 [(M + H)⁺, M = C₈H₉BrN₂O₄].

6-(3-Bromo-4-(methoxycarbonyl)pyrrol-2-yl)-1,1-dimethoxy-4,4-dimethyl-5-nitrohexan-2-one (10). Following a general procedure,⁶² a mixture of **8** (1.33 g, 4.80 mmol) and **9** (1.52 g, 9.60 mmol) was treated with DBU (3.60 mL, 24.0 mmol). The reaction mixture was stirred at room temperature for 16 h under argon. A saturated solution of cold aqueous NH₄Cl was added. The mixture was extracted with ethyl acetate. The combined organic phase was washed with brine, dried (Na₂SO₄) and concentrated. Column chromatography [silica, CH₂Cl₂/ethyl acetate (9:1)] afforded a pale yellow solid (1.57 g, 75% yield): mp 64–66 °C; ¹H NMR δ 1.15 (s, 3H), 1.28 (s, 3H), 2.63, 2.74 (AB, ²J = 18.8 Hz, 2H), 3.15–3.35 (m, 2H), 3.42 (s, 3H), 3.43 (s, 3H), 3.81 (s, 3H), 4.38 (s, 1H), 5.19 (dd, ³J = 2.4 Hz, ³J = 11.2 Hz, 1H), 7.33 (d, J = 3.6 Hz, 1H), 8.82 (brs, 1H); ¹³C NMR δ 24.1, 24.4, 25.5, 36.7, 45.0, 51.4, 55.3, 55.4, 93.5, 97.6, 104.8, 114.9, 124.6, 126.3, 163.8, 203.6; ESI-MS obsd 435.0766, calcd 435.0761 [(M + H)⁺, M = C₁₆H₂₃BrN₂O₇].

7-Bromo-2,3-dihydro-8-(methoxycarbonyl)-1-(1,1-dimethoxymethyl)-3,3-dimethyldipyrin (11). Following a general procedure,⁶² in a first flask, a solution of **10** (1.30 g, 3.00 mmol) in freshly distilled THF (10.0 mL) at 0 °C was treated with NaOMe (486 mg, 9.00 mmol). The mixture was stirred and deaerated by bubbling argon through the solution for 45 min. In a second flask purged with argon, TiCl₃ (12.0 mL, 20 wt % in 3% HCl solution, 19.0 mmol), 30.0 mL of THF and NH₄OAc (12.0 g, 156 mmol) were combined under argon, and the mixture was deaerated by bubbling argon for 45 min. Then, the first flask mixture was transferred via cannula to the buffered TiCl₃ mixture. The resulting mixture was stirred at room temperature for 16 h under argon. Then, the content was diluted with ethyl acetate and washed with saturated aqueous NaHCO₃. The organic layer was

separated, dried (Na₂SO₄) and concentrated. Column chromatography (silica, CH₂Cl₂) afforded a yellow solid (350 mg, 30% yield): mp 108–110 °C; ¹H NMR (300 MHz) δ 1.25 (s, 6H), 2.65 (s, 2H), 3.44 (s, 3H), 3.45 (s, 3H), 3.83 (s, 3H), 5.04 (s, 1H), 5.98 (s, 1H), 7.48 (d, *J* = 3.6 Hz, 1H), 11.22 (brs, 1H); ¹³C NMR δ 26.9, 29.2, 40.7, 48.7, 51.3, 54.8, 97.2, 102.5, 104.4, 114.5, 125.4, 130.7, 162.9, 164.2, 176.9; ESI-MS obsd 385.0749, calcd 385.0757 [(M + H)⁺, M = C₁₆H₂₁BrN₂O₄].

3-Bromo-2-(2-nitroethyl)-*N*-tosylpyrrole (13). Following a general procedure,⁶² a mixture of **12** (5.25 g, 16.0 mmol), potassium acetate (1.57 g, 16.0 mmol), and methylamine hydrochloride (1.08 g, 16.0 mmol) in absolute ethanol (8.00 mL) was treated with nitromethane (2.76 mL, 52.0 mmol). The resulting mixture was stirred at room temperature for 3 h, whereupon water was added. The resulting precipitate was separated by filtration, washed with water and dried under reduced pressure to afford a yellow solid, which was used directly in the next step. The crude solid material was dissolved in THF (69.0 mL) and cooled to –10 °C (using an acetone bath with a few pieces of dry ice). The solution was treated with 95% LiBH₄ (315 mg, 14.0 mmol) all-at-once under vigorous stirring. The reaction mixture was stirred for ~30 min at –10 °C, whereupon the reaction mixture was quenched by slowly adding a cold saturated aqueous NH₄Cl solution. The mixture was extracted with ethyl acetate. The organic solution was washed with brine, dried (Na₂SO₄) and concentrated. Column chromatography [silica, hexanes/CH₂Cl₂ (1:1)] afforded a white solid (1.20 g, 20% yield): mp 133–134 °C; ¹H NMR δ 2.44 (s, 3H), 3.43 (t, *J* = 8.0 Hz, 2H), 4.50 (t, *J* = 8.0 Hz, 2H), 6.32 (d, *J* = 3.6 Hz, 1H), 7.33 (d, *J* = 3.6 Hz, 1H), 7.36 (d, *J* = 8.4 Hz, 2H), 7.69 (d, *J* = 8.4 Hz, 2H); ¹³C NMR δ 21.8, 24.2, 72.9, 105.4, 114.7, 123.2, 125.1,

127.0, 130.7, 135.2, 146.2; ESI-MS obsd 394.9663, calcd 394.9672 [(M + Na)⁺, M = C₁₃H₁₃BrN₂O₄S].

6-(3-Bromopyrrol-2-yl)-1,1-dimethoxy-4,4-dimethyl-5-nitrohexan-2-one (14).

Following a general procedure,⁶² a mixture of **13** (1.20 g, 3.20 mmol) and **9** (1.90 g, 16.0 mmol) was treated with DBU (3.60 mL, 24.0 mmol). The reaction mixture was stirred at room temperature for 30 min under argon. A saturated solution of cold aqueous NH₄Cl was added at 0 °C. The mixture was extracted with ethyl acetate. The combined organic phase was washed with brine, dried (Na₂SO₄) and concentrated. Column chromatography [silica, CH₂Cl₂/ethyl acetate (9:1)] afforded a pale yellow solid (950 mg, 56% yield): mp 92–93 °C; ¹H NMR δ 1.13 (s, 3H), 1.29 (s, 3H), 2.43 (s, 3H), 2.66, 2.77 (AB, ²J = 18.8 Hz, 2H), 3.10 (dd, ³J = 3.2 Hz, ³J = 15.2 Hz, 1H), 3.42 (s, 3H), 3.43 (s, 3H), 3.56 (dd, ³J = 11.2 Hz, ³J = 15.2 Hz, 1H), 4.39 (s, 1H), 5.32 (dd, ³J = 2.8 Hz, ³J = 11.2 Hz, 1H), 6.26 (d, J = 3.6 Hz, 1H), 7.25 (d, J = 4.0 Hz, 1H), 7.33 (d, J = 8.4 Hz, 2H), 7.61 (d, J = 8.4 Hz, 2H); ¹³C NMR δ 21.9, 23.8, 24.0, 25.9, 36.8, 44.4, 55.2, 93.3, 104.7, 106.7, 116.0, 124.3, 126.5, 126.8, 130.5, 135.6, 145.9, 203.0; ESI-MS obsd 548.1060, calcd 548.1061 [(M + NH₄)⁺, M = C₂₁H₂₇BrN₂O₇S].

7-Bromo-2,3-dihydro-1-(1,1-dimethoxymethyl)-3,3-dimethyldipyrin (15).

Following a general procedure,⁶² in a first flask, a solution of **14** (530 mg, 1.00 mmol) in freshly distilled THF (5.0 mL) at 0 °C was treated with NaOMe (270 mg, 5.00 mmol). The mixture was stirred and deaerated by bubbling argon through the solution for 2 h. In a second flask purged with argon, TiCl₃ (7.00 mL, 20 wt % in 3% HCl solution, 11.0 mmol), THF (20 mL) and NH₄OAc (7.00 g, 90.0 mmol) were combined under argon, and the mixture was deaerated by bubbling with argon for 45 min. Then, the first flask mixture was

transferred via cannula to the buffered TiCl_3 mixture. The resulting mixture was stirred at room temperature for 18 h under argon. Then, the mixture was diluted with ethyl acetate and washed with saturated aqueous NaHCO_3 . The organic layer was separated, dried (Na_2SO_4) and concentrated. Column chromatography [silica, hexanes/ CH_2Cl_2 (1:1)] afforded a yellow oil (75.0 mg, 20% yield): ^1H NMR δ 1.24 (s, 6H), 2.63 (s, 2H), 3.45 (s, 6H), 5.02 (s, 1H), 5.93 (s, 1H), 6.19 (t, $J = 2.8$ Hz, 1H), 6.78 (t, $J = 2.8$ Hz, 1H), 10.75 (brs, 1H); ^{13}C NMR δ 19.3, 29.2, 40.6, 48.5, 54.7, 97.7, 102.7, 104.8, 111.2, 119.4, 128.8, 161.0, 175.4; ESI-MS obsd 327.0706, calcd 327.0703 [(M + H) $^+$, M = $\text{C}_{14}\text{H}_{19}\text{BrN}_2\text{O}_2$].

3,13-Bis[3,5-bis(*tert*-butoxycarbonyl)phenyl]-5-methoxy-8,8,18,18-tetramethylbacteriochlorin (pro-BC-6). Following a general procedure,²⁵ samples of **BC-9** (17.3 mg, 31.0 μmol), **4** (75.2 mg, 186 μmol), $\text{Pd}(\text{PPh}_3)_4$ (21.5 mg, 18.6 μmol), K_2CO_3 (51.5 mg, 373 μmol) and toluene/DMF [3.1 mL (2:1), deaerated by bubbling with argon for 45 min] was added to a Schlenk flask and deaerated by three freeze-pump-thaw cycles. The reaction mixture was stirred at 90 °C for 20 h. The reaction mixture was cooled to room temperature, concentrated to dryness, diluted with CH_2Cl_2 and washed with saturated aqueous NaHCO_3 . The organic layer was separated, dried (Na_2SO_4) and concentrated. Column chromatography [silica, hexanes/ CH_2Cl_2 (1:3)] afforded the title compound (18.4 mg, 62%): ^1H NMR δ -1.85 (brs, 1H), -1.60 (brs, 1H), 1.68 (s, 18H), 1.71 (s, 18H), 1.96 (s, 6H), 1.98 (s, 6H), 3.64 (s, 3H), 4.38 (s, 2H), 4.40 (s, 2H), 8.64–8.66 (m, 2H), 8.67 (s, 1H), 8.72 (s, 1H), 8.75 (t, $J = 2.4$ Hz, 1H), 8.80 (t, $J = 2.4$ Hz, 1H), 8.84 (d, $J = 2.4$ Hz, 1H), 8.88 (d, $J = 2.4$ Hz, 1H), 8.94 (d, $J = 2.4$ Hz, 1H); ^{13}C NMR δ 28.4, 28.5, 29.9, 31.3, 31.3, 45.8, 45.9, 47.8, 52.2, 63.4, 81.8, 82.1, 96.7, 97.1, 97.3, 122.6, 122.7, 127.5, 129.0, 129.5, 130.1, 131.9, 132.0, 132.2, 133.2, 134.2,

134.7, 135.1, 135.5, 135.6, 136.0, 136.5, 137.0, 138.9, 154.5, 160.9, 165.5, 165.8, 169.6, 170.1; MALDI-MS obsd 952.5; ESI-MS obsd 952.4989, calcd 952.4981 (C₅₇H₆₈N₄O₉); λ_{abs} (CH₂Cl₂) 364, 511, 731 nm.

3,13-Bis(3,5-dicarboxyphenyl)-5-methoxy-8,8,18,18-tetramethylbacteriochlorin (BC-6). A solution of **pro-BC-6** (4.0 mg, 4.2 μ mol) in CH₂Cl₂ (0.4 mL) was stirred at room temperature under argon for 2 min, followed by addition of TFA (0.1 mL). After 2 h, the reaction mixture was diluted with ethyl acetate and then washed with saturated aqueous NaHCO₃, 2 N HCl solution, and water. The organic layer was separated, dried (Na₂SO₄) and concentrated. The resulting solid was treated with hexanes and methanol (49:1), sonicated in a benchtop sonication bath, and then centrifuged. The supernatant was discarded to afford a green solid (2.7 mg, 88%): ¹H NMR (DMSO-*d*₆) δ -1.93 (brs, 1H), -1.69 (brs, 1H), 1.89 (s, 6H), 1.93 (s, 6H), 3.54 (s, 3H), 4.33 (s, 2H), 4.39 (s, 2H), 8.67 (d, *J* = 1.2 Hz, 1H), 8.71 (d, *J* = 1.2 Hz, 1H), 8.74 (s, 1H), 8.81 (m, 2H), 8.86 (s, 1H), 8.90–8.92 (m, 3H), 8.93 (s, 1H), 9.19 (s, 1H), 13.4–13.6 (br, 4H); MALDI-MS obsd 728.7; ESI-MS obsd 729.2559, calcd 729.2555 [(M + H)⁺, M = C₄₁H₃₆N₄O₉]; λ_{abs} (CH₂Cl₂) 365, 511, 731 nm; λ_{abs} (100 mM aqueous potassium phosphate buffer, pH 7.6) 357, 508, 730 nm; λ_{abs} (DMF) 362, 509, 727 nm.

2,12-Bis[3,5-bis(*tert*-butoxycarbonyl)phenyl]-3,13-bis(methoxycarbonyl)-5-methoxy-8,8,18,18-tetramethylbacteriochlorin (pro-BC-7). Following a general procedure,²⁵ a mixture of **BC-12** (25 mg, 0.037 mmol), **4** (90 mg, 0.22 mmol), Pd(PPh₃)₄ (25 mg, 0.022 mmol), and anhydrous K₂CO₃ (61 mg, 0.44 mmol) was deaerated under vacuum in a Schlenk flask for 1 h. Toluene/DMF [3.7 mL, (2:1), deaerated by bubbling argon] was

added and the reaction mixture was deaerated by four freeze-pump-thaw cycles. The reaction mixture was heated at 90 °C for 18 h. After cooling to room temperature, the solvent was evaporated. The crude reaction mixture was diluted with CH₂Cl₂ and washed with saturated aqueous NaHCO₃. The organic layer was separated, dried (Na₂SO₄) and concentrated. The residue was purified by column chromatography [silica, hexanes/ethyl acetate (9:1)] to afford a purple solid (13.4 mg, 33%): ¹H NMR δ -1.44 (brs, 1H), -1.15 (brs, 1H), 1.66 (s, 18H), 1.67 (s, 18H), 1.81 (s, 6H), 1.87 (s, 6H), 4.04 (s, 3H), 4.20 (s, 3H), 4.27 (s, 3H), 4.36 (s, 2H), 4.43 (s, 2H), 8.36 (s, 1H), 8.52 (s, 1H), 8.73 (d, *J* = 1.6 Hz, 2H), 8.89 (d, *J* = 1.2 Hz, 4H), 9.65 (s, 1H); ¹³C NMR δ 28.2, 28.4, 29.9, 30.8, 30.9, 45.8, 46.3, 47.9, 51.6, 51.9, 53.1, 64.6, 81.8, 81.9, 95.9, 98.1, 98.6, 118.8, 124.9, 128.4, 129.9, 130.2, 131.8, 132.2, 132.6, 133.3, 134.2, 134.5, 135.0, 135.7, 136.0, 136.2, 136.4, 137.0, 157.2, 161.9, 165.0, 165.3, 166.4, 168.7, 169.5, 173.3; MALDI-MS obsd 1069.3; ESI-MS obsd 1069.5167, calcd 1069.5169 [(M + H)⁺, M = C₆₁H₇₂N₄O₁₃]; λ_{abs} (DMF) 373, 531, 753 nm.

The procedure was repeated at larger scale following the above procedure but with several changes. **BC-12** (100 mg, 148 μmol), **4** (360 mg, 888 μmol), Pd(PPh₃)₄ (100 mg, 88.8 μmol) and Cs₂CO₃ (149 mg, 444 μmol) were reacted in toluene/DMF [10.0 mL, (2:1), deaerated by bubbling argon] for 22 h. After cooling to room temperature, the mixture was diluted with diethyl ether and washed (saturated aqueous NaHCO₃, 0.5 N HCl, water, and brine), dried (Na₂SO₄) and concentrated. Chromatography afforded the title compound (135 mg, 85%) with characterization data identical with those listed above.

2,12-Bis(3,5-dicarboxyphenyl)-3,13-bis(methoxycarbonyl)-5-methoxy-8,8,18,18-tetramethylbacteriochlorin (BC-7). A solution of **pro-BC-7** (5.7 mg, 5.3 μmol) in

anhydrous CH_2Cl_2 (1.4 mL) was treated with TFA (350 μL). The reaction mixture was stirred at room temperature under argon for 2 h. Ethyl acetate was added, and the mixture was washed with saturated aqueous NaHCO_3 . The aqueous phase was separated, acidified with 2 M HCl, and extracted with ethyl acetate. The organic layer was washed (brine, water), dried (Na_2SO_4) and concentrated. The resulting solid was washed with hexanes to give the title compound as a purple solid (4.0 mg, 89% yield): ^1H NMR ($\text{DMSO-}d_6$) δ -1.44 (brs, 1H), -1.15 (brs, 1H), 1.82 (s, 6H), 1.76 (s, 6H), 3.99 (s, 3H), 4.10 (s, 3H), 4.22 (s, 3H), 4.35 (s, 2H), 4.43 (s, 2H), 8.38 (s, 1H), 8.57 (s, 1H), 8.71 (d, $J = 1.2$ Hz, 2H), 8.75 (t, $J = 1.2$ Hz, 1H), 8.78 (t, $J = 1.6$ Hz, 1H), 8.86 (d, $J = 1.6$ Hz, 2H), 9.52 (s, 1H); MALDI-MS obsd 844.9; ESI-MS obsd 845.2648, calcd 845.2665 [(M + H) $^+$, M = $\text{C}_{45}\text{H}_{40}\text{N}_4\text{O}_{13}$]; λ_{abs} (DMF) 360, 374, 529, 743 nm; λ_{abs} (100 mM aqueous potassium phosphate buffer, pH 7.6) 370, 527, 750 nm.

2,12-Bis[3,5-bis(*tert*-butoxycarbonyl)phenyl]-5-methoxy-8,8,18,18-tetramethylbacteriochlorin (pro-BC-8). Following a general procedure,²⁵ a mixture of **BC-13** (18.6 mg, 33.3 μmol), **4** (80.4 mg, 200 μmol), $\text{Pd}(\text{PPh}_3)_4$ (23.1 mg, 20.0 μmol), and K_2CO_3 (55.3 mg, 400 μmol) in toluene/DMF [3.33 mL (2:1)] in a Schlenk flask was deaerated by three freeze-pump-thaw cycles. The flask was placed in an oil bath at 90 $^\circ\text{C}$ and stirred for 20 h. The reaction mixture was allowed to cool to room temperature, concentrated, diluted with CH_2Cl_2 and washed with saturated aqueous NaHCO_3 . The organic layer was dried (Na_2SO_4) and concentrated. Column chromatography [silica, CH_2Cl_2 /hexanes (2:1)] afforded a green solid (9.6 mg, 30% yield): ^1H NMR δ -1.80 (s, 1H), -1.68 (s, 1H), 1.70 (s, 36H), 1.93 (s, 6H), 1.94 (s, 6H), 4.43 (s, 2H), 4.44 (s, 2H), 4.51 (s, 3H), 8.73 (s, 1H), 8.74 (s, 1H), 8.76 (s, 1H), 8.82 (s, 1H), 8.84 (t, $J = 1.6$ Hz, 1H), 8.85 (t, $J = 1.6$

Hz, 1H), 9.00 (t, $J = 1.6$ Hz, 2H), 9.03 (t, $J = 1.6$ Hz, 2H), 9.07 (d, $J = 2.0$ Hz, 1H); ^{13}C NMR δ 25.1, 28.5, 29.9, 31.2, 31.3, 46.0, 46.3, 47.5, 51.9, 65.4, 82.0, 82.1, 95.4, 95.5, 98.4, 116.7, 121.7, 129.2, 129.7, 130.1, 132.3, 133.0, 133.2, 133.3, 134.7, 135.6, 135.7, 135.9, 136.8, 137.5, 153.6, 160.5, 165.4, 165.5, 170.2, 170.5; MALDI-MS obsd 953.8; ESI-MS 952.4982, calcd 952.4981 ($\text{C}_{57}\text{H}_{68}\text{N}_4\text{O}_9$); λ_{abs} (DMF) 368, 514, 735 nm.

2,12-Bis(3,5-dicarboxyphenyl)-5-methoxy-8,8,18,18-tetramethylbacteriochlorin (BC-8). A solution of **pro-BC-8** (3.1 mg, 3.2 μmol) in CH_2Cl_2 (300 μL) at room temperature was stirred under argon for 2 min followed by the addition of TFA (75 μL). The reaction mixture was stirred for 2 h. The mixture was diluted with ethyl acetate and treated with saturated aqueous NaHCO_3 . The ethyl acetate layer was then discarded. The aqueous phase (which contained the anionic bacteriochlorin) was separated, acidified with 2N HCl, and extracted with ethyl acetate. The organic layer was washed (water, brine), dried (Na_2SO_4) and concentrated. The resulting solid was treated with hexanes and methanol (49:1), sonicated in a benchtop sonication bath, and then centrifuged. The supernatant was discarded. The residue was dried to afford a purple solid (2.1 mg, 90%): ^1H NMR ($\text{DMSO-}d_6$) δ -1.78 (s, 1H), -1.68 (s, 1H), 1.86 (s, 6H), 1.88 (s, 6H), 4.37 (s, 2H), 4.42 (s, 2H), 4.49 (s, 3H), 8.71 (s, 1H), 8.73 (s, 1H), 8.76 (s, 2H), 8.89 (s, 1H), 9.03 (s, 2H), 9.06 (s, 2H), 9.19 (s, 2H); MALDI-MS obsd 729.2; ESI-MS obsd 729.2535, calcd 729.2555 [$(\text{M} + \text{H})^+$, $\text{M} = \text{C}_{41}\text{H}_{36}\text{N}_4\text{O}_9$]; λ_{abs} (DMF) 354, 512, 725 nm; λ_{abs} (100 mM aqueous potassium phosphate buffer, pH 7.6) 357, 511, 734 nm.

5-Methoxy-8,8,18,18-tetramethyl-3,13-diphenylbacteriochlorin (BC-10).

Following a general procedure,²⁵ a mixture of **BC-9** (20 mg, 0.036 mmol), **1** (22.0 mg, 0.108

mmol), Pd(PPh₃)₄ (12.5 mg, 0.0100 mmol), and anhydrous K₂CO₃ (60.0 mg, 0.432 mmol) was deaerated under vacuum in a Schlenk flask for 1 h. Toluene/DMF [3.6 mL, (2:1), deaerated by bubbling with argon] was added and the reaction mixture was deaerated by three freeze-pump-thaw cycles. The reaction mixture was heated at 90 °C for 18 h. After cooling to room temperature, the mixture was concentrated. The resulting residue was diluted with CH₂Cl₂, and washed with saturated aqueous NaHCO₃. The organic layer was separated, dried (Na₂SO₄) and concentrated. Column chromatography [silica, CH₂Cl₂: hexanes (1:1)] afforded a green solid (18.0 mg, 91%): ¹H NMR δ -1.91 (brs, 1H), -1.66 (brs, 1H), 1.94 (s, 6H), 1.97 (s, 6H), 3.64 (s, 3H), 4.38 (s, 4H), 7.51–7.57 (m, 1H), 7.58–7.68 (m, 3H), 7.72–7.79 (m, 2H), 8.09–8.13 (m, 2H), 8.16–8.20 (m, 2H), 8.61 (d, *J* = 2.4 Hz, 1H), 8.63 (s, 1H), 8.65 (s, 1H), 8.77 (d, *J* = 2.0 Hz, 1H), 8.79 (s, 1H); ¹³C NMR δ 31.2, 31.3, 45.7, 45.9, 47.7, 52.2, 63.4, 96.8, 96.9, 97.0, 122.3, 122.4, 127.0, 127.1, 127.8, 129.2, 131.3, 131.4, 133.9, 134.0, 135.4, 135.6, 136.3, 136.6, 136.7, 138.5, 153.9, 160.6, 169.0, 169.9; MALDI-MS obsd 552.2; ESI-MS obsd 553.2942, calcd 553.2962 [(M+ H)⁺, M = C₃₇H₃₆N₄O]; λ_{abs} (CH₂Cl₂) 361, 373, 508, 728 nm.

15-Bromo-5-methoxy-8,8,18,18-tetramethyl-3,13-diphenylbacteriochlorin (BC-11). Following a general procedure,²³ a solution of **BC-10** (15.0 mg, 0.0271 mmol, 2.0 mM) in dry THF (13.5 mL) was treated dropwise (10 min) with a solution of NBS (4.82 mg, 0.0271 mmol, 4.0 mM) in THF (6.75 mL) and stirred at room temperature under argon for 1 h. The reaction mixture was diluted with CH₂Cl₂ and washed with saturated aqueous NaHCO₃. The organic layer was separated, dried (Na₂SO₄) and concentrated. Column chromatography [silica, CH₂Cl₂: hexanes (1:1)] afforded a green solid (9.3 mg, 54%): ¹H

NMR δ -1.74 (brs, 1H), -1.45 (brs, 1H), 1.95 (s, 6H), 1.96 (s, 6H), 3.65 (s, 3H), 4.36 (s, 2H), 4.41 (s, 2H), 7.52–7.70 (m, 6H), 7.83–7.89 (m, 2H), 8.08–8.14 (m, 2H), 8.59 (s, 1H), 8.62–8.68 (m, 3H); ^{13}C NMR δ 31.4, 31.6, 45.5, 45.7, 48.2, 54.8, 63.7, 96.9, 98.5, 124.7, 125.8, 127.4, 127.8, 128.0, 129.6, 130.9, 131.2, 131.6, 132.4, 135.3, 136.3, 136.3, 137.7, 139.4, 157.2, 159.7, 168.0, 171.3; MALDI-MS obsd 631.9; ESI-MS obsd 631.2046, calcd 631.2067 [(M+H)⁺, M = C₃₇H₃₅BrN₄O]; λ_{abs} (CH₂Cl₂) 365, 520, 725 nm.

2,12-Dibromo-5-methoxy-3,13-bis(methoxycarbonyl)-8,8,18,18-tetramethylbacterio-chlorin (BC-12). Following a general procedure,²² a solution of **11** (289 mg, 750 μmol) in anhydrous CH₂Cl₂ (40.0 mL) was treated first with DTBP (2.87 g, 15.0 mmol) and second with TMSOTf (680 μL , 3.75 mmol). The reaction mixture was stirred at room temperature for 16 h. The mixture was washed with saturated aqueous NaHCO₃, dried (Na₂SO₄) and concentrated. Column chromatography [silica, CH₂Cl₂/hexanes (2:1)] afforded a dark purple solid (120 mg, 25% yield): ^1H NMR δ -1.54 (s, 1H), -1.26 (s, 1H), 1.93 (s, 6H), 1.94 (s, 6H), 4.23 (s, 3H), 4.31 (s, 3H), 4.32 (s, 3H), 4.33 (s, 2H), 4.37 (s, 2H), 8.66 (s, 1H), 8.86 (s, 1H), 9.53 (s, 1H); ^{13}C NMR δ 26.8, 29.9, 31.0, 31.2, 45.9, 46.2, 48.0, 51.7, 52.5, 53.6, 64.6, 95.7, 97.9, 98.6, 110.4, 115.4, 120.2, 126.6, 128.5, 131.9, 133.5, 135.1, 135.3, 157.5, 162.1, 165.3, 167.4, 170.0, 173.5; ESI-MS obsd 673.0636, calcd 673.0656 [(M+H)⁺, M = C₂₉H₃₀Br₂N₄O₅]; λ_{abs} (CH₂Cl₂) 356, 367, 527, 749 nm.

2,12-Dibromo-5-methoxy-8,8,18,18-tetramethylbacteriochlorin (BC-13). Following a general procedure,²² a solution of **15** (75.0 mg, 230 μmol) in anhydrous CH₂Cl₂ (13.0 mL) was treated first with DTBP (1.02 mL, 4.60 mmol) and second with TMSOTf (210

μL , 1.15 mmol). The reaction mixture was stirred under argon at room temperature for 18 h. The mixture was washed with saturated aqueous NaHCO_3 , dried (Na_2SO_4) and concentrated. Column chromatography [silica, CH_2Cl_2 /hexanes (2:1)] afforded a green solid (23.2 mg, 36% yield): ^1H NMR δ -2.06 (s, 1H), -1.95 (s, 1H), 1.94 (s, 6H), 1.96 (s, 6H), 4.33 (s, 2H), 4.35 (s, 2H), 4.43 (s, 3H), 8.54 (s, 1H), 8.67 (d, $J = 2.0$ Hz, 1H), 8.70 (s, 1H), 8.71 (s, 1H), 8.93 (d, $J = 2.0$ Hz, 1H); ^{13}C NMR δ 31.2, 31.4, 45.9, 46.2, 47.5, 51.9, 65.3, 95.3, 98.1, 109.6, 113.3, 118.9, 123.8, 130.0, 132.9, 134.3, 135.2, 135.7, 153.9, 160.8, 170.2, 170.6; MALDI-MS obsd 556.5; ESI-MS obsd 556.0468, calcd 556.0468 ($\text{C}_{25}\text{H}_{26}\text{Br}_2\text{N}_4\text{O}$); λ_{abs} (CH_2Cl_2) 348, 358, 369, 504, 724 nm.

15-Bromo-3,13-bis[3,5-bis(*tert*-butoxycarbonyl)phenyl]-5-methoxy-8,8,18,18-tetramethylbacteriochlorin (BC-14). Following a general procedure²³ in more dilute solution, a solution of **pro-BC-6** (27 mg, 28 μmol) in THF (58 mL) was treated with a solution of NBS (5.2 mg, 29 μmol) in THF (0.29 mL) at room temperature for 2 h. The reaction mixture was diluted with CH_2Cl_2 and washed with saturated aqueous NaHCO_3 . The organic layer was dried (Na_2SO_4), concentrated and chromatographed [silica, CH_2Cl_2 /ethyl acetate (7:3)] to afford a reddish solid (21 mg, 70%): ^1H NMR (300 MHz) δ -1.68 (s, 1H), -1.38 (s, 1H), 1.65 (s, 18H), 1.69 (s, 18H), 1.96 (s, 12H), 3.68 (s, 3H), 3.92 (d, $J = 17.6$ Hz, 1H), 4.08 (d, $J = 17.6$ Hz, 1H), 4.38 (s, 2H), 6.39–6.42 (m, 1H), 6.72 (s, 1H), 6.93–6.99 (m, 2H), 8.02 (br, 1H), 8.42 (t, $J = 1.6$ Hz, 1H), 8.63 (d, $J = 2.4$ Hz, 1H), 8.65 (s, 1H), 8.67 (d, $J = 2.4$ Hz, 1H), 8.76 (t, $J = 1.6$ Hz, 1H), 8.91 (d, $J = 1.2$ Hz, 2H); ^{13}C NMR δ 25.1, 28.5, 31.3, 31.4, 45.2, 46.0, 47.7, 52.0, 63.5, 81.8, 97.2, 97.5, 114.0, 114.2, 118.3, 121.0, 121.4, 123.1,

124.1, 125.2, 126.5, 128.1, 128.4, 129.1, 131.9, 132.3, 133.9, 134.0, 134.1, 135.8, 136.0, 136.2, 138.7, 139.0, 141.5, 145.9, 155.0, 161.1, 165.8, 169.2, 169.4; ESI-MS obsd 1030.4089, calcd 1030.4086 (C₅₇H₆₇BrN₄O₉); MALDI-MS obsd 1031.7; λ_{abs} (CH₂Cl₂) 367, 522, 727 nm.

15-(3-Aminophenyl)-3,13-bis[3,5-bis(*tert*-butoxycarbonyl)phenyl]-5-methoxy-8,8,18,18-tetramethylbacteriochlorin (BC-15). Following a general procedure,²³ samples of **BC-14** (21 mg, 20 μ mol), **16** (22 mg, 0.10 mmol), Pd(PPh₃)₄ (9.3 mg, 8.0 μ mol), and K₂CO₃ (33 mg, 0.24 mmol) were placed in a Schlenk flask, and deaerated under vacuum for 30 min. Toluene/DMF [2.0 mL, (2:1), deaerated by bubbling with argon] was added under argon and deaerated by three freeze-pump-thaw cycles. The reaction mixture was stirred at 90 °C for 18 h. The reaction mixture was cooled to room temperature, concentrated to dryness and diluted with CH₂Cl₂. The solution was washed with saturated aqueous NaHCO₃. The organic layer was separated, dried (Na₂SO₄) and concentrated. Column chromatography [silica, CH₂Cl₂/ethyl acetate (99:1)] provided a reddish solid (15 mg, 70%): ¹H NMR δ -1.57 (s, 1H), -1.23 (s, 1H), 1.64 (s, 18H), 1.69 (s, 18H), 1.80 (s, 3H), 1.90 (s, 3H), 1.97 (s, 3H), 1.99 (s, 3H), 3.66 (s, 3H), 4.37 (s, 2H), 4.41 (s, 2H), 8.60 (s, 1H), 8.63 (d, *J* = 1.2 Hz, 2H), 8.65 (s, 1H), 8.66 (d, *J* = 2.1 Hz, 1H), 8.69 (d, *J* = 2.1 Hz, 1H), 8.76–8.78 (m, 2H), 8.88 (d, *J* = 1.5 Hz, 2H); ¹³C NMR δ 28.5, 28.5, 31.4, 31.6, 45.6, 45.8, 48.2, 45.6, 45.8, 54.8, 63.7, 81.2, 81.9, 97.2, 97.3, 98.8, 125.0, 126.0, 129.4, 129.5, 130.2, 130.8, 131.9, 132.1, 132.5, 133.2, 134.3, 134.4, 135.4, 135.6, 135.8, 136.0, 136.1, 136.3, 138.1, 139.8, 157.7, 160.0, 165.7, 168.3, 171.8; MALDI-MS obsd 1044.6; ESI-MS obsd 1043.5406, calcd 1043.5408 (C₆₃H₇₃N₅O₉); λ_{abs} (CH₂Cl₂) 365, 517, 728 nm.

3,13-Bis[3,5-bis(*tert*-butoxycarbonyl)phenyl]-15-[(3-(4-maleimidobutyramido)phenyl)]-5-methoxy-8,8,18,18-tetramethylbacteriochlorin (pro-BC-16). A mixture of **17** (54 mg, 0.29 mmol), DCC (61 mg, 0.29 mmol) and DMAP (0.80 mg, 5.9 μ mol) in CH₂Cl₂ (2.5 mL) was treated with **BC-15** (31mg, 29 μ mol) in CH₂Cl₂ (0.5 mL) and stirred at room temperature for 2.5 h. The resulting mixture was filtered to remove insoluble material. The filtrate was concentrated and chromatographed [silica, CH₂Cl₂/ethyl acetate (24:1)] to afford a reddish solid (22 mg, 61%): ¹H NMR (300 MHz) δ -1.59 (s, 1H), -1.22 (s, 1H), 1.63 (s, 18H), 1.69 (s, 18H), 1.81 (s, 3H), 1.89 (s, 3H), 1.98–2.02 (m, 8H), 2.29 (t, *J* = 6.9 Hz, 2H), 3.63 (t, *J* = 6.3 Hz, 2H), 3.68 (s, 3H), 3.91 (d, *J* = 17.4 Hz, 1H), 4.03 (d, *J* = 17.4 Hz, 1H), 4.38 (s, 2H), 6.69 (s, 2H), 7.15 (t, *J* = 7.8 Hz, 1H), 7.34 (d, *J* = 7.2 Hz, 1H), 7.44–7.47 (m, 2H), 7.66 (s, 1H), 7.96 (s, 1H), 8.20 (s, 1H), 8.34 (t, *J* = 1.5 Hz, 1H), 8.63 (d, *J* = 2.7 Hz, 1H), 8.65 (t, *J* = 7.5 Hz, 2H), 8.68 (d, *J* = 2.1 Hz, 1H), 8.76 (t, *J* = 1.5 Hz, 1H), 8.91 (d, *J* = 1.8 Hz, 2H); ¹³C NMR δ 28.5, 28.5, 31.3, 31.4, 34.8, 37.3, 45.4, 46.0, 47.8, 52.2, 63.6, 81.6, 81.9, 97.2, 97.8, 113.3, 119.2, 123.3, 125.2, 126.6, 128.2, 128.3, 129.2, 129.4, 131.0, 132.0, 132.6, 133.8, 133.8, 134.3, 134.4, 134.9, 135.3, 136.0, 136.3, 137.4, 138.6, 139.0, 141.6, 155.3, 160.9, 165.8, 169.1, 169.6, 170.1, 171.3; MALDI-MS obsd 1210.9; ESI-MS obsd 1208.5848, calcd 1208.5829 (C₇₁H₈₀N₆O₁₂); λ_{abs} (CH₂Cl₂) 366, 517, 730 nm.

3,13-Bis(3,5-dicarboxyphenyl)-15-[3-(4-maleimidobutyramido)phenyl]-5-methoxy-8,8,18,18-tetramethylbacteriochlorin (BC-16). A solution of **pro-BC-16** (26 mg, 21 μ mol) in CH₂Cl₂ (2.0 mL) at room temperature was stirred under argon for 2 min, followed by addition of TFA (0.5 mL). After 2 h, the reaction mixture was diluted with ethyl acetate and washed with saturated NaHCO₃, 2 N HCl solution and water. The organic layer

was separated, dried (Na_2SO_4) and concentrated. The resulting solid was treated with a mixture solvent of hexanes and CH_2Cl_2 (3:2), sonicated in a benchtop sonication bath, and centrifuged. The supernatant was discarded to afford a green solid (17 mg, 82%): ^1H NMR ($\text{DMSO-}d_6$) δ -1.66 (s, 1H), -1.31 (s, 1H), 1.75 (s, 6H), 1.87 (s, 6H), 1.92 (s, 3H), 1.94 (s, 3H), 2.23 (t, $J = 7.2$ Hz, 2H), 3.43 (t, $J = 6.8$ Hz, 2H), 3.58 (s, 3H), 3.78 (d, $J = 16.8$ Hz, 1H), 4.09 (d, $J = 16.8$ Hz, 1H), 4.34 (s, 2H), 6.97–7.07 (m, 2H), 7.25–7.31 (m, 1H), 7.72 (s, 1H), 7.84 (br, 1H), 8.27 (s, 1H), 8.69 (s, 1H), 8.85–8.97 (m, 5H), 9.97 (s, 1H), 13.24 (br, 4H); ^{13}C NMR ($\text{DMSO-}d_6$) δ 24.5, 31.3, 31.4, 31.6, 34.2, 37.6, 45.3, 46.2, 47.5, 52.1, 63.7, 98.0, 98.4, 114.1, 117.5, 124.2, 127.6, 127.8, 127.9, 128.2, 128.5, 129.4, 130.5, 131.6, 132.1, 133.8, 134.1, 134.2, 135.2, 135.8, 135.9, 136.2, 138.5, 138.7, 139.5, 140.5, 155.5, 161.2, 164.2, 167.6, 169.1, 169.6, 169.8, 170.7, 171.8; MALDI-MS obsd 982.8; ESI-MS obsd 985.3403, calcd 985.3403 $[(\text{M} + \text{H})^+]$, $\text{M} = \text{C}_{55}\text{H}_{48}\text{N}_6\text{O}_{12}$; λ_{abs} (CH_3OH) 363, 514, 725 nm; λ_{abs} (100 mM aqueous potassium phosphate buffer, pH 7.6) 360, 516, 729 nm; λ_{abs} (DMF) 367, 516, 727 nm.

(VI) Preparation of β (-14Cys)BC-16

Stock solutions of DMF and Tris buffer (0.1 M, pH 8.6) were sonicated for 5 min, followed by bubbling with argon for 30 min to remove oxygen. A sample of β (-14Cys) (2.5 mg, 0.46 μmol) was dissolved in 92 μL of DMF, and 23 μL of Tris buffer (pH 8.6) was then added while the mixture was stirred under argon. The protein appeared to readily dissolve in DMF and stay in solution when Tris buffer was added. A sample of BC-16 (0.7 mg, 0.71 μmol) was dissolved in 92 μL of DMF and 23 μL of Tris buffer. The resulting BC-16

solution was then added dropwise to the β (-14Cys) solution under argon. The reaction mixture was stirred in the dark at room temperature for 3 h. The reaction mixture was treated with diethyl ether to cause precipitation. The resulting suspension was sonicated (benchtop sonication bath) and centrifuged (3800 rpm). The supernatant was discarded. The procedure (ether addition, sonication and centrifugation) was performed two additional times. The resulting greenish residue was dried under vacuum for 30 min. Addition of hexafluoroacetone trihydrate (50 μ L) to the greenish solid followed by sonication for 3 min completely dissolved the solid, affording a blue solution. Addition of 150 μ L of a solvent mixture that represented the initial HPLC eluant [composed of H₂O (50%), isopropanol (33.3%), acetonitrile (17.6%) and TFA (0.1%)] caused a change from blue back to green. This mixture was centrifuged to remove (visibly evident) insoluble particles. An aliquot (30 μ L) of the sample was injected into the HPLC instrument and a fraction at 15.5 min was collected. The fraction contained the title conjugate as well as unreacted peptide as observed upon ESI-MS analysis. The HPLC conditions are described in the Supplementary Information. An aliquot of the HPLC fraction was reinjected to assess homogeneity,⁷⁶ which showed the fraction to be essentially free of unreacted bacteriochlorin. The total (isolated) yield was determined to be 52% on the basis of absorption spectroscopy of the conjugate (bacteriochlorin Q_y band).⁷⁶ The fraction from the analytical HPLC was concentrated under vacuum to dryness and subjected to ESI-MS, which gave $m/z = 6410.0550$ for the monoisotopic ion (calcd 6410.0241 for M⁺, M = C₃₀₉H₄₁₇N₆₇O₈₂S) and $m/z = 6414.0708$ for the most intense peak. Such data can be compared with those for the peptide β (-14Cys),

which gave $m/z = 5425.7052$ for the monoisotopic ion (calcd 5425.6905 for M^+ , $M = C_{254}H_{369}N_{61}O_{70}S$) and $m/z = 5428.7056$ for the most intense peak.

Notes and references

- 1 H. Scheer, in *Chlorophylls and Bacteriochlorophylls: Biochemistry, Biophysics, Functions and Applications*, ed. B. Grimm, R. J. Porra, W. Rüdiger and H. Scheer, Springer, Dordrecht, The Netherlands, 2006, pp. 1–26.
- 2 Y. Chen, G. Li and R. K. Pandey, *Curr. Org. Chem.*, 2004, **8**, 1105–1134.
- 3 M. A. Grin, A. F. Mironov and A. A. Shtil, *Anti-Cancer Agents Med. Chem.*, 2008, **8**, 683–697.
- 4 J. M. Sutton, N. Fernandez and R. W. Boyle, *J. Porphyrins Phthalocyanines*, 2000, **4**, 655–658.
- 5 J. M. Sutton, O. J. Clarke, N. Fernandez and R. W. Boyle, *Bioconjugate Chem.*, 2002, **13**, 249–263.
- 6 A. M. G. Silva, A. C. Tomé, M. G. P. M. S. Neves, A. M. S. Silva and J. A. S. Cavaleiro, *J. Org. Chem.*, 2005, **70**, 2306–2314.
- 7 J. R. McCarthy, J. Bhaumik, N. Merbouh and R. Weissleder, *Org. Biomol. Chem.*, 2009, **7**, 3430–3436.
- 8 A. C. Tomé, M. G. P. M. S. Neves and J. A. S. Cavaleiro, *J. Porphyrins Phthalocyanines*, 2009, **13**, 408–414.
- 9 S. Singh, A. Aggarwal, S. Thompson, J. P. C. Tomé, X. Zhu, D. Samaroo, M. Vinodu, R. Gao and C. M. Drain, *Bioconjugate Chem.*, 2010, **21**, 2136–2146.
- 10 J. M. Dabrowski, L. G. Arnaut, M. M. Pereira, C. J. P. Monteiro, K. Urbanska, S.

- Simoes and G. Stochel, *ChemMedChem*, 2010, **5**, 1770–1780.
- 11 N. A. M. Pereira, S. M. Fonseca, A. C. Serra, T. M. V. D. Pinho e Melo and H. D. Burrows, *Eur. J. Org. Chem.*, 2011, 3970–3979.
- 12 J. M. Dąbrowski, K. Urbanska, L. G. Arnaut, M. M. Pereira, A. R. Abreu, S. Simões and G. Stochel, *ChemMedChem.*, 2011, **6**, 465–475.
- 13 Z. Yu and M. Ptaszek, *Org. Lett.*, 2012, **14**, 3708–3711.
- 14 V. M. Alexander, K. Sano, Z. Yu, T. Nakajima, P. L. Choyke, M. Ptaszek and H. Kobayashi, *Bioconjugate Chem.*, 2012, **23**, 1671–1679.
- 15 A. Kozyrev, M. Ethirajan, P. Chen, K. Ohkubo, B. C. Robinson, K. M. Barkigia, S. Fukuzumi, K. M. Kadish and R. K. Pandey, *J. Org. Chem.*, 2012, **77**, 10260–10271.
- 16 L. P. Samankumara, S. Wells, M. Zeller, A. M. Acuña, B. Röder and C. Brückner, *Angew. Chem. Int. Ed.*, 2012, **51**, 5757–5760.
- 17 M. M. Pereira, A. R. Abreu, N. P. F. Goncalves, M. J. F. Calvete, A. V. C. Simoes, C. J. P. Monteiro, L. G. Arnaut, M. E. Eusébio and J. Canotilho, *Green Chem.*, 2012, **14**, 1666–1672.
- 18 J. Ogikubo, E. Meehan, J. T. Engle, C. J. Ziegler and C. Brückner, *J. Org. Chem.*, 2013, **78**, 2840–2852.
- 19 M. Galezowski and D. T. Gryko, *Curr. Org. Chem.*, 2007, **11**, 1310–1338.
- 20 C. Brückner, L. Samankumara and J. Ogikubo, in *Handbook of Porphyrin Science*, ed. K. M. Kadish, K. M. Smith and R. Guilard, World Scientific Publishing Co., Singapore, 2012, vol. 17, pp. 1–112.
- 21 H.-J. Kim and J. S. Lindsey, *J. Org. Chem.*, 2005, **70**, 5475–5486.

- 22 M. Kraye, M. Ptaszek, H.-J. Kim, K. R. Meneely, D. Fan, K. Secor and J. S. Lindsey, *J. Org. Chem.*, 2010, **75**, 1016–1039.
- 23 D. Fan, M. Taniguchi and J. S. Lindsey, *J. Org. Chem.*, 2007, **72**, 5350–5357.
- 24 K. E. Borbas, C. Ruzié and J. S. Lindsey, *Org. Lett.*, 2008, **10**, 1931–1934.
- 25 C. Ruzié, M. Kraye, T. Balasubramanian and J. S. Lindsey, *J. Org. Chem.*, 2008, **73**, 5806–5820.
- 26 C. Muthiah, M. Taniguchi, H.-J. Kim, I. Schmidt, H. L. Kee, D. Holten, D. F. Bocian and J. S. Lindsey, *Photochem. Photobiol.*, 2007, **83**, 1513–1528.
- 27 S. Sharma, M. Kraye, F. F. Sperandio, L. Huang, Y.-Y. Huang, D. Holten, J. S. Lindsey and M. R. Hamblin, *J. Porphyrins Phthalocyanines*, **2013**, *17*, 73–85.
- 28 K. Aravindu, O. Mass, P. Vairaprakash, J. W. Springer, E. Yang, D. M. Niedzwiedzki, D. F. Bocian, D. Holten and J. S. Lindsey, *Chem. Sci.*, 2013, **4**, 3459–3477.
- 29 L. Huang, Y.-Y. Huang, P. Mroz, G. P. Tegos, T. Zhiyentayev, S. K. Sharma, Z. Lu, T. Balasubramanian, M. Kraye, C. Ruzié, E. Yang, H. L. Kee, C. Kirmaier, J. R. Diers, D. F. Bocian, D. Holten, J. S. Lindsey and M. R. Hamblin, *Antimicrob. Agents Chemother.*, 2010, **54**, 3834–3841.
- 30 K. R. Reddy, E. Lubian, M. P. Pavan, H.-J. Kim, E. Yang, D. Holten and J. S. Lindsey, *New J. Chem.*, 2013, **37**, 1157–1173.
- 31 E. Yang, C. Kirmaier, M. Kraye, M. Taniguchi, H.-J. Kim, J. R. Diers, D. F. Bocian, J. S. Lindsey and D. Holten, *J. Phys. Chem. B*, 2011, **115**, 10801–10816.

- 32 K. R. Reddy, J. Jiang, M. Krayner, M. A. Harris, J. W. Springer, E. Yang, J. Jiao, D. M. Niedzwiedzki, D. Pandithavidana, P. S. Parkes-Loach, C. Kirmaier, P. A. Loach, D. F. Bocian, D. Holten and J. S. Lindsey, *Chem. Sci.*, 2013, **4**, 2036–2053.
- 33 F. Giuntini, C. M. A. Alonso and R. W. Boyle, *Photochem. Photobiol. Sci.*, 2011, **10**, 759–791.
- 34 H. Tamiaki, M. Xu, T. Tanaka and T. Mizoguchi, *Bioorg. Med. Chem. Lett.*, 2013, **23**, 2377–2379.
- 35 N. Drogat, C. Gady, R. Granet and V. Sol, *Dyes Pigments*, 2013, **98**, 609–614.
- 36 M. A. Grin, I. S. Lonin, L. M. Likhoshevstov, O. S. Novikova, A. D. Plyutinskaya, E. A. Plotnikova, V. V. Kachala, R. I. Yakubovskaya and A. F. Mironov, *J. Porphyrins Phthalocyanines*, 2012, **16**, 1094–1109.
- 37 T. Maisch, C. Bosl, R.-M. Szeimies, N. Lehn and C. Abels, *Antimicrob. Agents Chemother.*, 2005, **49**, 1542–1552.
- 38 H. Taima, A. Okubo, N. Yoshioka and H. Inoue, *Tetrahedron Lett.*, 2005, **46**, 4161–4164.
- 39 H. Taima, A. Okubo, N. Yoshioka and H. Inoue, *Chem. Eur. J.*, 2006, **12**, 6331–6340.
- 40 G. Jori, C. Fabris, M. Soncin, S. Ferro, O. Coppellotti, D. Dei, L. Fantetti, G. Chiti and G. Roncucci, *Lasers Surg. Med.*, 2006, **38**, 468–481.
- 41 T. Maisch, C. Bosl, R.-M. Szeimies, B. Love and C. Abels, *Photochem. Photobiol. Sci.*, 2007, **6**, 545–551.
- 42 G. Simonneaux, P. Le Maux, S. Chevance and H. Srouf, in *Handbook of Porphyrin Science*, ed. K. M. Kadish, K. M. Smith and R. Guilard, World Scientific Publishing

- Co., Singapore, 2012, vol. 21, pp. 377–410.
- 43 C. Spagnul, R. Alberto, G. Gasser, S. Ferrari, V. Pierroz, A. Bergamo, T. Gianferrara and E. Alessio, *J. Inorg. Biochem.*, 2013, **122**, 57–65.
- 44 H. Garcia-Ortega and J. M. Ribo, *J. Porphyrins Phthalocyanines*, 2000, **4**, 564–568.
- 45 I. Batinic-Haberle, J. S. Rebouças, L. Benov and I. Spasojevic, in *Handbook of Porphyrin Science*, ed. K. M. Kadish, K. M. Smith and R. Guilard, World Scientific Publishing Co., Singapore, 2011, vol. 11, pp. 291–393.
- 46 S. J. Griffiths, P. F. Heelis, A. K. Haylett and J. V. Moore, *Cancer Lett.*, 1998, **125**, 177–184.
- 47 Y. Inaba, K. Ogawa and Y. Kobuke, *J. Porphyrins Phthalocyanines*, 2007, **11**, 406–417.
- 48 C. M. Nixon, K. Le Claire, F. Odobel, B. Bujoli and D. R. Talham, *Chem. Mater.*, 1999, **11**, 965–976.
- 49 K. E. Borbas, H. L. Kee, D. Holten, and J. S. Lindsey, *Org. Biomol. Chem.*, 2008, **6**, 187–194.
- 50 M. F. Grahn, A. Giger, A. McGuinness, M. L. de Jode, J. C. M. Stewart, H-B. Ris, H. J. Altermatt and N. S. Williams, *Lasers Med. Sci.*, 1999, **14**, 40–46.
- 51 R. Hornung, M. K. Fehr, H. Walt, P. Wyss, M. W. Berns and Y. Tadir, *Photochem. Photobiol.*, 2000, **72**, 696–700.
- 52 C.-L. Peng, M.-J. Shieh, M.-H. Tsai, C.-C. Chang and P.-S. Lai, *Biomaterials*, 2008, **29**, 3599–3608.

- 53 W. J. Kim, M. S. Kang, H. K. Kim, Y. Kim, T. Chang, T. Ohulchanskyy, P. N. Prasad and K. S. Lee, *J. Nanosci. Nanotechnol.*, 2009, **9**, 7130–7135.
- 54 G. Zheng, A. Graham, M. Shibata, J. R. Missert, A. R. Oseroff, T. J. Dougherty and R. K. Pandey, *J. Org. Chem.*, 2001, **66**, 8709–8716.
- 55 S. K. Pandey, X. Zheng, J. Morgan, J. R. Missert, T.-H. Liu, M. Shibata, D. A. Bellnier, A. R. Oseroff, B. W. Henderson, T. J. Dougherty and R. K. Pandey, *Mol. Pharmaceutics*, 2007, **4**, 448–464.
- 56 K. E. Borbas, V. Chandrashaker, C. Muthiah, H. L. Kee, D. Holten and J. S. Lindsey, *J. Org. Chem.*, 2008, **73**, 3145–3158.
- 57 A. Z. Muresan and J. S. Lindsey, *Tetrahedron*, 2008, **64**, 11440–11448.
- 58 M. Krayner, E. Yang, J. R. Diers, D. F. Bocian, D. Holten and J. S. Lindsey, *New J. Chem.*, 2011, **35**, 587–601.
- 59 T. Ishiyama, M. Murata and N. Miyaura, *J. Org. Chem.*, 1995, **60**, 7508–7510.
- 60 P. W. Shum and A. P. Kozikowski, *Tetrahedron Lett.*, 1990, **31**, 6785–6788.
- 61 B. L. Bray, P. H. Mathies, R. Naef, D. R. Solas, T. T. Tidwell, D. R. Artis and J. M. Muchowski, *J. Org. Chem.*, 1990, **55**, 6317–6328.
- 62 M. Krayner, T. Balasubramanian, C. Ruzié, M. Ptaszek, D. L. Cramer, M. Taniguchi and J. S. Lindsey, *J. Porphyrins Phthalocyanines*, 2009, **13**, 1098–1110.
- 63 O. Mass and J. S. Lindsey, *J. Org. Chem.*, 2011, **76**, 9478–9487.
- 64 H. C. Brown and B. Kanner, *J. Am. Chem. Soc.*, 1953, **75**, 3865.
- 65 T. Masquelin and D. Obrecht, *Synthesis*, 1995, 276–284.

- 66 L. Ghosez, C. Franc, F. Denonne, C. Cuisinier and R. Touillaux, *Can. J. Chem.*, 2001, **79**, 1827–1839.
- 67 T. Fukuda, T. Ohta, E.-I. Sudo and M. Iwao, *Org. Lett.*, 2010, **12**, 2734–2737.
- 68 T. Fukuda and M. Iwao, *Heterocycles*, 2012, **86**, 1261–1273.
- 69 M. Kobayashi, M. Akiyama, H. Kano and H. Kise, in *Chlorophylls and Bacteriochlorophylls: Biochemistry, Biophysics, Functions and Applications*, ed. B. Grimm, R. J. Porra, W. Rüdiger and H. Scheer, Springer, Dordrecht, The Netherlands, 2006, pp. 79–94.
- 70 The examination of absorption upon reciprocal change of concentration and pathlength is time-honored, dating 150 years ago to the development of Beer's law.^{a,b} Such studies have been carried out since to identify deviations from Beer's law particularly due to analyte association phenomena such as aggregation, oligomerization, or complexation.^{c,d} Early experiments relied on variable-pathlength cuvettes (e.g., Baly tubes^{e,f}) whereas a series of fixed-pathlength cuvettes provides more exacting examination across a larger concentration range. Representative chromophores examined in the latter manner include thionine,^{g,h} xanthene,ⁱ uroporphyrin,^j and synthetic *trans*-AB-porphyrins.⁵⁷ (a) Beer, *Ann. Phys. Chem.*, 1852, **86**, 78–88. (b) E. I. Stearns, *The Practice of Absorption Spectrophotometry*, Wiley-Interscience, New York, 1969, pp. 70–72. (c) W. C. Holmes, *Ind. Eng. Chem.*, 1924, **16**, 35–40. (d) W. E. Speas, *Phys. Rev.*, 1928, **31**, 569–578. (e) E. C. C. Baly and C. H. Desch, *Astrophys. J.*, 1906, **23**, 110–127. (f) G. R. Harrison, R. C. Lord and J. R. Loofbourow, *Practical Spectroscopy*, Prentice-Hall, Inc., New York, 1948,

- pp. 371–373. (g) L. F. Epstein, F. Karush and E. Rabinowitch, *J. Opt. Soc. Am.*, 1941, **31**, 77–84. (h) E. Rabinowitch and L. F. Epstein, *J. Am. Chem. Soc.*, 1941, **63**, 69–78. (i) J. E. Selwyn and J. I. Steinfeld, *J. Phys. Chem.*, 1972, **76**, 762–774. (j) D. Mauzerall, *Biochemistry*, 1965, **4**, 1801–1810.
- 71 J. W. Springer, P. S. Parkes-Loach, K. R.; Reddy, M. Krayner, J. Jiao, G. M. Lee, D. M. Niedzwiedzki, M. A. Harris, C. Kirmaier, D. F. Bocian, J. S. Lindsey, D. Holten, P. A. Loach, *J. Am. Chem. Soc.*, 2012, **134**, 4589–4599.
- 72 M. A. Harris, P. S. Parkes-Loach, J. W. Springer, K. R. Reddy, J. Jiang, E. C. Martin, P. Qian, J. Jiao, D. M. Niedzwiedzki, C. Kirmaier, J. D. Olsen, D. F. Bocian, D. Holten, C. N. Hunter, J. S. Lindsey and P. A. Loach, *Chem. Sci.*, 2013, **4**, 3924–3933.
- 73 H. Wolf-Klein, C. Kohl, K. Müllen and H. Paulsen, *Angew. Chem. Int. Ed.*, 2002, **41**, 3378–3380.
- 74 M. Escalante, A. Lenferink, Y. Zhao, N. Tas, J. Huskens, C. N. Hunter, V. Subramaniam and C. Otto, *Nano Lett.*, 2010, **10**, 1450–1457.
- 75 N. Srinivasan, C. A. Haney, J. S. Lindsey, W. Zhang and B. T. Chait, *J. Porphyrins Phthalocyanines*, 1999, **3**, 283–291.
- 76 J. Jiang, P. Vairaprakash, K. R. Reddy, T. Sahin, M. P. Pavan, E. Lubian and J. S. Lindsey, *Org. Biomol. Chem.*, 2014, **12**, 86–103.

CHAPTER 4

Evaluation of Motifs (Carboxylate, Phosphonate, Ammonium and PEG) for Water-Solubilization of Synthetic Bacteriochlorins

Preamble. A prior postdoctor from our group, Kanumuri Ramesh Reddy, synthesized bacteriochlorin **BC1** and corresponding precursors.

Introduction

Methods for the synthesis of hydrophilic tetrapyrroles provide an entrée into diverse areas of scientific investigation ranging from energy sciences to photomedicine. A generic design of hydrophilic tetrapyrroles is to introduce ionized groups (ammonium,¹⁻⁷ sulfonate,⁸⁻¹¹ carboxylate^{12,13} or phosphonate^{14,15}) or polar but nonionic groups (polyethylene glycol¹⁶⁻¹⁹ or glycoside^{20,21}) at synthetically accessible positions. While there are numerous reports concerning the synthesis of hydrophilic tetrapyrroles and their use in aqueous media, as in photodynamic therapy or biomedical imaging, most such reports describe one or a few target compounds of similar structure. Independent studies of water solubility are rarely performed, and the absence of comparative studies of distinct motifs across a common molecular architecture precludes meaningful conclusions about relative merits.

Our interests in preparing hydrophilic tetrapyrroles stems from our objectives in energy sciences, where such macrocycles can be incorporated with peptides to give self-assembled light-harvesting architectures. We previously prepared a hydrophilic bacteriochlorin bearing a 3,5-dicarboxyphenyl motif at the 3,13-positions as well as a maleimide tether for attachment to a peptide (cmpd XII, Chart 4.1).²²

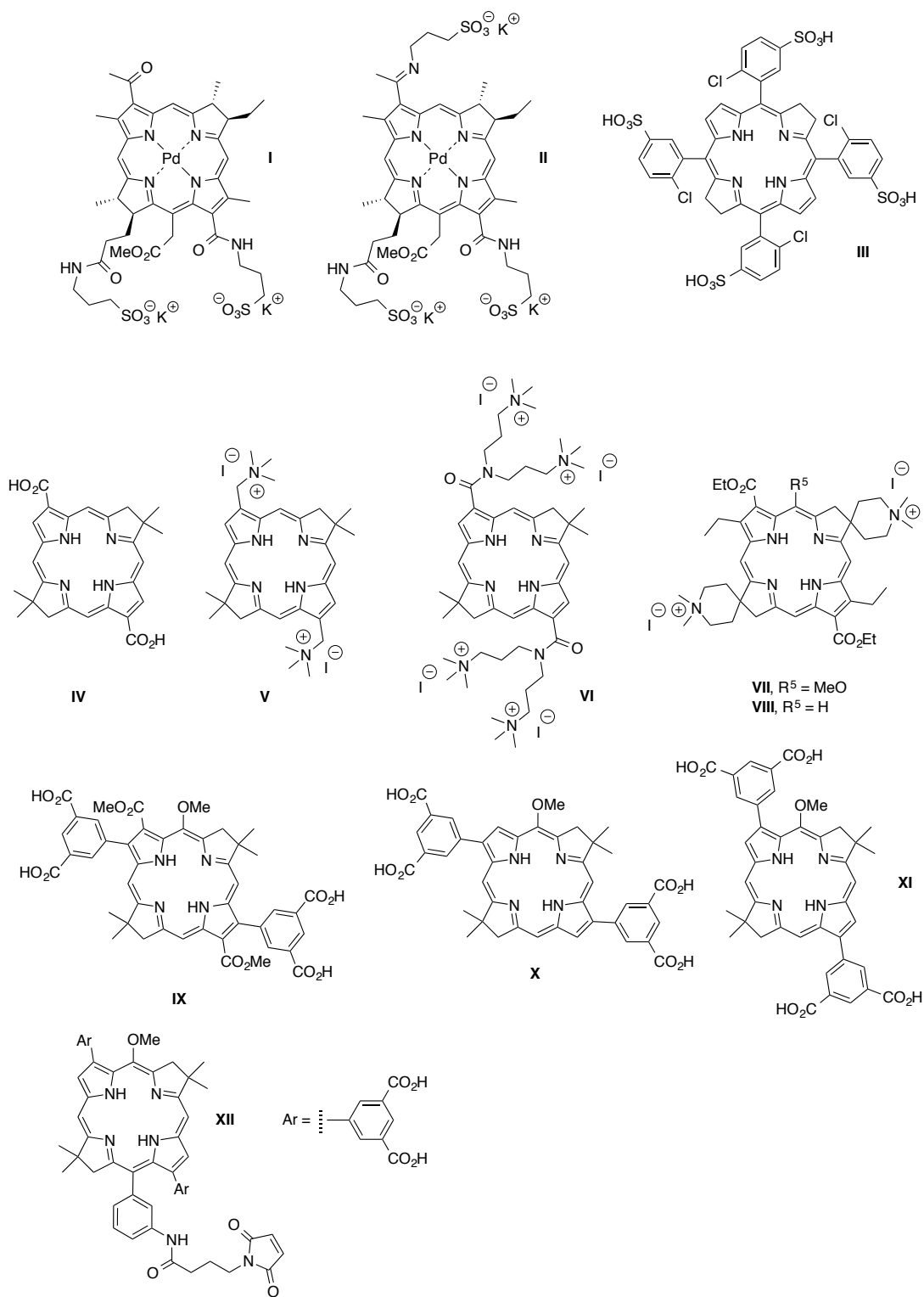


Chart 4.1. Representative hydrophilic bacteriochlorins **I–XII**.

A prevalent design element in the architectures displayed in Chart 4.2 entails positioning of the polar groups above and below the plane of the tetrapyrrole ring. The conceptual underpinning of this design is to shield the intrinsically hydrophobic faces of the tetrapyrrole π system from aqueous solution, by dint of steric bulk and/or electrostatic repulsion, and thereby suppress aggregation. To gain a better understanding of the virtues and limitations of the various types of solubilizing motifs, we prepared a set of bacteriochlorins (**BC1–BC5**) encompassing phosphonate (**BC1**), carboxylate (**BC2**), ammonium (for **BC3** and **BC4**), or PEG (**BC5**) moieties (Chart 4.2). Bacteriochlorins **BC3** and **BC4** both bear four ammonium groups but differ in that the former is more compact and has benzylammonium units whereas the latter contains alkylammonium groups attached via ester moieties. Bacteriochlorin **BC2** was prepared previously.²² Each bacteriochlorin in the set contains a common scaffold and was derived by Suzuki coupling with 3,13-dibromobacteriochlorin (**BC-Br**^{3,13}).

In this paper, we report the synthesis of the four new bacteriochlorins. A comprehensive comparison among the five bacteriochlorins has been made, regarding the synthesis amenability, photophysical properties (full-width-at-half-maximum, fwhm of absorption and fluorescence emission spectra, and Φ_f value), stability and ease of derivatization. The synthetic strategy, methods of evaluation, and results obtained should be applicable across the tetrapyrrole family of macrocycles.

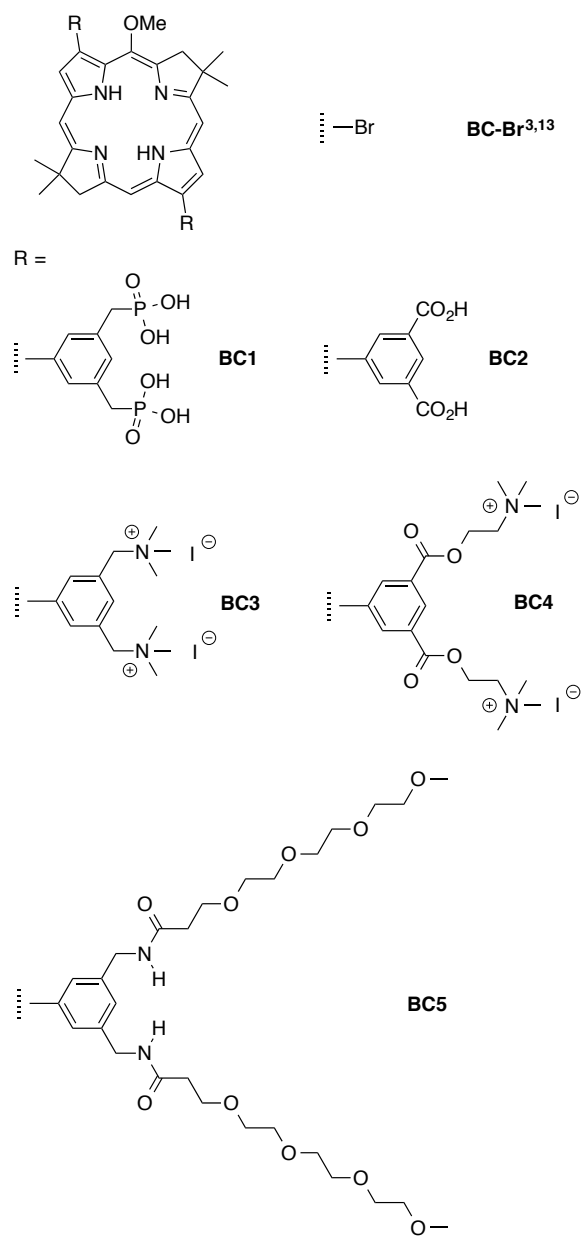
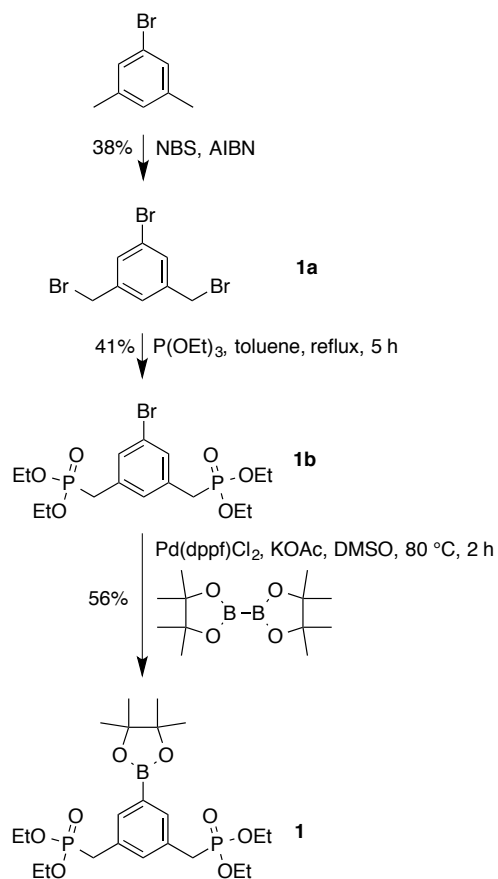


Chart 4.2. Bacteriochlorin scaffold and distinct water-solubilizing groups.

Results and discussion

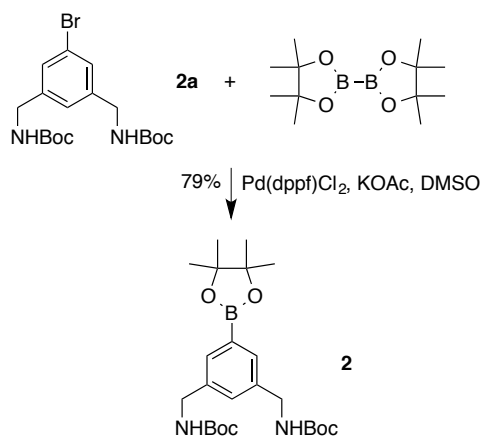
(I) Synthesis

(A) **Suzuki coupling partners.** The synthesis of all the bacteriochlorins entails Suzuki coupling of the dibromobacteriochlorin **BC-Br**^{3,13} with an aryl boronate ester. The synthesis of the phosphono Suzuki coupling partner is shown in Scheme 4.1. 1-Bromo-3,5-dimethylbenzene was dibrominated with NBS to give the known 1-bromo-3,5-bis(bromomethyl)benzene (**1a**),²³ which was prepared here at 14-fold larger scale, isolated without chromatography, and fully characterized. Treatment of **1a** with triethyl phosphite in toluene afforded the corresponding phosphonate **1b** in 41% yield. Pd-mediated coupling of **2** with bis(pinacolato)diboron gave diethyl phosphonate **1** in 56% yield.



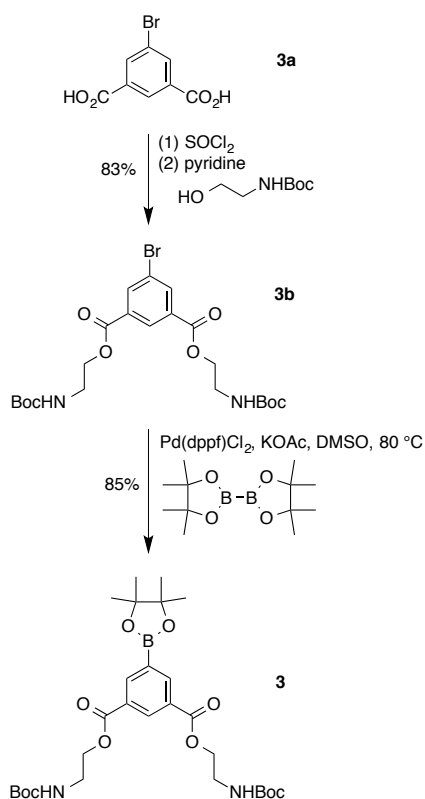
Scheme 4.1. Synthesis of diphosphono Suzuki coupling partner **1**.

Pd-mediated coupling of the known Boc-protected 3,5-bis(aminomethyl)bromobenzene **2a**²⁴ with bis(pinacolato)diboron gave the Suzuki coupling partner **2** in 79% yield (Scheme 4.2).



Scheme 4.2. Synthesis of bis(aminomethyl)phenyl Suzuki coupling partner **2**.

Acylation of commercially available 5-bromoisophthalic acid (**3a**) with thionyl chloride afforded 5-bromoisophthaloyl dichloride, which was directly treated with *N*-(*tert*-butoxycarbonyl)ethanolamine in pyridine at 0 °C to give Boc-protected 3,5-dicarboxy-5-bromobenzene **3b** in 83% yield for two steps (Scheme 4.3). Pd-mediated coupling of **3b** with bis(pinacolato)diboron gave Suzuki coupling partner **3** in 85% yield.

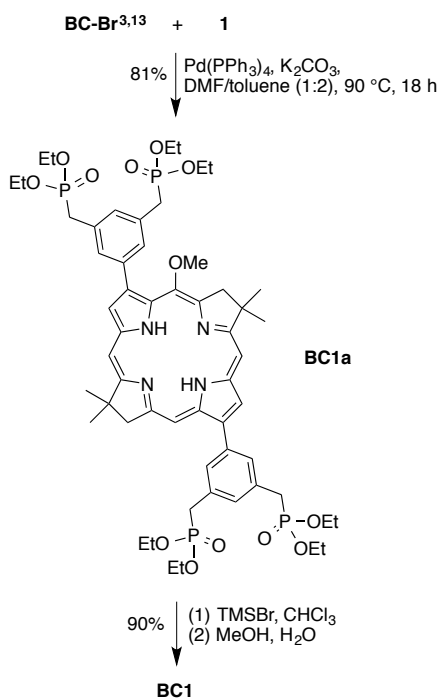


Scheme 4.3. Synthesis of Suzuki coupling partner **3**.

(B) Hydrophilic bacteriochlorins. The synthesis of the set of hydrophilic bacteriochlorin relies on the following strategy: (1) introduce the protected water-solubilizing moiety by Suzuki coupling reaction of **BC-Br**^{3,13} with the above-mentioned coupling partners **1–3**; and (2) remove the protecting group to give the hydrophilic bacteriochlorins directly (for **BC1** and **BC2**), or followed by quaternization (for **BC3** and **BC4**) or PEGylation (for **BC5**).

Suzuki coupling of **BC-Br**^{3,13} with **1** gave the protected phosphono bacteriochlorin **BC1a** in 81% yield. The ethyl protecting groups were removed by treatment with 80 equiv of bromotrimethylsilane (TMSBr)^{14,25} in CHCl₃ followed by hydrolysis in methanol and

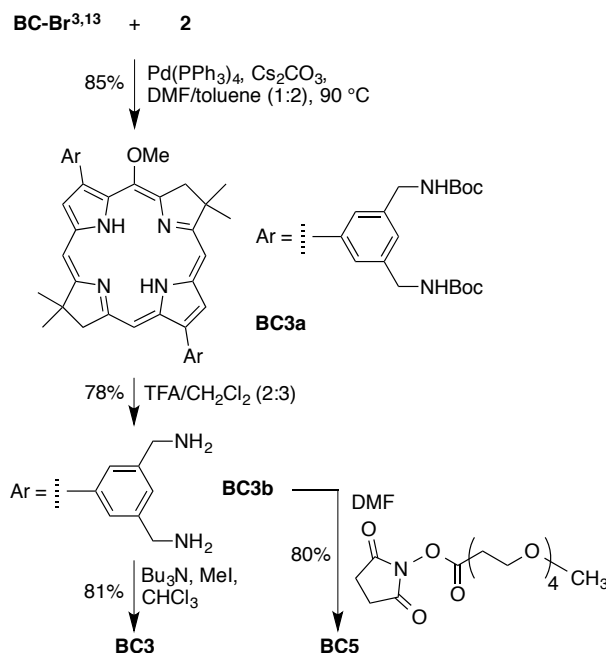
water (Scheme 4.4). In this manner, **BC1** was obtained from the respective protected counterparts in 90% yield. The chemoselectivity and essentially quantitative nature of the protecting group cleavage reactions enabled the resulting bacteriochlorin **BC1** to be characterized and used directly without purification.



Scheme 4.4. Synthesis of phosphono bacteriochlorin **BC1**.

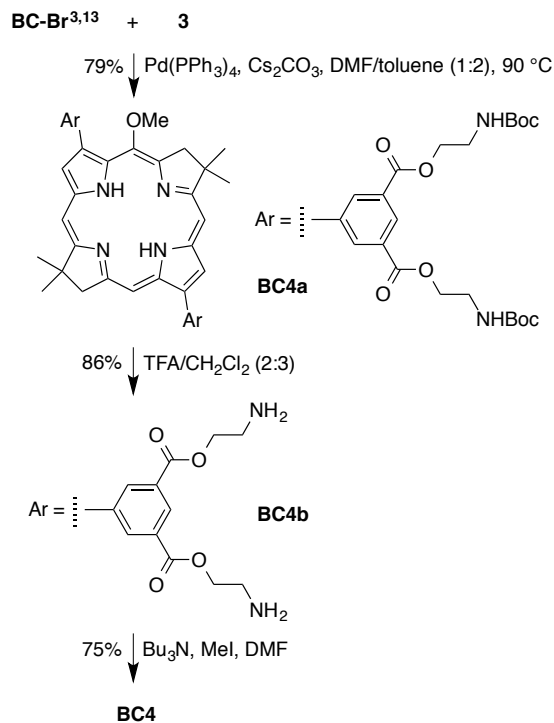
Suzuki reaction with coupling partner **2** gave the corresponding 3,13-diarylbacteriochlorin (**BC3a**), which upon exposure to TFA in CH₂Cl₂ gave bacteriochlorin **BC3b** in 78% yield (Scheme 4.5). The tetraaminobacteriochlorin provided a common precursor to both **BC3** and **BC5**. Quaternization with iodomethane in the presence of tributylamine (Bu₃N) gave ammoniobacteriochlorin **BC3** in 81% yield. The use of Bu₃N is

to (i) neutralize the protonated tetraamine derived from TFA, (ii) sponge up the byproduct HI, and (iii) facilitate removal of its protonated form by washing with THF. The removal of protonated Bu_3N by washing with THF is easier than that of triethylamine. PEGylation of **BC3b** with PEG4 NHS ester gave bacteriochlorin **BC5** in 80% yield.



Scheme 4.5. Synthesis of ammoniobacteriochlorin **BC3** and PEGylated bacteriochlorin **BC5**.

Suzuki reaction with coupling partner **3** gave the corresponding 3,13-bis(3,5-dicarboxyaryl)bacteriochlorin (**BC4a**) in 79% yield (Scheme 4.6). Following the same approach as with **BC3a**, deprotection of **BC4a** and subsequent quaternization afforded **BC4** in 86% and 75% yield for the two sequential steps.



Scheme 4.6. Synthesis of bacteriochlorin **BC4**.

The bacteriochlorins typically were characterized by absorption and fluorescence spectroscopy, ¹H NMR spectroscopy, ¹³C NMR spectroscopy (where quantity and solubility allowed), MALDI mass spectrometry, and ESI mass spectrometry. Exceptions include **BC1**, for which mass spectra could not be obtained (regardless of matrix examined for MALDI-MS), but each gave a clean ¹H NMR spectrum and characteristic bacteriochlorin absorption and emission spectra.

All five water-solubilizing motifs exhibit potentially distinct charged states in aqueous media, hence it is of interest to study the observed charged state from the mass spectrometry analysis. As summarized in Table 4.1, **BC1** did not give a detectable signal for

either MALDI/ESI-MS analysis. **BC2** and **BC5** each displayed a mono-cationic species upon both MALDI-MS and ESI-MS analysis. **BC3** and **BC4** are permanently charged (tetraammonio) and no signal was obtained upon MALDI-MS analysis using various matrices (POPOP, CHCA and sinapic acid). On the other hand, a quadruply charged species ($m/z = \text{obsd } 210.1528$ for **BC3** and 268.1584 for **BC4**, respectively, where $z = 4$) was observed upon ESI-MS analysis.

Table 4.1. Detected charge states of **BC1–BC5** upon MALDI- and ESI-MS analysis.

Compound	MALDI-MS charge state	ESI-MS charge state
BC1	N.O. ^a	N.O.
BC2	+1	+1
BC3	N.O.	+4
BC4	N.O.	+4
BC5	+1	+1

^aNot observed.

(II) Photophysical properties

(A) Absorption and emission spectra. The absorption and emission spectra were collected in *N,N*-dimethylformamide (DMF), aqueous potassium phosphate buffer (0.5 M, pH 7.0), and in one case, water. The parameters of interest include (1) the position of the long-wavelength absorption (Q_y) band, (2) the position of the fluorescence emission band, (3) the sharpness of the absorption Q_y band and fluorescence emission band, measured by the fwhm, and (4) the fluorescence quantum yield (Φ_f). All of these parameters are listed in

Table 4.1. All five bacteriochlorins exhibit similar absorption and emission patterns, hence the spectrum of only one representative bacteriochlorin (**BC3**, in phosphate buffer) is displayed in Figure 4.1.

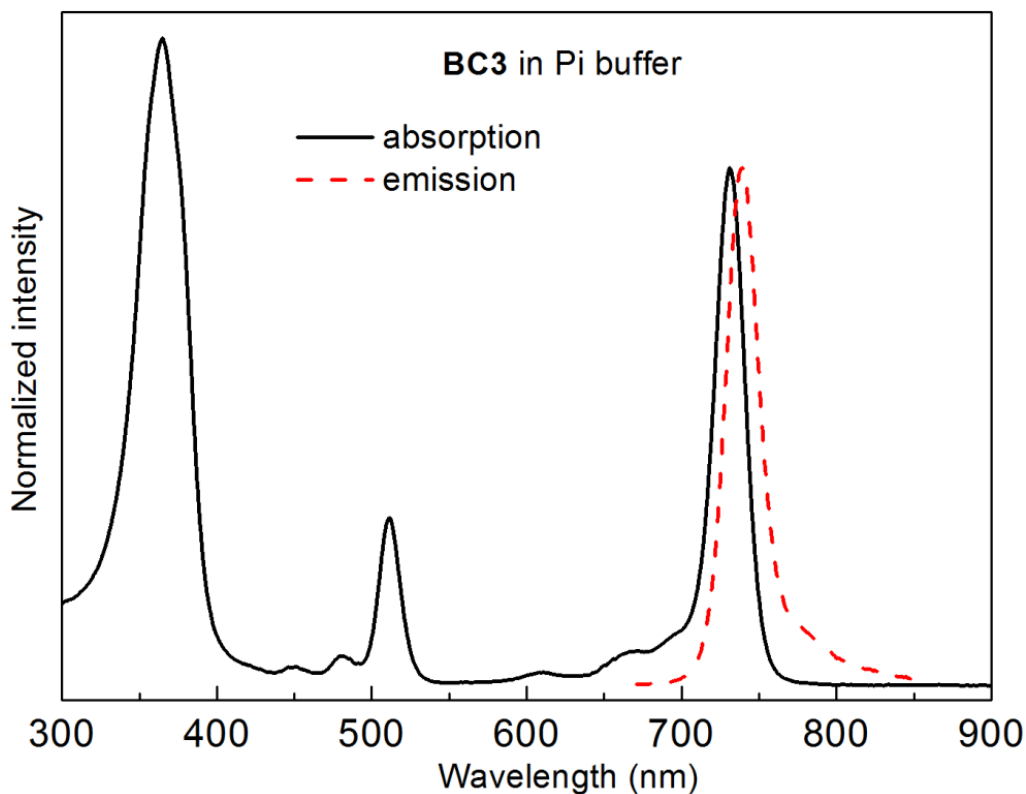


Figure 4.1. Normalized absorption spectra (solid) and emission spectra (dashed) of **BC3** in aqueous potassium phosphate buffer (0.5 M, pH 7.0) at room temperature. Spectral parameters are given in Table 4.2.

The key findings are as follows: (1) all bacteriochlorins exhibit characteristic absorption peaks of the bacteriochlorin chromophores: strong Soret bands in the UV region, modest Q_x band in the green-yellow region, and intense Q_y band in the NIR region; (2) all bacteriochlorins displayed sharp absorption and emission bands with fwhm 21–31 nm; (3) the hydrophilic bacteriochlorins and

the corresponding precursors exhibited similar F_f values in DMF, indicating that the introduction of the water-solubilizing motifs to bacteriochlorins do not impart a significant adverse effect on the excited-state properties; while the F_f values of the hydrophilic bacteriochlorins in aqueous solutions decrease to ~30–90% of the same compounds in DMF. A similar diminution upon examination in aqueous solution was observed with hydrophilic chlorins²³⁶ and bacteriochlorins.³¹²

(B) Effect of concentration on spectral properties. Absorption versus concentration studies were conducted to assess the aqueous solution properties of the bacteriochlorins over a concentration range of 1000-fold (~200–600 μM to ~0.2–0.6 μM). This type of study has been explained in detail,²² and the same approach was adopted herein. The experimental approach entails reciprocal variation of concentration and cuvette pathlength (0.1 – 10 cm) upon absorption spectroscopy, as outlined in Figure 4.2. Aqueous potassium phosphate buffer (0.5 M, pH 7.0) was used for **BC1–BC4**, and neat water was used for **BC5**. The initial dissolution was facilitated by use of 5% DMSO. The co-solvent was not needed in all cases, but was included in each sample for consistency.

Table 4.2. Absorption and fluorescence properties of bacteriochlorins.^a

reference	Compound	Solvent	λ_{abs} , nm	FWHM nm (Abs)	λ_{em} , nm	FWHM nm (Flu)	Φ_f
here	BC1a	DMF	729	21	736	23	0.20
here	BC1^b	Pi buffer ^c	730	29	735	28	0.060
312	BC2a	DMF	731	24	738	25	0.18
312	BC2	DMF	729	22	735	23	0.19
312	BC2	Pi buffer ^c	730	26	736	26	0.078
here	BC3a	DMF	729	21	734	23	0.20
here	BC3	DMF	731	23	737	24	0.17
here	BC3	Pi buffer ^c	732	25	739	26	0.11
here	BC4a	DMF	730	23	738	23	0.19
here	BC4	DMF	732	23	738	24	0.16
here	BC4	Pi buffer ^c	731	31	738	24	0.053
here	BC5	DMF	729	22	736	23	0.16
here	BC5	Water	728	23	733	23	0.14

^aEach sample in aqueous solution contains 1% DMF to facilitate initial dissolution. ^b**BC1** does not dissolve in DMF, so no data were collected in DMF. ^cPi buffer: 0.5 M potassium phosphate pH 7.0.

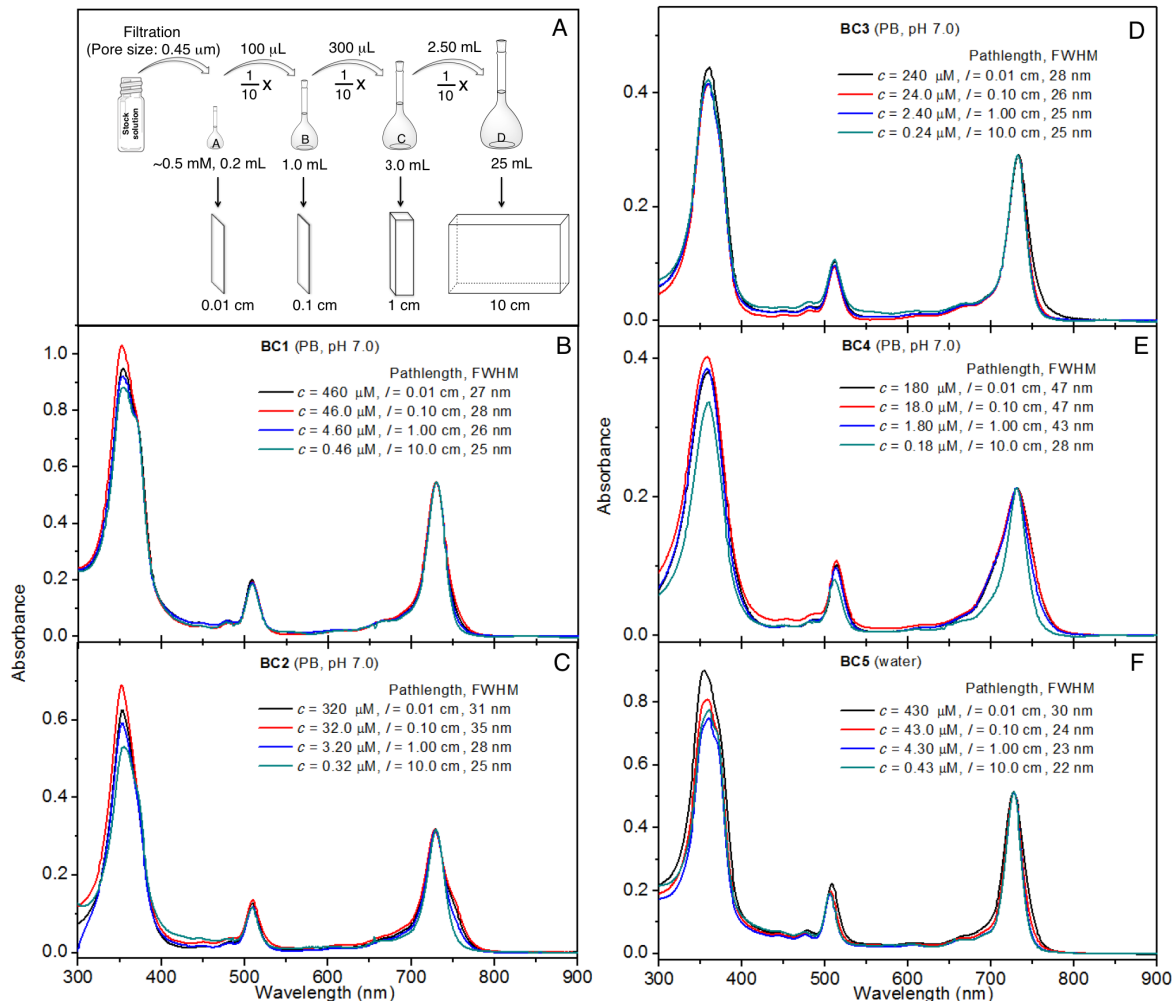


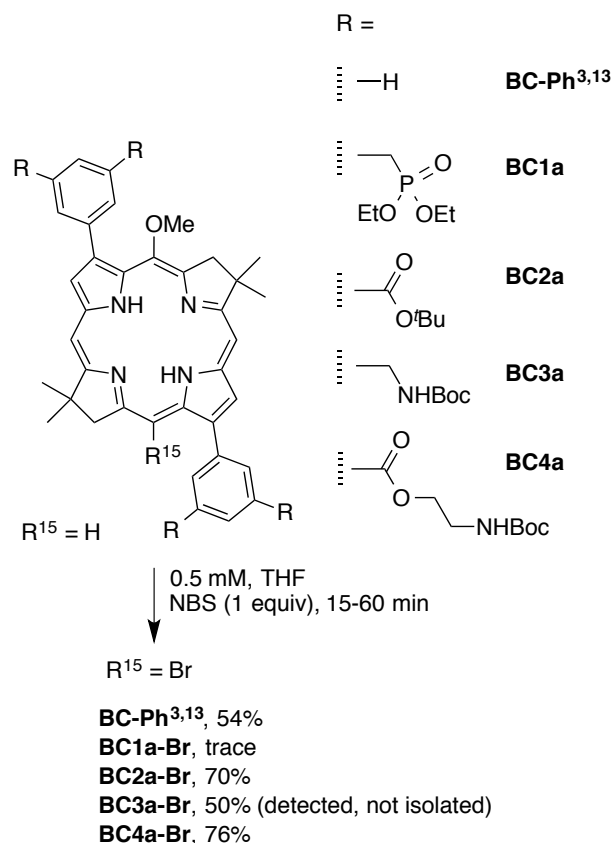
Figure 4.2. Flowchart for absorption versus concentration study (panel A). Absorption versus concentration of **BC1–BC5** each over a range of 1000-fold (panels B–F). All spectra were normalized at the Q_y band. The concentration was calculated based on absorption in the 1-cm cuvette, assuming $\epsilon(Q_y) = 120,000 \text{ M}^{-1}\text{cm}^{-1}$.

The spectra for each bacteriochlorin are shown in Figure 4.2. While **BC2** and **BC4** displayed obvious band broadening showing some degree of aggregation, **BC1**, **BC3** and **BC5** exhibited almost unchanged spectroscopic properties though the concentration changes

over a range of 1000-fold. At all concentrations for all five bacteriochlorins, the samples remained clear upon visual inspection indicating the absence of precipitates.

(III) 15-Bromination study

A potential application of the hydrophilic bacteriochlorins entails the introduction of a conjugatable tether for attachment to proteins or surfaces. One strategy in this regard relies on bromination at the 15-position of the macrocycle,²⁷ which is known to occur with a high degree of regioselectivity for many but not all 5-methoxybacteriochlorins. The known examples of 15-bromination of 5-methoxybacteriochlorins bearing diverse substituents at the β -positions (2, 12, 3, 13 positions) have been summarized.²² In this regard, the 5-methoxybacteriochlorin bearing phenyl groups at the 3,13-positions underwent bromination at the 15-position to give the corresponding bromobacteriochlorin in 54% yield.²² **BC2a** similarly gave the 15-brominated bacteriochlorin in 70% yield.²² These examples and the results with the three other bacteriochlorin precursors are shown in Scheme 4.7.



Scheme 4.7. 15-Bromination of bacteriochlorin precursors **BC1a–BC4a**.

Treatment of **BC1a** under similar or somewhat more forcing bromination conditions (50 °C and reaction time prolonged to 12 h) afforded only a trace amount of the desired product **BC1a-Br**, measured by MADLI-MS, whereas the majority was unreacted material. **BC3a** exhibited better activity and gave an almost 1:1 mixture of brominated product **BC3a-Br** and starting material, measured by MALDI-MS assuming equal ionization efficiencies of these two species; however, the reaction mixture could not be isolated. **BC4a** showed similar activity to **BC2a** (both bear alkoxy carbonylmethylaryl moieties), and yielded the desired isolated product **BC4a-Br** in 76% yield.

(IV) Comparison

The suitability of the solubilization motifs incorporated in **BC1–BC5** for bioconjugation studies depends on a host of factors including synthetic accessibility and photophysical parameters. Six features were considered in this regard. The features include (1) synthesis yield from the common precursor **BC-Br**^{3,13}, (2) ease of 15-bromination, (3) fwhm of the long-wavelength (Q_y) absorption band, (4) Φ_f in aqueous solution, (5) stability upon standing, and (6) ease of purification of the target compound. Synthesis amenability is measured here by the total yield beginning with the Suzuki coupling reaction of the 3,13-dibromobacteriochlorin and all subsequent steps. The rationale for emphasis on the 15-bromination is because low yields in this step present a difficult separation problem; hence, 15-bromination can be a key bottleneck in preparation of bioconjugatable analogues. Bacteriochlorin stability is measured by the extent of bacteriochlorin (%) remaining after standing for 48 h at 4 °C in the dark, determined by the Q_y absorption intensity. Methods for purification of hydrophilic compounds **BC1–BC5** vary with the distinct solubilization motifs.

The results for the five bacteriochlorins assessed against these criteria are listed in Table 4.3. Little distinction was observed for synthesis yields, with the range of 51-73% likely subject to improvement for any of the bacteriochlorins via further optimization. **BC1** shows a relatively broad Q_y band, low Φ_f value, and the least stability of the set, but most importantly, the precursor of **BC1** is the only bacteriochlorin examined herein that could not be brominated. Until methods of 15-bromination or alternative strategies for incorporation of a bioconjugatable tether are identified, this latter result at present disqualified the phosphonate motif for a variety of applications. **BC2** and **BC4** gave high stability, and their

precursors (an aryldiester) gave facile 15-bromination, yet both gave lower Φ_f values. **BC3** and **BC5** gave the narrowest band shape and the highest Φ_f values. **BC3** and **BC5** also share a common precursor (**BC3a**), which upon 15-bromination yielded a mixture of starting material and the desired product.

The purification procedures for the final compounds vary considerably. The final step in the synthesis of **BC1** entailed TMS-Br-mediated cleavage of the ethyl phosphonate protecting groups. **BC1** was purified by deprotonation of the phosphonic acid with sodium hydroxide solution (so as to make the compound more polar) followed by reversed phase column chromatography (C18, 5-cm length and 1-cm diameter) using H₂O/MeOH (from 99:1 to 99:5) as the co-eluent. The final step in the synthesis of **BC2** entailed TFA-mediated cleavage of the *tert*-butyl carboxylate protecting groups. **BC2** was purified by partitioning into the organic phase (from aqueous acid) followed by washing the solid with hexanes/methanol (49:1).²² The final step in the syntheses of ammonium bacteriochlorins **BC3** and **BC4** does not entail deprotection but rather quaternization of the free amines with methyl iodide. **BC3** and **BC4** were purified by addition of ether/THF (1:1) followed by sonication, centrifugation and decanting of the supernatant to remove excessive methyl iodide and protonated tributylamine. The final step in the synthesis of **BC5** also does not entail deprotection, but rather amidation of the free amines with the PEG-NHS ester. Purification was achieved first by washing with aqueous NaHCO₃ solution to remove DMF, followed by washing the residue with hexanes/CH₂Cl₂ (19:1) to remove excessive PEG4-NHS ester or the hydrolyzed product PEG4 carboxylic acid.

Table 4.3. Properties of hydrophilic bacteriochlorins **BC1–BC5**.

Cmpd	Synthesis yield	Derivatization ^b (15-bromination)	fwhm nm (Flu) ^a	Φ_f^a	Stability	Purification methods
BC1	73%	No	29	0.060	85%	C18 chromatography
BC2	55%	Yes	26	0.078	96%	Ppt, washing with hexanes/methanol (49:1)
BC3	54%	Yes, mixture	25	0.11	82%	Ppt, washing with ether/THF (1:1)
BC4	51%	Yes	31	0.053	96%	
BC5	53%	Yes, mixture	23	0.14	95%	Ppt, washing with hexanes/CH ₂ Cl ₂ (19:1)

^aData collected from samples in potassium phosphate buffer (0.5 M, pH 7.0).

^bBromination was conducted on the relevant precursors (**BC1a**, **BC2a**, **BC3a**, **BC4a**).

In summary, the ammonium-, carboxylate-, and PEG-substituted bacteriochlorins all appear suitable for use with bioconjugatable tethers. The particular choice depends, of course, on application. For applications where fluorescence (Φ_f , sharpness of emission) is an important parameter, the nonionic yet polar PEG-bacteriochlorin appears superior, with the incomplete 15-bromination as the only drawback if this route is employed to install a bioconjugatable tether.

Experimental section

(I) General methods

^1H NMR and ^{13}C NMR spectroscopies were performed at room temperature. ^{31}P (162 MHz) chemical shifts are reported versus the resonance of phosphoric acid (H_3PO_4) as an external reference (insert tube). Tetramethylsilane was used as internal reference for CDCl_3 . In ^{13}C NMR spectroscopy of selected compounds, not all quaternary carbons were observed. MALDI-MS was performed with the matrix 1,4-bis(5-phenyl-2-oxazol-2-yl)benzene (POPOP) for bacteriochlorins,²⁸ except that α -cyano-4-hydroxycinnamic acid (CHCA) was used for **BC5**. Electrospray ionization mass spectrometry (ESI-MS) data are reported for the molecular ion. Silica gel (40 μm average particle size) was used for column chromatography. All solvents were reagent grade and were used as received unless noted otherwise. THF was freshly distilled from sodium/benzophenone ketyl. CHCl_3 was stabilized with amylenes ($\leq 1\%$). Known compounds **1a**,²³ **2a**,²⁴ **BC-Br**,^{3,13,29} **BC2a**,²² and **BC2**²² were prepared following literature procedures. All other compounds were used as received from commercial sources. For ammoniobacteriochlorins **BC3** and **BC4**, yield calculations were carried on the assumption of the presence of the tetraiodide salt.

(II) Synthesis

1-Bromo-3,5-bis(bromomethyl)benzene (1a). Following a general procedure,²³ a mixture of 1-bromo-3,5-dimethylbenzene (14.8 g, 80.0 mmol), NBS (28.5 g, 160 mmol), and AIBN (0.657 g, 4.00 mmol, 5 mol%) in acetonitrile (400 mL) was refluxed under argon for 5 h. The mixture was concentrated. CCl_4 (75.0 mL) was added with heating to dissolve the crude product. The reaction mixture was allowed to cool and then filtered to remove any

undissolved succinimide. The filtrate was concentrated to afford the crude product, which upon crystallization from ethanol afforded white crystals (10.5 g, 38%): mp 91–93 °C; ^1H NMR (300 MHz, CDCl_3) δ 4.40 (s, 4H), 7.32–7.35 (m, 1H), 7.47 (d, $J = 1.8$ Hz, 2H); ^{13}C NMR δ 31.7, 122.9, 128.5, 132.2, 140.5; Anal. Calcd. C, 28.03; H, 2.06. Found C, 28.03; H, 1.98.

1-Bromo-3,5-bis(diethylphosphonomethyl)benzene (1b). Following a general procedure,²³ a solution of **1a** (19.0 g, 55.0 mmol) and triethyl phosphite (18.6 g, 100 mmol) in toluene (30.0 mL) was refluxed under argon for 5 h. The reaction mixture was allowed to cool to room temperature whereupon toluene was removed by rotary evaporation. The resulting oily liquid was dissolved in CHCl_3 , washed with water, dried (Na_2SO_4), concentrated and purified by a short chromatography column [silica, ethyl acetate/hexanes (1:1)] to obtain a colorless liquid (10.5 g, 41%): ^1H NMR (300 MHz, CDCl_3) δ 1.27 (t, $J = 7.2$ Hz, 12H), 3.09 (t, $J = 22.2$ Hz, 4H), 3.94–4.10 (m, 8H), 7.14–7.18 (m, 1H), 7.33–7.37 (m, 2H); ^{13}C NMR δ 16.5–16.6 [m, (this multiplet contains three peaks at δ 16.51, 16.53, 16.56, which may stem from merging of a doublet of doublets)], 33.4 (d, $J = 138$ Hz), 62.4–62.5 [m (this multiplet contains three peaks at δ 62.42, 62.46, 62.49, which may stem from merging of a doublet of doublets)], 122.5, 130.0–130.3 [m, (this multiplet contains three peaks at δ 130.04, 130.10, 130.17, may be because of merging doublet of doublet)], 131.2–131.5 [m, (this multiplet contains three peaks at δ 131.38, 131.44, 131.48, which may stem from merging of a doublet of doublets)], 134.0–134.4 [m, (which may stem from merging of a doublet of doublets)]; ^{31}P NMR δ 25.86; ESI-MS obsd 457.0540, calcd 457.0539 [(M + H)⁺, M = $\text{C}_{16}\text{H}_{27}\text{BrO}_6\text{P}_2$].

2-[3,5-Bis(diethylphosphonomethyl)phenyl]-3,3,4,4-tetramethyl-1,3,2-dioxaborolane (1). Following a general procedure,³⁰ a mixture of Pd(dppf)Cl₂ (0.132 g, 0.180 mmol, 3 mol%), KOAc (1.76 g, 18.0 mmol) and bis(pinacolato)diboron (1.67 g, 6.60 mmol) in a Schlenk flask was deaerated under high vacuum for 20 min. Then, a solution of DMSO (18 mL) containing **1b** (2.74 g, 6.00 mmol) (degassed for 10 min) was added under argon, and the reaction mixture was degassed by three freeze–pump–thaw cycles. The mixture was stirred at 80 °C for 2 h. The starting material and product co-chromatograph upon TLC analysis (silica, ethyl acetate/hexanes (1:1)). Hence, progress of the reaction mixture was monitored by ¹H NMR spectroscopy (the aromatic protons of the product are deshielded compared with those of the starting material) whereupon a new peak was observed at δ 1.33 ppm. The reaction mixture was allowed to cool to room temperature. The mixture was diluted with ethyl acetate, washed with water, dried (Na₂SO₄), and concentrated. The resulting residue was purified by column chromatography [silica, ethyl acetate/hexanes (1:1)] to obtain a light brown liquid (1.7 g, 56%): ¹H NMR (300 MHz, CDCl₃) δ 1.22–1.29 (m, 12H), 1.33 (s, 12H), 3.14 (d, *J* = 21.6 Hz, 4H) 3.95–4.10 (m, 8H), 7.34–7.38 (m, 1H), 7.58–7.64 (m, 2H); ¹³C NMR (75 MHz, CDCl₃) δ 16.5 (d, *J* = 6.8 Hz), 25.0, 33.6 (d, *J* = 137.2 Hz), 62.3 (d, *J* = 6.8 Hz), 84.0, 131.5, 133.8–134.2 [m, (this multiplet contains three peaks at δ 133.97, 134.03, 134.09, perhaps due to merging of a doublet of doublets)], 134.8–135.1 [m, (this multiplet contains three peaks at δ 134.92, 134.97, 135.02, perhaps due to merging of a doublet of doublets)]; ³¹P NMR, δ 26.91; ESI-MS obsd 505.2288, calcd 505.2286 [(M + H)⁺, M = C₂₂H₃₉BO₈P₂].

2-[3,5-Bis(*tert*-butoxycarbonamidomethyl)phenyl]-3,3,4,4-tetramethyl-1,3,2-dioxaborolane (2). Following a general procedure,³⁰ samples of **2a** (1.25 g, 3.00 mmol), bis(pinacolato)diboron (761 mg, 3.00 mmol), Pd(dppf)Cl₂ (65.9 mg, 90.0 μmol), KOAc (883 mg, 9.00 mmol), and DMSO (20.0 mL, deaerated by bubbling with argon for 30 min) were added to a Schlenk flask. The reaction mixture was deaerated by three freeze-pump-thaw cycles. The reaction mixture was stirred at 80 °C under argon for 16 h. The reaction mixture was cooled to room temperature, diluted with ethyl acetate and washed with brine. The organic layer was separated, dried (Na₂SO₄) and concentrated. Column chromatography [silica, hexanes/CH₂Cl₂ (3:2)] provided a viscous liquid (1.10 g, 79%): ¹H NMR (400 MHz, CDCl₃) δ 1.34 (s, 12H), 1.46 (s, 18H), 4.32 (d, *J* = 5.2 Hz, 4H), 4.82 (br, 2H), 7.31 (s, 1H), 7.61 (s, 2H); ¹³C NMR (100 MHz, CDCl₃) δ 25.1, 28.6, 44.8, 84.2, 129.8, 133.0, 138.8, 156.1; ESI-MS obsd 485.2792, calcd 485.2793 [(M + Na)⁺, M = C₂₄H₃₉BN₂O₆].

Bis[2-(*tert*-butoxycarbonamido)ethyl] 5-bromoisophthalate (3b). A sample of 5-bromoisophthalic acid (**3a**, 490 mg, 2.00 mmol) in SOCl₂ (5.00 mL) was stirred under argon at 65 °C for 16 h. The solvent was removed under vacuum. The residue was slowly treated with a solution of *N*-(*tert*-butoxycarbonyl)ethanolamine (800 mg, 5.00 mmol) in pyridine (4.50 mL) in an ice bath. The reaction mixture was stirred under argon at room temperature for 16 h. The reaction mixture was diluted with ethyl acetate, and then washed with 1 N HCl solution and brine. The aqueous solution was extracted three times with ethyl acetate. The combined organic extract was dried (Na₂SO₄), concentrated and chromatographed [silica, CH₂Cl₂/ethyl acetate (9:1)] to afford a white sticky solid (882 mg, 83%): ¹H NMR (400 MHz, CDCl₃) δ 1.44 (s, 18H), 3.53–3.59 (m, 4H), 4.42 (t, *J* = 5.2 Hz, 4H), 5.20 (br, 2H), 8.32 (d, *J*

= 1.6 Hz, 2H), 8.58 (s, 1H); ^{13}C NMR (100 MHz, CDCl_3) δ 28.6, 39.8, 65.4, 79.8, 122.8, 129.6, 132.3, 136.9, 156.1, 164.6; ESI-MS obsd 553.1148, calcd 553.1156 [(M + Na) $^+$, M = $\text{C}_{22}\text{H}_{31}\text{O}_8\text{N}_2\text{Br}$].

Bis[2-(*tert*-butoxycarbonamido)ethyl] 5-(4,4,5,5-tetramethyl-1,3,2-dioxaborolan-2-yl)isophthalate (3). Following a general procedure,³⁰ samples of **3b** (0.593 g, 1.12 mmol), bis(pinacolato)diboron (283 mg, 1.116 mmol), Pd(pddf)Cl₂ (40.8 mg, 55.8 μmol), KOAc (329 mg, 3.35 mmol), and DMSO (5.6 mL, deaerated by bubbling with argon for 30 min) were added to a Schlenk flask. The reaction mixture was deaerated by three freeze-pump-thaw cycles. The reaction mixture was stirred at 80 °C for 4 h. The reaction mixture was cooled to room temperature, diluted with ethyl acetate and washed with brine. The organic layer was separated, dried (Na_2SO_4) and concentrated. Column chromatography [silica, CH_2Cl_2 /ethyl acetate (17:3)] provided a white sticky solid (548 mg, 85%): ^1H NMR (400 MHz, CDCl_3) δ 1.34 (s, 12H), 1.43 (s, 18H), 3.58 (m, 4H), 4.45 (t, J = 5.2 Hz, 4H), 5.42 (s, 2H), 8.61 (d, J = 2.0 Hz, 2H), 8.74 (t, J = 2.0 Hz, 1H); ^{13}C NMR (100 MHz, CDCl_3) δ 25.0, 28.5, 39.8, 64.9, 79.5, 84.6, 130.0, 133.6, 140.2, 156.1, 165.9; ESI-MS obsd 601.2908, calcd 601.2903 [(M + Na) $^+$, M = $\text{C}_{28}\text{H}_{43}\text{BN}_2\text{O}_{10}$].

3,13-Bis[3,5-bis(diethylphosphonomethyl)phenyl]-5-methoxy-8,8,18,18-tetramethylbacteriochlorin (BC1a). Following a general procedure,³¹ samples of **BC-Br**^{3,13} (45 mg, 80 μmol), Pd(PPh₃)₄ (28 mg, 24 μmol) and anhydrous K_2CO_3 (0.13 g, 0.96 mmol) were placed in a Schlenk flask and dried under high vacuum for 1 h. Toluene/DMF [8.0 mL (2:1), degassed by bubbling with argon for 10 min] was added along with **1** (0.12 g, 0.24 mmol), and the resulting reaction mixture was degassed by three freeze-pump-thaw

cycles. The reaction mixture was heated at 90 °C for 18 h. After allowing to cool to room temperature, the toluene was removed by rotary evaporation. The resulting residue was diluted with CH₂Cl₂, and the resulting solution was washed with aqueous NaHCO₃ solution. The organic layer was separated, dried (Na₂SO₄) and concentrated. The residue was purified by column chromatography [silica, MeOH/CH₂Cl₂ (1:24)] to afford a green solid (75 mg, 81%): ¹H NMR (400 MHz, CDCl₃) δ -1.93 (brs, 1H), -1.67 (brs, 1H), 1.30–1.40 (m, 24H), 1.95 (s, 6H), 1.97 (s, 6H), 3.37 (d, *J* = 15.2 Hz, 4H), 3.42 (d, *J* = 15.6 Hz, 4H), 3.66 (s, 3H), 4.04–4.24 (m, 16H), 4.35 (s, 2H), 4.39 (s, 2H), 7.43 (s, 1H), 7.48 (s, 1H), 7.94 (d, *J* = 1.6 Hz, 2H), 8.02 (s, 2H), 8.58 (d, *J* = 2.0 Hz, 1H), 8.61 (s, 1H), 8.64 (s, 1H), 8.76 (d, *J* = 2.0 Hz, 1H), 8.80 (s, 1H); ¹³C NMR (100 MHz, CDCl₃) δ 16.7 (d, *J* = 3.0 Hz), 31.3, 31.4, 34.0 (dd, *J* = 138.2 Hz & 14.5 Hz), 45.7, 45.8, 47.8, 52.1, 62.4 (dd, *J* = 16.0 Hz & 6.8 Hz), 63.3, 96.9, 122.3, 122.6, 127.4, 129.9, 130.5, 131.2, 131.5, 132.9 (d, *J* = 11.3 Hz), 133.3, 134.0, 135.2, 135.5, 135.8, 136.3, 137.0, 138.8, 154.0, 160.6, 169.1, 169.72, ³¹P NMR δ 26.9, 27.1; MALDI-MS obsd 1153.2964; ESI-MS obsd 577.2407, calcd 577.2409 [(M + 2H)²⁺, M = C₅₇H₈₀N₄O₁₃P₄], λ_{abs} (CH₂Cl₂) 363, 510, 730 nm.

2,12-Bis[3,5-bis(phosphonomethyl)phenyl]-5-methoxy-8,8,18,18-tetramethylbacteriochlorin (BC1). Following a reported procedure,²⁹ a solution of **BC1a** (3.1 mg, 2.7 μmol) in anhydrous CHCl₃ (0.14 mL) was treated with TMSBr (29 μL, 0.22 mmol, 80 equiv) under argon, and the reaction mixture was stirred in the dark for 16 h. Methanol (0.30 mL) was then added, and the mixture was stirred for 3 h. The solvent was removed by rotary evaporation, and the residue was dried under high vacuum for 1 h. A solution of 0.25 M NaOH (1.0 mL) was added to the dried reaction mixture to give a

greenish solution. The solution was concentrated to dryness. The residue was dissolved in a minimum amount of water and chromatographed [C18 silica, H₂O/MeOH (from 99:1 to 99:5)] to afford a dark greenish solid (2.5 mg, 90%): ¹H NMR [300 MHz, CDCl₃/CD₃OD (1:1), two pyrrolic protons were not observed] δ 1.81 (s, 6H), 1.87 (s, 6H), 2.96–3.06 (m, 8H), 3.63 (s, 3H), 4.32 (s, 2H), 4.51 (s, 2H), 7.41 (s, 1H), 7.47 (s, 1H), 7.73 (s, 2H), 7.93 (s, 2H), 8.69 (s, 1H), 8.73 (s, 1H), 8.75 (s, 1H), 8.85 (s, 1H), 8.95 (s, 1H); λ_{abs} (0.5 M phosphate buffer, pH 7.0) 353, 508, 730 nm.

3,13-Bis[3,5-bis(*tert*-butoxycarbonamidomethyl)phenyl]-5-methoxy-8,8,18,18-tetramethylbacteriochlorin (BC3a). Following a general procedure,³² samples of **BC-Br**^{3,13} (44.6 mg, 80.0 μmol), **2** (81.4 mg, 176 μmol), Pd(PPh₃)₄ (55.6 mg, 48.1 μmol), Cs₂CO₃ (156 mg, 480 μmol) and toluene/DMF [4.00 mL (2:1), deaerated by bubbling with argon for 45 min] were added to a Schlenk flask. The mixture was deaerated by three freeze-pump-thaw cycles. The reaction mixture was stirred at 90 °C for 18 h. The reaction mixture was cooled to room temperature, concentrated to dryness, diluted with CH₂Cl₂ and washed with saturated aqueous NaHCO₃. The organic layer was separated, dried (Na₂SO₄), concentrated and chromatographed [silica, CH₂Cl₂/ethyl acetate (4:1)]. The resulting solid was treated with hexanes/ethyl acetate (4:1), sonicated in a benchtop sonication bath and centrifuged. The supernatant was discarded to afford a greenish solid (72.7 mg, 85%): ¹H NMR (300 MHz, CDCl₃) δ -1.92 (s, 1H), -1.66 (s, 1H), 1.50 (s, 36H), 1.95 (s, 6H), 1.97 (s, 6H), 3.62 (s, 3H), 4.37 (s, 2H), 4.39 (s, 2H), 4.54–4.61 (m, 8H), 5.05 (br, 4H), 7.38 (s, 1H), 7.44 (s, 1H), 7.94 (s, 2H), 7.98 (s, 2H), 8.59–8.64 (m, 3H), 8.73 (d, *J* = 5.7 Hz, 2H); ¹³C NMR (100 MHz, CDCl₃) δ 28.70, 28.76, 31.33, 31.41, 44.67, 44.79, 45.00, 45.09, 45.76,

45.90, 47.9, 52.2, 63.4, 79.75, 79.82, 79.95, 84.2, 97.0, 113.6, 117.7, 122.45, 122.53, 125.2, 125.5, 125.7, 127.5, 128.4, 129.2, 129.5, 130.2, 130.8, 133.6, 134.1, 134.86, 134.92, 134.98, 135.26, 135.32, 135.39, 135.6, 136.2, 136.4, 137.3, 138.8, 139.1, 140.2, 140.4, 140.9, 150.0, 141.7, 154.2, 156.30, 156.40, 156.47, 157.6, 160.8, 169.2, 169.9; MALDI-MS obsd 1070.7317; ESI-MS obsd 1068.6043, calcd 1068.6043 (M^+ , $M = C_{61}H_{80}N_8O_9$); λ_{abs} (CH_2Cl_2) 363, 510, 729 nm.

3,13-Bis[3,5-bis(aminomethyl)phenyl]-5-methoxy-8,8,18,18-tetramethylbacteriochlorin (BC3b). A solution of **BC3a** (20.4 mg, 19.1 μmol) in CH_2Cl_2 (1.15 mL) was stirred under argon for 2 min, followed by addition of TFA (768 μL). After 20 min, the reaction mixture was diluted with CHCl_3 and dried under an argon flow. Tributylamine (77.8 mg, 0.420 mmol) was added to the solid residue, and the mixture was sonicated for 3 min in a benchtop sonication bath. A mixture of THF and hexanes (1:1) was then added and the resulting suspension was sonicated for 5 min followed by centrifugation. The supernatant was discarded to afford a green solid (9.9 mg, 78%): ^1H NMR (300 MHz, CD_3OD , the four primary amino and two pyrrolic protons were not observed) δ 1.99 (s, 6H), 2.01 (s, 6H), 3.70 (s, 3H), 4.40 (s, 2H), 4.41 (s, 4H), 4.45 (s, 2H), 4.47 (s, 4H), 7.72 (s, 1H), 7.80 (s, 1H), 8.28 (d, $J = 1.8$ Hz, 2H), 8.34 (d, $J = 1.8$ Hz, 2H), 8.74 (s, 1H), 8.77 (s, 1H), 8.83 (s, 1H), 8.87 (s, 1H), 8.99 (s, 1H); MALDI-MS obsd 668.6777; ESI-MS obsd 669.4026, calcd 669.4024 [$(M + H)^+$, $M = C_{41}H_{48}N_8O$]; λ_{abs} (methanol) 360, 507, 726 nm.

3,13-Bis[3,5-bis(*N,N,N*-trimethylammoniomethyl)phenyl]-5-methoxy-8,8,18,18-tetramethylbacteriochlorin diiodide (BC3). A mixture of **BC3b** (4.0 mg, 6.0 μmol) and tributylamine (44 mg, 0.24 mmol) in DMF (0.20 mL) was stirred under argon for 2 min,

followed by addition of iodomethane (45 μ L, 0.72 mmol). After 16 h, ether/THF (1:1) was added to the reaction mixture to precipitate the crude product. The suspension was sonicated for 3 min on a benchtop sonication bath followed by centrifugation. The supernatant was discarded to afford a green solid. This procedure (ether addition/sonication/centrifugation) was carried out three additional times to afford a green solid (6.5 mg, 81%): ^1H NMR (300 MHz, DMSO- d_6 , the 12 ammoniomethyl peaks were overlapped with the solvent peak) δ – 1.93 (s, 1H), –1.69 (s, 1H), 1.91 (s, 6H), 1.93 (s, 6H), 3.25 (s, 36H), 3.58 (s, 3H), 4.30 (s, 2H), 4.37 (s, 2H), 4.81 (s, 4H), 4.87 (s, 4H), 7.84 (s, 1H), 7.90 (s, 1H), 8.40 (s, 2H), 8.56 (s, 2H), 8.80 (s, 1H), 8.87–8.90 (m, 2H), 8.95 (s, 1H), 9.16 (s, 1H); obsd 210.1528, calcd 210.1530 [(M – 4I) $^{4+}$, M = C₅₃H₇₆I₄N₈O]; λ_{abs} (0.5 M phosphate buffer, pH 7.0) 363, 519, 731 nm.

3,13-Bis[3,5-bis(2-(*tert*-butoxycarbonamido)ethoxycarbonyl)phenyl]-5-methoxy-8,8,18,18-tetramethylbacteriochlorin (BC4a). Following a general procedure,³² samples of **BC-Br**^{3,13} (44.6 mg, 80.0 μ mol), **3** (44.5 mg, 134 μ mol), Pd(PPh₃)₄ (12.4 mg, 10.7 μ mol) and Cs₂CO₃ (34.9 mg, 107 μ mol) were placed in a Schlenk flask and dried under high vacuum for 30 min. Toluene/DMF [2.70 mL (2:1), deaerated by bubbling with argon for 45 min] was added to the Schlenk flask under argon and deaerated by three freeze-pump-thaw cycles. The reaction mixture was stirred at 90 °C for 13 h. The reaction mixture was cooled to room temperature, concentrated to dryness, diluted with CH₂Cl₂ and washed with saturated aqueous NaHCO₃. The organic layer was separated, dried (Na₂SO₄), concentrated and chromatographed [silica, CH₂Cl₂/ethyl acetate (4:1)]. Treatment of the resulting solid with hexanes/CH₂Cl₂ (4:1) afforded a suspension, which was sonicated in a benchtop sonication bath followed by centrifugation. The supernatant was discarded to afford a greenish solid

(82.3 mg, 79%): ^1H NMR (300 MHz, CDCl_3) δ -1.80 (s, 1H), -1.56 (s, 1H), 1.42 (s, 36H), 1.96 (s, 6H), 1.98 (s, 6H), 3.62–3.66 (m, 11H), 4.38 (s, 2H), 4.40 (s, 2H), 4.50–4.60 (m, 8H), 5.02–5.07 (m, 4H), 8.66 (s, 1H), 8.69 (s, 3H), 8.87 (s, 2H), 8.92 (s, 1H), 9.02–9.04 (m, 4H); ^{13}C NMR (100 MHz, CDCl_3) δ 28.6, 31.30, 31.38, 40.0, 45.8, 46.0, 47.8, 52.2, 63.4, 65.21, 65.32, 79.9, 96.6, 97.41, 97.49, 122.6, 123.1, 127.3, 128.3, 129.5, 129.9, 130.1, 131.44, 131.46, 134.18, 134.23, 135.1, 135.6, 136.32, 136.39, 136.8, 137.6, 139.3, 154.6, 156.1, 161.3, 166.1, 166.4, 169.8, 170.5; MALDI-MS obsd 1302.6920; ESI-MS obsd 1301.6335, calcd 1301.6340 $[(\text{M} + \text{H})^+]$, $\text{M} = \text{C}_{69}\text{H}_{88}\text{N}_8\text{O}_{17}$; λ_{abs} (CH_2Cl_2) 364, 511, 732 nm.

3,13-Bis[3,5-bis(2-aminoethoxycarbonyl)phenyl]-5-methoxy-8,8,18,18-tetramethylbacteriochlorin (BC4b). A solution of **BC4a** (42.0 mg, 32.3 μmol) in CH_2Cl_2 (1.94 mL) was stirred under argon for 2 min, followed by addition of TFA (1.29 mL). After 1 h, the reaction mixture was diluted with CHCl_3 and dried under an argon flow. Tributylamine (300 μL) was added to the solid residue, and the resulting suspension was sonicated for 3 min in a benchtop sonication bath. A mixture of THF and ether (1:1) was then added, and the resulting suspension was sonicated for 5 min followed by centrifugation. The supernatant was discarded to afford a green solid (25 mg, 86%): ^1H NMR (300 MHz, $\text{CD}_3\text{OD}/\text{CDCl}_3$, the NH_2 and pyrrolic protons were not observed) δ 1.98 (s, 6H), 2.01 (s, 6H), 3.44–4.51 (m, 8H), 3.64 (s, 3H), 4.40 (s, 2H), 4.42 (s, 2H), 4.70–4.77 (m, 8H), 8.74 (s, 1H), 8.80 (d, $J = 2.7$ Hz, 2H), 8.87 (s, 1H), 8.99 (t, $J = 1.5$ Hz, 1H), 9.03 (t, $J = 1.5$ Hz, 1H), 9.06 (s, 1H), 9.10 (d, $J = 1.5$ Hz, 2H), 9.15 (d, $J = 1.5$ Hz, 2H); MALDI-MS obsd 900.3985; obsd 301.1462, calcd 301.1463 $[(\text{M} + 3\text{H})^{3+}]$, $\text{M} = \text{C}_{49}\text{H}_{56}\text{N}_8\text{O}_9$; λ_{abs} (methanol) 361, 508, 727 nm.

3,13-Bis[3,5-bis(2-(*N,N,N*-trimethylammonio)ethoxycarbonyl)phenyl]-5-methoxy-8,8,18,18-tetramethylbacteriochlorin diiodide (BC4). A mixture of **BC4b** (6.2 mg, 6.9 μmol) and tributylamine (51 mg, 0.28 mmol) in DMF (0.20 mL) was stirred under argon for 2 min, followed by addition of iodomethane (51 μL , 0.83 mmol). After 16 h, ether/THF (1:1) was added to the reaction mixture to precipitate the crude product. The suspension was sonicated for 3 min in a benchtop sonication bath followed by centrifugation. The supernatant was discarded to afford a green solid. This procedure (ether addition/sonication/centrifugation) was carried out three more times to afford a green solid (8.2 mg, 75%): $^1\text{H NMR}$ (300 MHz, $\text{DMSO-}d_6$) δ -1.87 (s, 1H), -1.62 (s, 1H), 1.91 (s, 6H), 1.95 (s, 6H), 3.25 (s, 36H), 3.54 (s, 3H), 3.91 (br, 8H), 4.29 (s, 2H), 4.34 (s, 2H), 4.86 (br, 8H), 8.72–8.82 (m, 3H), 8.90 (s, 1H), 8.94–9.04 (m, 6H), 9.20 (s, 1H); obsd 268.1584, calcd 268.1585 [($M - 4\text{I}$) $^{4+}$, $M = \text{C}_{61}\text{H}_{84}\text{I}_4\text{N}_8\text{O}_9$]; λ_{abs} (0.5 M phosphate buffer, pH 7.0) 363, 519, 731 nm.

3,13-Bis[3,5-bis(2,5,8,11-tetraoxatetradecan-14-amido)phenyl]-5-methoxy-8,8,18,18-tetramethylbacteriochlorin (BC5). A mixture of **BC3b** (5.00 mg, 7.47 μmol) and PEG4 NHS ester (100 mg, 299 μmol) in DMF (100 μL) was stirred at room temperature under argon for 20 h. The reaction mixture was diluted with CH_2Cl_2 and washed with saturated aqueous NaHCO_3 . The combined organic extract was dried (Na_2SO_4) and concentrated. A mixture of hexanes/ CH_2Cl_2 (19:1) was added to the residue. The resulting suspension was sonicated for 3 min on a benchtop sonication bath followed by centrifugation. The supernatant was discarded to afford a green solid. This procedure (solvent addition/sonication/centrifugation) was carried out three more times to afford a green solid

(9.2 mg, 80%): ^1H NMR (300 MHz, CDCl_3) δ -1.94 (s, 1H), -1.69 (s, 1H), 1.95 (s, 6H), 1.97 (s, 6H), 2.52–2.61 (m, 16H), 3.24 (s, 6H), 3.25 (s, 6H), 3.33–3.87 (m, 51H), 4.35 (s, 2H), 4.39 (s, 2H), 4.67 (d, $J = 6.0$ Hz, 4H), 4.72 (d, $J = 6.0$ Hz, 4H), 7.13–7.15 (m, 4H), 7.38 (s, 1H), 7.45 (s, 1H), 7.94 (s, 2H), 7.97 (s, 2H), 8.58–8.63 (m, 3H), 8.74–8.75 (m, 2H); MALDI-MS obsd 1541.8276; ESI-MS obsd 1563.8470, calcd 1563.8460 $[(\text{M} + \text{Na})^+]$, $\text{M} = \text{C}_{81}\text{H}_{120}\text{N}_8\text{O}_{21}$]; λ_{abs} (water) 359, 506, 728 nm.

15-Bromo-3,13-bis[3,5-bis(2-(*tert*-butoxycarbonamido)ethoxycarbonyl)phenyl]-5-methoxy-8,8,18,18-tetramethylbacteriochlorin (BC4a-Br). Following a general procedure,³² a solution of **BC4a** (42.6 mg, 32.7 μmol) in THF (65.4 mL) was treated with NBS (5.80 mg, 32.7 μmol) in THF (327 μL) at room temperature for 15 min. The reaction mixture was diluted with CH_2Cl_2 and washed with saturated aqueous NaHCO_3 . The organic layer was dried (Na_2SO_4), concentrated and chromatographed [silica, CH_2Cl_2 /ethyl acetate (7:3)] to afford a reddish solid (34.3 mg, 76%): ^1H NMR (300 MHz, CDCl_3) δ -1.63 (s, 1H), -1.33 (s, 1H), 1.40 (s, 18H), 1.42 (s, 18H), 1.96 (s, 6H), 1.97 (s, 6H), 3.57–3.64 (m, 11H), 4.37 (s, 2H), 4.41 (s, 2H), 4.48–4.54 (m, 8H), 4.98 (br, 2H), 5.07 (br, 2H), 8.63 (s, 1H), 8.67 (s, 1H), 8.69 (d, $J = 2.4$ Hz, 1H), 8.74–8.76 (m, 3H), 8.89 (t, $J = 1.5$ Hz, 2H), 8.89 (d, $J = 1.5$ Hz, 2H); ^{13}C NMR (100 MHz, CDCl_3) δ 28.63, 28.65, 31.5, 31.7, 40.1, 45.6, 45.9, 48.2, 54.8, 63.7, 65.3, 79.9, 97.2, 97.5, 99.0, 125.1, 126.2, 129.4, 129.87, 129.97, 130.12, 130.3, 130.9, 132.6, 133.6, 133.8, 135.4, 136.2, 136.7, 137.0, 138.6, 140.4, 156.2, 157.8, 160.3, 166.3, 168.7, 172.0; ESI-MS obsd 1379.5458, calcd 1379.5445 $[(\text{M} + \text{H})^+]$, $\text{M} = \text{C}_{69}\text{H}_{87}\text{BrN}_8\text{O}_{17}$]; MALDI-MS obsd 1382.5555; λ_{abs} (CH_2Cl_2) 368, 523, 729 nm.

(III) Absorption versus concentration study.

For each bacteriochlorin, four different solutions (solution *A*, *B*, *C* and *D*) in aqueous potassium phosphate buffer (0.5 M, pH = 7.0) were prepared. The concentration of the solution *A* (~500 μM) afforded absorbance (A) ~0.5 for the Q_y transition measured with a 0.01-cm pathlength cuvette. Successive serial dilution (10 times each) with buffer gave bacteriochlorin concentrations as follows: [solution *A*] = 10 x [solution *B*] = 100 x [solution *C*] = 1000 x [solution *D*].

A typical experiment proceeded as follows: a stock solution was prepared by adding a small amount of DMSO (12.5–37.5 μL , to facilitate dissolution) to bacteriochlorin (~0.1–0.3 mg; ~0.1–0.3 μM) in a small vial followed by addition of aqueous potassium phosphate buffer (237.5–712.5 μL , 0.5 M, pH = 7.0). The resulting sample was sonicated for one minute and then filtered (poly-vinylidene difluoride high-volume low pressure filter, pore size 0.45 μm) to obtain solution *A* (~500 μM). The absorbance of solution *A* was measured in a 0.01-cm pathlength cuvette. Solution *B* was obtained by mixing solution *A* (100–200 μL) with buffer (900–1800 μL) in a small vial. The absorbance of solution *B* was measured in a 0.1-cm pathlength cuvette. For further dilution, solution *B* (300 μL) was mixed with buffer (2.70 mL) in a 1-cm pathlength cuvette to obtain solution *C* and the absorbance was measured. Solution *C* (2.50 mL) was transferred into a 25 mL volumetric flask and made up to the mark with buffer. The absorbance of the resulting solution *D* was measured in a 10-cm pathlength cuvette. The procedure was followed for each bacteriochlorin **BC1 – BC5**. Note

that the range of volumes employed depends on the initial quantity of bacteriochlorin, which was added to the initial vial without weighing.

(IV) Fluorescence yield determinations

The Φ_f values (in DMF, water, or aqueous potassium phosphate buffer) were determined relative to that of 5-methoxy-8,8,18,18-tetramethyl-2,12-di-*p*-tolylbacteriochlorin in toluene ($\Phi_f = 0.18$)²⁶ without correction for refractive index differences.

References

- 1 T. Maisch, C. Bosl, R.-M. Szeimies, N. Lehn and C. Abels, *Antimicrob. Agents Chemother.*, 2005, **49**, 1542–1552.
- 2 C. Spagnul, R. Alberto, G. Gasser, S. Ferrari, V. Pierroz, A. Bergamo, T. Gianferrara and E. Alessio, *J. Inorg. Biochem.*, 2013, **122**, 57–65.
- 3 H. Taima, A. Okubo, N. Yoshioka and H. Inoue, *Tetrahedron Lett.*, 2005, **46**, 4161–4164.
- 4 H. Taima, A. Okubo, N. Yoshioka and H. Inoue, *Chem. Eur. J.*, 2006, **12**, 6331–6340.
- 5 T. Maisch, C. Bosl, R.-M. Szeimies, B. Love and C. Abels, *Photochem. Photobiol. Sci.*, 2007, **6**, 545–551.
- 6 G. Jori, C. Fabris, M. Soncin, S. Ferro, O. Coppellotti, D. Dei, L. Fantetti, G. Chiti and G. Gabrio Roncucci, *Lasers Surg. Med.*, 2006, **38**, 468–481.
- 7 G. Simonneaux, P. Le Maux, S. Chevance, H. Srouf, In: *Handbook of Porphyrin Science*, ed. K. Kadish, K. M. Smith and R. Guilard, World Scientific: Singapore, 2012, Vol. 21, pp. 377–410.
- 8 J. M. Dabrowski, L. G. Arnaut, M. M. Pereira, C. J. P. Monteiro, K. Urbanska, S.

- Simoes and G. Stochel, *ChemMedChem*, 2010, **5**, 1770–1780.
- 9 J. M. Dabrowski, K. Urbanska, L. G. Arnaut, M. M. Pereira, A. R. Abreu, S. Simoes and G. Stochel, *ChemMedChem.*, 2011, **6**, 465–475.
- 10 H. Garcia-Ortega and J. M. Ribo, *J. Porphyrins Phthalocyanines*, 2000, **4**, 564–568.
- 11 I. Batinic-Haberle, J. S. Reboucas, L. Benov and I. Spasojevic, In: *Handbook of Porphyrin Science*, ed. K. Kadish, K. M. Smith and R. Guilard, World Scientific, Singapore, 2011, Vol. 11, pp. 291–393.
- 12 Y. Inaba, K. Ogawa and Y. Kobuke, *J. Porphyrins Phthalocyanines*, 2007, **11**, 406–417.
- 13 S. J.Griffiths, P. F. Heelis, A. K. Haylett and J. V. Moore, *Cancer Lett.*, 1998, **125**, 177–184.
14. K. E. Borbas, H. L. Kee, D. Holten, J. S. Lindsey, *Org. Biomol. Chem.* 2008, **6**, 187–194.
- 15 C. M. Nixon, K. L. Claire, F. Odobel, B. Bujoli and D. R. Talham, *Chem. Mater.*, 1999, **11**, 965–976.
- 16 W. J. Kim, M. S. Kang, H. K. Kim, Y. Kim, T. Chang, T. Ohulchanskyy, P. N. Prasad and K. S. Lee, *J. Nanosci. Nanotechnol.*, 2009, **9**, 7130–7135.
- 17 C.-L. Peng, M.-J. Shieh, M.-H. Tsai, C.-C. Chang and P.-S. Lai, *Biomaterials*, 2008, **29**, 3599–3608.
- 18 M. F. Grahn, A. Giger, A. McGuinness, M. L. de Jode, J. C. M. Stewart, H.-B. Ris, H. J. Altermatt and N. S. Williams, *Lasers Med. Sci.*, 1999, **14**, 40–46.

- 19 R. Hornung, M. K. Fehr, H. Walt, P. Wyss, M. W. Berns and Y. Tadir, *Photochem. Photobiol.*, 2000, **72**, 696–700.
- 20 S. K. Pandey, X. Zheng, J. Morgan, J. R. Missert, T. H. Liu, M. Shibata, D. A. Bellnier, A. R. Oseroff, B. W. Henderson, T. J. Dougherty and R. K. Pandey, *Mol. Pharmaceutics*, 2007, **4**, 448–464.
- 21 G. Zheng, A. Graham, M. Shibata, J. R. Missert, A. R. Oseroff, T. J. Dougherty and R. K. Pandey, *J. Org. Chem.*, 2001, **66**, 8709–8716.
- 22 J. Jiang, P. Vairaprakash, K. R. Reddy, T. Sahin, M. P. Pavan, E. Lubian and J. S. Lindsey, *Org. Biol. Chem.*, 2014, **12**, 86–103.
- 23 E. Diez-Barra, J. C. Garcia-Martinez, S. Merino, R. D. Rey, J. Rodriguez-lopez, P. Sanchez-Verdu and J. Tejada, *J. Org. Chem.*, 2001, **66**, 5664–5670.
- 24 B. Sookcharoenpinyo, E. Klein, Y. Ferrand, D. B. Walker, P. R. Brotherhood, C. Ke, M. P. Crump and A. P. Davis, *Angew. Chem. Int. Ed.*, 2012, **51**, 4586–4590.
- 25 M. Krayner, M. Ptaszek, H.-J. Kim, K. R. Meneely, D. Fan, K. Secor and J. S. Lindsey, *J. Org. Chem.*, 2010, **75**, 1016–1039.
- 26 H.-J. Kim and J. S. Lindsey, *J. Org. Chem.*, 2005, **70**, 5475–5486.
- 27 D. Fan, M. Taniguchi and J. S. Lindsey, *J. Org. Chem.*, 2007, **72**, 5350–5357.
- 28 N. Srinivasan, C. A. Haney, J. S. Lindsey, W. Zhang and B. T. Chait, *J. Porphyrins Phthalocyanines*, 1999, **3**, 283–291.
- 29 K. E. Borbas, V. Chandrashaker, C. Muthiah, H. L. Kee, D. Holten and J. S. Lindsey, *J. Org. Chem.*, 2008, **73**, 3145–3158.
- 30 T. Ishiyama, M. Murata and N. Miyaura, *J. Org. Chem.*, 1995, **60**, 7508–7510.

31. C. Ruzié, M. Krayner, T. Balasubramanian, J. S. Lindsey, *J. Org. Chem.* 2008, **73**, 5806–5820.
32. K. R. Reddy, J. Jiang, M. Krayner, M. A. Harris, J. W. Springer, E. Yang, J. Jiao, D. M. Niedzwiedzki, D. Pandithavidana, P. S. Parkes-Loach, C. Kirmaier, P. A. Loach, D. F. Bocian, D. Holten and J. S. Lindsey, *Chem. Sci.*, 2013, **4**, 2036–2053.

CHAPTER 5

Polarity-Tunable and Wavelength-Tunable Bacteriochlorins Bearing a Single Carboxylic Acid or NHS Ester. Use in a Protein Bioconjugation Model System

Preamble. The contents in this chapter have been published⁸⁰ with contributions from the following individuals. Chih-Yian Chen: bioconjugation and photophysical property study on conjugates (together with Jianbing). Nuonuo Zhang: photophysical property study on bacteriochlorins (together with Jianbing). Pothiappan Vairaprakash, together Jianbing, is involved for the molecular designs.

Introduction

The conjugation of chromophores to biological molecules has a rich history both in methods and applications.¹⁻⁹ Yet, a comparatively unexplored topic in this domain concerns the use of NIR-active chromophores. The challenge to filling this lacuna entails synthetic tailoring of NIR-active chromophores to achieve the molecular design requirements. The latter typically include polarity of the overall chromophore, tuning the wavelength of absorption/emission, and incorporation of a single bioconjugatable tether. Examples of synthetic NIR chromophores range from long-chain cyanine dyes to quantum dots.¹⁰⁻¹³ Nature's NIR-active chromophores are built around the bacteriochlorin π -system (i.e., a *trans*-tetrahydroporphyrin), which provide the basis for bacterial photosynthesis (Bchl *a*, *b* and *g*)¹⁴ and unknown roles in other organisms (e.g., tolyporphins)¹⁵⁻²¹ (Chart 5.1).

While natural bacteriochlorins are in principle available in large quantities, and semisynthesis therefrom has been a mainstay for tailoring bacteriochlorins,^{22,23} the presence of a number of substituents about the perimeter of the macrocycle limits synthetic

manipulations particularly for wavelength tuning, polarity tuning, and installation of a single bioconjugatable tether. Regardless of the synthetic challenges, a chief advantage of the tetrapyrrole family of compounds (porphyrin, chlorin, bacteriochlorin – and more broadly – the dipyrroles and phthalocyanines) is that the π -chromophoric system is neutral, whereas many pigment classes are intrinsically charged.²⁴ The anionic fluorescein and the cationic cyanine dyes are archetypes in this regard. A neutral non-polar chromophore can be used as is, or alternatively, derivatized to bear cationic or anionic charges, whereas chromophores that are intrinsically charged in principle can be rendered zwitterionic but are always intrinsically polar.

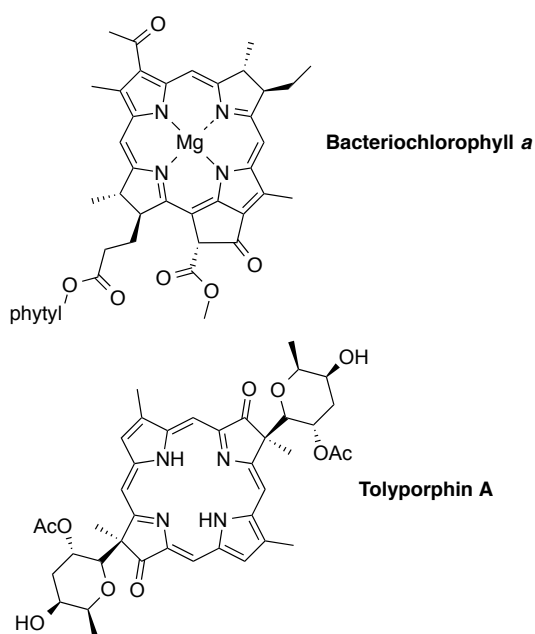


Chart 5.1. Representative bacteriochlorophylls and tolyporphins.

Methods to prepare synthetic bacteriochlorins are under active investigation²⁵⁻⁴⁵ and have been recently reviewed.^{46,47} Two approaches that likely define the range of such methods include (1) double addition to a porphyrin thereby converting two, opposite pyrrole rings to pyrroline rings, and (2) *de novo* synthesis wherein the pyrroline rings are incorporated as pre-made constituents upon macrocycle formation. Only two *de novo* routes to bacteriochlorins are known: the total synthesis of tolyporphins by Kishi and coworkers,⁴⁸⁻⁵¹ and the route to gem-dimethyl-substituted bacteriochlorins developed in our group.⁴¹⁻⁴⁵ The synthetic simplicity of the porphyrin-modification approach is offset by the typical formation of isomeric mixtures and limited wavelength tuning, whereas the full scope of versatility offered by *de novo* synthesis is counterbalanced by the necessary synthetic investment in constructing the macrocycle. Both approaches have merit, and indeed, bioconjugatable bacteriochlorins have been prepared by both approaches, as illustrated by the representative examples shown in Chart 5.2. Bacteriochlorin **I** or **II** was prepared by OsO₄ treatment of a porphyrin,^{26,28} whereas the set of **III-V** were prepared by *de novo* synthesis.⁵²⁻⁵⁶ Note the nature of the bioconjugatable groups [isothiocyanate (**I**), carboxylic acid (**II**), maleimide (**III**, **IV**), and NHS ester (**V**)] as well as the polarity: bacteriochlorin members of sets **III** and **V** are hydrophobic, whereas **IV** is hydrophilic.

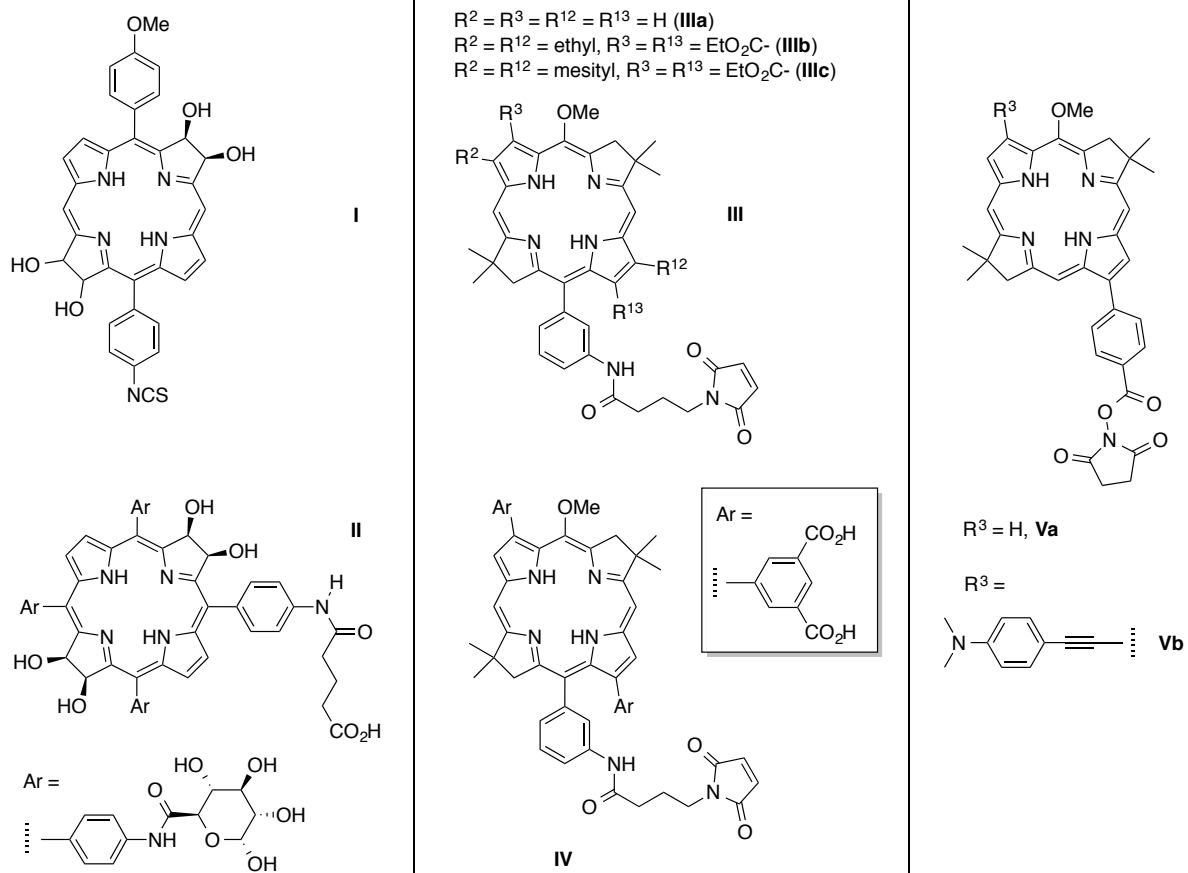


Chart 5.2. Representative bioconjugatable synthetic bacteriochlorins.

The ability to tune the position of the long-wavelength absorption band (and hence the position of the fluorescence emission band) relies on introduction of auxochromes at the perimeter of the macrocycle.⁵⁷ The long-wavelength absorption (Q_y) band stems from a transition that is polarized along the long axis of the molecule, as shown in Figure 5.1. Accordingly, the introduction of substituents at the β -pyrrole positions (2, 3, 12, 13) or adjacent meso-positions (5, 15) enables the band to be shifted from ~ 700 to nearly 900 nm. For the members of set **III**, the Q_y band ranges from 713 to 756 nm.^{52,54} Such

bacteriochlorins have been incorporated into light-harvesting architectures by bioconjugation to analogues of the native membrane-spanning peptides of the light-harvesting complexes of photosynthetic bacteria. The resulting biohybrid light-harvesting architectures self-assemble in aqueous-detergent media. The appended synthetic bacteriochlorins – attached via a maleimide-cysteinyll linkage – absorb NIR light and funnel the resulting excited-state energy to lower-energy-absorbing chromophores as part of the light-harvesting process.^{52,54,58}

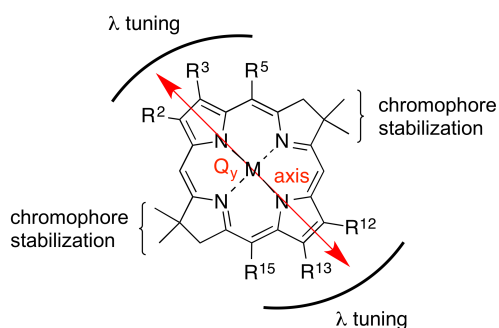


Figure 5.1. Molecular design features of synthetic bacteriochlorins.

We set out to develop a more broadly viable set of wavelength-tunable and polarity-tunable bacteriochlorins, with multiple objectives. First, the reliance on a maleimide-cysteinyll linkage to incorporate the bacteriochlorins was effective but also limiting, because the peptides examined contained only one cysteine.^{52,54,58} Given concerns about handling of peptides containing multiple cysteines (due to oxidative crosslinking), we sought a family of bacteriochlorins wherein each member contains a single carboxylic acid in lieu of a maleimide unit. The carboxylic acid or NHS ester derived therefrom is readily conjugated with amines,⁵⁹ which are more prevalent and manageable than cysteines. To our knowledge,

the only bacteriochlorin-NHS esters prepared by *de novo* synthesis are **Va** and **Vb** of Chart 5.2. Second, for a long time we have been enamored of the work of Cellarius and Mauzerall, who employed polystyrene nanoparticles bearing surface-adsorbed pheophytins as prototypical photoreactors.⁶⁰ Their ingenious strategy “combines the structural features of an interface with the simplicity of studying photochemistry in solution” and in particular enabled studies of pigment loading, pigment-pigment interactions, excited-state energy transfer, and perhaps exciton trapping.⁶⁰ From the vantage of 50-years hence, the work was unavoidably limited by the polydispersity of the particles (24–260 nm diameter) and by the adsorption rather than covalent attachment of the tetrapyrrole chromophore. Accordingly, we felt that a modern analogue of the pheophytin-on-polystyrene particles could be constructed of bioconjugatable bacteriochlorins covalently attached to a globular protein, with the latter providing a ‘particle’ with known surface derivatization sites and uniform nanoscale size (~5 nm diameter).

We prepared two families of bacteriochlorins. The first family (**BC1–BC6**) is lipophilic and includes five free-base bacteriochlorins and one zinc bacteriochlorin (Chart 5.3). On the basis of analogous bacteriochlorins (lacking a carboxylic acid tether), absorption in the NIR region (730–820 nm) is expected. Metalation of the bacteriochlorin with zinc(II) imparts a bathochromic shift (12–16 nm) versus that of the free base bacteriochlorin.⁴⁵ Moreover, insertion of the zinc does not significantly shorten the singlet excited-state lifetime, which enables ensuing photochemical processes.⁴⁵ The second set (**BC7–BC10**) includes four hydrophilic bacteriochlorins. Members of the set of bacteriochlorins are expected to provide absorption covering the near infrared (NIR) region

(726–823 nm) and thereby find diverse use in the construction of novel light-harvesting architectures.

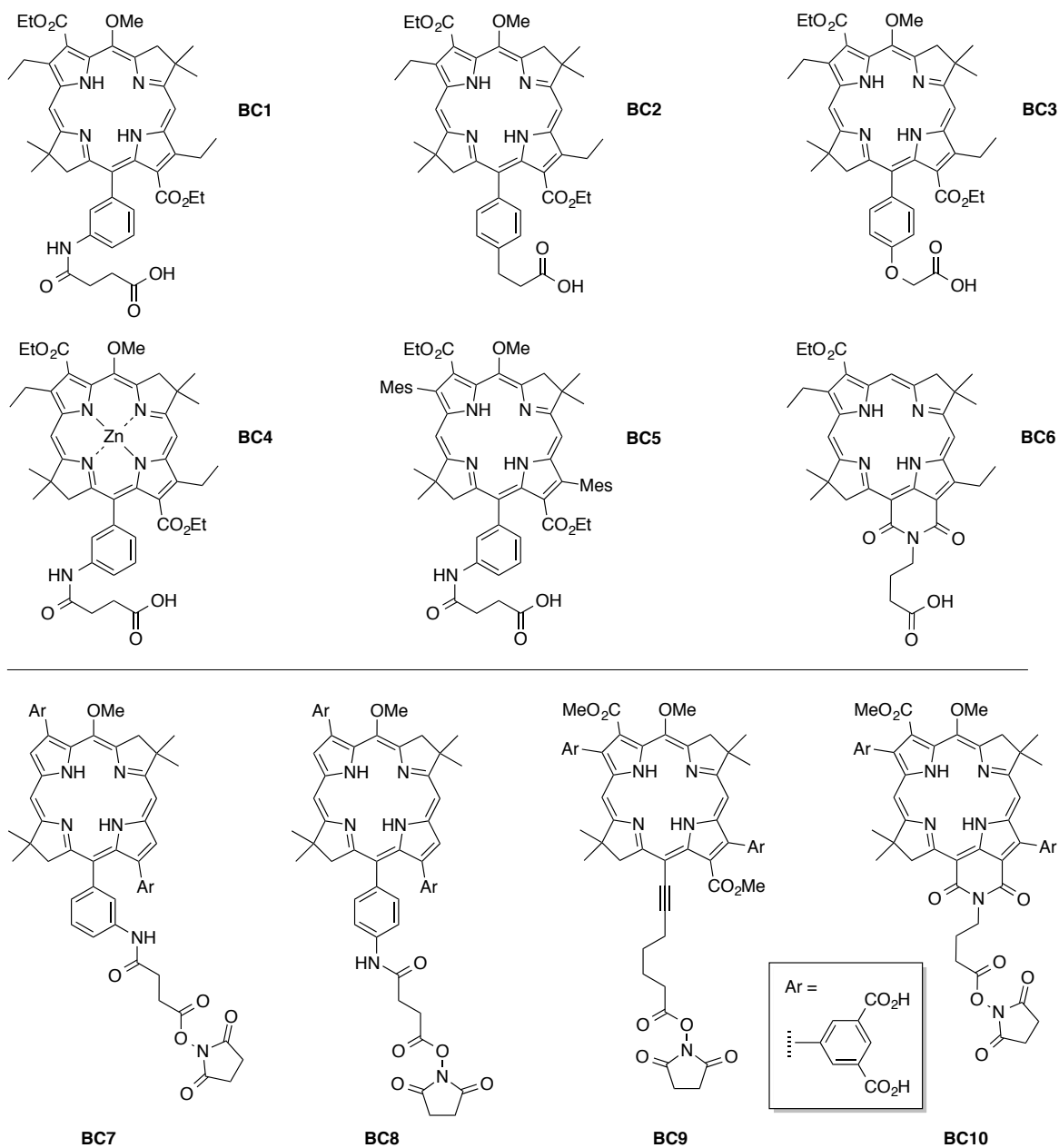


Chart 5.3. Structures of six lipophilic monocarboxy-bacteriochlorins (top) and four hydrophilic tetracarboxy-bacteriochlorins bearing an NHS ester (below).

In this paper, we report the synthesis of the 10 bacteriochlorins along with their absorption and fluorescence properties in DMF and/or aqueous solution. We have employed Mb as a globular protein for bioconjugation with selected hydrophilic bacteriochlorins. The absorption and fluorescence properties of the resulting Mb–bacteriochlorin conjugates have been examined in aqueous solution in the presence or absence of the heme ligand. Taken together, the studies afford a new set of stable, synthetic bacteriochlorins for use in cases where aqueous or membrane solubility is sought; where wavelength tunability (726 to 823 nm) is sought; and where bioconjugation via one of the simplest joining reactions (amidation) is desired.

Results and discussion

(I) Synthesis

(A) Lipophilic bacteriochlorins. The six monocarboxy-bacteriochlorins (**BC1–BC6**) were derivatized from three known bacteriochlorin building blocks (**BC11**,⁵² **BC12**,⁴³ **BC13**⁵⁴) bearing distinct substituents at the 2,3,12,13,15 positions for wavelength tailoring and derivatization (Chart 5.4). Three distinct methods were employed to introduce the carboxylic acid group. (1) For bacteriochlorins with a 3-aminophenyl group, nucleophilic ring-opening of succinic anhydride gave the carboxylic acid group directly (**BC1**, **BC4** and **BC5**). (2) For 15-brominated bacteriochlorins, Suzuki coupling with compounds bearing a protected carboxylic acid group, followed by deprotection with trifluoroacetic acid (TFA) unveiled the carboxylic acid group (**BC2** and **BC3**). (3) Pd-mediated carbonylation with a BOC-protected amine formed the bacteriochlorin–imide, followed by TFA deprotection

unveiled the carboxylic acid group (**BC6**). All of these methods proceeded smoothly to afford the monocarboxy-bacteriochlorins in good to excellent yields.

Reaction of aminophenylbacteriochlorin **BC11** with succinic anhydride in CHCl_3 afforded **BC1** in 67% yield (Scheme 5.1). Metalation⁴⁵ of bacteriochlorin **BC11** with zinc triflate in the presence of sodium hydride afforded **BC14** in 52% yield. Reaction of **BC14** with succinic anhydride gave the carboxy-bacteriochlorin **BC4** in 62% yield. In a similar manner to that of **BC1** and **BC4**, treatment of bacteriochlorin **BC13** with succinic anhydride afforded **BC5** in 71% yield.

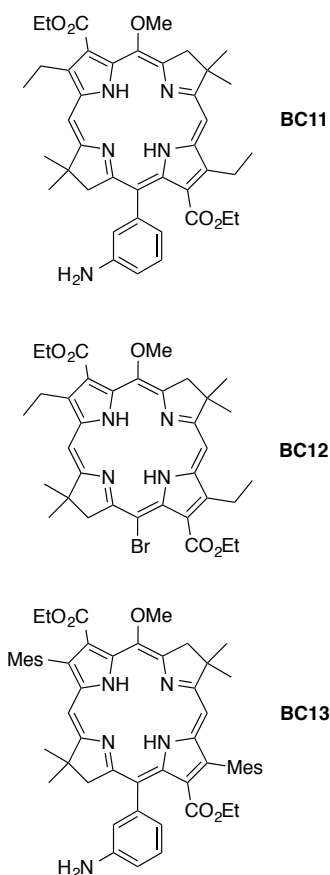
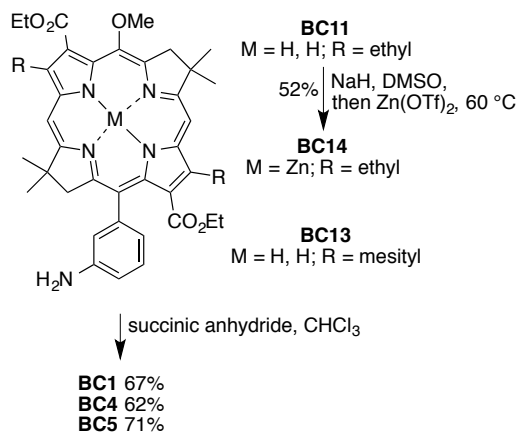
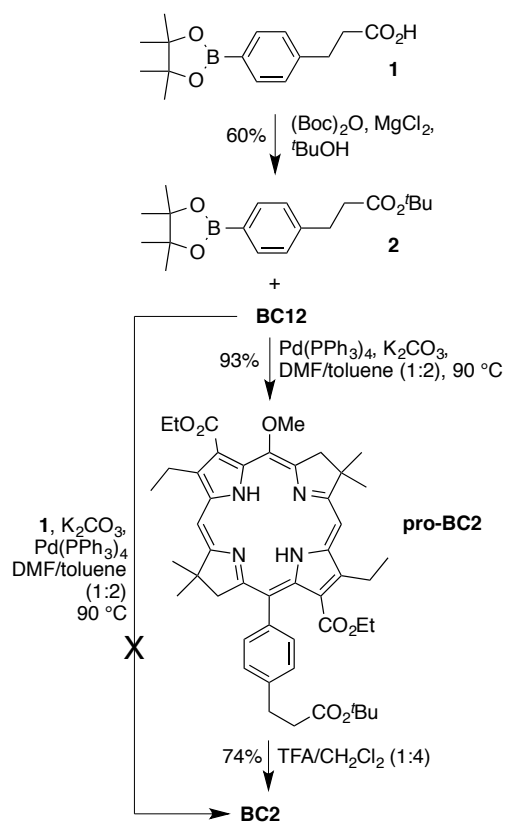


Chart 5.4. Three known bacteriochlorin building blocks.



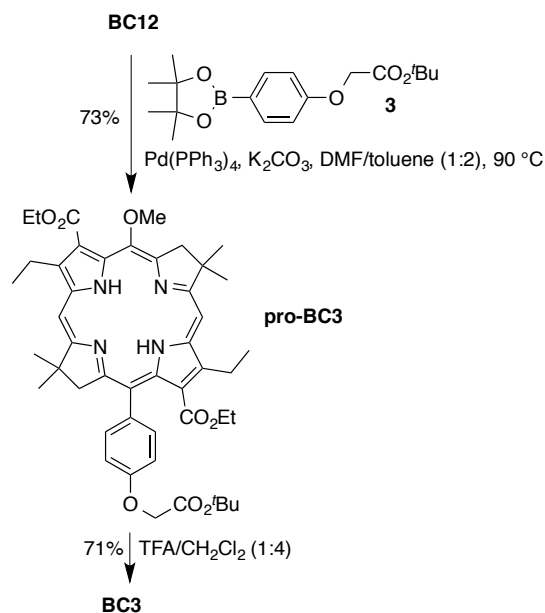
Scheme 5.1. Synthesis of monocarboxy-bacteriochlorins **BC1**, **BC4** and **BC5**.

Suzuki coupling of bacteriochlorin **BC12** with compound **1** failed to give the desired carboxy-bacteriochlorin **BC2**, presumably because of the presence of the free carboxy group of **1** (Scheme 5.2). Alternatively, the free carboxylic acid group of **1** was protected with *tert*-butyl group. Treatment of **1** with di-*tert*-butyl dicarbonate [(Boc)₂O] in the presence of MgCl₂⁶¹ afforded the *tert*-butyl ester **2** in 60% yield. Suzuki coupling of bacteriochlorin **BC12** with **2** gave **pro-BC2** in excellent yield (93%). Cleavage of the *tert*-butyl protecting group in 20% TFA gave **BC2** in 74% yield.⁵³



Scheme 5.2. Synthesis of monocarboxy-bacteriochlorin **BC2**.

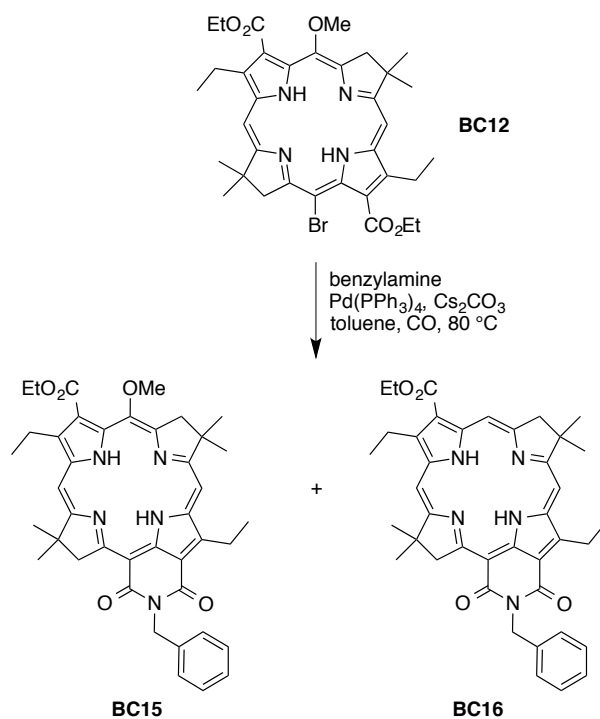
BC3 was obtained in a similar manner as for **BC2**, using the known Suzuki coupling partner **3**⁴² (Scheme 5.3).



Scheme 5.3. Synthesis of monocarboxy-bacteriochlorin **BC3**.

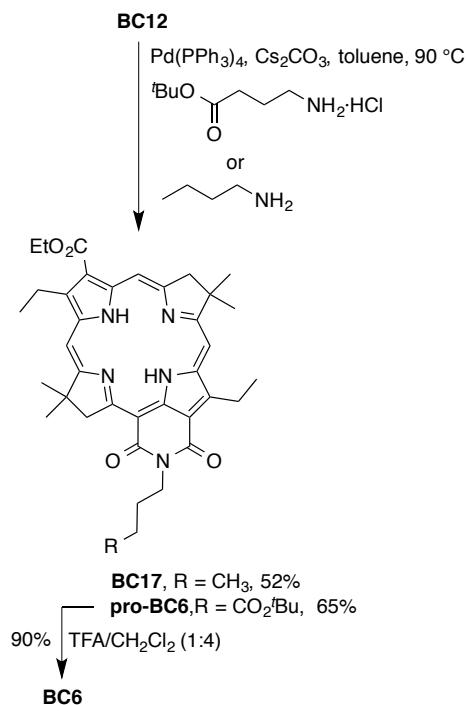
Bacteriochlorin-13,15-dicarboximides with a methoxy group at the 5-position have been synthesized previously.⁴⁴ The imide-forming reaction entails treatment of a bacteriochlorin (bearing a 13-carboethoxy group and a 15-bromo group; e.g., **BC12**) to Pd-mediated carbamoylation in the presence of an amine and CO. The reaction is carried out in the presence of a base, typically Cs_2CO_3 . Thus, **BC12** was converted to **BC15** in 62% yield upon use of 3 equivalents of Cs_2CO_3 .⁴⁴ Upon repeating this synthesis, **BC15** was obtained in 55% yield and we noted the presence of a trace amount (<5%) of the corresponding bacteriochlorin-imide lacking the 5-methoxy group (**BC16**). When the reaction was repeated with 9 equivalents of Cs_2CO_3 , the ratio reversed: the demethoxylated **BC16** was obtained in 84% yield whereas the 5-methoxybacteriochlorin **BC15** was obtained in <5% yield (Scheme 5.4). The reaction is readily monitored by absorption spectroscopy (as well as MALDI-MS),

given that the long-wavelength absorption maximum is at 726 nm (**BC12**), 798 nm (**BC15**) and 820 nm (**BC16**). Removal of the 5-methoxy group thus provides a convenient means to impart a bathochromic shift of the long-wavelength absorption band of the bacteriochlorin.



Scheme 5.4. Demethoxylation upon imide formation (see text).

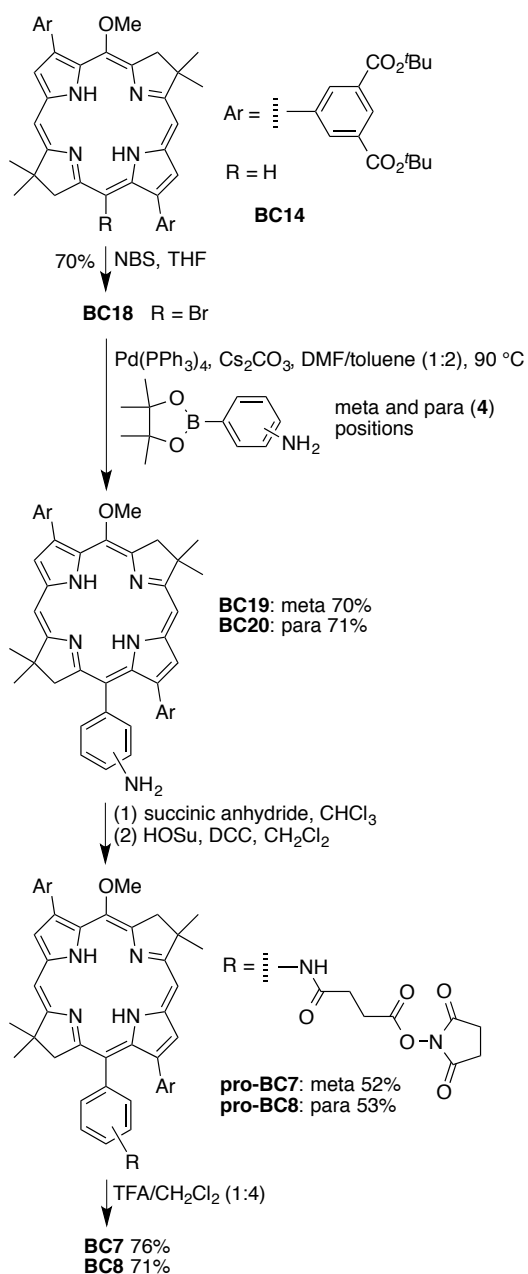
Herein, 15 equivalents of Cs₂CO₃ were used to form the bacteriochlorin–imide as well as remove the 5-methoxy group. The synthesis was first carried out with *n*-butylamine, which gave the 5-demethoxylated bacteriochlorin-imide **BC17** in 52% yield (Scheme 5.5). Similar use of *tert*-butyl 4-aminobutyrate gave **pro-BC6** in 65% yield. Cleavage of the protecting group with TFA gave the monocarboxy-bacteriochlorin **BC6** in 90% yield.



Scheme 5.5. Synthesis of monocarboxy-bacteriochlorin **BC6**.

(B) Hydrophilic bacteriochlorin. The generic route for the synthesis of the four tetracarboxy-bacteriochlorin-NHS esters (**BC7–BC10**, Chart 5.3) is as follows: (1) self-condensation of a bromodihydrodipyrrin–acetal to form the 3,13-dibromo-5-methoxybacteriochlorin macrocycle;^{41,43} (2) Pd-mediated Suzuki coupling to install the 3,13-bis(3,5-di-*tert*-butoxycarbonylphenyl) groups;⁵³ (3) regioselective bromination at the 15-position;⁴² (4) Pd-mediated Suzuki or Sonogashira coupling to install the unprotected carboxylic acid tether at the 15-position;⁴² (5) reaction with *N*-hydroxysuccinimide (HOSu) in the presence of *N,N*-dicyclohexylcarbodiimide (DCC) or 1-ethyl-3-(3-dimethylaminopropyl)carbodiimide hydrochloride (EDC) to afford the penultimate, fully protected bacteriochlorin target, bearing four *tert*-butyl esters and one NHS esters; and (6)

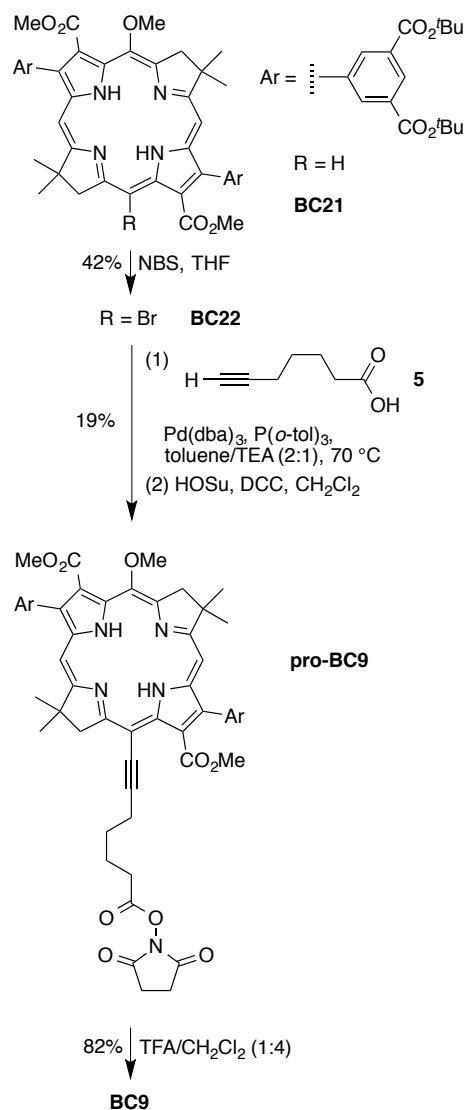
selective cleavage of the *tert*-butyl groups to give tetracarboxy-bacteriochlorin bearing a single NHS ester.



Scheme 5.6. Synthesis of tetracarboxy-bacteriochlorin-NHS esters **BC7** and **BC8**.

The synthesis of the bacteriochlorin-NHS esters **BC7** and **BC8** are shown in Scheme 5.6. **BC18** and **BC19** were reported in our previous paper,⁵³ and are presented here for comparison. Suzuki coupling reaction of bacteriochlorin **BC18** with *p*-anilinoboronic ester (**4**) afforded **BC20** in 71% yield. Treatment of **BC19** or **BC20** with succinic anhydride in CHCl₃ afforded the intermediate 15-carboxybacteriochlorin, which was partially purified by column chromatography, and used directly in the next step. Esterification of each crude bacteriochlorin with HOSu in the presence of DCC gave **pro-BC8** or **pro-BC9** in 52% or 53% yield (for two steps), respectively. Treatment of **pro-BC8** or **pro-BC9** with 20% TFA in CH₂Cl₂ unveiled the four carboxylic acid groups in 76% or 71% yield, respectively, while keeping the bacteriochlorin chromophore and NHS ester intact.

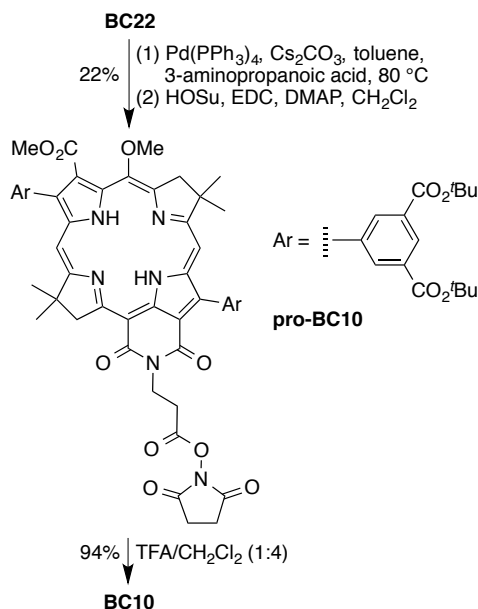
Treatment of bacteriochlorin **BC21**⁵³ with *N*-bromosuccinimide (NBS) in THF afforded the 15-brominated product **BC22** in 42% yield. The presence of the 3,13-aryldiester substituents on the bacteriochlorin ring caused a slightly adverse effect given that the yield was lower than that of bacteriochlorin **BC18** (70%).⁵³ The copper-free Sonogashira reaction^{62,63} of **BC22** and 6-heptynoic acid (**5**) was carried out in toluene/triethylamine (TEA, 2:1) containing Pd₂(dba)₃ and P(*o*-tol)₃ at 70 °C (Scheme 5.7). The resulting monocarboxy-bacteriochlorin was esterified to afford the bacteriochlorin-NHS ester **pro-BC9** in 19% yield for two steps. The low yield could be attributed to two factors: (1) the presence of the free carboxylic acid on **5** was deprotonated under the basic reaction conditions, which would result in low solubility; and (2) bacteriochlorin **pro-BC9** was purified by preparative TLC (instead of column chromatography), from which recovery was poor. Finally, cleavage of the *tert*-butyl ester with 20% TFA in CH₂Cl₂ give the final bacteriochlorin **BC9** in 82% yield.



Scheme 5.7. Synthesis of tetracarboxy-bacteriochlorin-NHS ester **BC9**.

Pd-mediated carbonylation of 15-bromobacteriochlorin **BC22** with 3-aminopropanoic acid in toluene afforded the bacteriochlorin-imide, which was purified by column chromatography and used directly in the next step. Treatment with HOSu/EDC and 4-dimethylaminopyridine (DMAP) gave the bacteriochlorin-NHS ester **pro-BC10** in 22% yield

for two steps (Scheme 5.8). Cleavage of the protecting group with TFA gave the free tetracarboxy-bacteriochlorin **BC10** in 94% yield.



Scheme 5.8. Synthesis of the tetracarboxy-bacteriochlorin–imide bearing an NHS ester.

The bacteriochlorins **BC1–BC10** and precursors typically were characterized by absorption and fluorescence spectroscopy, ¹H NMR spectroscopy, ¹³C NMR spectroscopy (where quantity and solubility allowed), MALDI mass spectrometry, and ESI mass spectrometry.

(II) Photophysical properties

The parameters of interest include (1) the position of the long-wavelength (Q_y) absorption band, (2) the position of the fluorescence emission band, and (3) the sharpness of the absorption Q_y band and fluorescence emission band, measured by the full-width-half-

maximum (fwhm). The absorption and emission spectra of the lipophilic bacteriochlorins were collected in *N,N*-dimethylformamide (DMF) (Figure 5.2). All of these parameters, including the Φ_f values, are listed in Table 5.1. Each bacteriochlorin gave characteristic absorption and fluorescence spectra,⁶⁴ indicating the absence of any adverse effect due to the presence of the bioconjugatable tether. The set of six carboxy-bacteriochlorins exhibits long-wavelength absorption band (Q_y) in the NIR region, ranging from 730–820 nm. As expected, an increase in the number of electron-withdrawing groups (e.g., ester or imide moieties) along the y-axis of the bacteriochlorin caused a bathochromatic shift in the absorption and emission spectra.

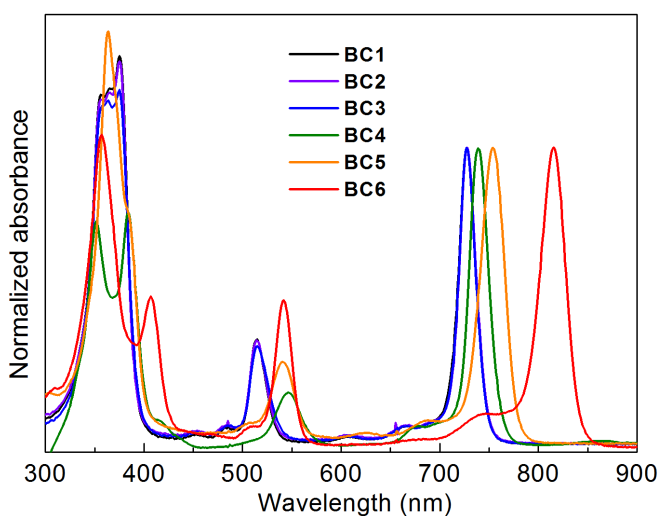


Figure 5.2. Normalized absorption spectra in DMF at room temperature. Spectral parameters are given in Table 5.1.

Table 5.1. Absorption and fluorescence properties of lipophilic bacteriochlorins **BC1–BC6**.^a

Compounds	λ_{abs} , nm	fwhm nm (Abs)	λ_{em} , nm	fwhm nm (Flu)	Φ_f
BC1	727	21	733	24	0.18
BC2	728	20	734	24	0.18
BC3	727	19	733	24	0.19
BC4	737	24	745	39	0.14
BC5	754	28	764	27	0.18
BC6	816	30	822	27	0.037

^aAll spectra were recorded in DMF at room temperature.

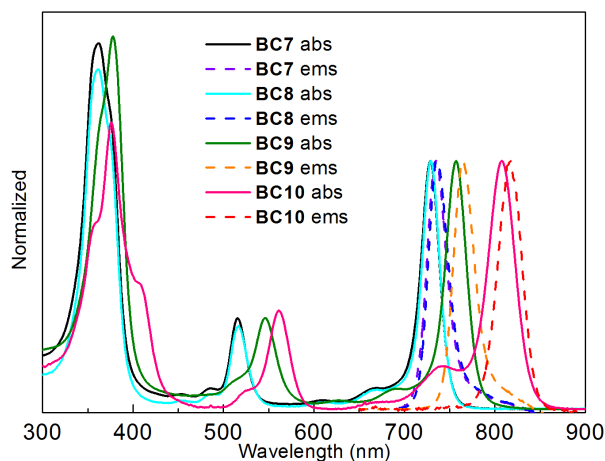


Figure 5.3. Normalized absorption and fluorescent spectra in potassium phosphate buffer (0.5 M, pH 7, for **BC7-9**) and DMF (for **BC10**) at room temperature.

The absorption and emission spectra of the hydrophilic bacteriochlorins were collected in DMF and in aqueous potassium phosphate buffer (Figure 5.3). The spectroscopic parameters are listed in Table 5.2.

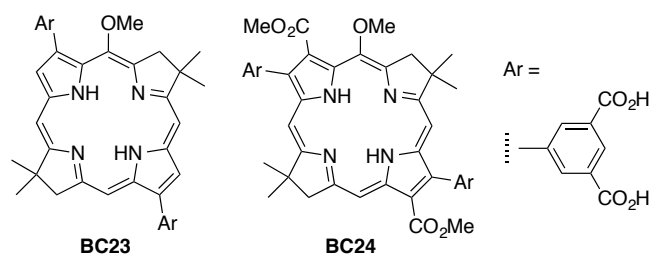


Chart 5.5. Parent bacteriochlorins lacking bioconjugatable tethers.

Table 5.2. Absorption and fluorescence properties of bacteriochlorins.^a

Compounds	solvent	λ_{abs} , nm	fwhm nm (Abs)	λ_{em} , nm	fwhm nm (Flu)	Φ_f
BC23^b	DMF	729	22	735	23	0.19
BC23^b	buffer	730	26	736	26	0.078
BC24^b	DMF	746	31	753	23	0.16
BC24^b	buffer	749	35	758	37	0.11
BC7	DMF	727	23	732	24	0.17
BC7	buffer	729	24	735	26	0.12
BC8	DMF	727	21	733	24	0.19
BC8	buffer	729	23	736	26	0.13
BC9	DMF	754	26	760	24	0.133
BC9	buffer	757	27	765	27	0.13
BC10	DMF	808	35	818	33	0.037
BC10	buffer	823	50	829	N/A ^c	0.0011

^aEach sample contains 1% DMF to facilitate initial dissolution. The buffer is potassium phosphate (0.5 M, pH 7.0). ^bData reported in Ref 53. ^cLow signal-to-noise ratio precluded the determination of the fwhm value.

Each bacteriochlorin exhibited absorption and fluorescence in DMF characteristic of the bacteriochlorin chromophore: a strong B band in the UV region, modest Q_x band in the green-yellow region, and intense Q_y band in the NIR region. **BC7–BC9** gave similar spectra in aqueous phosphate buffer, whereas that of **BC10** was significantly broadened characteristic of aggregation. Other than this lone exception, all bacteriochlorins displayed sharp absorption and emission bands with fwhm 22–35 nm. As with the lipophilic bacteriochlorins, introduction of the bioconjugatable tether in **BC7** and **BC8** caused little absorption or emission shift (by comparison with the parent compound **BC23**), while the ethynyl group in **BC9** and the 13,15-imide moiety in **BC10** gave the expected bathochromic shift (in comparison with **BC24**). The Φ_f values ranged from 0.037–0.19, with exception for (aggregated) **BC10** in buffer, which gave 0.0011. It is noteworthy that the Φ_f values in aqueous medium were diminished versus those in organic media, as observed previously for chlorins.⁶⁵

(III) Bioconjugation study

We examined bioconjugation of selected hydrophilic bacteriochlorins with the protein Mb. The specific goals of this investigation include (1) quantitative analysis of the bacteriochlorin/Mb ratios, and (2) comparison of the spectral properties (absorption, fluorescence, Φ_f) of the bacteriochlorins bound to Mb with those for the bacteriochlorins free in solution. More broadly, we felt preparation of bacteriochlorin–Mb conjugates could provide a more exacting analogue of the pheophytin-on-particles system of Cellarius and Mauzerall,⁶⁰ and their spectroscopic examination could provide a testbed that is more simple

and controlled than those in typical fluorophore–protein conjugation studies. The latter range from the widespread conjugation of fluorophores to antibodies⁶⁶⁻⁷⁰ to our own use of biomimetic light-harvesting peptides.^{52,54,58} For these experiments we chiefly examined bacteriochlorin **BC7** but also looked briefly at **BC8**.

Mb was selected for the bioconjugation for the following reasons: (1) Mb is a water-soluble globular protein (diameter ~ 50 Å) containing 19 lysine residues,⁷¹ of which six are involved in stabilizing electrostatic interactions (Lys16-Asp122, Lys47-Asp44, Lys56-Glu52, Lys77-Glu18, Lys79-Glu4 and Lys133-Glu6).^{72,73} The remaining 14 primary amines (13 Lys residues and 1 *N*-terminus amine) are considered accessible for the amine-NHS ester ligation. (2) The heme chromophore absorbs strongly at 408 nm ($\epsilon = 188,000 \text{ M}^{-1}\text{cm}^{-1}$).⁷⁴ The heme absorption is a better reference peak for calculation of intensely absorbing chromophore/protein ratios than the frequently used, weaker, broad (often non-descript) protein absorption at 280 nm (for apomyoglobin (apoMb), $\epsilon_{280 \text{ nm}} = 15,900 \text{ M}^{-1}\text{cm}^{-1}$),⁷⁵ a wavelength where solvent, impurities, and even the chromophore typically also absorb. A diarylbacteriochlorin⁴¹ (e.g., **BC7–BC10**), for example, exhibits $\epsilon_{280 \text{ nm}} = 52,900 \text{ M}^{-1}\text{cm}^{-1}$, which dwarfs that of Mb even for a 1:1 loading. (3) The heme ligand can be removed from the protein binding pocket as needed by organic (2-butanone) extraction. (4) Mb can be purchased at low price in large quantity (hundreds of mgs) and with high purity (95-100%). We chose Mb from equine skeletal muscle for bioconjugation studies, although Mbs from different organisms have similar primary, secondary (helicity, 8 helical segments) and tertiary structures.⁸⁰

The rationale for focus on Mb versus the more prevalent use of antibodies for fluorophore conjugation warrants emphasis: Mb is more compact (~17 kDa versus ~150 kDa); Mb is abundantly available as a pure compound; Mb and conjugates thereof readily afford MALDI-MS data; and the presence of the heme provides a convenient (removable) absorption spectrometric internal calibrant. The attachment of fluorophores to antibodies is an essential step for use in flow cytometry or cellular staining,^{66,68,69} for example, yet for fundamental spectroscopic and photochemical studies, a small globular protein such as Mb (or apoMb) affords distinct advantages, as described below.

In one study, the bioconjugation of **BC7** was carried out at room temperature with 2, 10, or 50 equiv of the bacteriochlorin-NHS ester versus Mb. Purification by PD-10 gel permeation chromatography (GPC) with potassium phosphate buffer (0.5 M, pH 7.0) caused elution of the conjugate as a clear dark green band, while the free bacteriochlorin (unreacted or hydrolyzed bacteriochlorin-NHS ester) remained on top of the column. The resultant conjugate solution was subjected to centrifugal Amicon filtration, and the absence of the bacteriochlorin absorption of the filtrates indicated the thorough removal of the free bacteriochlorin.

The absorption spectrum in potassium phosphate buffer of the Mb–bacteriochlorin conjugate **Mb-BC7** closely resembled the sum of the component parts in each case (2, 10 or 50 equiv) although a small amount of tailing (to long wavelength) of the bacteriochlorin Q_y band was observed. The spectrum of the conjugate prepared with 50 equiv is shown in Figure 5.4 (panel A) along with that of Mb and **BC7**.⁸⁰

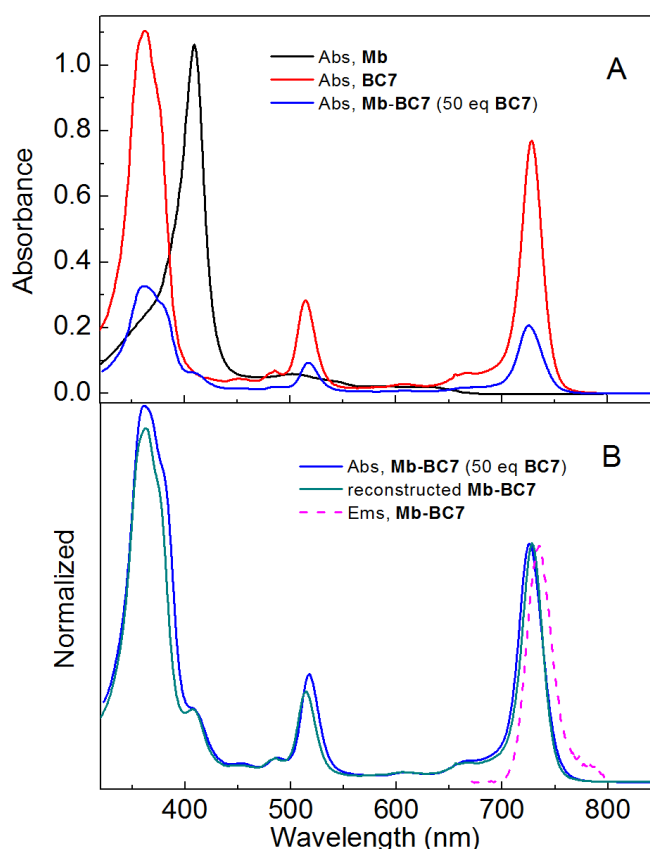


Figure 5.4. (A). Absorption spectra of Mb, **BC7** and conjugate **Mb-BC7** in potassium phosphate buffer (0.5 M, pH 7.0). The concentration of each component is chosen arbitrarily. (B). The normalized experimental (blue), reconstructed (cyan) absorption, and emission (magenta, dashed) spectra of conjugate **Mb-BC7**. Spectral parameters are given in Table 5.3.

Multicomponent analysis (using the known absorption spectrum of **Mb** and of **BC7**) in each case was carried out using PhotochemCAD^{76,77} to assess the bacteriochlorin/Mb ratio. The characteristic absorption peaks of Mb (408 nm) and bacteriochlorins (362, 516, 729 nm) were selected for the calculation. Reconstruction of the absorption of the conjugate versus the experimental absorption visually shows the accuracy of the absorption deconvolution for calculation of the bacteriochlorin/Mb ratio (Figure 5.4, panel B). The results are listed in

Table 5.3. The use of 2, 10, and 50 equiv of **BC7** resulted in 0.62, 1.6, and 7.1 bacteriochlorins per Mb.

Table 5.3. Absorption and fluorescence properties of conjugate **Mb-BC7** with different equivalents of **BC7** input.^a

Compound	Degree of loading ^b	λ_{abs} , nm	fwhm nm (Abs)	λ_{em} , nm	fwhm nm (Flu)	Φ_f
Mb-BC7 (2 equiv)	0.62	729	27	735	26	0.019
apoMb-BC7 (2 equiv)		726	23	730	23	0.091
Mb-BC7 (10 equiv)	1.6	728	26	734	27	0.020
apoMb-BC7 (10 equiv)		726	24	732	24	0.071
Mb-BC7 (50 equiv)	7.1	726	27	735	27	0.018
apoMb-BC7 (50 equiv)		721	30	731	27	0.023

^aAll data determined in potassium phosphate buffer (0.5 M, pH 7.0) at room temperature.

^bThe ratio of **BC7** to Mb, determined by multicomponent absorption spectral analysis.

The same three conjugates were examined by MALDI-MS using α -cyano-4-hydroxycinnamic acid (CHCA) as matrix. The data are shown in Figure 5.5. The increase in loading with number of equivalents of **BC7** was clearly seen, with a distribution of peaks separated by $\Delta m = 920$ Da, which corresponds to **BC7** minus the NHS moiety. The

distribution shifts to higher mass with increasing number of equivalents. For the conjugate prepared with 50 equiv of **BC7**, which gave an average loading of 7.1 (by absorption spectroscopy), individual peaks in the progression of 0–9 were clearly observed. Since ionization efficiencies may vary with different amounts of chromophores attached, the MALDI-MS results, while insightful, are not reliable for calculations of bacteriochlorin/Mb ratios. Yet the minimum conclusion is that the distribution is narrow for 10 equiv (1.6 loading) yet quite broad for 50 equiv (7.1 loading). In a separate experiment, **BC7** and **BC8** were conjugated at 60 equiv relative to Mb, affording conjugates that also were quite soluble in aqueous solution. In both cases, the resulting loading was 9 and 12, respectively. The shift of the peaks in the distribution to higher mass was readily observed upon MALDI-MS analysis.⁸⁰

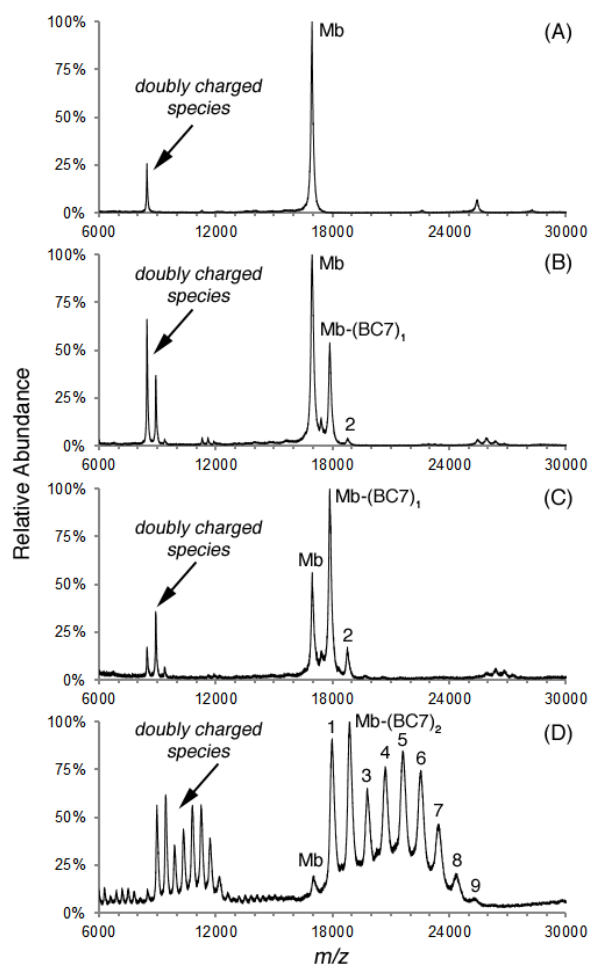


Figure 5.5. The MALDI spectra of the conjugate samples of Mb to (A) 0, (B) 2, (C) 10, and (D) 50 equiv of **BC7**. Peaks that match the mass of labeled Mb were marked by **Mb-(BC7)_x**, where x indicates the number of the bacteriochlorins attached.

The fluorescence properties of the **Mb-BC7** conjugates were examined. The spectrum for the conjugate derived from 50 equiv of **BC7** is shown in Figure 5.4 (panel B). The Φ_f value upon attachment to the protein was decreased to ~ 0.02 , to be compared with the value of 0.12 for **BC7** in aqueous solution. The Φ_f value was essentially indifferent to the level of loading. To distinguish possible effects of heme as a quencher, the heme was

removed by extraction with 2-butanone,⁷⁸ to afford the corresponding apoMb conjugates. In each case, the resulting **apoMb-BC7** conjugate (derived from 2, 10 or 50 equiv of **BC7**) gave a characteristic bacteriochlorin absorption spectrum.⁸⁰ Indeed, no trace of tailing of the long-wavelength, Q_y absorption band was observed. Unlike for **Mb-BC7**, however, the Φ_f values now were a function of loading (i.e., **BC7**/Mb ratio). The results are illustrated in Figure 5.6. The Φ_f value for the lowest-loading conjugate (2 equiv of **BC7**, average 0.62 bacteriochlorins/Mb) was 0.091, only decreased by 25% from that of the parent **BC7** monomer. On the other hand, the decline with loading (to 0.023 for 50 equiv, average 7.1 bacteriochlorins/Mb) is attributed to self-quenching of the bacteriochlorins on the protein. Thus, a distinction between quenching due to the presence of heme versus quenching due to bacteriochlorin self-interactions is clearly obtained.

loading	Φ_f values	
	Mb-BC7	apoMb-BC7
0.62 (2 equiv)	0.019	0.091
1.6 (10 equiv)	0.020	0.071
7.1 (50 equiv)	0.018	0.023

Arrows labeled "heme quenching" point from the apoMb-BC7 values to the Mb-BC7 values for each loading level. A vertical arrow labeled "self-quenching" points downwards from the apoMb-BC7 value at 0.62 equiv to the value at 7.1 equiv.

Figure 5.6. Fluorescence quantum yield values as a function of loading and \pm heme.

The origin of self-quenching is unclear. The absorption spectra and the emission spectra of the **apoMb-BC7** conjugates were essentially identical to those of the monomeric **BC7**. Calculations of the Förster through-space energy transfer (using PhotochemCad^{76,77})

showed that the self-exchange process for bacteriochlorin–bacteriochlorin energy transfer exhibits $R_0 = 59 \text{ \AA}$. Given the diameter of Mb is $\sim 50 \text{ \AA}$ from most distant points, a considerable degree of energy transfer between bacteriochlorins attached to Mb is expected to be permissible. Hence, any excited-state trapping site(s) at/near the protein are likely to be encountered upon successive transfer steps.

Outlook

The ability to synthesize hydrophilic/hydrophobic bacteriochlorins with some degree of wavelength tunability and that bear a single carboxylic acid (or NHS-ester) opens the door to a wide variety of studies, particularly upon bioconjugation to proteins. The lipophilic bacteriochlorins will be used for attachment to the hydrophobic region of membrane-spanning light-harvesting peptides to give rise to self-assembled artificial photosynthetic architectures. The attachment of a hydrophilic bacteriochlorin to Mb affords a water-soluble NIR-active protein architecture that is likely a more exacting and versatile analogue of the Cellarius-Mauzerall use of pheophytin-on-polystyrene particles first reported nearly 50 years ago. The bioconjugation of bacteriochlorins to Mb described herein also affords several attractive attributes as a testbed for attachment of chromophores to proteins: (1) the presence of heme provides a convenient absorption calibration standard for determining average loading of intensely absorbing chromophores, which often is difficult when relying solely on the weakly absorbing 280-nm band of proteins; (2) mass spectrometry of the Mb-chromophore conjugate provides a more granular view of the loading distribution; and (3) heme can be readily removed following loading determination to assess spectral properties in the resulting apoMb, including absorption and fluorescence spectra as well as Φ_f values.

Experimental section.

(I) General methods.

¹H NMR and ¹³C NMR spectroscopies were performed at room temperature. Tetramethylsilane was used as internal reference for CDCl₃. MALDI-MS was performed with the matrix 1,4-bis(5-phenyl-2-oxazol-2-yl)benzene for bacteriochlorins,⁷⁹ and α -cyano-4-hydroxycinnamic acid (CHCA) for Mb and conjugates. Electrospray ionization mass spectrometry (ESI-MS) data are reported for the molecular ion. Silica gel (40 μ m average particle size) was used for column chromatography. All solvents were reagent grade and were used as received unless noted otherwise. THF was freshly distilled from sodium/benzophenone ketyl. CHCl₃ was stabilized with amylenes (\leq 1%). Compounds **1**, **2**, **4** and **5** were obtained from commercial sources. Known compound **3**⁴² and bacteriochlorins **BC11**,⁵² **BC12**,⁴³ **BC13**,⁵⁴ **BC14**,⁵³ **BC18**,⁵³ and **BC19**⁵³ were prepared following literature procedures. Equine Mb was obtained in 95-100% purity and used as received.

(II) Synthesis

2-[4-(2-(*tert*-Butoxycarbonyl)ethyl)phenyl]-3,3,4,4-tetramethyl-1,3,2-dioxaborolane (2). Following a general procedure,⁶¹ a mixture of **1** (0.28 g, 1.0 mmol), di-*tert*-butyl dicarbonate (0.28 g, 1.3 mmol) and MgCl₂ (9.5 mg, 0.10 mmol) in *tert*-butyl alcohol (0.49 mL) and acetonitrile (0.15 mL) was stirred under argon for 16 h. The crude reaction mixture was diluted with water (10 mL) and extracted with ethyl acetate (3 x 10 mL). The combined extract was dried (Na₂SO₄), concentrated and chromatographed [silica, hexanes/ethyl acetate (9:1)] to afford a viscous colorless liquid (0.20 g, 60%): ¹H NMR (300 MHz, CDCl₃) δ 1.33 (s, 12H), 1.41 (s, 9H), 2.53 (t, J = 7.5 Hz, 2H), 2.92 (t, J = 7.5 Hz, 2H),

7.21 (d, $J = 7.8$ Hz, 2H), 7.73 (d, $J = 7.8$ Hz, 2H); ^{13}C NMR (75 MHz, CDCl_3) δ 25.1, 28.3, 31.5, 37.1, 80.6, 83.9, 100.3, 128.0, 135.2, 144.4, 172.3; ESI-MS obsd 354.2083, calcd 354.2087 $[(\text{M} + \text{Na})^+, \text{M} = \text{C}_{19}\text{H}_{29}\text{BO}_4]$.

15-[3-(3-Carboxypropionylamino)phenyl]-3,13-bis(ethoxycarbonyl)-2,12-diethyl-8,8,18,18-tetramethylbacteriochlorin (BC1). Following a general procedure,⁵² a solution of **BC11** (9.8 mg, 14 μmol) in CHCl_3 (0.60 mL) was treated with succinic anhydride (1.7 mg, 21 μmol) and stirred for 4 h at room temperature. 2 N HCl solution (~ 20 mL) was added to the reaction mixture, which then was extracted twice with CH_2Cl_2 . The extract was dried (Na_2SO_4), concentrated and chromatographed (silica, ethyl acetate) to afford a greenish solid (7.5 mg, 67%): ^1H NMR (300 MHz, $\text{DMSO}-d_6$) δ -1.99 (s, 1H), -1.69 (s, 1H), 1.20 (t, $J = 6.9$ Hz, 3H), 1.19 (t, $J = 7.2$ Hz, 3H), 1.78 (d, $J = 5.1$ Hz, 6H), 1.82 (s, 6H), 1.94 (d, $J = 4.8$ Hz, 6H), 2.09 (d, $J = 3.3$ Hz, 6H), 2.21 (s, 3H), 2.49 (s, 3H), 2.87 (m, 4H), 3.65 (s, 3H), 3.68 (s, 2H), 4.24 (d, $J = 2.4$ Hz, 2H), 4.32 (q, $J = 7.2$ Hz, 2H), 4.42 (q, $J = 7.2$ Hz, 2H), 6.56 (s, 1H), 6.64 (s, 1H), 7.08–7.15 (m, 4H), 7.34 (s, 1H), 7.39 (s, 1H), 7.47 (d, $J = 7.2$ Hz, 1H), 7.70 (d, $J = 8.7$ Hz, 2H), 7.79 (d, $J = 8.1$ Hz, 2H), 8.58 (br, 1H), 9.61 (s, 1H), 9.63 (s, 1H), 9.87 (s, 1H); MALDI-MS obsd 791.7302; ESI-MS obsd 792.3957, calcd 792.3967 $[(\text{M} + \text{H})^+, \text{M} = \text{C}_{45}\text{H}_{53}\text{N}_5\text{O}_8]$; λ_{abs} (CH_2Cl_2) 356, 375, 515, 727 nm.

15-[4-(2-(tert-Butoxycarbonyl)ethyl)phenyl]-3,13-bis(ethoxycarbonyl)-2,12-diethyl-8,8,18,18-tetramethylbacteriochlorin (pro-BC2). Following a general procedure,⁵² samples of **BC12** (34.0 mg, 50.0 μmol), **2** (49.8 mg, 150 μmol), $\text{Pd}(\text{PPh}_3)_4$ (17.3 mg, 15.0 μmol), and K_2CO_3 (83.0 mg, 600 μmol) were placed in a Schlenk flask which was then pump-purged three times with argon. DMF/toluene [5.0 mL, (1:2), degassed by bubbling

with argon for 30 min] was added to the Schlenk flask, and the reaction mixture was stirred at 90 °C for 18 h. The reaction mixture was cooled to room temperature, concentrated to dryness, and diluted with CH₂Cl₂. The resulting solution was washed with aqueous NaHCO₃. The organic layer was separated, dried (Na₂SO₄), concentrated and chromatographed [silica, CH₂Cl₂/ethyl acetate (49:1)] to obtain a greenish solid (37.6 mg, 93%): ¹H NMR (400 MHz, CDCl₃) δ -1.81 (brs, 1H), -1.51 (brs, 1H), 1.29 (t, *J* = 7.2 Hz, 3H), 1.55 (s, 9H), 1.63–1.70 (m, 6H), 1.77 (t, *J* = 8.0 Hz, 3H), 1.83 (s, 6H), 1.95 (s, 6H), 2.77 (t, *J* = 7.6 Hz, 2H), 3.16 (t, *J* = 7.6 Hz, 2H), 3.79 (q, *J* = 7.6 Hz, 2H), 3.83–3.89 (m, 6H), 4.27 (s, 3H), 4.38 (s, 2H), 4.80 (q, *J* = 7.2 Hz, 2H), 7.47 (d, *J* = 8.0 Hz, 2H), 7.73 (d, *J* = 8.0 Hz, 2H), 8.57 (s, 1H), 8.61 (s, 1H); ¹³C NMR (75 MHz, CDCl₃) δ 14.4, 14.9, 17.8, 20.2, 20.3, 28.5, 31.2, 31.3, 31.4, 37.4, 45.2, 46.3, 47.5, 52.3, 61.4, 62.0, 64.4, 80.8, 94.5, 94.7, 112.9, 123.2, 126.2, 127.7, 127.8, 132.4, 132.6, 133.4, 135.0, 138.6, 139.7, 140.2, 154.7, 161.0, 168.1, 168.5, 169.2, 172.7; MALDI-MS obsd 804.6556; ESI-MS obsd 805.4520, calcd 805.4535 [(M + H)⁺, M = C₄₈H₆₀N₄O₇]; λ_{abs} (CH₂Cl₂) 356, 365, 376, 515, 729 nm.

15-[4-(2-Carboxyethyl)phenyl]-3,13-bis(ethoxycarbonyl)-2,12-diethyl-8,8,18,18-tetramethylbacteriochlorin (BC2). Following a general procedure,⁵³ a sample of **pro-BC2** (9.0 mg, 11 μmol) in CH₂Cl₂ (2.0 mL) was stirred under argon for 2 min, followed by addition of TFA (0.40 mL). After 1 h, the reaction mixture was washed with saturated aqueous NaHCO₃, 2 N HCl, and water. The organic layer was separated, dried (Na₂SO₄) and concentrated. The resulting solid was treated with hexanes, sonicated in a benchtop sonication bath, centrifuged, and the supernatant was discarded to afford a reddish solid (6.2 mg, 74%): ¹H NMR (400 MHz, DMSO-*d*₆) δ -1.97 (brs, 1H), -1.67 (brs, 1H), 1.17 (t, *J* = 7.2

Hz, 3H), 1.50–1.56 (m, 6H), 1.63 (t, $J = 7.6$ Hz, 3H), 1.77 (s, 6H), 1.90 (s, 6H), 2.73 (t, $J = 7.2$ Hz, 2H), 3.03 (t, $J = 7.2$ Hz, 2H), 3.68–3.81 (m, 8H), 4.17 (s, 3H), 4.31 (s, 2H), 4.66 (q, $J = 7.6$ Hz, 2H), 7.45 (d, $J = 7.6$ Hz, 2H), 7.73 (d, $J = 7.6$ Hz, 2H), 8.67 (s, 1H), 8.72 (s, 1H), 12.30 (br, 1H); MALDI-MS obsd 747.9117; ESI-MS obsd 749.3912, calcd 749.3909 [(M + H)⁺, M = C₄₄H₅₂N₄O₇]; λ_{abs} (CH₂Cl₂) 356, 365, 376, 515, 729 nm.

15-[4-(*tert*-Butoxycarbonylmethoxy)phenyl]-3,13-bis(ethoxycarbonyl)-2,12-diethyl-8,8,18,18-tetramethylbacteriochlorin (pro-BC3). Following a general procedure,⁵² samples of **BC12** (34 mg, 50 μmol), **3** (50 mg, 0.15 mmol), Pd(PPh₃)₄ (17 mg, 15 μmol), and K₂CO₃ (83 mg, 0.60 μmol) were placed in a Schlenk flask which was then pump-purged three times with argon. DMF/toluene [5.0 mL, (1:2), degassed by bubbling with argon for 30 min] was added to the Schlenk flask, and the reaction mixture was stirred at 90 °C for 18 h. The reaction mixture was cooled to room temperature, concentrated to dryness, diluted with CH₂Cl₂ and washed with aqueous NaHCO₃. The organic layer was separated, dried (Na₂SO₄) and concentrated. Column chromatography [silica, CH₂Cl₂/ethyl acetate (49:1)] provided a greenish solid (29 mg, 73%): ¹H NMR (400 MHz, CDCl₃) δ -1.83 (brs, 1H), -1.53 (brs, 1H), 1.30 (t, $J = 7.2$ Hz, 3H), 1.59 (s, 9H), 1.62–1.69 (m, 6H), 1.76 (t, $J = 7.6$ Hz, 3H), 1.82 (s, 6H), 1.94 (s, 6H), 3.76 (q, $J = 8.0$ Hz, 2H), 3.82–3.89 (m, 4H), 3.95 (q, $J = 7.2$ Hz, 2H), 4.26 (s, 3H), 4.36 (s, 2H), 4.72 (s, 2), 4.78 (q, $J = 7.2$ Hz, 2H), 7.14 (d, $J = 8.4$ Hz, 2H), 7.71 (d, $J = 8.4$ Hz, 2H), 8.56 (s, 1H), 8.60 (s, 1H); ¹³C NMR (75 MHz, CDCl₃) δ 14.5, 14.9, 17.9, 20.2, 20.3, 28.4, 31.2, 31.4, 45.2, 46.3, 47.6, 52.3, 61.6, 62.0, 64.4, 66.1, 82.8, 94.5, 94.7, 112.4, 113.9, 123.2, 126.4, 127.7, 132.4, 132.5, 132.8, 134.4, 135.0, 135.1, 135.2, 138.5, 154.7, 157.7, 161.3, 168.2, 168.4, 168.6, 169.3; MALDI-MS obsd 806.6729;

ESI-MS obsd 807.4323, calcd 807.4327 [(M + H)⁺, M = C₄₇H₅₈N₄O₈]; λ_{abs} (CH₂Cl₂) 356, 364, 376, 515, 729 nm.

15-[4-(Carboxymethoxy)phenyl]-3,13-bis(ethoxycarbonyl)-2,12-diethyl-8,8,18,18-tetramethylbacteriochlorin (BC3). Following a general procedure,⁵³ a sample of **pro-BC3** (14 mg, 17 μmol) in CH₂Cl₂ (3.1 mL) was stirred under argon for 2 min, followed by addition of TFA (0.62 mL). After 1 h, the reaction mixture was washed with saturated aqueous NaHCO₃, 2 N HCl, and water. The organic layer was separated, dried (Na₂SO₄) and concentrated. The resulting solid was treated with hexanes. The resulting suspension was sonicated in a benchtop sonication bath and centrifuged. The supernatant was discarded to afford a reddish solid (9.2 mg, 71%): ¹H NMR (400 MHz, DMSO-*d*₆) δ -1.97 (brs, 1H), -1.67 (brs, 1H), 1.22 (t, *J* = 7.2 Hz, 3H), 1.51–1.59 (m, 6H), 1.65 (t, *J* = 7.6 Hz, 3H), 1.80 (s, 6H), 1.92 (s, 6H), 3.70–3.88 (m, 8H), 4.19 (s, 3H), 4.32 (s, 2H), 4.68 (q, *J* = 8.0 Hz, 2H), 4.87 (s, 2H), 7.15 (d, *J* = 8.4 Hz, 2H), 7.64 (d, *J* = 8.4 Hz, 2H), 8.69 (s, 1H), 8.74 (s, 1H), 13.13 (br, 1H); MALDI-MS obsd 750.5661; ESI-MS obsd 751.3706, calcd 751.3701 [(M + H)⁺, M = C₄₃H₅₀N₄O₈]; λ_{abs} (CH₂Cl₂) 357, 365, 375, 515, 728 nm.

Zn(II)-15-[3-(3-Carboxypropionylamino)phenyl]-3,13-bis(ethoxycarbonyl)-2,12-diethyl-8,8,18,18-tetramethylbacteriochlorin (BC4). Following a general procedure,⁵² a solution of **BC14** (14.3 mg, 18.9 μmol) in CHCl₃ (1.00 mL) was treated with succinic anhydride (2.50 mg, 25.0 μmol) and stirred at room temperature for 4 h. The resulting mixture was chromatographed (silica, ethyl acetate) to afford a reddish solid (10.0 mg, 62%): ¹H NMR (300 MHz, THF-*d*₈) δ 1.21 (t, *J* = 6.9 Hz, 3H), 1.51–1.69 (m, 9H), 1.82 (s, 3H), 1.83 (s, 3H), 1.95 (s, 6H), 2.61–2.63 (m, 4H), 3.61–3.84 (m, 8H), 3.97 (s, 1H), 4.14 (s, 3H),

4.38 (s, 2H), 4.61 (t, $J = 7.2$ Hz, 2H), 7.35–7.43 (m, 2H), 7.61 (s, 1H), 8.14 (d, $J = 7.5$ Hz, 1H), 8.46 (s, 1H), 8.450 (s, 1H), 9.28 (s, 1H); MALDI-MS obsd 853.40; ESI-MS obsd 854.3029, calcd 854.3107 [(M + H)⁺, M = C₄₅H₅₁N₅O₈Zn]; λ_{abs} (CH₂Cl₂) 353, 384, 551, 735 nm.

15-[3-(3-Carboxypropionylamino)phenyl]-3,13-bis(ethoxycarbonyl)-2,12-dimesityl-8,8,18,18-tetramethylbacteriochlorin (BC5). Following a general procedure,⁵² a solution of **BC13** (14.2 mg, 16.3 μmol) in CHCl₃ (652 μL) was treated with succinic anhydride (8.10 mg, 81.4 μmol) and stirred for 1 h at room temperature. The reaction mixture was dried and chromatographed [silica, CH₂Cl₂/ethyl acetate (9:1) to CH₂Cl₂/methanol (4:1)] to yield a greenish solid (11.2 mg, 71%): ¹H NMR (400 MHz, THF-*d*₈, the CO₂H proton was not observed) δ -0.80 (s, 1H), -0.47 (s, 1H), 0.97 (t, $J = 7.2$ Hz, 3H), 1.09 (t, $J = 7.2$ Hz, 3H), 1.77 (s, 3H), 1.81 (s, 3H), 1.83 (s, 3H), 1.87 (s, 3H), 1.93 (s, 6H), 2.07 (s, 3H), 2.09 (s, 3H), 2.24 (s, 3H), 2.47 (s, 3H), 2.59–2.67 (m, 4H), 3.63 (s, 3H), 3.75 (d, $J = 2.4$ Hz, 2H), 4.20–4.27 (m, 4H), 4.31 (t, $J = 7.2$ Hz, 2H), 6.45 (s, 1H), 6.72 (s, 1H), 6.97–7.04 (m, 2H), 7.10 (s, 2H), 7.54 (d, $J = 8.0$ Hz, 1H), 7.65 (s, 1H), 8.94 (s, 1H), 9.68 (s, 1H), 9.72 (s, 1H); ¹³C NMR (100 MHz, THF-*d*₈) δ 16.9, 17.0, 24.2, 24.4, 24.7, 32.3, 34.0, 34.1, 34.2, 35.2, 48.9, 49.6, 50.7, 55.7, 63.59, 63.65, 65.8, 119.0, 121.1, 124.4, 124.8, 128.2, 129.1, 130.8, 131.09, 131.16, 131.20, 131.7, 136.1, 137.5, 138.1, 138.6, 138.8, 139.7, 139.9, 140.4, 140.5, 140.6, 141.2, 141.9, 144.1, 160.1, 166.3, 169.08, 169.18, 172.9, 173.8, 174.7, 177.2; MALDI-MS obsd 971.0664; ESI-MS obsd 972.4897, calcd 972.4906 [(M + H)⁺, M = C₅₉H₆₅N₅O₈]; λ_{abs} (CH₂Cl₂) 364, 543, 756 nm.

15²-[N-(3-(*tert*-Butoxycarbonyl)propyl)-3-ethoxycarbonyl-2,12-diethyl-8,8,18,18-tetramethylbacteriochlorin-13,15-dicarboximide (pro-BC6). Following a reported procedure,⁴⁴ a mixture of **BC12** (19.0 mg, 28.0 μmol), Pd(PPh₃)₄ (51.7 mg, 44.7 μmol), Cs₂CO₃ (137 mg, 419 μmol) and *tert*-butyl 4-aminobutyrate (22.0 mg, 112 μmol) was placed in a Schlenk flask, and deaerated under high vacuum for 40 min. The flask was then filled with CO and toluene (3.0 mL, deaerated by bubbling with argon for 30 min, and then with CO for 30 min). The reaction mixture was stirred at 90 °C for 14 h under a CO atmosphere at ambient pressure. The reaction mixture was cooled to room temperature, dried and washed (saturated aqueous NaHCO₃ solution). The combined organic layer was dried (Na₂SO₄), concentrated and chromatographed [silica, CH₂Cl₂/ethyl acetate (22:3)]. The resulting solid was extracted with hexanes, sonicated in a benchtop sonication bath and centrifuged. The supernatant was discarded to afford a reddish solid (13.0 mg, 65%): ¹H NMR (400 MHz, CDCl₃) δ -0.72 (s, 1H), -0.51 (s, 1H), 1.47 (s, 9H), 1.68–1.78 (m, 9H), 1.92 (s, 6H), 1.93 (s, 6H), 2.25–2.32 (m, 2H), 2.54 (t, *J* = 8.4 Hz, 2H), 4.08 (q, *J* = 7.2 Hz, 2H), 4.21 (q, *J* = 7.2 Hz, 2H), 4.33 (s, 2H), 4.50 (t, *J* = 7.2 Hz, 2H), 4.73 (s, 2H), 4.77 (q, *J* = 7.2 Hz, 2H), 8.57 (s, 1H), 8.70 (s, 1H), 9.55 (s, 1H); ¹³C NMR (100 MHz, CDCl₃) δ 14.8, 17.4, 17.6, 20.1, 20.9, 24.7, 28.4, 30.0, 31.2, 31.6, 33.8, 39.6, 45.7, 46.1, 52.1, 53.3, 61.5, 80.4, 94.7, 99.2, 99.5, 102.0, 115.0, 122.1, 133.4, 134.6, 136.2, 136.9, 140.3, 144.4, 162.8, 163.3, 165.9, 168.3, 168.5, 170.4, 172.9, 176.2; MALDI-MS obsd 709.4791; ESI-MS obsd 710.3921, calcd 710.3912 [(M + H)⁺, M = C₄₁H₅₁N₅O₆]; λ_{abs} (CH₂Cl₂) 358, 408, 544, 819 nm.

15²-[N-(3-(Carboxypropyl)-3-ethoxycarbonyl-2,12-diethyl-8,8,18,18-tetramethylbacteriochlorin-13,15-dicarboximide (BC6). Following a general procedure,⁵³

a solution of **pro-BC6** (14.5 mg, 20.0 μmol) in CH_2Cl_2 (1.60 mL) was stirred under argon for 2 min, followed by addition of TFA (400 μL). After 30 min, the reaction mixture was diluted with ethyl acetate and then washed with saturated aqueous NaHCO_3 . The organic layer was separated, dried (Na_2SO_4) and concentrated. The resulting solid was treated with hexanes, sonicated in a benchtop sonication bath and centrifuged. The supernatant was discarded to afford a reddish solid (12.0 mg, 90%): ^1H NMR (400 MHz, CDCl_3 , the COOH proton was not observed) δ -0.70 (s, 1H), -0.50 (s, 1H), 1.64–1.75 (m, 9H), 1.90 (s, 12H), 2.23–2.27 (m, 2H), 2.54 (t, $J = 7.2$ Hz, 2H), 4.03 (q, $J = 7.2$ Hz, 2H), 4.17 (q, $J = 7.2$ Hz, 2H), 4.30 (s, 2H), 4.42 (t, $J = 7.2$ Hz, 2H), 4.68 (s, 2H), 4.77 (q, $J = 7.2$ Hz, 2H), 8.53 (s, 1H), 8.66 (s, 1H), 9.52 (s, 1H); ^{13}C NMR (100 MHz, CDCl_3) δ 14.8, 17.4, 17.5, 20.1, 20.9, 24.3, 31.1, 31.5, 32.1, 39.3, 45.6, 46.2, 52.1, 53.3, 61.5, 94.7, 99.1, 99.6, 102.0, 114.6, 122.2, 133.3, 134.5, 136.3, 137.1, 140.2, 144.5, 162.8, 163.4, 165.8, 168.46, 168.49, 170.4, 176.5, 178.3; MALDI-MS obsd 654.1035; ESI-MS obsd 654.329, calcd 654.3286 [(M + H)⁺, M = $\text{C}_{37}\text{H}_{43}\text{N}_5\text{O}_6$]; λ_{abs} (CH_2Cl_2) 357, 408, 544, 819 nm.

3,13-Bis[3,5-bis(*tert*-butoxycarbonyl)phenyl]-5-methoxy-15-[3-(4-(*N*-succinimidooxy)-1,4-dioxobutylamino)phenyl]-8,8,18,18-tetramethylbacteriochlorin (pro-BC7**). Following a general procedure,⁵² a solution of **BC16** (14.7 mg, 14.0 μmol) in CHCl_3 (560 μL) was treated with succinic anhydride (2.80 mg, 27.8 μmol) and stirred for 2 h at room temperature. The crude reaction mixture was chromatographed [silica, CH_2Cl_2 /ethyl acetate (23:2)] to afford a greenish solid, which was used directly in the next step. The greenish solid was dissolved in CH_2Cl_2 (1.23 mL) followed by addition of DCC (38.1 mg,**

0.185 mmol). The mixture was stirred under argon for 3 min. Then HOSu (21.3 mg, 0.185 mmol) was added. The resulting mixture was stirred for 40 min and then filtered to remove insoluble material. The filtrate was concentrated and chromatographed [silica, CH₂Cl₂/ethyl acetate (9:1)] to yield a greenish solid (9.0 mg, 40%): ¹H NMR (300 MHz, CDCl₃) δ -1.59 (s, 1H), -1.21 (s, 1H), 1.64 (s, 18H), 1.69 (s, 18H), 1.90 (s, 6H), 2.00 (s, 6H), 2.74–2.81 (m, 6H), 3.06 (t, *J* = 7.5 Hz, 2H), 3.70 (s, 3H), 3.91–4.18 (m, 2H), 4.38 (s, 2H), 7.14 (t, *J* = 7.8 Hz, 1H), 7.38 (d, *J* = 5.4 Hz, 1H), 7.41–7.43 (m, 3H), 7.58 (s, 1H), 7.96 (s, 1H), 8.18 (s, 1H), 8.38 (s, 1H), 8.66 (t, *J* = 9.9 Hz, 2H), 8.76 (s, 1H), 8.91 (s, 2H); ¹³C NMR (100 MHz, CDCl₃) δ 14.4, 22.9, 25.2, 25.78, 25.81, 26.9, 28.48, 28.54, 31.4, 34.2, 45.4, 46.0, 47.8, 49.4, 52.1, 63.6, 81.9, 97.3, 97.8, 113.2, 119.6, 123.4, 125.5, 126.6, 128.16, 128.27, 128.31, 129.2, 129.6, 132.0, 132.6, 133.71, 133.75, 134.3, 134.9, 135.2, 136.0, 136.3, 137.1, 138.6, 139.0, 141.6, 155.4, 157.0, 160.8, 165.8, 168.20, 168.37, 169.1, 169.2, 169.7; MALDI-MS obsd 1242.5563; ESI-MS obsd 1241.5811, calcd 1241.5811 [(M + H)⁺, M = C₆₁H₇₁BrN₄O₁₃]; λ_{abs} (CH₂Cl₂) 366, 517, 730 nm.

3,13-Bis(3,5-dicarboxyphenyl)-5-methoxy-15-[3-(4-(*N*-succinimidooxy)-1,4-dioxobutylamino)phenyl]-8,8,18,18-tetramethylbacteriochlorin (BC7). Following a general procedure,⁵³ a solution of **pro-BC7** (32.2 mg, 26.0 μmol) in CH₂Cl₂ (4.00 mL) was stirred under argon for 2 min, followed by addition of TFA (1.00 mL). After 2 h, the reaction mixture was diluted with ethyl acetate and then washed with brine until the aqueous phase was neutral (pH paper). The organic layer was separated, dried (Na₂SO₄) and concentrated. The resulting solid was treated with CH₂Cl₂, sonicated in a benchtop sonication bath and centrifuged. The supernatant was discarded to afford a green solid (20.0 mg, 76%): ¹H NMR

(300 MHz, DMSO-*d*₆) δ -1.67 (s, 1H), -1.32 (s, 1H), 1.74 (s, 3H), 1.86 (s, 3H), 1.92 (s, 3H), 1.94 (s, 3H), 2.67 (t, *J* = 5.1 Hz, 2H), 2.77 (s, 4H), 2.94 (t, *J* = 5.1 Hz, 2H), 3.58 (s, 3H), 3.80 (d, *J* = 13.2 Hz, 1H), 4.06 (d, *J* = 13.2 Hz, 1H), 4.34 (s, 2H), 7.05 (t, *J* = 5.4 Hz, 1H), 7.26 (t, *J* = 8.1 Hz, 2H), 7.77 (s, 1H), 7.87 (s, 1H), 8.10 (s, 1H), 8.27 (d, *J* = 1.2 Hz, 1H), 8.69 (d, *J* = 1.2 Hz, 1H), 8.85–8.97 (m, 6H), 9.88 (s, 1H), 13.4–13.6 (br, 4H); MALDI-MS obsd 1015.4610; ESI-MS obsd 1017.3289, calcd 1017.3301 [(M + H)⁺, M = C₅₅H₄₈N₆O₁₄]; λ_{abs} (0.5 M potassium phosphate buffer, pH 7.0) 362, 516, 729 nm.

3,13-Bis[3,5-bis(*tert*-butoxycarbonyl)phenyl]-5-methoxy-15-[4-(4-(*N*-succinimidooxy)-1,4-dioxobutylamino)phenyl]-8,8,18,18-tetramethylbacteriochlorin (pro-BC8). Following a general procedure,⁵² a solution of **BC20** (18 mg, 17 μ mol) in CHCl₃ (0.63 mL) was treated with succinic anhydride (6.2 mg, 62 μ mol) and stirred for 1 h at room temperature. The crude reaction mixture was chromatographed (silica, ethyl acetate) to afford a greenish solid (14 mg), which was used directly in the next step. The resulting greenish solid (8.0 mg) was dissolved in CH₂Cl₂ (0.70 mL) followed by the addition of DCC (14 mg, 70 μ mol), and the mixture was stirred under argon for 3 min. HOSu (8.1 mg, 70 μ mol) was then added. The resulting mixture was stirred for 40 min and then filtered to remove insoluble material. The filtrate was concentrated and chromatographed [silica, CH₂Cl₂/ethyl acetate (4:1)]. The resulting solid was treated with hexanes/CH₂Cl₂ (9:1), sonicated in a benchtop sonication bath and centrifuged. The supernatant was discarded to afford a green solid (6.5 mg, 53%): ¹H NMR (300 MHz, CDCl₃, the NH proton peaks were not observed) δ -1.58 (s, 1H), -1.20 (s, 1H), 1.63 (s, 18H), 1.69 (s, 18H), 1.84 (s, 6H), 1.98

(s, 6H), 2.85–2.90 (m, 6H), 3.15 (t, $J = 6.6$ Hz, 2H), 3.68 (s, 3H), 3.95 (s, 2H), 4.38 (s, 2H), 7.25–7.27 (m, 1H), 7.41–7.46 (m, 3H), 8.01(d, $J = 1.8$ Hz, 2H), 8.40 (s, 1H), 8.66–8.69 (m, 4H), 8.76 (t, $J = 1.8$ Hz, 1H), 8.91 (d, $J = 1.8$ Hz, 2H); MALDI-MS 1240.4706; ESI-MS obsd 1241.5795, calcd 1241.5805 [(M + H)⁺, M = C₇₁H₈₀N₆O₁₄]; λ_{abs} (CH₂Cl₂) 366, 518, 730 nm.

3,13-Bis(3,5-dicarboxyphenyl)-5-methoxy-15-[4-(4-(*N*-succinimidooxy)-1,4-dioxobutylamino)phenyl]-8,8,18,18-tetramethylbacteriochlorin (BC8). Following a general procedure,⁵³ a solution of **pro-BC8** (6.5 mg, 5.2 μmol) in CH₂Cl₂ (0.42 mL) was stirred under argon for 2 min, followed by addition of TFA (0.11 mL). After 1.5 h, the reaction mixture was diluted with ethyl acetate and then washed with brine until the aqueous phase was neutral (pH paper). The organic layer was separated, dried (Na₂SO₄) and concentrated. The resulting solid was treated with CH₂Cl₂, sonicated in a benchtop sonication bath, and centrifuged. The supernatant was discarded to afford a green solid (3.8 mg, 71%): ¹H NMR (300 MHz, CD₃OD/CDCl₃, the COOH and NH proton peaks were not observed) δ 1.87 (s, 6H), 2.01 (s, 6H), 2.88–2.92 (m, 6H), 3.14 (t, $J = 7.2$ Hz, 2H), 3.68 (s, 3H), 3.97 (s, 2H), 4.40 (s, 2H), 7.37–7.45 (m, 4H), 8.15 (d, $J = 1.5$ Hz, 2H), 8.52 (s, 1H), 8.73–8.76 (m, 4H), 8.91 (s, 1H), 9.02 (d, $J = 1.5$ Hz, 2H); MALDI-MS obsd 1016.2656; ESI-MS obsd 1017.3289, calcd 1017.3301 [(M + H)⁺, M = C₅₅H₄₈N₆O₁₄]; λ_{abs} (0.5 M potassium phosphate buffer, pH 7.0) 362, 516, 729 nm.

2,12-Bis[3,5-bis(*tert*-butoxycarbonyl)phenyl]-3,13-bis(methoxycarbonyl)-5-methoxy-15-[7-(*N*-succinimidooxy)-7-oxohept-1-ynyl]-8,8,18,18-tetramethylbacteriochlorin (pro-BC9). Following a general procedure⁴² for copper-free Sonogashira reaction,^{62,63} a mixture of **BC22** (26 mg, 23 μmol), 6-heptynoic acid (**5**, 15 μL ,

0.12 mmol), Pd₂(dba)₃ (6.2 mg, 6.7 μmol), and P(*o*-tol)₃ (11 mg, 35 μmol) were placed in a Schlenk flask and dried under high vacuum for 30 min. Toluene/TEA [2.4 mL, (2:1), deaerated by bubbling with argon for 30 min] was added to the Schlenk flask under argon and deaerated by three freeze-pump-thaw cycles. The reaction mixture was stirred at 70 °C for 18 h. The reaction mixture was cooled to room temperature, concentrated to dryness, diluted with CH₂Cl₂ and washed (saturated aqueous NaHCO₃ solution). The organic layer was separated, dried (Na₂SO₄) and concentrated. Column chromatography [silica, CH₂Cl₂/EtOAc (19:1) to CH₂Cl₂/CH₃OH (19:1)] provided a reddish solid (8.0 mg, total yield is given below): MALDI-MS obsd 1192.7728; ESI-MS obsd 1193.5701, calcd 1193.5693 [(M + H)⁺, M = C₆₈H₈₀N₄O₁₅]; λ_{abs} (CH₂Cl₂) 382, 547, 756 nm. Half of the product (4.0 mg), DCC (6.9 mg, 34 μmol) and HOSu (3.9 mg, 34 μmol) was stirred in CH₂Cl₂ (0.34 mL) under argon at room temperature for 40 min. The resulting mixture was filtered to remove insoluble material. The filtrate was concentrated and separated by preparative TLC [silica, CH₂Cl₂/methanol (99:1)] to yield a reddish solid (2.8 mg, 19%): ¹H NMR (300 MHz, CDCl₃) δ -1.22 (s, 1H), -0.97 (s, 1H), 1.54–1.58 (m, 2H), 1.66 (s, 36H), 1.82 (s, 6H), 1.83 (s, 6H), 2.22–2.28 (m, 2H), 2.78–2.91 (m, 8H), 4.12 (s, 3H), 4.17 (s, 3H), 4.26 (s, 3H), 4.32 (s, 2H), 4.42 (s, 2H), 8.45 (s, 1H), 8.49 (s, 1H), 8.82 (s, 1H), 8.83 (s, 1H), 8.86–8.87 (m, 4H); MALDI-MS 1289.4308; ESI-MS obsd 1290.5865, calcd 1290.5857 [(M + H)⁺, M = C₇₂H₈₃N₅O₁₇]; λ_{abs} (CH₂Cl₂) 381, 547, 756 nm.

2,12-Bis(3,5-dicarboxyphenyl)-3,13-bis(methoxycarbonyl)-5-methoxy-15-[7-(*N*-succinimidooxy)-7-oxohept-1-ynyl]-8,8,18,18-tetramethylbacteriochlorin (BC9).

Following a general procedure,⁵³ a solution of **pro-BC9** (3.4 mg, 2.6 μmol) in CH₂Cl₂ (0.22

mL) was stirred under argon for 2 min, followed by addition of TFA (44 μ L). After 1.5 h, the reaction mixture was diluted with ethyl acetate and then washed with brine until the aqueous phase was neutral (checked by pH paper). The organic layer was separated, dried (Na_2SO_4) and concentrated. The resulting solid was treated with CH_2Cl_2 , sonicated in a benchtop sonication bath and centrifuged. The supernatant was discarded to afford a reddish solid (2.3 mg, 82%): ^1H NMR (300 MHz, $\text{CD}_3\text{OD}/\text{CDCl}_3$, the COOH and NH proton peaks were not observed) δ 1.26–1.30 (m, 2H), 1.85 (s, 12H), 2.02–2.22 (m, 2H), 2.78–2.93 (m, 8H), 4.14 (s, 3H), 4.18 (s, 3H), 4.29 (s, 3H), 4.42 (s, 2H), 4.55 (s, 2H), 8.50 (s, 1H), 8.53 (s, 1H), 8.95 (s, 1H), 8.96 (s, 1H), 8.99–9.01 (m, 4H); MALDI-MS obsd 1068.5653; ESI-MS obsd 1066.3371, calcd 1066.3353 $[(\text{M} + \text{H})^+]$, $\text{M} = \text{C}_{56}\text{H}_{51}\text{N}_5\text{O}_{17}$; λ_{abs} (0.5 M potassium phosphate buffer, pH 7.0) 378, 546, 757 nm.

15²-N-(3-Succinimidooxypropyl)-3-methoxycarbonyl-2,12-bis[3,5-bis(*tert*-butoxycarbonyl)phenyl]-8,8,18,18-tetramethylbacteriochlorin-13,15-dicarboximide (pro-BC10). Following a reported procedure,⁴⁴ a mixture of **BC22** (12 mg, 10 μ mol), $\text{Pd}(\text{PPh}_3)_4$ (12 mg, 10 μ mol), Cs_2CO_3 (10 mg, 30 μ mol) and 3-aminopropanoic acid (4.0 mg, 40 μ mol) was placed in a Schlenk flask, and deaerated under high vacuum for 40 min. The flask was then filled with CO and toluene (1.0 mL, deaerated by bubbling with argon for 30 min, and then with CO for 30 min). The reaction mixture was stirred at 80 $^\circ\text{C}$ for 18 h under a CO atmosphere at ambient pressure. The reaction mixture was cooled to room temperature, dried and washed (saturated aqueous NaHCO_3 solution). The combined organic layer was dried (Na_2SO_4), concentrated and chromatographed [silica, CH_2Cl_2 /methanol (4:1)]. The resulting solid was mixed with EDC (9.6 mg 50 μ mol), DMAP (0.20 mg, 2.0 μ mol) and

HOSu (5.7 mg, 50 μ mol) in CH₂Cl₂ (0.20 mL) and stirred under argon for 3 h. The reaction residue was chromatographed [silica, CH₂Cl₂/ethyl acetate (19:1 to 4:1)] to afford a reddish solid (2.7 mg, 22%): ¹H NMR (300 MHz, CDCl₃) δ -0.43 (s, 1H), 0.09 (s, 1H), 1.66 (s, 18H), 1.67 (s, 18H), 1.79 (s, 6H), 1.82 (s, 6H), 2.83 (s, 4H), 3.31 (t, *J* = 6.6 Hz, 2H), 4.18 (s, 3H), 4.25 (s, 2H), 4.27 (s, 3H), 4.70 (s, 2H), 4.83 (t, *J* = 6.6 Hz, 2H), 8.38 (s, 1H), 8.45 (s, 1H), 8.83 (d, *J* = 2.1 Hz, 2H), 8.84 (d, *J* = 2.1 Hz, 2H), 8.89 (t, *J* = 1.5 Hz, 2H); MALDI-MS obsd 1248.9579; ESI-MS obsd 1249.5371, calcd 1249.5340 [(M + H)⁺, M = C₆₈H₇₆N₆O₁₇]; λ_{abs} (CH₂Cl₂) 377, 564, 811 nm.

15²-N-(3-Succinimidooxypropyl)-3-methoxycarbonyl-2,12-bis(3,5-dicarbonylphenyl)-8,8,18,18-tetramethylbacteriochlorin-13,15-dicarboximide (BC10).

Following a general procedure,⁵³ a solution of **pro-BC10** (2.6 mg, 2.1 μ mol) in CH₂Cl₂ (0.12 mL) was stirred under argon for 2 min, followed by addition of TFA (92 μ L). After 1 h, the reaction mixture was diluted with ethyl acetate and then washed with brine until the aqueous phase was neutral (checked by pH paper). The organic layer was separated, dried (Na₂SO₄) and concentrated. The resulting solid was treated with CH₂Cl₂, sonicated in a benchtop sonication bath and centrifuged. The supernatant was discarded to afford a reddish solid (2.0 mg, 94%): ¹H NMR (300 MHz, THF-*d*₈, four CO₂H protons were not observed) δ -0.24 (s, 1H), 0.29 (s, 1H), 1.99 (s, 6H), 2.01 (s, 6H), 2.93 (s, 4H), 3.43 (t, *J* = 7.2 Hz, 2H), 4.28 (s, 3H), 4.46 (s, 3H), 4.50 (s, 2H), 4.90–4.93 (m, 4H), 8.70 (s, 1H), 8.74 (s, 1H), 9.12–9.15 (m, 6H); MALDI-MS obsd 1025.4487; ESI-MS obsd 1025.2875, calcd 1025.2836 [(M + H)⁺, M = C₅₂H₄₄N₆O₁₇]; λ_{abs} (0.5 M potassium phosphate buffer, pH 7.0) 377, 570, 824 nm.

Zn(II)-15-(3-Aminophenyl)-3,13-bis(ethoxycarbonyl)-2,12-diethyl-5-methoxy-8,8,18,18-tetramethylbacteriochlorin (BC14). Following a general procedure,⁴⁵ a mixture of **BC11** (16.0 mg, 23.1 μmol) and NaH (16.6 mg, 1.20 mmol, 30.0 equiv) was added to DMSO (2.30 mL) under argon and stirred for 5 min. $\text{Zn}(\text{OTf})_2$ (252 mg, 694 μmol , 30.0 equiv) was then added, and the suspension was stirred for 16 h in an oil bath at 80 °C. The crude mixture was washed with water and extracted with ethyl acetate. The combined extract was dried (Na_2SO_4), concentrated and chromatographed [silica, CH_2Cl_2 /ethyl acetate (9:1)] to afford a reddish solid (9.1 mg, 52%): ^1H NMR (300 MHz, $\text{THF}-d_8$) δ 1.25 (t, $J = 7.2$ Hz, 3H), 1.51–1.69 (m, 9H), 1.81 (s, 3H), 1.83 (s, 3H), 1.94 (s, 6H), 3.61–3.76 (m, 4H), 3.89–4.02 (m, 4H), 4.13 (s, 3H), 4.37 (s, 2H), 4.55 (s, 2H), 4.61 (t, $J = 7.5$ Hz, 2H), 6.71–6.74 (m, 1H), 6.92–6.94 (m, 2H), 7.17 (t, $J = 7.8$ Hz, 1H), 8.44 (s, 1H), 8.48 (s, 1H); MALDI-MS obsd 753.39; ESI-MS obsd 754.2917, calcd 754.2947 [(M + H)⁺, M = $\text{C}_{41}\text{H}_{47}\text{N}_5\text{O}_5\text{Zn}$]; λ_{abs} (CH_2Cl_2) 355, 385, 553, 738 nm.

15²-N-Butyl-3-ethoxycarbonyl-2,12-diethyl-8,8,18,18-tetramethylbacteriochlorin-13,15-dicarboximide (BC17). Following a reported procedure,⁴⁴ a mixture of **BC12** (25.0 mg, 36.8 μmol), $\text{Pd}(\text{PPh}_3)_4$ (68.0 mg, 58.9 μmol), Cs_2CO_3 (180 mg, 552 μmol) and *n*-butylamine (18.0 μL , 184 μmol) was placed in a Schlenk flask, and deaerated under high vacuum for 40 min. The flask was then filled with CO and toluene (4.0 mL, deaerated by bubbling with argon for 30 min, and then with CO for 30 min). The reaction mixture was stirred at 90 °C for 18 h under a CO atmosphere at ambient pressure. The reaction mixture was cooled to room temperature, dried and washed with saturated aqueous NaHCO_3 solution. The combined organic layer was dried (Na_2SO_4), concentrated and chromatographed [silica,

hexanes/CH₂Cl₂ (5:5 to 3:7)] to afford a reddish solid (11.9 mg, 52%): ¹H NMR (400 MHz, CDCl₃) δ -0.74 (s, 1H), -0.54 (s, 1H), 1.10 (t, *J* = 7.2 Hz, 3H), 1.62–1.79 (m, 13H), 1.92 (s, 6H), 1.93 (s, 6H), 4.08 (q, *J* = 7.2 Hz, 2H), 4.22 (q, *J* = 7.2 Hz, 2H), 4.33 (s, 2H), 4.44 (t, *J* = 8.0 Hz, 2H), 4.74 (s, 2H), 4.78 (q, *J* = 7.2 Hz, 2H), 8.58 (s, 1H), 8.71 (s, 1H), 9.56 (s, 1H); ¹³C NMR (100 MHz, CDCl₃) δ 14.3, 14.8, 17.4, 17.6, 20.1, 20.9, 21.0, 30.0, 31.2, 31.3, 31.6, 40.4, 45.7, 46.1, 52.1, 53.36, 53.45, 61.5, 94.7, 99.4, 99.5, 101.9, 115.2, 122.0, 133.5, 134.6, 136.2, 136.8, 140.3, 144.3, 162.6, 163.4, 165.9, 168.2, 168.5, 170.5, 176.0; MALDI-MS obsd 622.9292; ESI-MS obsd 624.3532, calcd 624.3544 [(M + H)⁺, M = C₃₇H₄₅N₅O₄]; λ_{abs} (CH₂Cl₂) 357, 408, 543, 818 nm.

15-(4-Aminophenyl)-3,13-bis[3,5-bis(*tert*-butoxycarbonyl)phenyl]-5-methoxy-8,8,18,18-tetramethylbacteriochlorin (BC20). Following a general procedure,⁵² samples of bacteriochlorin **BC18** (53.0 mg, 51.4 μmol), **4** (56.3 mg, 0.257 mmol), Pd(PPh₃)₄ (23.7 mg, 20.6 μmol), and Cs₂CO₃ (101 mg, 0.308 mmol) were placed in a Schlenk flask and dried under high vacuum for 30 min. Toluene/DMF [5.1 mL, (2:1), deaerated by bubbling with argon for 30 min] was added to the Schlenk flask under argon and deaerated by three freeze-pump-thaw cycles. The reaction mixture was stirred at 90 °C for 18 h. The reaction mixture was cooled to room temperature, concentrated to dryness, diluted with CH₂Cl₂ and washed with saturated aqueous NaHCO₃. The organic layer was separated, dried (Na₂SO₄), concentrated and chromatographed [silica, CH₂Cl₂/ethyl acetate (23:2)] to provide a greenish solid (38.0 mg, 71%): ¹H NMR (300 MHz, CDCl₃) δ -1.52 (s, 1H), -1.18 (s, 1H), 1.65 (s, 18H), 1.69 (s, 18H), 1.85 (s, 6H), 1.98 (s, 6H), 3.60 (s, 2H), 3.68 (s, 3H), 4.00 (s, 2H), 4.38 (s, 2H), 6.41 (d, *J* = 8.4 Hz, 2H), 7.22 (d, *J* = 8.1 Hz, 1H), 7.26 (s, 1H), 7.62 (d, *J* = 8.1 Hz, 1H),

8.48 (t, $J = 1.5$ Hz, 1H), 8.64–8.67 (m, 4H), 8.76 (t, $J = 1.5$ Hz, 1H), 8.91 (d, $J = 1.5$ Hz, 1H) (two anilino NH protons were not observed); ^{13}C NMR (100 MHz, CDCl_3) δ 25.1, 28.5, 31.27, 31.38, 45.1, 46.0, 47.7, 52.4, 63.5, 81.4, 81.8, 83.5, 97.31, 97.37, 114.1, 114.3, 122.9, 127.0, 127.5, 128.0, 129.1, 131.07, 131.12, 131.9, 132.1, 133.9, 134.1, 134.2, 134.8, 136.0, 136.2, 136.6, 138.7, 138.9, 145.5, 154.8, 161.9, 165.6, 165.8, 169.06, 169.22; MALDI-MS 1043.6068; ESI-MS obsd 1044.5475, calcd 1044.5481 $[(\text{M} + \text{H})^+]$, $\text{M} = \text{C}_{63}\text{H}_{73}\text{N}_5\text{O}_9$; λ_{abs} (CH_2Cl_2) 366, 520, 729 nm.

15-Bromo-2,12-bis[3,5-bis(*tert*-butoxycarbonyl)phenyl]-3,13-dimethoxycarbonyl-5-methoxy-8,8,18,18-tetramethylbacteriochlorin (BC22). Following a general procedure,⁴³ a solution of bacteriochlorin **BC21** (44 mg, 41 μmol) in THF (8.3 mL) was treated with NBS (7.3 mg, 41 μmol) in THF (0.41 mL) at room temperature for 1.5 h. The reaction mixture was diluted with CH_2Cl_2 and washed with saturated aqueous NaHCO_3 . The organic layer was dried (Na_2SO_4), concentrated and chromatographed [silica, CH_2Cl_2 /ethyl acetate (19:1)] to afford a reddish solid (20 mg, 42%): ^1H NMR (300 MHz, CDCl_3) δ -1.52 (s, 1H), -1.25 (s, 1H), 1.66 (s, 36H), 1.83 (s, 6H), 1.86 (s, 6H), 4.16 (s, 3H), 4.20 (s, 3H), 4.28 (s, 3H), 4.37 (s, 2H), 4.44 (s, 2H), 8.50 (s, 2H), 8.83–8.85 (m, 2H), 8.87–8.88 (m, 4H); ^{13}C NMR (100 MHz) δ 14.4, 28.5, 29.9, 31.0, 31.3, 46.0, 47.9, 53.27, 53.39, 54.7, 64.6, 82.04, 82.10, 94.6, 96.7, 97.1, 98.2, 125.2, 126.0, 129.2, 130.0, 130.4, 131.5, 132.8, 133.1, 133.4, 133.7, 133.9, 134.4, 134.5, 136.3, 136.6, 158.2, 160.8, 165.08, 165.14, 168.6, 168.8, 169.2, 173.4; ESI-MS obsd 1147.4245, calcd 1147.4274 $[(\text{M} + \text{H})^+]$, $\text{M} = \text{C}_{61}\text{H}_{71}\text{BrN}_4\text{O}_{13}$; λ_{abs} (CH_2Cl_2) 375, 531, 740 nm.

(III) Protocol for preparation of Mb conjugate

The following procedure pertains to the use of 60 equiv of bacteriochlorin/Mb. A sample of equine Mb (0.57 mg, 33 nmol) was dissolved in potassium phosphate buffer (0.1 M, pH 8.3, 0.17 mL). In a separate vial, bacteriochlorin **BC7** or **BC8** (2.0 mg, 2.0 μ mol, 60 equiv) was initially dissolved in DMSO (33 μ L) and then 137 μ L of the same phosphate buffer was added with stirring to make a homogeneous bacteriochlorin solution. The resulting bacteriochlorin solution was then transferred to the Mb solution, and incubated in the dark for 3 h at room temperature (\sim 23 $^{\circ}$ C). The final concentration of Mb was 0.1 mM, in which DMSO accounts for 10% by volume.

The crude bacteriochlorin–Mb conjugate **Mb-BC7** or **Mb-BC8** was purified by passage (gravity-elution) over a PD-10 GPC column (Sephadex G-25 medium, bed dimension: 14.5 x 50 mm) with potassium phosphate buffer (0.5 M, pH 7.0) as eluent. The conjugate eluted as a clear dark green band, while free bacteriochlorin (unreacted or hydrolyzed bacteriochlorin-NHS ester) remained on top of the column. The resultant conjugate solution was subjected to centrifugal Amicon® Ultra-4 filtration (regenerated cellulose, molecular weight cutoff = 10K) for 30 min. The resulting filtrate lacked bacteriochlorin absorption, consistent with the thorough removal of any unconjugated bacteriochlorin. The solution that did not pass through the filter constituted the purified bacteriochlorin–Mb conjugate. MALDI-MS for **Mb-BC7**: m/z = 198812, 20695, 21509, 22484 (most intense), 23401, and 24319. MALDI-MS for **Mb-BC8**: m/z = 21589, 22509, 23432 (most intense), 24354 and 25330. Further data are provided in the ref 80.

The following protocol describes the use of 2, 10, or 50 equiv of bacteriochlorin/Mb. A sample of Mb (0.52 mg, 30 nmol) was dissolved in potassium phosphate buffer (0.1 M, pH 8.3, 0.15 mL). In a separate vial, bacteriochlorin **BC7** (60 μg , 60 nmol, 2 equiv or 0.30 mg, 0.30 μmol , 10 equiv, or 1.5 mg, 1.5 μmol , 50 equiv) was initially dissolved in DMSO (30 μL) and then 120 μL of the same phosphate buffer was added with stirring to make a homogeneous bacteriochlorin solution. The resulting bacteriochlorin solution was then pipetted into the Mb solution, and incubated in the dark for 3 h at room temperature (~ 23 $^{\circ}\text{C}$). The final concentration of Mb was 0.1 mM, and DMSO accounts for 10% by volume. The remainder of the protocol is identical for that above with 60 equiv of bacteriochlorin/Mb. The characterization data are provided in the body of the paper.

(IV) Heme-removal protocol

Following a general procedure,⁷⁸ the **Mb-BC7** conjugate (2, 10, or 50 equiv of **BC7**) in potassium phosphate buffer (100 mM, pH 8.3) was diluted with 2 N HCl to adjust to pH \sim 2 (pH paper). An equal volume of 2-butanone was added. The mixture was shaken gently and allowed to stand for 10 min. The organic layer was discarded. This procedure (2-butanone addition/phase separation/2-butanone removal) was repeated three times (total of four extractions). The aqueous phase containing the resulting **apoMb-BC7** conjugate was titrated with 2 M NaOH to adjust to pH \sim 8 (pH paper) for subsequent spectroscopic studies. The characterization data are provided in the body of the paper.

(V) Fluorescence quantum yield measurements

The Φ_f values were determined by excitation into the bacteriochlorin Q_x band (511–570 nm) with emission integrated from 650–850 nm. Samples were examined in a 1-cm

pathlength cuvette at room temperature with absorption of the Q_x band of $\sim 0.02\text{--}0.03$. The absorption of the corresponding Q_y band was typically ≤ 0.1 thereby avoiding the inner filter effect. The yields were determined in the standard manner (with corrected spectra) by ratioing to 3,13-bis(3,5-dicarboxyphenyl)-5-methoxy-8,8,18,18-tetramethylbacteriochlorin ($\Phi_f = 0.078$) for studies in aqueous solution,⁵³ or to 2,12-di-*p*-tolyl-5-methoxy-8,8,18,18-tetramethylbacteriochlorin ($\Phi_f = 0.18$ in toluene) for studies in DMF.⁴¹

(VI) Förster energy-transfer calculations.

The following parameters were utilized in the calculation:^{76,77} dielectric constant $n = 1.33$; orientation factor $\kappa^2 = 0.67$; assumed $\epsilon = 120,000 \text{ M}^{-1}\text{cm}^{-1}$ for **BC7** at 728 nm; $\Phi_f = 0.12$ for **BC7**. The calculated R_0 was 59 Å for **BC7-BC7**.

References

- 1 M. Köhn and R. Breinbauer, *Angew. Chem. Int. Ed.*, 2004, **43**, 3106–3116.
- 2 R. K. V. Lim and Q. Lin, *Sci. China Chem.*, 2010, **53**, 61–70.
- 3 L. I. Willems, W. A. Van der Linden, N. Li, K.-Y. Li, N. Liu, S. Hoogendoorn, G. A. Van der Marel, B. I. Florea and H. S. Overkleeft, *Acc. Chem. Res.*, 2011, **44**, 718–729.
- 4 Y.-X. Chen, G. Triola and H. Waldmann, *Acc. Chem. Res.*, 2011, **44**, 762–773.
- 5 S. S. van Berkel, M. B. van Eldijk and J. C. M. van Hest, *Angew. Chem. Int. Ed.*, 2011, **50**, 8806–8827.
- 6 C. I. Schilling, N. Jung, M. Biskup, U. Schepers and S. Bräse, *Chem. Soc. Rev.*, 2011, **40**, 4840–4871.
- 7 E. M. Sletten and C. R. Bertozzi, *Acc. Chem. Res.*, 2011, **44**, 666–676.

- 8 F. Giuntini, C. M. A. Alonso and R. W. Boyle, *Photochem. Photobiol. Sci.*, 2011, **10**, 759–791.
- 9 D. M. Patterson, L. A. Nazarova and J. A. Prescher, *ACS Chem. Biol.*, 2014, **9**, 592–605.
- 10 A. S. Tatikolov, *J. Photochem. Photobiol. C: Photochem. Rev.*, 2012, **13**, 55–90.
- 11 M. Ptaszek, *Prog. Mol. Biol. Transl. Sci.*, 2013, **113**, 59–108.
- 12 K. Umezawa, D. Citterio and K. Suzuki, *Anal. Sci.*, 2014, **30**, 327–349.
- 13 J. Pichaandi and F. C. J. M. van Veggel, *Coord. Chem. Rev.*, 2014, **263–264**, 138–150.
- 14 H. Scheer, in *Chlorophylls and Bacteriochlorophylls: Biochemistry, Biophysics, Functions and Applications*, ed. B. Grimm, R. J. Porra, W. Rüdiger and H. Scheer, Springer, Dordrecht, The Netherlands, 2006, pp. 1–26.
- 15 M. R. Prinsep, F. R. Caplan, R. E. Moore, G. M. L. Patterson and C. D. Smith, *J. Am. Chem. Soc.*, 1992, **114**, 385–387.
- 16 C. D. Smith, M. R. Prinsep, F. R. Caplan, R. E. Moore and G. M. L. Patterson, *Oncol. Res.*, 1994, **6**, 211–218.
- 17 M. R. Prinsep, G. M. L. Patterson, L. K. Larsen and C. D. Smith, *Tetrahedron*, 1995, **51**, 10523–10530.
- 18 M. R. Prinsep, G. M. L. Patterson, L. K. Larsen and C. D. Smith, *J. Nat. Prod.*, 1998, **61**, 1133–1136.
- 19 P. Morlière, J.-C. Mazière, R. Santus, C. D. Smith, M. R. Prinsep, C. C. Stobbe, M. C. Fenning, J. L. Golberg and J. D. Chapman, *Cancer Res.*, 1998, **58**, 3571–3578.

- 20 T. G. Minehan, L. Cook-Blumberg, Y. Kishi, M. R. Prinsep and R. E. Moore, *Angew. Chem. Int. Ed.*, 1999, **38**, 926–928.
- 21 M. R. Prinsep and J. Puddick, *Phytochem. Anal.*, 2011, **22**, 285–290.
- 22 Y. Chen, G. Li and R. K. Pandey, *Curr. Org. Chem.*, 2004, **8**, 1105–1134.
- 23 M. A. Grin, A. F. Mironov and A. A. Shtil, *Anti-Cancer Agents Med. Chem.*, 2008, **8**, 683–697.
- 24 R. W. Wagner and J. S. Lindsey, *Pure Appl. Chem.*, 1996, **68**, 1373–1380.
Corrigendum: R. W. Wagner and J. S. Lindsey, *Pure Appl. Chem.*, 1998, **70** (8), p. i.
- 25 J. M. Sutton, N. Fernandez and R. W. Boyle, *J. Porphyrins Phthalocyanines*, 2000, **4**, 655–658.
- 26 J. M. Sutton, O. J. Clarke, N. Fernandez and R. W. Boyle, *Bioconjugate Chem.*, 2002, **13**, 249–263.
- 27 A. M. G. Silva, A. C. Tomé, M. G. P. M. S. Neves, A. M. S. Silva and J. A. S. Cavaleiro, *J. Org. Chem.*, 2005, **70**, 2306–2314.
- 28 J. R. McCarthy, J. Bhaumik, N. Merbouh and R. Weissleder, *Org. Biomol. Chem.*, 2009, **7**, 3430–3436.
- 29 A. C. Tomé, M. G. P. M. S. Neves and J. A. S. Cavaleiro, *J. Porphyrins Phthalocyanines*, 2009, **13**, 408–414.
- 30 S. Singh, A. Aggarwal, S. Thompson, J. P. C. Tomé, X. Zhu, D. Samaroo, M. Vinodu, R. Gao and C. M. Drain, *Bioconjugate Chem.*, 2010, **21**, 2136–2146.
- 31 J. M. Dabrowski, L. G. Arnaut, M. M. Pereira, C. J. P. Monteiro, K. Urbanska, S. Simoes and G. Stochel, *ChemMedChem.*, 2010, **5**, 1770–1780.

- 32 N. A. M. Pereira, S. M. Fonseca, A. C. Serra, T. M. V. D. Pinho e Melo and H. D. Burrows, *Eur. J. Org. Chem.*, 2011, 3970–3979.
- 33 J. M. Dąbrowski, K. Urbanska, L. G. Arnaut, M. M. Pereira, A. R. Abreu, S. Simões and G. Stochel, *ChemMedChem.*, 2011, **6**, 465–475.
- 34 Z. Yu and M. Ptaszek, *Org. Lett.*, 2012, **14**, 3708–3711.
- 35 V. M. Alexander, K. Sano, Z. Yu, T. Nakajima, P. L. Choyke, M. Ptaszek and H. Kobayashi, *Bioconjugate Chem.*, 2012, **23**, 1671–1679.
- 36 A. Kozyrev, M. Ethirajan, P. Chen, K. Ohkubo, B. C. Robinson, K. M. Barkigia, S. Fukuzumi, K. M. Kadish and R. K. Pandey, *J. Org. Chem.*, 2012, **77**, 10260–10271.
- 37 L. P. Samankumara, S. Wells, M. Zeller, A. M. Acuña, B. Röder and C. Brückner, *Angew. Chem. Int. Ed.*, 2012, **51**, 5757–5760.
- 38 M. M. Pereira, A. R. Abreu, N. P. F. Goncalves, M. J. F. Calvete, A. V. C. Simoes, C. J. P. Monteiro, L. G. Arnaut, M. E. Eusébio and J. Canotilho, *Green Chem.*, 2012, **14**, 1666–1672.
- 39 J. Ogikubo, E. Meehan, J. T. Engle, C. J. Ziegler and C. Brückner, *J. Org. Chem.*, 2013, **78**, 2840–2852.
- 40 A. Aggarwal, S. Thompson, S. Singh, B. Newton, A. Moore, R. Gao, X. Gu. S. Mukherjee and C. M. Drain, *Photochem. Photobiol.*, 2014, **90**, 419–430.
- 41 H.-J. Kim and J. S. Lindsey, *J. Org. Chem.*, 2005, **70**, 5475–5486.
- 42 D. Fan, M. Taniguchi and J. S. Lindsey, *J. Org. Chem.*, 2007, **72**, 5350–5357.
- 43 M. Krayner, M. Ptaszek, H.-J. Kim, K. R. Meneely, D. Fan, K. Secor and J. S. Lindsey, *J. Org. Chem.*, 2010, **75**, 1016–1039.

- 44 M. Krayner, E. Yang, J. R. Diers, D. F. Bocian, D. Holten and J. S. Lindsey, *New J. Chem.*, 2011, **35**, 587–601.
- 45 C.-Y. Chen, E. Sun, D. Fan, M. Taniguchi, B. E. McDowell, E. Yang, J. R. Diers, D. F. Bocian, D. Holten and J. S. Lindsey, *Inorg. Chem.*, 2012, **51**, 9443–9464.
- 46 M. Galezowski and D. T. Gryko, *Curr. Org. Chem.*, 2007, **11**, 1310–1338.
- 47 C. Brückner, L. Samankumara and J. Ogikubo, in *Handbook of Porphyrin Science*, ed. K. M. Kadish, K. M. Smith and R. Guilard, World Scientific Publishing Co., Singapore, 2012, vol. 17, pp. 1–112.
- 48 T. G. Minehan and Y. Kishi, *Tetrahedron Lett.*, 1997, **38**, 6811–6814.
- 49 T. G. Minehan and Y. Kishi, *Tetrahedron Lett.*, 1997, **38**, 6815–6818.
- 50 T. G. Minehan and Y. Kishi, *Angew. Chem. Int. Ed.*, 1999, **38**, 923–925.
- 51 W. Wang and Y. Kishi, *Org. Lett.*, 1999, **1**, 1129–1132.
- 52 K. R. Reddy, J. Jiang, M. Krayner, M. A. Harris, J. W. Springer, E. Yang, J. Jiao, D. M. Niedzwiedzki, D. Pandithavidana, P. S. Parkes-Loach, C. Kirmaier, P. A. Loach, D. F. Bocian, D. Holten and J. S. Lindsey, *Chem. Sci.*, 2013, **4**, 2036–2053.
- 53 J. Jiang, P. Vairaprakash, K. R. Reddy, T. Sahin, M. P. Pavan, E. Lubian and J. S. Lindsey, *Org. Biol. Chem.*, 2014, **12**, 86–103.
- 54 M. A. Harris, J. Jiang, D. M. Niedzwiedzki, J. Jiao, M. Taniguchi, C. Kirmaier, P. A. Loach, D. F. Bocian, J. S. Lindsey, D. Holten and P. S. Parkes-Loach, *Photosyn. Res.*, 2014, **121**, 35–48.
- 55 Z. Yu and M. Ptaszek, *Org. Lett.*, 2012, **14**, 3708–3711.

- 56 T. Harada, K. Sano, K. Sato, R. Watanabe, Z. Yu, H. Hanaoka, T. Nakajima, P. L. Choyke, M. Ptaszek and H. Kobayashi, *Bioconjugate Chem.*, 2014, **25**, 362–369.
- 57 E. Yang, C. Kirmaier, M. Krayner, M. Taniguchi, H.-J. Kim, J. R. Diers, D. F. Bocian, J. S. Lindsey and D. Holten, *J. Phys. Chem. B*, 2011, **115**, 10801–10816.
- 58 J. Jiang, K. R. Reddy, M. P. Pavan, E. Lubian, M. A. Harris, J. Jiao, C. Kirmaier, P. S. Parkes-Loach, P. A. Loach, D. F. Bocian, D. Holten and J. S. Lindsey, *Photosyn. Res.*, 2014, 10.1007/s11120-014-0021-9.
- 59 G. T. Hermanson, *Bioconjugate Techniques*; Academic Press: San Diego, 1996.
- 60 R. A. Cellarius and D. Mauzerall, *Biochim. Biophys. Acta*, 1966, **112**, 235–255.
- 61 G. Bartoli, M. Bosco, A. Carlone, R. Dalpozzo, E. Marcantoni, P. Melchiorre and L. Sambri, *Synthesis*, 2007, 3489–3496.
- 62 R. W. Wagner, T. E. Johnson, F. Li and J. S. Lindsey, *J. Org. Chem.*, 1995, **60**, 5266–5273.
- 63 R. W. Wagner, Y. Ciringh, C. Clausen and J. S. Lindsey, *Chem. Mater.*, 1999, **11**, 2974–2983.
- 64 M. Kobayashi, M. Akiyama, H. Kano and H. Kise, in *Chlorophylls and Bacteriochlorophylls: Biochemistry, Biophysics, Functions and Applications*, ed. B. Grimm, R. J. Porra, W. Rüdiger and H. Scheer, Springer, Dordrecht, The Netherlands, 2006, pp. 79–94.
- 65 K. E. Borbas, V. Chandrashaker, C. Muthiah, H. L. Kee, D. Holten and J. S. Lindsey, *J. Org. Chem.*, 2008, **73**, 3145–3158.

- 66 B. Abrams, Z. Diwu, O. Guryev, S. Aleshkov, R. Hingorani, M. Edinger, R. Lee, J. Link and T. Dubrovsky, *Anal. Biochem.*, 2009, **386**, 262–269.
- 67 A. S. Manjappa, K. R. Chaudhari, M. P. Venkataraju, P. Dantuluri, B. Nanda, C. Sidda, K. K. Sawant and R. S. R. Murthy, *J. Control. Release*, 2011, **150**, 2–22.
- 68 P. K. Chattopadhyay, B. Gaylord, A. Palmer, N. Jiang, M. A. Raven, G. Lewis, M. A. Reuter, A. K. M. N. Rahman, D. A. Price, M. R. Betts and M. Roederer, *Cytometry Part A*, 2012, **81A**, 456–466.
- 69 D. Majonis, O. Ornatsky, D. Weinrich and M. A. Winnik, *Biomacromol.*, 2013, **14**, 1503–1513.
- 70 F. Bryden, A. Maruani, H. Savoie, V. Chudasama, M. E. B. Smith, S. Caddick and R. W. Boyle, *Bioconjugate Chem.*, 2014, **25**, 611–617.
- 71 M. Dautrevaux, Y. Boulanger, K. Han and G. Biserte, *Eur. J. Biochem.*, 1969, **11**, 267–277.
- 72 B. Garcia-Moreno E., L. X. Chen, K. L. March, R. S. Gurd and F. R. N. Gurd, *J. Biol. Chem.*, 1985, **260**, 14070–14082.
- 73 C. H. I. Ramos, M. S. Kay and R. L. Baldwin, *Biochemistry*, 1999, **38**, 9783–9790.
- 74 A. Castro-Forero, D. Jiménez, J. López-Garriga and M. Torres-Lugo, *J. Appl. Polym. Sci. Symp.*, 2008, **107**, 881–890.
- 75 S. C. Harrison and E. R. Blout, *J. Biol. Chem.*, 1965, **240**, 299–303.
- 76 H. Du, R.-C. A. Fuh, J. Li, L. A. Corkan and J. S. Lindsey, *Photochem. Photobiol.*, 1998, **68**, 141–142.

- 77 J. M. Dixon, M. Taniguchi and J. S. Lindsey, *Photochem. Photobiol.*, 2005, **81**, 212–213.
- 78 F. W. J. Teale, *Biochim. Biophys. Acta*, 1959, **35**, 543.
- 79 N. Srinivasan, C. A. Haney, J. S. Lindsey, W. Zhang and B. T. Chait, *J. Porphyrins Phthalocyanines*, 1999, **3**, 283–291.
- 80 J. Jiang, C.-Y. Chen, N. Zhang, P. Vairaprakash and J. S. Lindsey, *New J. Chem.*, 2015, **39**, 403–419.

CHAPTER 6

Amphiphilic, Hydrophilic, or Hydrophobic Synthetic Bacteriochlorins in Biohybrid Light-Harvesting Architectures. Consideration of Molecular Designs

Preamble. The contents in this chapter have been published⁵⁸ with contributions from the following individuals/groups. Kanumuri Ramesh Reddy: synthesis of **B1** and corresponding precursors. M. Phani Pavan and Elisa Lubian, together with Kanumuri Ramesh Reddy, are involved in the bacteriochlorin molecular design. Michelle A. Harris and Christine Kirmaier (the Holten group): Photophysical property studies on dyads. Jieying Jiao (the Bocian group): FT-IR for the peptide-chromophore conjugates.

Introduction

Facile access to light-harvesting antennas – designed from first principles and created from simple materials – would enrich our fundamental understanding of photosynthetic light capture and may prove useful for applications in solar-energy conversion. While absorption of light, the first act in photosynthesis, is ostensibly simple, photosynthetic systems deploy 100s to 1000s of pigments in elaborate architectures to capture sunlight that is dilute (low flux) and spectrally rich (~300 to ~1000 nm); the resulting energy is funneled in sub-nanoseconds to reaction centers where the processes of energy transduction and ultimate storage begins. Photosynthesis in all of its diverse formats provides a deep knowledge base for molecular-based solar-energy conversion, yet earnest efforts over several decades to recreate photosynthetic-like light-harvesting processes by purely chemical means have fallen far short of the efficiency and versatility of the natural systems.¹⁻⁴ Chief challenges stem from the diverse spectral range of incoming solar radiation, the ephemeral nature of the

singlet excited state derived from photon absorption, the sensitivity of highly energetic excited states and energy funneling processes to 3-dimensional organization, and the requirement to deploy large numbers of chromophores over mesoscale dimensions while retaining exacting architectural control at the atomic and sub-nanoscale level.

A central objective is to create a ‘science of design’ that fulfills such daunting objectives, wherein from first principles and readily accessible constituents, mesoscale antennas can be created with tailorable performance specifications with regards to spectral coverage, absorbance intensity, and efficiency of excitation delivery and transduction. In a preceding paper in this journal, we described our ongoing studies in the development of biohybrid antennas.⁵ Such antennas are comprised of peptides derived from photosynthetic bacteria (or synthetic peptide analogues), bacteriochlorophyll *a* (BChl *a*) and synthetic chromophores. The general strategy relies on the self-assembly of the photosynthetic peptides (α and β) and BChl *a* to form a dyad composed of two peptides and two BChl *a* molecules (**Figure 6.1A**); the resulting $\alpha\beta$ -dyad then self-associates to give $(\alpha\beta)_n$ -cyclic oligomers that resemble the native light-harvesting antennas LH1 or LH2. The two-tier assembly process is accompanied by a shift in the long-wavelength (Q_y) absorption band from ~ 780 nm for the BChl-*a* monomer to ~ 820 nm for BChl-*a* pair in the $\alpha\beta$ -dyad, and to ~ 875 nm for the BChl-*a* array in the $(\alpha\beta)_n$ -oligomer (**Figure 6.1B**). The synthetic chromophores are covalently attached to one or both of the peptides and then are piggybacked into the cyclic oligomers via the two-tiered self-assembly process. To date, synthetic chromophores have been attached covalently to β -peptide analogues at positions – 34, –21, –17, –14, –10, –6, –2 (**Figure 6.1A**).⁵⁻⁸ The use of appropriately chosen synthetic

chromophores enables the spectral coverage of the resulting antenna to be broadened beyond that provided by the native antenna.

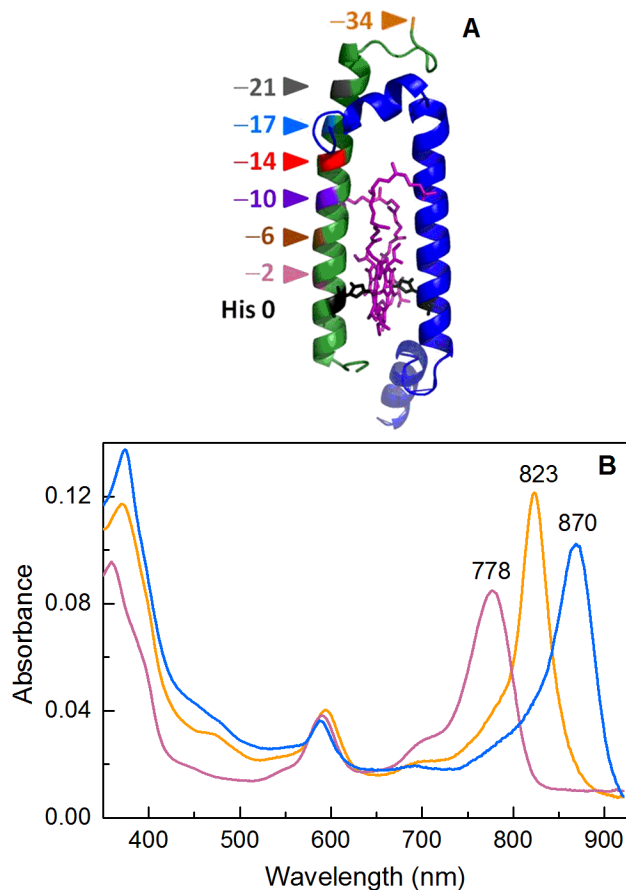


Figure 6.1. (A) $\alpha\beta$ -subunit of the LH2 (B800–850) antenna of *Phaeospirillum (Phs.) molischianum*, showing sites used previously for conjugation of synthetic chromophores on the presumed equivalent structure in the *Rb. sphaeroides* LH1 β -peptide. Coordinating histidines are illustrated (black). (B) Absorption spectra of BChl *a* in 0.90% octG (mauve), $\alpha\beta$ -dyad (which contains the BChl-*a* pair B820) reconstituted from native *Rb. sphaeroides* α - and β -polypeptides and BChl *a* (gold) in 0.66% octG, and LH1-type $(\alpha\beta)_n$ -oligomers (which contain the BChl-*a* array B870) formed from subunits ($\alpha\beta$ -dyads) by overnight chilling at 6 °C (blue).

The biohybrid approach (1) integrates the blueprint of biological photosynthesis with the malleability imparted by synthetic chemistry, (2) employs semisynthesis to combine photosynthetic constituents with compounds produced by the exquisite control of modern synthetic chemistry, (3) exploits the two-tiered self-assembly process of the natural system to convert synthetically tailorable modular constituents into functional mesoscale antennas, and (4) enables designer antennas to be rapidly fabricated with features for use in solutions, patterned surfaces, and films. A considerable virtue of the biohybrid antenna approach versus that of total (i.e., *de novo*) chemical synthesis is the reliance on molecules and designs that have been selected by the “fine comb of evolution”^{9,10} and the ensuing self-assembly processes to readily form mesoscale constructs. Few if any *de novo* synthetic routes are available that afford the requisite control over 3-dimensional molecular structure, organize a large number of non-identical pigments (with energy gradients in some cases), and achieve facile scaling by stitching together readily available small molecules to reach the mesoscale size. The inherent semisynthetic nature of the biohybrid approach fulfills such criteria and thereby offers atomic-level control of a mesoscale architecture.

Our work to date on biohybrid antennas⁵⁻⁸ has given rise to the question “how many synthetic chromophores can be attached to the peptides while retaining the requisite features for dyad/oligomer self-assembly processes?” To complement the absorption provided by the native array of BChl *a* molecules in an oligomer antenna, we have to date attached (1) two identical synthetic chromophores to a given peptide to enhance the absorption at select wavelengths compared to a single unit, or (2) two different chromophores to further expand the solar coverage and to make more efficient use of distant sites via two-step relay energy

transfer. This work has so far identified seven distinct sites (**Figure 6.1A**) on the β -peptide that can be used individually or in combinations to afford self-assembly of the resulting chromophore-peptide conjugate with the α -peptide and BChl *a* to give the corresponding $(\alpha\beta)_n$ -oligomer.

A subsidiary design feature not yet explored concerns the molecular polarity of the appended chromophore. The photosynthetic antenna peptides assemble in the native system in bilayer lipid membranes. Accordingly, the biohybrid antennas are assembled in an aqueous detergent medium. The detergent employed to date is the nonionic surfactant *n*-octyl β -D-glucoside (octG), which affords micelles under the assembly conditions employed. The synthetic chromophores examined to date include rather hydrophobic molecules such as a coumarin¹¹ or bacteriochlorin^{6-8,12}, or somewhat polar xanthenes such as Oregon Green and Rhodamine Red.^{6,8,11} As a prelude to addressing the aforementioned question of loading, we sought to examine whether the use of polar chromophores offered any advantage in the assembly process. Although the assembly is carried out in a micellar milieu, a very real concern was that the use of three, four or more hydrophobic synthetic chromophores would result in precipitation thereby thwarting assembly. An examination of the question of polarity must employ a neutral chromophore that can be tailored with polar groups; such a requirement eliminates most synthetic dyes, which are intrinsically charged.¹³ Hence we have turned to derivatization of synthetic bioconjugatable bacteriochlorins to systematically examine this aspect of molecular design.

In the work reported herein, a new amphiphilic bioconjugatable bacteriochlorin (**B1**, *vide infra*) has been synthesized. The bacteriochlorin is attached to a native (full-length) β -

peptide analogue that contains a single cysteine in lieu of a methionine at a position near the middle of the main, α -helical region of the β -peptide. The resulting conjugate is combined with BChl *a* to give the corresponding $\beta\beta$ -dyad (a homo dimer), which cannot self-associate to give β_n -oligomers.^{13,14} An analogous hydrophilic bioconjugatable bacteriochlorin (**B2**) was similarly employed to prepare a $\beta\beta$ -dyad. Static fluorescence and time-resolved absorption spectroscopies were utilized to assess the efficiency of energy transfer from the synthetic bacteriochlorin to the pair of BChl *a* molecules embedded in the core of the peptide dyad. The results are compared with those found previously using hydrophobic bioconjugatable bacteriochlorins (e.g., **B3**). Collectively, the results are valuable in guiding the design of more elaborate biohybrid antennas.

Results and discussion

(I) Synthetic bioconjugatable bacteriochlorins

(A) Reconnaissance. Recent advances in synthesis have afforded access to analogues of natural bacteriochlorophylls,¹⁹⁻²¹ bacteriochlorins derived from porphyrins,²²⁻²⁸ and *de novo* synthesized bacteriochlorins.²⁹⁻³⁴ The synthetic methodology we have developed to access bacteriochlorins is distinguished by (1) incorporation of geminal dimethyl groups at the 8 and 18 positions to secure the chromophore from oxidative dehydrogenation leading to chlorins or porphyrins, (2) scalability, and (3) amenability to diverse reaction conditions. The bacteriochlorins shown in **Chart 6.1** exemplify three distinct polarity classes, as **B1** (newly described here) is amphiphilic, **B2** is hydrophilic,¹² and **B3** is hydrophobic.⁷ Each bears a maleimido group for bioconjugation.

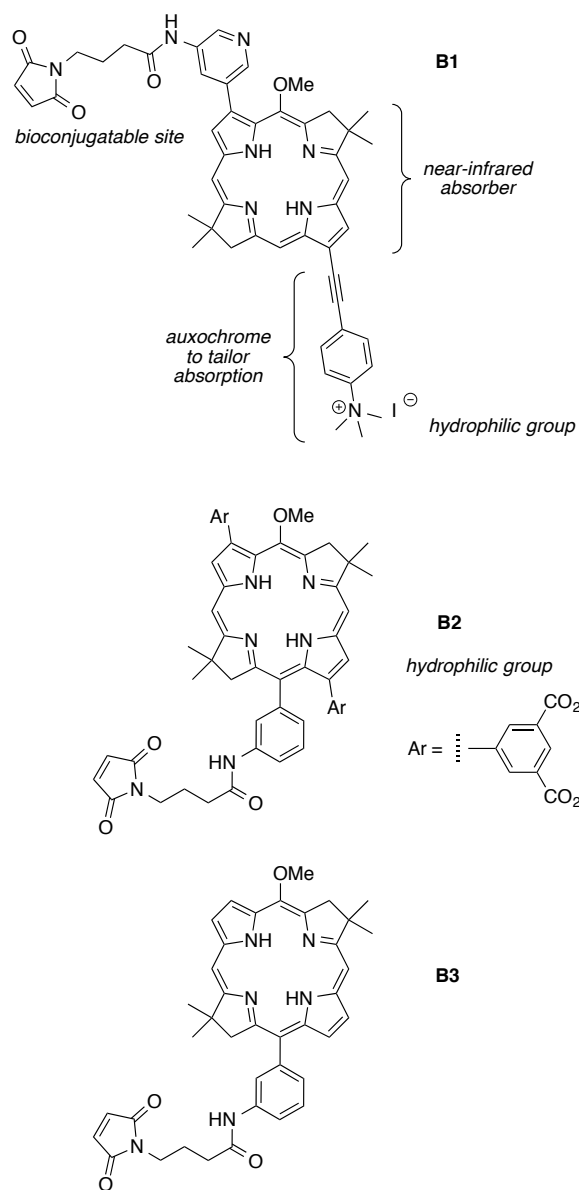
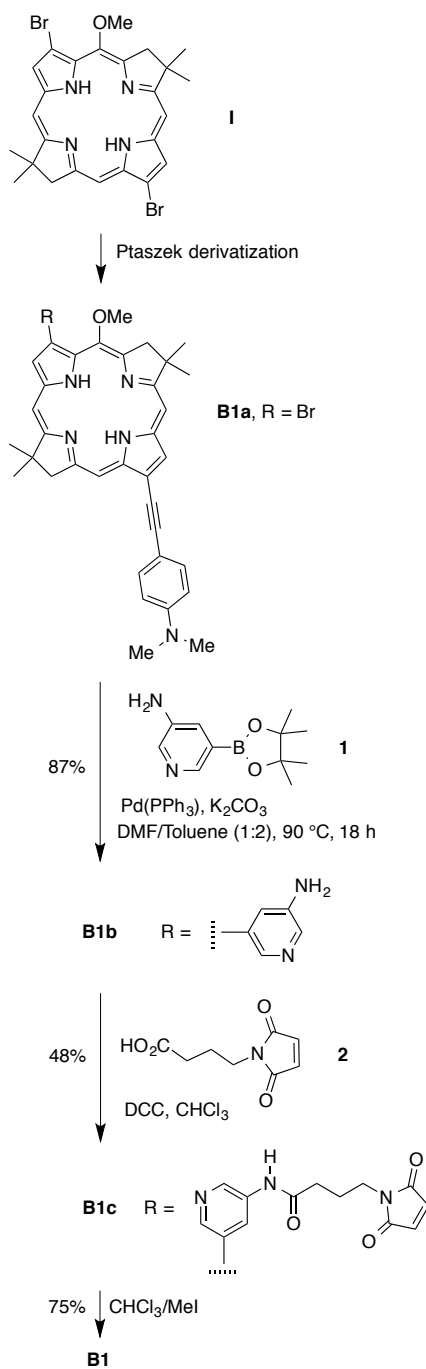


Chart 6.1. Amphiphilic (**B1**), hydrophilic (**B2**) and hydrophobic (**B3**) bioconjugatable bacteriochlorins.

A sizable family of “hydrophobic, bioconjugatable, wavelength-tunable bacteriochlorins” (including **B3**) has been prepared and members therein have been incorporated in biohybrid antennas.⁶⁻⁸ Members of the general family of “hydrophilic,

bioconjugatable, bacteriochlorins” have been created previously.^{35,36} The first example with geminal-dimethyl substituents, **B2**, was conjugated to a light-harvesting peptide in a proof-of-principle experiment¹² but the corresponding biohybrid antennas were not previously investigated. The development of amphiphilic bacteriochlorins requires tailoring such that one side of the molecule is polar and the other is nonpolar.³⁷ The design of the “amphiphilic, bioconjugatable bacteriochlorin” **B1** shown in **Chart 6.1** includes a charged, trimethylanilinium as the polar unit, and the bioconjugatable tether as the nonpolar moiety on the opposite side of the molecule. Synthetic access to such Janus-like molecules is made possible by recent advances in synthesis, as described in the next section.

(B) Synthesis of amphiphilic bacteriochlorin B1. A 3,13-dibromo-5-methoxybacteriochlorin (**I**, **Scheme 6.1**) was subjected to selective Sonogashira coupling reaction to give **B1a**,¹⁷ which provided a route to bioconjugatable bacteriochlorins for use in biomedical imaging studies.^{38,39} The selectivity of coupling (13-position then 3-position) accrued from the steric hindrance imparted by the 5-methoxy group. To introduce a bioconjugatable group, we treated **B1a** to a Suzuki coupling with boronate **1**, which afforded the multifunctional bacteriochlorin **B1b** in 87% yield (**Scheme 6.1**). Coupling with 4-maleimidobutyric acid (**2**) mediated by *N,N*-dicyclohexylcarbodiimide (DCC) gave bacteriochlorin **B1c** in 48% yield. Subsequent quaternization with methyl iodide provided the bacteriochlorin **B1** in 75% yield. Bacteriochlorin **B1** was characterized by ¹H NMR spectroscopy, MALDI-MS and ESI-MS, absorption spectroscopy, and fluorescence spectroscopy. The bacteriochlorin exhibited absorption spectral features characteristic of bacteriochlorins including native bacteriochlorophylls.⁴⁰



Scheme 6.1. Synthesis of amphiphilic bioconjugatable bacteriochlorin **B1**.

(II) Bacteriochlorin–peptide conjugate

(A) Peptide choice. We have employed the native β -peptide analogue **$\beta(-14\text{Cys})$** to form $\beta\beta$ -dyads for the following reasons: (1) the β -peptide dimerizes in the presence of BChl *a* to form $\beta\beta$ -dyads, yet such dyads do not continue to form β_n -oligomers;^{13,14} (2) the β -peptide can be readily customized and obtained commercially in ample quantities (>50 mg), (3) the composition of the $\beta\beta$ -dyad is well defined as are the conditions for its formation, (4) an equilibrium is established during formation of the $\beta\beta$ -dyad, hence thermodynamic properties may be determined. By contrast, the native α -peptide from *Rb. sphaeroides* LH1 alone with BChl *a* does not form dyads or oligomers. On the other hand, $\beta\beta$ -dyads are less stable than LH1-type antennas so that care must be taken to measure their energy-transfer properties promptly at low temperature (10 °C employed herein).

(B) Bioconjugate formation and characterization. The bioconjugation reaction was carried out with **$\beta(-14\text{Cys})$** at 2 mM and a 50% excess of **B1** (3 mM) in a 1:4 solvent mixture of Tris buffer (pH 8.6) and *N,N*-dimethylformamide (DMF) at room temperature for 3 hours. The resulting conjugate is hereafter simply denoted **β -B1**. The desired conjugate was obtained in 57% yield following reverse-phase HPLC purification and exhibited the expected peaks upon mass spectrometric analysis.⁵⁸ The absorption spectrum of the purified conjugate **β -B1** showed bands due to the peptide in the ultraviolet region (283 nm) and the bacteriochlorin in the near-ultraviolet Soret (B_y , B_x) region (365 nm), visible Q_x region (519 nm), and near-infrared Q_y region (748 nm).

The fluorescence quantum yield (Φ_f) for conjugate **β -B1** in aqueous buffered detergent solution is 0.13, compared to 0.09 for **β -B2**¹² and 0.15 for **β -B3**⁸ (Table 6.1). The fluorescence properties of the conjugates can be compared with those of the monomeric bacteriochlorins. Bacteriochlorin **B1** showed a Φ_f of 0.092 in DMF and $\Phi_f = 0.023$ in the mixed solvent of 80% water and 20% DMF. A diminished fluorescence yield in aqueous media is often found for bacteriochlorins.¹² For example, the Φ_f for **B2** is 0.16 in DMF and 0.074 in aqueous buffer.¹² In comparison, the average Φ_f for about three-dozen hydrophobic bacteriochlorins in nonpolar media (e.g. toluene) is 0.15 ± 0.03 .^{41,42}

FTIR spectra of peptide–bacteriochlorin conjugates **β -B1**, **β -B2** and **β -B3** are shown in ref 58. The spectra are compared with that of peptide **$\beta(-14Cys)$** to which the bacteriochlorins are conjugated and to that of the native β -peptide. All of the spectra show the amide I and amide II vibrations at 1546 and 1664 cm^{-1} , respectively, that are characteristic of α -helical peptides. The similarity of the spectra indicates that replacement of the native methionine at the –14-position with Cys and subsequent conjugation of a synthetic bacteriochlorin at this site do not compromise the α -helical structure of the peptide.

Table 6.1. Energy-Transfer Parameters for Dyads^a

Parameters	$\beta\beta$ -dyad formed from conjugate listed			
	β -B1	β -B2	β -B3	β -OGR
Experimental Φ_{EET}	0.85	0.40	0.85	0.50
Chromophore Donor Φ_{f}^b	0.13	0.090	0.15	0.30
Chromophore Donor λ_{em} (nm)	751	732	717	524
B820 Acceptor ϵ ($\text{M}^{-1}\text{cm}^{-1}$)	172,000	172,000	172,000	172,000
J ($\times 10^{-13}$) (cm^6)	6.4	4.0	3.6	0.59
R_0 (\AA)	50	43	46	37
Calculated Φ_{EET} (@ $R = 29\text{\AA}$)	0.96	0.92	0.94	0.85
Calculated Φ_{EET} (@ $R = 41\text{\AA}$)	0.77	0.59	0.68	0.41

^aThe calculations use the “ R_0 method” in which R_0 is the distance at which $\Phi_{\text{EET}} = 0.5$, and thus $\Phi_{\text{ET}} = R_0^6 / (R_0^6 + R^6)$, where $R_0^6 = (8.8 \times 10^{23}) \kappa^2 \Phi_{\text{f}} J n^{-4}$. Here, J is the spectral overlap integral, n is the refractive index (1.333), and κ^2 is the orientation factor (dynamically averaged value of 2/3). The fluorescence quantum yield of the donor chromophore in the absence of energy transfer was measured for the peptide–chromophore conjugate in aqueous phosphate buffer (pH 7.6) containing 0.66% octG using as a reference 5-methoxy-2,12-di-*p*-tolylbacteriochlorin ($\Phi_{\text{f}} = 0.18$ in deoxygenated toluene) and/or free base *meso*-tetraphenylporphyrin ($\Phi_{\text{f}} = 0.069$ in non-deoxygenated toluene) at room temperature. ^cThe molar absorptivity (ϵ) of the acceptor B820 (BChl pair) at the Q_y maximum is twice the value per BChl for an $\alpha\beta$ -dyad determined in ref 43. The Förster energy-transfer efficiencies were calculated using approximate minimum and maximum distances between the attached donor chromophore and B820 obtained from molecular modeling. The efficiencies listed in the last two rows correspond to the values at those two distances.

(C) Comparison of hydrophilic, hydrophobic or amphiphilic bacteriochlorins.

We have previously employed hydrophobic maleimido–bacteriochlorins for attachment to peptides analogous to those found in the natural light-harvesting antennas of bacterial photosynthesis.^{6-8,12} The resulting conjugates were then examined in aqueous detergent

(micellar) solutions. The native peptide is very hydrophobic whereas bacteriochlorin **B1** (amphiphilic) and **B2** (hydrophilic) are more polar. Each conjugate herein dissolved well in the solvent hexafluoroacetone-trihydrate/acetonitrile/isopropanol (50:17:33) for HPLC analysis. The total isolated yields [including reaction, work-up and HPLC purification] of 57% and 50%¹² for peptide conjugate **β -B1** and **β -B2**, respectively, are far higher than our previous yield (17%) for a hydrophobic chromophore-peptide.⁷ Accordingly, the introduction of hydrophilic/amphiphilic bacteriochlorin to the hydrophobic β -peptide appears to facilitate handling and purification.

(III) $\beta\beta$ -Dyads

(A) Formation. Procedures for the formation of bb-dyads were described previously^{6,7,14} and are provided in the Experimental section for completeness. The procedures are analogous to those used for the formation of $\alpha\beta$ -dyads.^{5,8,43-47} Dyad formation is a self-assembly process that is sensitive to the composition of the medium, in particular the nature and concentration of micelles. The dependency of octG micelle formation in water exhibits a steep and negative temperature dependence over the range 5–40 °C;⁴⁸ accordingly, a decrease in temperature increases the critical micelle concentration (CMC) of octG (i.e., decreases the concentration of octG micelles). The association of α - and β - (or β - and β -) peptides with each other and BChl *a* to give dyads can be promoted by (1) decreasing the concentration of octG (i.e., by simply adding phosphate buffer to the aqueous detergent solution), or (2) keeping the concentration of octG fixed but lowering the temperature. The diminished micelle concentration forces interaction between the

hydrophobic surfaces of the conjugates, thereby driving assembly.⁵ The experimental processes are illustrated in **Figure 6.2**.

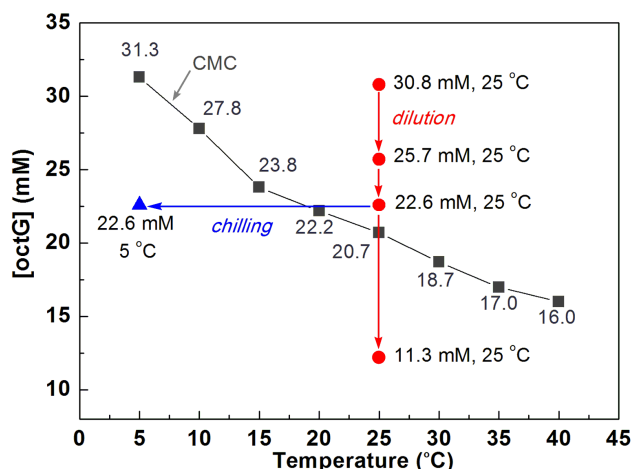


Figure 6.2. Dyad formation as a function of concentration of octG and temperature. The black squares show the temperature dependence of the CMC.⁴⁸ The formation of $\beta\beta$ -dyads occurs at room temperature by dilution with buffer to bring the detergent concentration below the CMC (red circles and arrows) or by chilling the sample to raise the CMC to above the given detergent concentration (blue triangle and arrow).

The peptide for forming dyads was initially contained in an aqueous solution containing octG at 30.8 mM (~0.90%), whereupon BChl *a* was added as well as phosphate buffer solution (100 mM, pH 7.6, lacking octG). The peptide–pigment conjugates examined in this manner include β -B1, β -B2, β -B3, as well as the conjugate with Oregon Green (β -OGR). When the octG concentration declined to 22.6 mM (~0.66%) by addition of aqueous phosphate buffer, dyad formation was noticeable. Dyad formation reached completion upon further dilution [for β -B2 only] of octG to 11.3 mM as shown in the red (vertical) arrow of **Figure 6.2**. Alternatively, dyad formation also could be induced by chilling the solution at

5 °C for 1 h as shown by the blue (horizontal) arrow of **Figure 6.2**. The latter process was explored with all four of the peptide–chromophore conjugates. Spectra that illustrate dyad formation for **β -B1**, **β -B3** and **β -OGR** are shown for **β -B2** in **Figure 6.3**.

In summary, the formation of $\beta\beta$ -dyads entails assembly of four constituents: 2 β -peptides and two Bchl *a* molecules. As such, *a priori* one expects that the extent of association at equilibrium should increase with an increase in concentration of reactants. The paradoxical increase in extent of association upon *dilution* of reactants is attributed to the decrease in concentration of the detergent octG in micelles, which in turn promotes hydrophobic interactions of the dyad constituents.

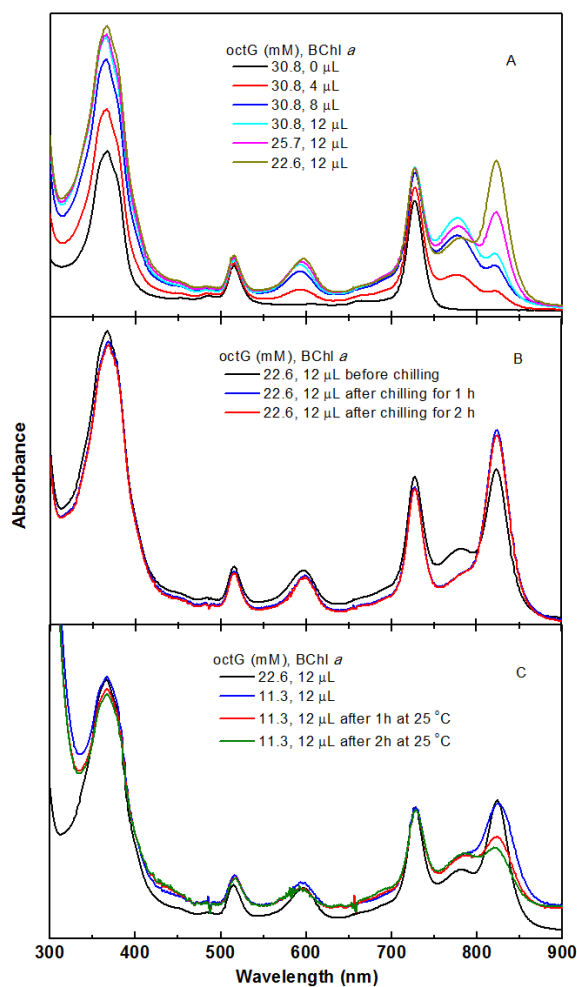
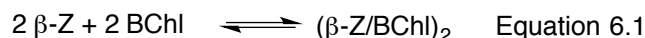


Figure 6.3. Absorption spectra for formation of dyads from β -B2 signaled by the peak at 823 nm. (A) Titration of β -B2 at 30.8 mM octG with no BChl *a* (black) with aliquots of BChl *a* (red, blue, cyan) followed by decreasing concentrations of octG (magenta, dark yellow); in total 12 μ L of BChl *a* was added. (B) Samples at 22.6 mM octG with 12 μ L total of BChl *a* before (black) and after 1 h (blue) and 2 h (red) chilling at 5 °C. (C) Samples at 22.6 mM with 12 μ L total of BChl *a* before (black) and after dilution of octG concentration to 11.3 mM for 0 (blue), 1 (red) and 2 (green) hours. The spectra were corrected for dilution, so that each sample would have the same concentration as the initial sample before dilution. The initial sample (30.8 mM octG) prior to addition of BChl *a* (in panel A) gave an absorbance at 727 nm of 0.22 in a 1-cm cuvette. In panel C, a lamp artifact at 655 nm was manually smoothed.

(B) Quantitation of assembly. A quantitative estimate of the extent of dyad formation was assessed by multicomponent analysis of the absorption spectrum, making use of the known spectra of the BChl *a* monomer and the BChl *a* pair B820 in aqueous buffered octG solutions, which have Q_y peak molar absorptivities of 55,000 M⁻¹ cm⁻¹ and 172,000 M⁻¹ cm⁻¹.⁴³ A set of concentrations of 30.8, 25.7, 22.6 and 11.3 mM was examined for (**β-B2/BChl**)₂ at room temperature. A simple statement of the reaction equilibrium is given by eq 1, where two molecules of free bacteriochlorin–peptide conjugate and two molecules of BChl *a* assemble to give the dyad, denoted generically (**β-Z/BChl**)₂. Eqs 1 and 2 have been regarded as incomplete because the interactive role of detergent is not taken into account.⁴⁷ Regardless, the relevant species are free bacteriochlorin–peptide conjugate, free BChl *a*, and dyad. The percentage of association to give dyad is given by eq 3, where [β-Z]₀ denotes the initial concentration of the bacteriochlorin–peptide conjugate.



$$K_{\text{assoc}} = \frac{[(\beta\text{-Z/BChl})_2]}{[\beta\text{-Z}]^2 \cdot [\text{BChl}]^2} \quad \text{Equation 6.2}$$

$$A_{\%} = \frac{2 \cdot [(\beta\text{-Z/BChl})_2]}{[\beta\text{-Z}]_0} \quad \text{Equation 6.3}$$

Z = B1, B2, B3 or OGR

Multicomponent analysis of the absorption spectra for the room-temperature samples in the Q_y region determines the concentrations of the dyad, free bacteriochlorin–peptide

conjugate, and free BChl *a*. For the case of the amphiphilic bacteriochlorin–peptide conjugate, the concentration of dyad (**β -B1/BChl**)₂, free conjugate **β -B1** and free BChl *a* at 0.75% was found to be 0.85, 0.16 and 2.18 μ M, respectively (note that BChl *a* was used in excess). The resulting K_{assoc} was calculated to be $700 \times 10^{16} \text{ M}^3$ on the basis of eq 2. This value can be compared with the reported value of $\geq 300 \times 10^{16} \text{ M}^3$ under the same conditions for native dyads without any chromophores attached.⁴⁹ The percentage of association is calculated to be 94%, on the basis of eq 3, where $[\beta\text{-BC}]_0$ is 1.8 μ M for **β -B1**. Similar analysis on the other chromophore–peptide conjugates was conducted and results are shown in ref 58.

(C) Equilibrium study. The reversibility of dyad formation was examined by a variable-temperature study. A solution containing the dyad (**β -B2/BChl**)₂ and excess BChl *a* at 22.6 mM octG was examined in a 1-cm pathlength cuvette. The temperature was varied over the range 15–35 °C with a 5 °C increment, with no sample addition or withdrawal from the solution during the study. The constant absorbance at 516 and 728 nm indicates that the volume change induced by the temperature change is negligible. Two cycles (each cycle is 25→20→15→20→25→30→35→30→25 °C) were conducted. The results from the first cycle are shown in **Figure 6.4**. A decrease from 25 to 15 °C induced the formation of dyad, and a subsequent increase from 15 to 35 °C caused the dyad to dissociate, as shown by the decrease in the 823-nm absorbance of the dyad and the increase in absorbance of the 779-nm absorbance of free BChl *a*. A subsequent decrease from 35 to 25 °C gave the same dyad concentration as the initial state. An isosbestic peak at 800 nm is consistent with a two-state process of BChl *a* that is free in the monomer form versus paired in the dyad. This study

unambiguously shows that the dyad formation process is reversible as the temperature is varied.

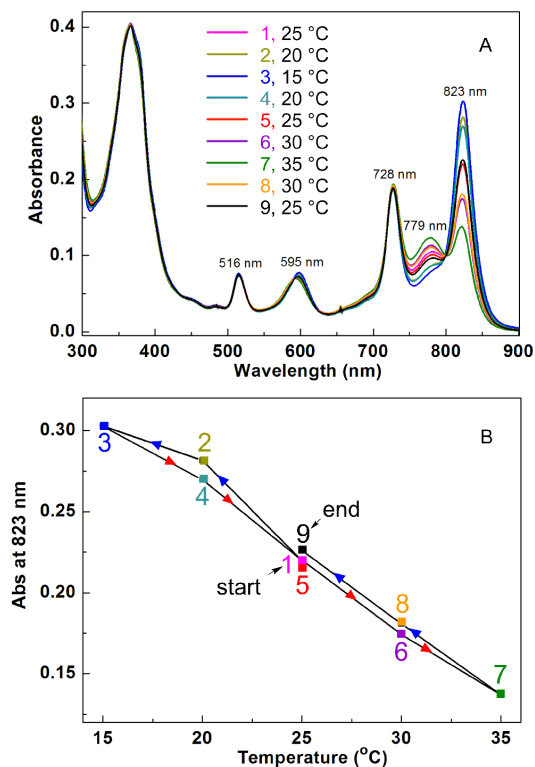


Figure 6.4. Variable-temperature study of (β -B2/BChl)₂ dyad assembly/disassembly at 22.6 mM octG in aqueous phosphate buffer. (A) The absorbance at 728 nm is from the synthetic bacteriochlorin, at 779 nm is from the free BChl *a*, and at 823 nm is from the BChl *a* in the dyad. (B) The absorbance of dyad at 823 nm at various temperatures.

(D) Energy-transfer studies. The efficiency of excitation energy transfer (Φ_{EET}) from the attached chromophore (**B1**, **B2**, **B3**, **OGR**) to the BChl-*a* pair (B820) in each $\beta\beta$ -dyad was determined by static and time-resolved optical studies. The most straightforward measurement is to compare the excitation spectrum of the B820 fluorescence and the

absorbance ($1 - T$) spectrum (where T is transmittance). Representative results are shown in **Figure 6.5**. The Φ_{EET} obtained from these studies for the $\beta\beta$ -dyad containing the respective attached chromophore is 0.85 (**B1**), 0.40 (**B2**), 0.85 (**B3**) or 0.40 (**OGR**).

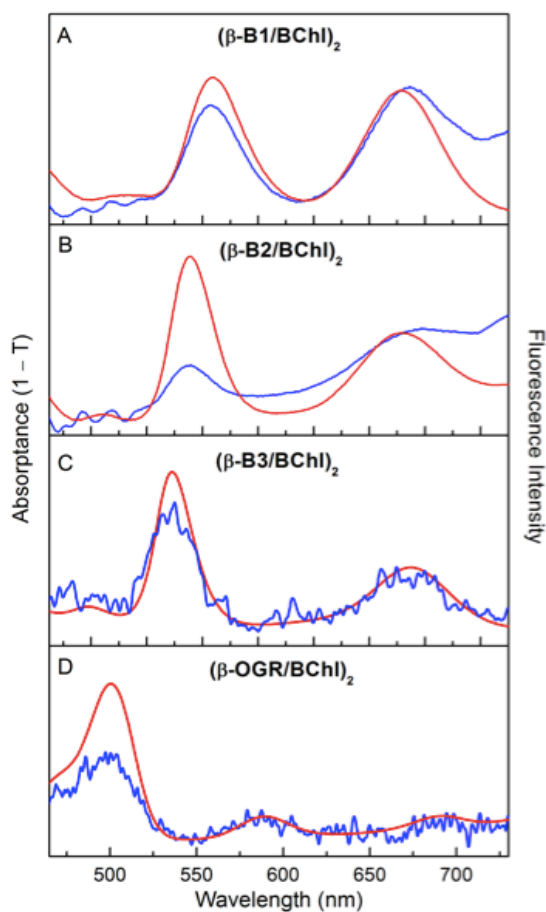


Figure 6.5. Absorbance ($1 -$ transmittance) spectrum (red) versus fluorescence excitation spectrum (blue) at $10\text{ }^{\circ}\text{C}$ using ($\lambda_{\text{det}} = 835\text{--}840\text{ nm}$ for $\beta\beta$ -dyads (**$\beta\text{-B1/BChl}$**)₂ (A), (**$\beta\text{-B2/BChl}$**)₂ (B), (**$\beta\text{-B3/BChl}$**)₂ (C) and (**$\beta\text{-OGR/BChl}$**)₂ (D).

Our experience⁵⁻⁸ is that the Φ_{EET} value obtained from the absorbance versus excitation spectral analysis is typically near the mean of the values from the various other measurements performed, which include (1) the B820 fluorescence yield exciting the attached chromophore versus B820 directly, (2) the reduction of the chromophore fluorescence intensity and excited-state lifetime in the presence of B820 in the dyad versus in its absence in the peptide conjugate, and (3) the dynamics for formation (and decay) of excited B820 following excitation of the attached chromophore as probed by ultrafast transient absorption spectroscopy. Such is the case here, and the average value ($\pm 10\%$) from such studies for each $\beta\beta$ -dyad is listed in the top row of Table 6.1.

Representative results from ultrafast transient absorption studies are shown in **Figure 6.6**. Panels A–D show the decay of the lowest singlet excited state of the chromophore (B1*, B2*, B3*, OGR*) as probed by decay of ground-state bleaching or excited-state absorption in a select wavelength region; similar decays are found across the visible and near-infrared regions and analyzed globally. Panels A and C shows the first ~ 50 ps and panels B and D show a longer time scale (the data extend to ~ 8 ns). Although the decays are all multi-exponential, visual inspection shows that the excited-state decays are faster in the $\beta\beta$ -dyad versus the peptide–bacteriochlorin conjugate because energy transfer to B820 occurs in the former but not the latter.

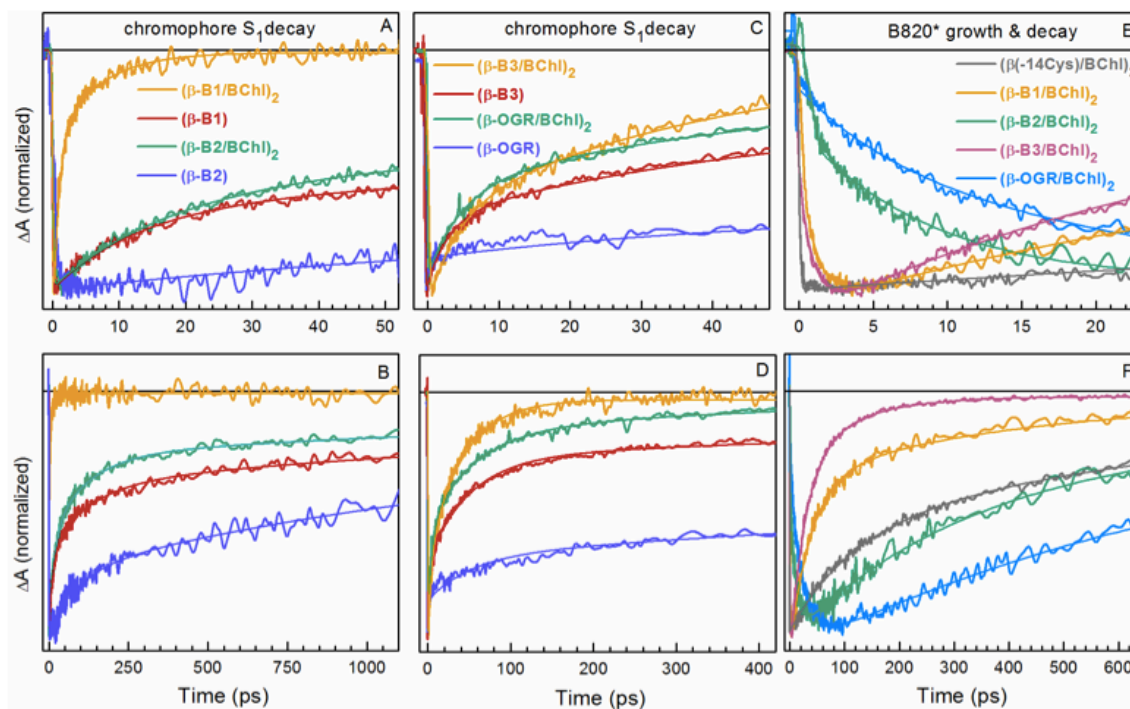


Figure 6.6. Representative transient absorption kinetics obtained at 10 °C for chromophore–peptide conjugates or dyads and probing the decay of the Q_y bleaching of the chromophore (A–D) or the formation and decay of B820* in the dyad (E, F) using excitation of the attached chromophore [**B1** (520 nm), **B2** (520 nm), **B3** (710 nm), **OGR** (480 nm)] or B820 directly (590 nm) for dyad $(\beta(-14\text{Cys})/\text{BChl})_2$, which lacks an attached chromophore. The solid lines are fits to a function containing the instrument response function convolved with two or three exponentials plus a constant.

For the **B1** pair, the amplitude-weighted lifetime of ~ 3 ps for B1^* in dyad $(\beta\text{-B1}/\text{BChl})_2$ is substantially faster than that of ~ 700 ps in conjugate $\beta\text{-B1}$, consistent with the high $\Phi_{\text{ENT}} = 0.85$ measured for this dyad by fluorescence-excitation versus 1 – T analysis. The analogous pairs of values for the other chromophores are ~ 400 ps versus ~ 1 ns for **B2**, ~ 30 ps versus ~ 1 ns for **B3**, and ~ 100 ps versus ~ 1.8 ns for **OGR**. The dyad versus conjugate difference for **B2** is consistent with the modest $\Phi_{\text{EET}} = 0.4$ obtained from fluorescence-

excitation versus 1 – T spectra, and that for **B3** with the high $\Phi_{\text{EET}} = 0.85$ similarly derived. In the case of **OGR**, the lifetime pair indicates a larger Φ_{EET} than 0.4 obtained from the fluorescence-excitation studies, contributing the average value of 0.5 (Table 6.1).

There can be many reasons for the multi-exponential excited-state decays of the chromophore attached to the peptide or in the dyad. These include multiple conformations, locations or orientations of the chromophore with respect to the peptide that afford a range of chromophore–peptide interactions that alter to varying degrees the inherent decay rate constants (fluorescence, internal conversion, intersystem crossing), provide electron-transfer quenching pathways, or give energy transfer to the BChl-*a* pair B820 with various rate constants in the case of the $\beta\beta$ -dyads. Such effects may occur not only in a single unit (one conjugate or one dyad) but also in “aggregates” if formed to some extent, and this tendency may be affected by the inherent properties of the attached chromophore.

If such effects on chromophore properties (other than energy transfer to B820) occur to different degrees in the dyad versus conjugate alone, then the extent to which the latter is a good benchmark for the former for deducing Φ_{EET} may be compromised. This latter point is an issue in deducing Φ_{EET} from chromophore excited-state lifetime or fluorescence yield reduction, but not for the fluorescence-excitation versus absorbance studies because both types of spectra are run solely on the dyad with no conjugate control. In the case of **OGR**, it is known that the nature of the medium and particularly the protonation state of the carboxylic acid in this dye (a fluorescein relative) can dramatically affect photophysical properties such as fluorescence yield and excited-state lifetime.⁸ The same may be true to some degree for hydrophilic bacteriochlorin **B2**, which contains four carboxylic acid groups

(**Chart 6.1**). Such has been found for some (amphiphilic) chlorins and bacteriochlorins bearing carboxylic acid functionalities depending on aqueous (micellar) environment.³⁷ Such properties may contribute to the multi-exponential excited-state decays and to the lower Φ_{EET} of 0.4 or 0.5 in the dyad containing **B2** or **OGR** compared to 0.85 for those housing **B1** or **B3**.

Panels E and F in **Figure 6.6** show the profiles for the formation and subsequent decay of the excited BChl-*a* pair (B820) in a set of $\beta\beta$ -dyads. Panel C shows data for the first ~ 25 ps and panel D the next 600 ps (the data set extends to ~ 8 ns). Dyad (β -**14Cys**)/**BChl**)₂ (black traces) has the native sequence except for replacement of Met with Cys at the -14 position and has no attached chromophore. Direct excitation of B820 at 590 nm results in an instrument-limited rise in the combined Q_y bleaching and B820* stimulated emission (**Figure 6.6E**), followed by essentially complete decay to the ground state with two components with time constants of 810 ps (53%) and 115 ps (40%), giving an amplitude-weighted lifetime of ~ 480 ps (**Figure 6.6F**).

In contrast, dyads (β -**B1**)/**BChl**)₂ (gold traces) and (β -**B3**)/**BChl**)₂ (mauve traces) show a detectable but short lag of 1-2 ps (**Figure 6.6E**) in the formation of the B820 bleaching and B820* stimulated emission due to energy transfer from **B1** or **B3** to B820 ($\Phi_{\text{EET}} = 0.85$). In both cases, the rise is consistent with a short B1* or B3* lifetime component (**Figure 6.6A,C**). As noted above, such fast B1* or B3* decay components compared to the nanosecond time-scale amplitude-weighted decay in the absence of energy transfer are also consistent with the high Φ_{EET} (0.85) in these dyads. The B820* decay for (β -**B1**)/**BChl**)₂ (gold trace in **Figure 6.6F**) has a mean time constant of ~ 400 ps that is similar

to that for the attached-chromophore-lacking dyad ($\beta(-14\text{Cys})/\text{BChl}$)₂ (black trace) but is weighted toward the shorter phases. The decay of B820* for dyad ($\beta\text{-B3}/\text{BChl}$)₂ is faster still (mauve trace) with an amplitude-weighted lifetime of ~50 ps. This faster decay could represent extended interactions between the BChl-*a* contributing to B820 if the attached highly hydrophobic **B3** promotes the formation of aggregates or provides a quenching pathway for B820*.

In contrast, the apparent B820* decay for dyads ($\beta\text{-B2}/\text{BChl}$)₂ (green trace) and ($\beta\text{-OGR}/\text{BChl}$)₂ (blue trace) both show considerably longer lags in the formation of B820* via energy transfer than for the dyads containing **B1** and **B3** (**Figure 6.6E**). The lag for ($\beta\text{-B2}/\text{BChl}$)₂ is ~10 ps and that for ($\beta\text{-OGR}/\text{BChl}$)₂ has two components with time constants of ~6 ps and ~26 ps with an amplitude-weighted value of 20 ps. These lags are consistent with B2* and OGR* lifetime components in these time scales measured in the same dyads (**Figure 6.6B,D**). Furthermore, the decay of B820* is slower in both of these dyads compared to the dyad ($\beta(-14\text{Cys})/\text{BChl}$)₂ that has no attached chromophore. The amplitude-weighted B820* decay time is ~600 ps for ($\beta\text{-B2}/\text{BChl}$)₂ and ~850 ps for ($\beta\text{-OGR}/\text{BChl}$)₂. The longer apparent B820* decays are due in part to contributions on top of the inherent B820* decay with a mean time constant of ~400 ps (found in the absence of attached chromophore). Such contributions are limited by the slower components of the decay of B3* or OGR* (**Figure 6.6A–D**) that reflect the slow phases of B3* → B820 or OGR* → B820 energy transfer and the modest Φ_{EET} of 0.40 for ($\beta\text{-B2}/\text{BChl}$)₂ and 0.50 for ($\beta\text{-OGR}/\text{BChl}$)₂ (Table 6.1). Collectively, the time-resolved absorption data fully support the conclusions

derived from the static fluorescence measurements that the efficiency of energy transfer (Φ_{EET}) from amphiphilic **B1** and hydrophobic **B3** to the BChl-*a* pair B820 in the $\beta\beta$ -dyads is about two-fold greater than for hydrophilic **B2** and **OGR**.

(E) Studies of multi-exponential decays in dyads. The multi-exponential decay of B820* in the $\beta\beta$ -dyads even in the absence of a covalently attached chromophore could arise from a number of sources, as we have discussed previously for 31mer $\beta\beta$ -dyads and $(\beta\beta)_n$ -oligomers and full-length $\alpha\beta$ -dyads and $(\alpha\beta)_n$ -oligomers.⁵⁻⁸ These possibilities include multiple conformers associated with different degrees of interactions between the two BChl-*a* of a dyad, or a range of interactions between neighboring BChl-*a* pairs if dyads associate with one another and modify the inherent B820* decay properties.

If such “aggregation” occurs and more than two BChl-*a* are interacting in a fraction of a sample, then that fraction would be more prone to the effects of exciton annihilation if the excitation intensity is too high. The latter possibility was explored in **Figure 6.7A**, in which the decay of the combined B820 ground-state absorption bleaching and B820* stimulated emission decay was monitored as a function of the energy of the ~120 fs excitation pulse. The lack of a laser energy (intensity) dependence indicates that exciton annihilation does not make a major contribution to the ~115 ps and ~840 ps decay components for dyad $(\beta(-14\text{Cys})/\text{BChl})_2$, which lacks attached chromophores. (Studies of dyads and oligomers at higher intensities often show the development of faster components likely associated with annihilation.)

The decay kinetics for the case of 1 μJ energy per pulse in **Figure 6.7B** shows the same ~120 ps and ~850 ps components with relative amplitudes of 0.51 and 0.39 found in

Figure 6.6D (black). The long component is on the same order of that found for the B820* in $\alpha\beta$ -dyads⁵⁰ and B850* in LH2 rings.^{51,52} Shorter decays on the order of 30–300 ps also have been found in LH2 and attributed to exciton annihilation involving adjacent but interacting rings.⁵³⁻⁵⁴ In principle the same could occur for “aggregated” dyads, although a dependence on intensity is not obvious, at least for $\beta\beta$ -dyads in the absence of attached chromophores (**Figure 6.7A**). As noted above, an alternative is that the inter-BChl-*a* interactions are not the same within each BChl-*a* pair (or with neighboring dyads) and thus have different degrees of reduction of the lifetime compared to monomeric BChl *a*, which is on the order of 2–4 ns.^{50,55}

Förster calculations were performed to estimate the efficiency of energy transfer (Φ_{EET}) from the attached chromophore (**B1, B2, B3, OGR**) to the BChl-*a* pair target site in the associated $\beta\beta$ -dyad. The calculations were performed using PhotochemCAD.⁵⁶ In prior papers^{5,6,8} where a larger number of cases (e.g., sites, attached chromophores, multiple chromophores) were explored, variations in the Φ_{EET} generally were found to follow expectations based on the distance, spectral overlap, and donor photophysical properties that underpin the Förster through-space mechanism, despite limitations in knowledge of some parameters (e.g., precise distances and orientations.)

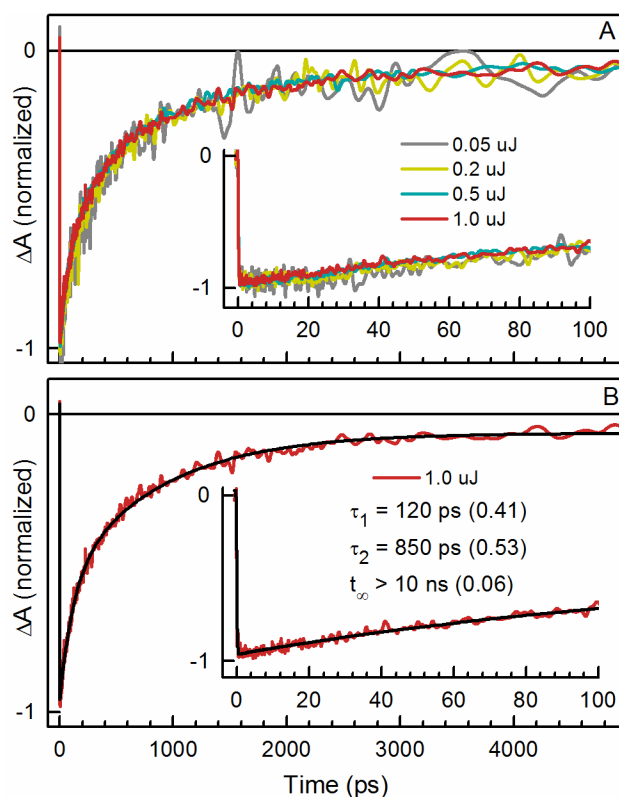


Figure 6.7. (A) Representative time profile for decay of B820 bleaching plus stimulated emission averaged for a $\beta\beta$ -dyad with native β -peptide sequence except for replacement of Met by Cys at the -14 position. The signals were probed over the interval 825–835 nm following excitation with a ~ 100 fs flash at 590 nm using different excitation energies per pulse, for samples held at 10 °C. (B) The decay profile obtained using 1 μ J per pulse along with a fit to a function consisting of the convolution of the instrument response and two-exponentials plus a constant. The components have time constants of 120 and 850 ps with amplitudes of 41% and 53%, with the other 6% due to the constant asymptote.

For each $\beta\beta$ -dyad studied here, calculations were performed using estimated maximum and minimum distances between the BChl-*a* acceptor and the attached chromophore, given the length and flexibility of the linker (Table 6.1). The calculated values bracket the experimental values for the dyads containing amphiphilic **B1** and hydrophobic **B3**. The yields are smaller than expected for hydrophilic **B2**, even though **B2** has similar spectral

overlap that those operational for **B1** and **B3**. Similarly the measured yield for the dyad containing **OGR** is smaller than expected, although the apparent fluorescence yield of **OGR** appears medium dependent and the best choice of system (chromophore, conjugate, medium) for comparison is an issue. The orientation factor is likely involved in these differences, but given the flexibility of the linkers, to do more than use an orientation-averaged value is beyond the current level of the calculations. Regardless, the observed Φ_{EET} value is less than that calculated for the closest expected interchromophore distance for each of the biohybrid antennas.

Outlook

The realization of a science of design that enables rapid *de novo* construction of tailor-made light-harvesting antennas remains a great challenge. The work described herein is aimed at gaining a deeper understanding of the requisite polarity properties of the molecular constituents for use in the biohybrid approach toward such antennas. While one or a few compounds does not provide the basis for far-reaching conclusions, the amphiphilic or hydrophilic bacteriochlorins afford ease of handling of the corresponding conjugate versus that of the hydrophobic conjugates. Moreover, the amphiphilic bacteriochlorin–peptide conjugate gave a larger K_{assoc} for $\beta\beta$ -dyad formation and a higher yield of energy transfer versus those of the hydrophilic conjugate.

Key molecular design issues concern whether amphiphilic character or merely a limited amount of polarity of the attached synthetic chromophore suffices to give rise to the observed effects, and whether the disparate results from the amphiphilic versus hydrophilic bacteriochlorins reflects the fact that the former is (singly) positively charged whereas the

latter has (up to four) negative charges. Regardless, the present results indicate the viability of the biohybrid approach for the rapid construction of light-harvesting architectures. The chromophores examined to date afford increased light-gathering capabilities to the resulting semisynthetic architectures by funneling energy to the native BChl *a* molecules. A study wherein a very long-wavelength absorbing chromophore (a terrylene) was covalently attached to a chlorophyll–light-harvesting protein demonstrated energy flow from the chlorophyll to the synthetic chromophore.⁵⁷ The access to diverse synthetic chromophores and synthetic peptides, in concert with the blueprint of native photosynthesis, augurs well for the systematic design of tailorable light-harvesting architectures for fundamental studies as well as applications in photonics and solar-energy conversion.

Experimental section

(I) General methods

¹H NMR (400 MHz) spectroscopy was performed at room temperature in CDCl₃ (with tetramethylsilane as internal reference) unless noted otherwise. **B1** and bacteriochlorin precursors typically exhibited insufficient solubility to be characterized by ¹³C NMR spectroscopy. Silica gel (40 μm average particle size) was used for column chromatography. All solvents were reagent grade and were used as received unless noted otherwise. THF was freshly distilled from sodium/benzophenone ketyl. Matrix-assisted laser-desorption mass spectrometry (MALDI-MS) was performed with the matrix 1,4-bis(5-phenyl-2-oxazol-2-yl)benzene¹⁵ unless noted otherwise. Electrospray ionization mass spectrometry (ESI-MS) data are reported for the molecular ion or quasimolecular ion. The peptides employed herein were the native α-peptide and an analogue of the β-peptide from LH1 of *Rb. sphaeroides*.

The α -peptide was obtained as described previously.¹⁶ The β -peptide analogue contains Cys in place of Met at position -14 (measured from the His at position 0):

ADKSDLGYTGLTDEQAQELHSVYCSGLWLFSAVAIVAH⁰LAVYIWRPWF.

The β -peptide analogue is termed **$\beta(-14\text{Cys})$** and was purchased from Bio-Synthesis (Lewisville, Texas) in 90% purity. BChl *a* that contains a phytyl esterifying alcohol was obtained from Sigma. Known bacteriochlorin **B1a** was prepared following literature procedures.¹⁷ Conjugate **$\beta\text{-B2}$** ¹² and **$\beta\text{-B3}$** ⁸ were prepared as described previously. All other compounds were used as received from commercial sources.

The variable temperature study of dyad assembly/disassembly was conducted on an Agilent 8453 UV-visible spectrophotometer, equipped with a Peltier (solid-state) temperature controller. Real-time temperature was read with a thermocouple inserted into the cuvette. Mild magnetic stirring (200 rpm) was employed to ensure rapid and uniform heating/cooling processes.

Static and time-resolved optical studies and single-reflection Fourier transform infrared (FTIR) measurements were performed as described.⁶⁻⁸ FTIR studies were performed on samples at room temperature. Optical studies were conducted on samples at 10 °C, slightly higher than the temperature at which the dyads were prepared by chilling (and stored) to minimize water condensation on the optical cells.

(II) Synthesis

3-(5-Amino-3-pyridyl)-5-methoxy-8,8,18,18-tetramethyl-13[2-(4-*N,N*-dimethyl-aminophenyl)ethynyl]bacteriochlorin (B1b). Following a general procedure,⁷ a mixture of 3-bromo-5-methoxy-8,8,18,18-tetramethyl-13-[2-(4-*N,N*-dimethylamino-

phenyl)ethynyl]bacteriochlorin (**B1a**, 102 mg, 0.164 mmol), 4,4,5,5-tetramethyl-2-(5-amino-3-pyridyl)-1,3,2-dioxaborolane (**1**, 108 mg, 0.492 mmol), Pd(PPh₃)₄ (57.0 mg, 49.0 μmol) and anhydrous K₂CO₃ (272 mg, 1.97 mmol) was dried in a Schlenk flask for 1 h. DMF/toluene [16.4 mL (1:2), degassed by bubbling argon for 30 min] was added, and the reaction mixture was deaerated by three “freeze–pump–thaw” cycles. The reaction mixture was heated at 90 °C for 18 h. After cooling to room temperature, the solvent was removed. The resulting solid was dissolved in CH₂Cl₂ and washed with saturated aqueous NaHCO₃ solution. The organic layer was separated, dried (Na₂SO₄), and concentrated. The residue was chromatographed [silica, ethyl acetate/triethylamine (5:1)] to afford a green solid that contained a small amount of triphenylphosphine oxide. The triphenylphosphine oxide was removed by washing with Et₂O/hexanes (3:2) to provide a green solid (90 mg, 87%): ¹H NMR δ –1.80 (brs, 1H), –1.66 (brs, 1H), 1.95 (s, 12H), 3.09 (s, 6H), 3.69 (s, 3H), 3.88 (brs, 2H), 4.33 (s, 2H), 4.43 (s, 2H), 6.82 (d, *J* = 9.2 Hz, 2H), 7.74–7.80 (m, 3H), 8.28 (d, *J* = 2.8 Hz, 1H), 8.55 (s, 1H), 8.57–8.61 (m, 2H), 8.74–8.80 (m, 2H), 8.95 (s, 1H); MALDI-MS obsd 635.3; ESI-MS obsd 636.3448; calcd 636.3445 [(M + H)⁺, M = C₄₀H₄₁N₇O]; λ_{abs} (CH₂Cl₂) 364, 517, 747 nm.

3-[5-(4-Maleimidobutyramido)-3-pyridyl]-5-methoxy-8,8,18,18-tetramethyl-13-[2-(4-(*N,N*-dimethylamino)phenyl)ethynyl]bacteriochlorin (B1c**).** A mixture of **B1b** (10.0 mg, 0.0157 mmol), 4-maleimidobutyric acid (**2**, 2.87 mg, 15.7 μmol) and DCC (3.20 mg, 15.7 μmol) in CHCl₃ (1.5 mL, 10 mM) was stirred at room temperature for 24 h. Then the reaction mixture was washed with aqueous NaHCO₃ solution, dried (Na₂SO₄), concentrated and chromatographed [silica, CH₂Cl₂/MeOH (1:1)] to provide a green solid (6.0 mg, 48%)

yield, 95% purity): $^1\text{H NMR } \delta$ -1.66 (brs, 1H), -1.56 (brs, 1H), 1.94 (s, 12H), 2.08–2.16 (m, 2H), 2.49 (t, $J = 6.4$ Hz, 2H), 3.09 (s, 6H), 3.64 (s, 3H), 3.71 (t, $J = 6.4$ Hz, 2H), 4.29 (brs, 2H), 4.24 (s, 2H), 6.73 (s, 2H), 6.82 (d, $J = 8.8$ Hz, 2H), 7.76 (d, $J = 8.8$ Hz, 2H), 8.51 (s, 1H), 8.56 (s, 1H), 8.60 (d, $J = 2.4$ Hz, 1H), 8.73 (d, $J = 2.2$ Hz, 2H), 8.92 (s, 2H), 9.06 (s, 1H), 9.11 (s, 1H); MALDI-MS obsd 800.3; ESI-MS obsd 801.3860; calcd 801.3871 [(M + H)⁺, M = C₄₈H₄₈N₈O₄], λ_{abs} (CH₂Cl₂) 363, 517, 747 nm.

3-[5-(4-Maleimidobutyramido)-3-pyridyl]-5-methoxy-8,8,18,18-tetramethyl-13[2-(4-*N,N,N*-trimethylammonio)phenyl]ethynyl]bacteriochlorin iodide (B1). Following a general method for quaternization,¹⁸ a solution of **B1c** (6.0 mg, 7.5 μmol) in CHCl₃ (1.0 mL, stabilized with EtOH) was treated with MeI (37 μL , 0.60 mmol), and reaction mixture was stirred under argon for 24 h. At this time a solid had settled on the walls and bottom of the vial. Excess MeI was removed, and anhydrous Et₂O (10 mL) was added. The suspension was sonicated for 2 min and then centrifuged. The supernatant was decanted. The remaining solid was dried under high vacuum to afford a pink solid (5.2 mg, 75%): $^1\text{H NMR}$ (CD₃OD) δ 1.94 (s, 6H), 1.95 (s, 6H), 1.96–1.97 (m, 2H), 2.60 (t, $J = 7.2$ Hz, 2H), 3.08 (s, 9H), 3.67 (t, $J = 7.2$ Hz, 2H), 3.71 (s, 3H), 4.28 (s, 2H), 4.40 (s, 2H), 6.85 (s, 2H), 6.88 (d, $J = 9.3$ Hz, 2H), 7.69 (d, $J = 9.3$ Hz, 2H), 8.59 (d, $J = 4.8$ Hz, 2H), 8.70 (s, 1H), 8.78 (d, $J = 3.0$ Hz, 2H), 8.91 (s, 1H), 9.36 (s, 1H), 9.67 (s, 1H), two *N*-pyrrolic protons and one amide proton are missing due to the use of CD₃OD; MALDI-MS obsd 816.7 (M⁺), 801.7 (M–Me)⁺, 786.6 (M–Me₂)⁺; ESI-MS obsd 815.4030; calcd 815.4028 [(M – I)⁺, M = C₄₉H₅₁N₈O₄]; λ_{abs} (H₂O) 366, 522, 749 nm.

(III) Preparation of β -B1

A sample of $\beta(-14\text{Cys})$ (1.5 mg, 0.28 μmol) was dissolved in DMF (56 μL) whereupon Tris buffer (14 μL , pH 8.6) was added while the mixture was stirred under a steady flow of argon. The protein appeared to readily go into solution in DMF and stay in solution when Tris buffer was added. Similarly, a sample of **B1** (0.40 mg, 0.42 μmol) was dissolved in DMF (56 μL) whereupon Tris buffer (14 μL , pH 8.6) was added. The bacteriochlorin solution was then added dropwise to the peptide solution over 2 min with stirring under argon. The reaction vessel was stoppered and stirred at room temperature for 2 h in the dark. The reaction mixture was treated with DMF (200 μL) and sonicated for 3 min, followed by centrifugation at 4000 rpm for 10 min. The supernatant was gently decanted and the procedure was repeated twice in an effort to completely remove excess (unreacted) **B1**. Analytical HPLC was performed as described in ref 8 and repeated herein for completion: Analytical HPLC was performed on a Hewlett-Packard 1100 series instrument using a C4 column (Vydac, 10 μm , 300 \AA , 150 mm x 4.6 mm) in series with a guard column. The HPLC solvent system consisted of (A) 0.1% trifluoroacetic acid in water as the aqueous solvent and (B) 0.1% trifluoroacetic acid in 1:2 (v/v) acetonitrile/2-propanol as the organic solvent. The original composition of A/B is 50/50 (v/v), and the use of a gradient afforded the final composition of A/B (30/70) at 48 min. In other words, the HPLC solvent was initially H₂O (50%), CH₃CN (16.7%), isopropanol (33.3%), and trifluoroacetic acid (0.1%), which has pH 2.01. The use of a gradient afforded a final composition of H₂O (30%), CH₃CN (23.3%), isopropanol (46.6%), and trifluoroacetic acid (0.1%) at 48 min. The flow

rate was 0.8 mL/min for the analytical. The conjugate was injected (10–40 μ L) at a concentration of 0.5–1.0 mM in a solution of hexafluoroacetone trihydrate (25%), water (37.5%), CH₃CN (12.5%), and isopropanol (25%). The conjugate was first dissolved in neat hexafluoroacetone trihydrate and then the other solvents were added to give the injection sample; the conjugate was soluble in this solvent mixture. The resulting brownish residue was dried under vacuum for 30 min. Addition of hexafluoroacetone trihydrate (40 μ L) to the brownish solid followed by sonication for 3 min completely dissolved the solid. Addition of 80 μ L of a solvent mixture [composed of H₂O (50%), isopropanol (33.3%), acetonitrile (17.6%) and trifluoroacetic acid (0.1%)] caused a change from pink back to brownish. This mixture was centrifuged to remove (visibly evident) insoluble particles. The resulting supernatant was analyzed by HPLC. The total (isolated) yield was determined to be 57% on the basis of absorption spectroscopy of the conjugate versus the starting peptide.

The resulting bacteriochlorin–peptide conjugate **β -B1** was examined by mass spectrometry. ESI-MS analysis afforded a set of peaks with varying number of charges, which upon hypermass ion reconstruction gave the base peak at $m/z = 6242.1240$.⁵⁸ The bacteriochlorin–peptide conjugate in native form bears a single permanent charge due to the trimethylammonium group. To determine the monoisotopic mass, the observed peak ($m/z = 1041.0274$; $z = 6$) corresponds to the monoisotopic value of 6241.1644 [for the singly charged species, **β -B1**, which agreed well (11.3 ppm) with the theoretical value of 6241.0938 (M^+ , $M = C_{303}H_{420}N_{69}O_{74}S$). Such data can be compared with those for the peptide **β -(14Cys)**, which gave $m/z = 5425.7052$ (calcd 5425.6905, M^+ , $M = C_{254}H_{369}N_{61}O_{70}S$) and $m/z = 5428.7056$ as the base peak.⁵⁸ Analysis also was carried out by MALDI-MS analysis (with

the matrix α -cyano-4-hydroxycinnamic acid). The data for β -B1 (obsd 6231.6763) can be compared with those of the peptide β (-14Cys): obsd 5429.4814. In both cases a small, systematic mass displacement error occurred owing to the choice of calibrants.

(IV) Dyad formation from β -B1

Under dim light, a sample of β -B1 (~0.03 mg) was solubilized in 10 μ L of hexafluoroacetone trihydrate, diluted with 0.5 mL of 154 mM octG in 100 mM phosphate buffer solution (pH 7.6), and then diluted 3-fold with the same buffer (lacking octG) to bring the octG concentration to 30.8 mM. This detergent solution containing β -B1 was neutralized by addition of 15 μ L of 3 M potassium hydroxide solution. Aliquots of BChl *a* in degassed acetone (~1.5 mM) were then added (4.0 μ L first, then 4.0 μ L x 2 to give 12 μ L total) to the solution; the change in absorption upon such additions of BChl *a* is shown in **Figure 6.8**. Formation of dyads was then induced by (1) addition of 100 mM phosphate buffer solution (pH 7.6, lacking octG) to decrease the octG concentration first to 30.8 mM, 25.7 mM and then to 22.6 mM, followed by (2) chilling the sample at 5 °C. The dilution of the octG detergent and the chilling processes change the respective protein and micelle concentrations.

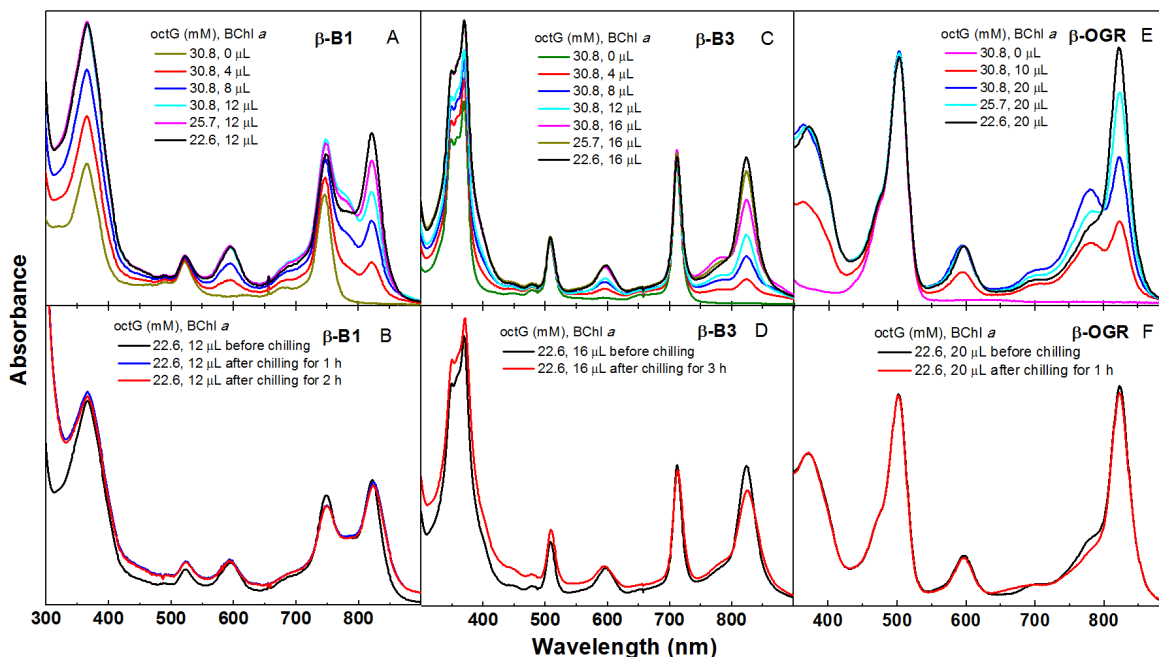


Figure 6.8. Absorption spectra for formation of dyads signaled by the peak at 822 nm. Titration of β -B1 (A), β -B3 (C) or β -OGR (E) in aqueous phosphate buffer containing 30.8 mM octG with BChl *a* (in acetone) followed by phosphate buffer without octG (to dilute the octG ultimately to 22.6 mM). Samples of β -B1 (B), β -B3 (D) and β -OGR (F) in 22.6 mM octG before and after chilling at 5 °C. The spectra were corrected for dilution. The initial sample (30.8 mM octG) prior to addition of BChl *a* gave an absorbance at 745 nm of 0.22 for β -B1 (A), at 727 nm of 0.63 for β -B3 (C) and at 502 nm of 0.34 for β -OGR (E), all in a 1-cm cuvette. The last trace (black) in panel A, C, or E is the first trace in panel B, D, or F, respectively.

References

- 1 H. D. Harvey, In: *The porphyrin handbook*, ed. K. M. Kadish, K. M. Smith and R. Guilard, Academic Press, San Diego, CA, 2003, Vol. 18, pp. 63–250.
- 2 N. Aratani, A. Osuka, In: *Handbook of porphyrin science*, ed. K. M. Kadish, K. M. Smith and R. Guilard, world scientific publishing Co., Singapore, 2010, Vol. 1, pp. 1–132.

- 3 P. D. Harvey, C. Stern, R. Guilard, In *Handbook of porphyrin science*, ed. K. M. Kadish, K. M. Smith and R. Guilard, world scientific publishing Co., Singapore, 2010, Vol. 1, pp. 1–179.
- 4 J. S. Lindsey, O. Mass and C. Y. Chen, *New J. Chem.*, 2011, **35**, 511–516.
- 5 M. A. Harris, J. Jiang, D. M. Niedzwiedzki, J. Jiao, M. Taniguchi, C. Kirmaier, P. A. Loach, D. F. Bocian, J. S. Lindsey, D. Holten and P. S. Parkes-Loach, *Photosynth. Res.*, 2014, **121**, 35–48.
- 6 J. W. Springer, P. S. Parkes-Loach, K. R. Reddy, M. Krayner, J. Jiao, G. M. Lee, D. M. Niedzwiedzki, M. A. Harris, C. Kirmaier, D. F. Bocian, J. S. Lindsey, D. Holten and P. A. Loach, *J. Am. Chem. Soc.*, 2012, **134**, 4589–4599.
- 7 K. R. Reddy, J. Jiang, M. Krayner, M. A. Harris, J. W. Springer, E. Yang, J. Jiao, D. M. Niedzwiedzki, D. Pandithavidana, P. S. Parkes-Loach, C. Kirmaier, P. A. Loach, D. F. Bocian, D. Holten and J. S. Lindsey JS, *Chem. Sci.*, 2013, **4**, 2036–2053.
- 8 M. A. Harris, P. S. Parkes-Loach, J. W. Springer, J. Jiang, E. C. Martin, P. Qian, J. Jiao, D. M. Niedzwiedzki, C. Kirmaier, J. D. Olsen, D. F. Bocian, D. Holten, C. N. Hunter, J. S. Lindsey and P. A. Loach, *Chem. Sci.*, 2011, **4**, 3924–3933.
- 9 D. Mauzerall, *Ann NY. Acad. Sci.*, 1973, **206**, 483–494.
- 10 D. Mauzerall, *Photosynth. Res.*, 1992, **33**, 163–170.
- 11 C. J. Law, J. Chen, P. S. Parkes-Loach and P. A. Loach, *Photosynth. Res.*, 2003, **75**, 193–210.
- 12 J. Jiang, P. Vairaprakash, K. R. Reddy, T. Sahin, M. P. Pavan, E. Lubian and J. S. Lindsey, *Org. Biomol. Chem.*, 2014, **12**, 86–103.

- 13 P. A. Loach, P. S. Parkes-Loach, C. M. Davis and B. A. Heller, *Photosynth. Res.*, 1994, **40**, 231–245.
- 14 K. A. Meadows, K. Iida, T. Kazuichi, P. A. Recchia, B. A. Heller, B. Antonio, M. Nango, P. A. Loach, *Biochemistry*, 1995, **34**, 1559–1574.
- 15 N. Srinivasan, C. A. Haney, J. S. Lindsey, W. Zhang and B. T. Chait, *J. Porphyrins Phthalocyanines*, 1999, **3**, 283–291
- 16 P. S. Parkes-Loach, J. R. Sprinkle and P. A. Loach PA, *Biochemistry*, 1988, **27**, 2718–2727
- 17 Z. Yu and M. Ptaszek, *Org. Lett.*, 2012, **14**, 3708–3711.
- 18 C. Ruzié, M. Krayner, T. Balasubramanian and J. S. Lindsey, *J. Org. Chem.*, 2008, **73**, 5806–5820.
- 19 Y. Chen, G. Li and R. K. Pandey, *Curr. Org. Chem.*, **8**, 1105–1134.
- 20 M. A. Grin, A. F. Mironov and A. A. Shtil, *Anti-Cancer Agents Med. Chem.*, 2008, **8**, 683–697.
- 21 A. Kozyrev, M. Ethirajan, P. Chen, K. Ohkubo, B. C. Robinson, K. M. Barkigia, S. Fukuzumi, K. M. Kadish and R. K. Pandey RK, *J. Org. Chem.*, 2012, **77**, 10260–10271.
- 22 A. M. G. Silva, A. C. Tomé, M. G. P. M. S. Neves, A. M. S. Silva, J. A. S. Cavaleir, *J. Org. Chem.*, 2005, **70**, 2306–2314.
- 23 A. C. Tomé, M. G. P. M. S. Neves and J. A. S. Cavaleiro JAS, *J. Porphyrins Phthalocyanines*, 2009, **13**, 408–414.

- 24 S. Singh, A. Aggarwal, S. Thompson, J. P. C. Tomé, X. Zhu, D. Samaroo, M. Vinodu, R. Gao and C. M. Drain, *Bioconjugate Chem.*, 2010, **21**, 2136–2146.
- 25 N. A. M. Pereira, S. M. Fonseca, A. C. Serra, T. M. V. D. Pinho e Melo and H. D. Burrows, *Eur. J. Org. Chem.*, 2011, 3970–3979.
- 26 J. M. Dąbrowski, K. Urbanska, L. G. Arnaut, M. M. Pereira, R. R. Abreu, S. Simões, G. Stochel, *ChemMedChem.*, 2011, **6**, 465–475.
- 27 L. P. Samankumara, S. Wells, M. Zeller, A. M. Acuña, B. Röder, C. Brückner, *Angew. Chem. Int. Ed.*, 2012, **51**, 5757–5760.
- 28 A. Aggarwal, S. Thompson, S. Singh, B. Newton, A. Moore, R. Gao, X. Gu, S. Mukherjee and C.M. Drain, *Photochem. Photobiol.*, 2014, **90**, 419–430.
- 29 T. G. Minehan, Y. Kishi, *Angew. Chem. Int. Ed.*, 1999, **38**, 923–925.
- 30 W. Wang, Y. Kishi, *Org. Lett.*, 1999, **1**, 1129–1132.
- 31 H. J. Kim and J. S. Lindsey, *J. Org. Chem.*, 2005, **70**, 5475–5486.
- 32 M. Krayner, M. Ptaszek, H. J. Kim, K. R. Meneely, D. Fan, K. Secor, J. S. Lindsey, 2010, *J. Org. Chem.*, **75**, 1016–1039.
- 33 M. Galezowski and D. T. Gryko, *Curr. Org. Chem.*, 2007, **11**, 1310–1338.
- 34 C. Brückner, L. Samankumara and J. Ogikubo, In *Handbook of porphyrin science*, ed. K. M. Kadish, K. M. Smith and R. Guilard, world scientific, Singapore, 2012, Vol. 17, pp.1–112.
- 35 J. M. Sutton, O. J. Clarke, N. Fernandez and R. W. Boyle, *Bioconjugate Chem.*, 2002, **13**, 249–263.
- 36 J. R. McCarthy, J. Bhaumik, N. Merbouh and R. Weissleder, *Org. Biomol. Chem.*,

- 2009, **7**, 3430–3436.
- 37 K. Aravindu, O. Mass, P. Vairaprakash, J. W. Springer, E. Yang, D. M. Niedzwiedzki, D. F. Bocian, D. Holten and J. S. Lindsey, *Chem. Sci.*, 2013, **4**, 3459–3477.
- 38 V. M. Alexander, K. Sano, Z. Yu, T. Nakajima, P. L. Choyke, M. Ptaszek and H. Kobayashi H, *Bioconjugate Chem.*, 2012, **23**, 1671–1679.
- 39 T. Harada, K. Sano, K. Sato, R. Watanabe, Z. Yu, H. Hanaoka, T. Nakajima, P. L. Choyke, M. Ptaszek and H. Kobayashi H, *Bioconjugate Chem.*, 2014, **25**, 362–369.
- 40 M. Kobayashi, M. Akiyama, H. Kano, H. Kise, In *Chlorophylls and bacteriochlorophylls: biochemistry, biophysics, functions and applications*, ed. B. Grimm, R. J. Porra, W. Rüdiger and H. Scheer H, Springer, Dordrecht, The Netherlands, 2006, pp. 79–94.
- 41 E. Yang, C. Kirmaier, M. Krayner, M. Taniguchi, H. J. Kim, J. R. Diers, D. F. Bocian, J. S. Lindsey and D. Holten D, *J Phys. Chem. B*, 2011, **115**, 10801–10816.
- 42 C.-Y. Chen, E. Sun, D. Fan, M. Taniguchi, B. E. McDowell, E. Yang, D. F. Diers, D. Bocian, D. Holten and J. S. Lindsey, *Inorg. Chem.*, 2012, **51**, 9443–9464.
- 43 K. A. Meadows, P. S. Parkes-Loach, J. W. Kehoe and P. A. Loach, *Biochemistry*, 1998, **37**, 3411–3417.
- 44 A. Pandit, R. W. Visschers, I. H. M. van Stokkum, R. Kraayenhof, R. van Grondelle, *Biochemistry*, 2001, **40**, 12913–12924.
- 45 A. Pandit, H. Ma, I. H. M. van Stokkum, M. Gruebele, R. van Grondelle, *Biochemistry*, 2002, **41**, 15115–15120.

- 46 P. A. Loach and P. S. Parkes-Loach, In *Advances in photosynthesis: Anoxygenic photosynthetic bacteria*, ed. R. E. Blankenship, M. T. Madigan and C. E. Bauer, Kluwer Academic Publishers, Dordrecht, 1995, pp. 437–471.
- 47 P. A. Loach and P. S. Parkes-Loach, In *The purple phototropic bacteria*, ed. C. N. Hunter, F. Daldal, M. C. Thurnauer and J. T. Beatty, Springer, Dordrecht, 2009, pp. 181–198.
- 48 M. da Graça Miguel, O. Eidelman, M. Ollivon and A. Walter, *Biochemistry*, 1989, **28**, 8921–8928.
- 49 J. B. Todd, P. A. Recchia, P. S. Parkes-Loach, J. D. Olsen, G. J. S. Fowler, P. McGlynn, N. C. Hunter and P. A. Loach, *Photosynth. Res.*, 1999, **62**, 85–98.
- 50 M. C. Chang, P. M. Callahan, P. S. Parkes-Loach, T. M. Cotton and P. A. Loach, *Biochemistry*, 1990, **29**, 421–429.
- 51 H. H. Billsten, J. L. Herek, G. Garcia-Asua, L. Hashøj, T. Polívka, C. N. Hunter and V. Sundström, *Biochemistry*, 2002, **41**, 4127–4136.
- 52 C. N. Hunter, H. Bergström, R. van Grondelle and V. Sundström, *Biochemistry*, 1990, **29**, 3203–3207.
- 53 A. Schubert, A. Stenstam, W. J. D. Beenken, J. L. Herek, R. Cogdell, T. Pullerits and V. Sundström, *Biophys. J.*, 2004, **86**, 2363–2373.
- 54 T. Pflock, M. Dezi, G. Venturoli, R. J. Cogdell, J. Köhler and S. Oellerich, *Photosynth. Res.*, 2008, **95**, 291–298
- 55 J. S. Connolly, E. B. Samuel and A. F. Janzen, *Photochem. Photobiol.*, 1982, **36**, 565–574.

- 56 H. Du, R. C. A. Fuh, J. Li, L. A. Corkan and J. S. Lindsey, *Photochem. Photobiol.*, 1998, **68**, 141–142.
- 57 H. Wolf-Klein, C. Kohl, K. Müllen and H. Paulsen, *Angew. Chem. Int. Ed.*, 2002, **41**, 3378–3380.
- 58 J. Jiang, K. R. Reddy, M. P. Pavan, E. Lubian, M. A. Harris, J. Jiao, D. M. Niedzwiedzki, C. Kirmaier, P. S. Parkes-Loach, P. A. Loach, D. F. Bocian, D. Holten and J. S. Lindsey, *Photosynth. Res.*, 2014, **122**, 187–202.

CHAPTER 7

Versatile Design of Biohybrid Light-Harvesting Architectures to Tune Location, Density and Spectral Coverage of Attached Synthetic Chromophores for Enhanced Energy Capture

Preamble. The contents in this chapter have been published⁶¹ with contributions from the following individuals/groups. Michelle A. Harris and Christine Kirmaier (the Holten group): photophysical property studies on biohybrids. Jieying Jiao (the Bocian group): FT-IR study on peptide-chromophore conjugates. Pamela S. Parkes-Loach (the Loach group): construction of biohybrids from peptide-chromophore conjugate.

Introduction

The design of next generation solar light collectors may serve a broad range of applications. Applications for maximum energy output require broad spectral coverage to harvest as much solar energy as possible, whereas light-activated sensors or switches may only utilize one of several narrow spectral windows. In both types of applications, the light-harvesting features must be tailored to the downstream needs with avoidance of deleterious processes such as excited-state quenching or formation of reactive (oxygen) species. A ‘science of design’ is required to fulfill such daunting objectives, wherein the molecular architecture is chosen from first principles and the requisite constituents are then assembled in a straightforward and rational manner. While photosynthesis in all of its diverse formats provides blueprints for molecular-based solar energy conversion, earnest efforts over several decades to recreate photosynthetic-like processes by purely chemical means have fallen far short of the efficiency and versatility of the natural systems. Indeed, with relatively few

albeit notable exceptions,¹⁻³ extant synthetic light-harvesting architectures generally rely on covalent linkages for organization rather than supramolecular self-assembly, contain far fewer chromophores than those in the natural systems, and generally absorb light in the visible rather than the photon-rich near-infrared (NIR) region.⁴⁻⁶ Whereas most synthetic light-harvesting architectures contain <10 chromophores or so, the natural photosynthetic light-harvesting systems ultimately deploy hundreds of chromophores (e.g., chlorophylls, bacteriochlorophylls, carotenoids, bilins) in self-assembled architectures that span mesoscale dimensions.

As a step towards developing a versatile platform technology to create molecular light-harvesting architectures that rival natural photosynthetic antennas and exhibit the design latitude suitable for next generation solar energy conversion, we have turned to a semisynthesis approach.⁷⁻⁹ Semisynthesis combines modern synthetic chemistry and abundant natural constituents. The semisynthesis approach we have explored builds on the light-harvesting blueprint from photosynthetic bacteria, where nanoscale antenna complexes are formed by a two-tiered self-assembly process. The light-harvesting complexes in photosynthetic bacteria are comprised of cyclic oligomers of discrete subunits, each of which contains two small (5–6 kDa) peptides, α and β , that provide the scaffold and organization for two bacteriochlorophyll *a* (BChl *a*) molecules.¹⁰⁻¹¹ The semisynthesis approach employs synthetic analogues of one or both of the peptides, to which are attached synthetic chromophores. The subsequent self-assembly process affords a ‘biohybrid antenna’ resembling the native antenna in size and complexity yet also contains synthetic chromophores that confer added spectral coverage.

The success of the biohybrid approach stems in part from the robustness of the peptides and the choice of placement of the synthetic chromophores therein. The peptides do not lose their α -helicity despite being lyophilized and dissolved in organic solvents or in aqueous detergent solutions.^{9,12,13} The reconstitution of the separately isolated native components, or engineered native-like analogues, is a two-tier assembly process analogous to that in the formation of natural bacterial antenna systems. The two BChl *a* molecules associate with the α - and β -peptides to form a dyad ‘subunit’ (**Figure 7.1a**) under specific conditions.^{14,15} The conditions can then be altered to favor assembly of subunits into cyclic LH1-type oligomers (**Figure 7.1b** and **7.1c**).⁹ Whereas the long-wavelength (Q_y) band of monomeric BChl *a* is at ~ 780 nm, the dyad of two interacting BChl *a* (denoted B820) in the subunit absorbs at ~ 820 nm, and the absorption of the larger array of BChl *a* (denoted B875) in the LH1-type oligomer is shifted to still longer wavelengths, typically ~ 875 nm (**Figure 7.1d**). In some native membranes, the cyclic oligomer structures can associate to form large, two-dimensional antenna arrays.¹⁶⁻¹⁸ The peptides can also be modified at the N and C termini to facilitate preparation of monolayers on metallic surfaces.¹⁹

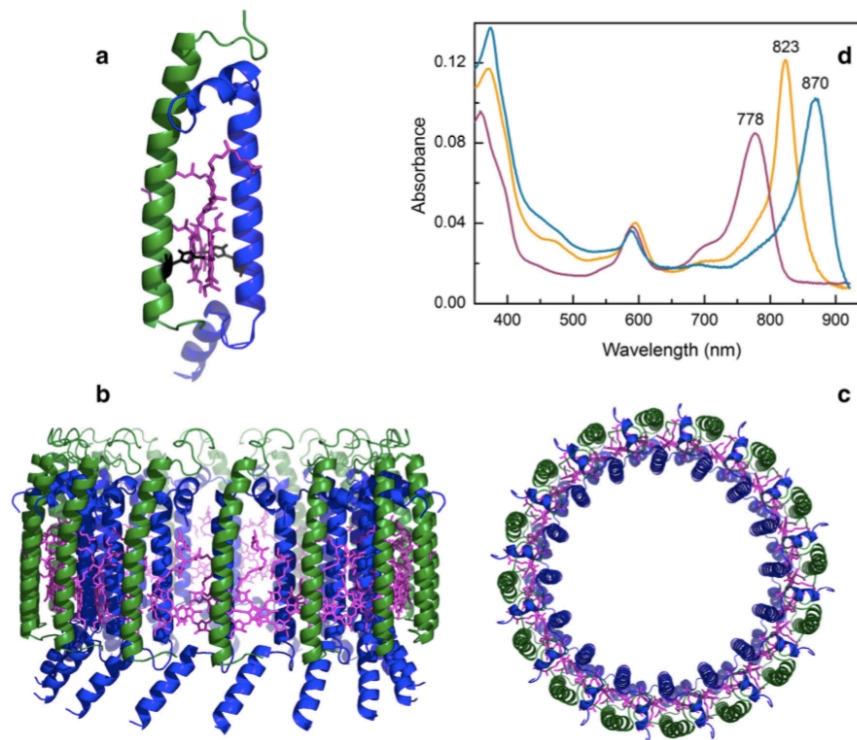


Figure 7.1. (a) $\alpha\beta$ -subunit of the LH2 (B800–850) complex of *Phaeospirillum (Phs.) molischianum*.²⁰ Coordinating histidines are illustrated (black). (b and c) Side and top view of a model of the *Rb. sphaeroides* LH1 oligomer; the model is in ref 21, which lacks protein PufX and thus shows a closed ring. The α -peptides (blue) are on the inside of the ring and the β -peptides (green) are on the outside. BChl *a* are colored magenta. (d) Absorption spectra of BChl *a* in 0.90% octyl glucoside (mauve), $\alpha\beta$ -dyad (B820) reconstituted from native *Rb. sphaeroides* α - and β -peptides and BChl *a* (gold) in 0.66% octyl glucoside and LH1-type ($\alpha\beta$)_n-oligomers formed from subunits ($\alpha\beta$ -dyads) by overnight chilling at 6 °C (blue).

Using knowledge from crystal structures of analogous LH2 bacterial antenna structures^{20,22,23} and from structure-function reconstitution work,¹⁴⁻¹⁵ the peptides were modified so that a chromophore could be covalently attached without disrupting the assembly of the peptides and BChl *a* to form subunits (B820-containing $\alpha\beta$ -dyads) and LH1-type complexes (B875-containing ($\alpha\beta$)_n-oligomers). On the basis of spectroscopic analogy with

native LH1 complexes^{21,24-27} as well as direct examination by electron microscopy, the biohybrid LH1-type oligomers were found to exist as rings with a distribution of sizes that on the whole were slightly smaller than the natural complexes.⁹ Given the distribution of rings with 14–16 dyads, the overall light-harvesting architecture contain an average of 30 non-covalently bound BChl *a* (B875) and hence an average of 15 additional covalently bound synthetic chromophores.

In previous work,⁷⁻⁹ a palette of bacteriochlorins was synthesized and members therein were attached to the peptides to form dyads containing the synthetic bacteriochlorin and BChl *a*. These bacteriochlorins can be designed to have the long-wavelength (Q_y) band at a specific wavelength in the NIR region (see subset in **Figure 7.2a**)^{8,28} and, in so doing make the antenna spectrally tunable. Other chromophores such as Oregon Green (**OGR**) or Rhodamine Red were also attached to the peptides. By attaching such chromophores, one per peptide, the spectral coverage of the light-harvesting complex was increased. These covalently attached chromophores have been shown to have a high efficiency of excitation energy transfer (Φ_{EET}) to B875 (the BChl *a* array) in the oligomer. Moreover, the assembly of two distinct dyads was examined wherein each contains a distinct chromophore to give a heterogeneous mixture of oligomers. In so doing, the Φ_{EET} from a distant chromophore to B875 was significantly enhanced by relay energy transfer via a more proximal chromophore.⁹

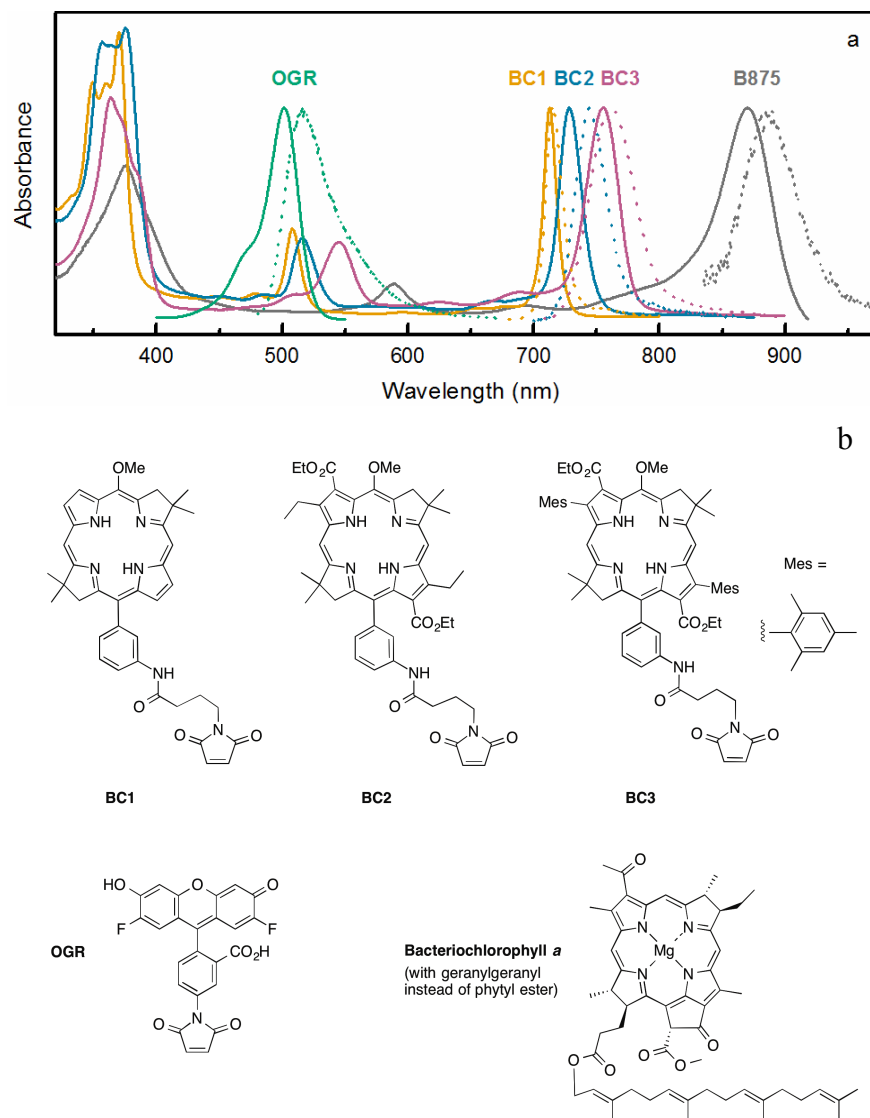


Figure 7.2. (a) Normalized absorption (solid) and fluorescence (dashed) spectra of the commercial dye Oregon Green 488 maleimide (**OGR**), bioconjugatable bacteriochlorins **BC1**, **BC2** and **BC3**, and BChl *a* ring B875 in LH1-type antenna. (b) Structures of **BC1**, **BC2**, **BC3**, **OGR**, and BChl *a*.

The present work extends our knowledge of the biohybrid antennas in three ways. First, seven different sites for the covalent attachment of chromophores to the peptide have been explored and the resulting conjugates tested for the capacity to form dyad subunits and

LH1-type oligomers. To correlate the distance between the attached chromophore and B875 with the energy-transfer efficiency, the same bacteriochlorin was attached to each of the different sites and Φ_{EET} measured. Second, to test the effects of increasing chromophore density, two identical chromophores were attached to the same peptide and reconstituted into an LH1-type oligomer, and Φ_{EET} was measured. Finally, to further explore ways to increase spectral coverage, a mixture of three distinct conjugates, each consisting of a β -peptide and a distinct single chromophore, were used to form heterogeneous LH1-type oligomers. Collectively, the results further the development of a versatile platform technology for the design and assembly of modular light-harvesting complexes for specific purposes.

Methods and materials

(I) Peptides

Six synthetic peptides (Bio-Synthesis, Lewisville, TX) were used in these studies. Each contained 48 amino acids with a sequence identical to that of the β -peptide of *Rhodobacter (Rb.) sphaeroides* LH1 except for the substitutions shown in Table 7.1. The substitution(s) of each residue in the respective peptides is to install a cysteine residue, with one exception entailing the introduction of propargyl glycine (PGly). The former enables conjugation with maleimide-tethered chromophores as described herein whereas the latter is employed in click chemistry (not examined herein). Each peptide exhibited >90% purity on the basis of HPLC data and each gave the expected peak upon mass spectrometry.⁶¹ The α -peptide used in these studies was the native LH1 α -peptide of *Rb. sphaeroides*, isolated from the LH2-less mutant, *puc705BA*, as previously described.⁹

Table 7.1. Synthetic peptides,^a conjugates, and oligomer antenna.

Peptide	Modification	Chromophore	Chromophore–Peptide Conjugate
$\beta(-2)$	Val(-2)→Cys	BC2	$\beta(-2)BC2$
$\beta(-6)$	Ala(-6)→Cys	BC2	$\beta(-6)BC2$
$\beta(-14)$	Met(-14)→Cys	BC1	$\beta(-14)BC1$
$\beta(-14)$	Met(-14)→Cys	BC2	$\beta(-14)BC2$
$\beta(-14)$	Met(-14)→Cys	BC3	$\beta(-14)BC3$
$\beta(-34)$	Ser(-34)→Cys	BC2	$\beta(-34)BC2$
$\beta(-10,-21)$	Trp(-10)→Cys, Gln(-21)→Cys	OGR	$\beta(-10)OGR(-21)OGR$
$\beta(-10,-21)$	Trp(-10)→Cys, Gln(-21)→Cys	BC2	$\beta(-10)BC2(-21)$
$\beta(-10,-21)$	Trp(-10)→Cys, Gln(-21)→Cys	BC2	$\beta(-10)(-21)BC2$
$\beta(-10,-21)$	Trp(-10)→Cys, Gln(-21)→Cys	BC2	$\beta(-10)BC2(-21)BC2$
$\beta(-10,-17)$	Trp(-10)→PGly, Ser(-17)→Cys	BC2	$\beta(-10PGly)(-17)BC2$

^aThe sequence of the native *Rb. sphaeroides* LH1 β -peptide is as follows: ADKS⁻³⁴DLGYTGLTDEQAQ⁻²¹ELHS⁻¹⁷VYM⁻¹⁴SGLW⁻¹⁰LFS^{A-6}VAIV⁻²AH⁰LAVYIWRPWF where H is position 0 and the designated amino acids are the positions modified herein.

(II) Chromophores

The structures of the chromophores used in this work are shown in **Figure 7.2b**. Bacteriochlorophyll *a* with a geranylgeranyl esterifying alcohol ($Q_y \lambda_{\max} = 777 \text{ nm}$) was isolated from membranes of the G9 carotenoidless mutant of *Rhodospirillum (Rsp.) rubrum*.²⁹ The geranylgeranyl bacteriochlorophyll *a*³⁰ is hereafter referred to as BChl *a* for simplicity. The dye Oregon Green 488 maleimide (**OGR**, $\lambda_{\max} = 488 \text{ nm}$) was purchased from Invitrogen: Molecular Probes. The synthetic bacteriochlorins **BC1** ($Q_y \lambda_{\max} = 713 \text{ nm}$) and **BC2** ($Q_y \lambda_{\max} = 729 \text{ nm}$) were synthesized as described previously (Reddy et al. 2013). Bacteriochlorin **BC3** ($Q_y \lambda_{\max} = 758 \text{ nm}$) was prepared⁶¹ by attachment of a maleimide tether to 3,13-diethoxycarbonyl-2,12-dimesityl-5-methoxy-8,8,18,18-tetramethylbacteriochlorin²⁸ using established methods.⁸ The three synthetic bacteriochlorins exhibit spectroscopic and photochemical features⁸ resembling those of native bacteriochlorophylls.³¹

(III) Chromophore–peptide conjugates

Synthetic bacteriochlorins **BC1**, **BC2**, **BC3** and commercial dye **OGR** were individually conjugated to the appropriate peptide in a solution of *N,N*-dimethylformamide and aqueous Tris buffer using standard procedures⁹ to produce 1:1 chromophore–peptide conjugates or, in the case of the diCys peptide $\beta(-10,-21)$, 1:1 or 2:1 chromophore–peptide conjugates (Table 7.1). The ratio of chromophore/peptide in the HPLC-purified products was determined on the basis of molar absorption coefficients of the peptide at 289 nm and the bacteriochlorin at its Q_y maximum (**Figure 7.3A**). The stoichiometry of chromophore per peptide for each conjugate was confirmed by electrospray ionization mass spectral analysis.³²⁻³⁴ Further details are given in the ref 61.

(IV) Formation of subunits and LH1-type complexes

Specific chromophore–peptide conjugates were mixed with α -peptide and BChl *a* to form subunits with $\lambda_{\text{max}} \sim 820$ nm (**Figure 7.1d**) as described previously.^{8,9} Careful titration of BChl *a* to the conjugate is especially important to maximize the formation of subunits and minimize the amount of free BChl *a* and free conjugate. This objective is achieved by adding BChl *a* in small increments until the absorbance increase upon addition is larger at 781 nm (free BChl *a*) than at 823 nm (subunit), as is illustrated in **Figure 7.3b**. The LH1-type biohybrid antenna, which exhibit $\lambda_{\text{max}} \sim 875$ nm (**Figure 7.1d**), are then formed as previously described.^{8,9}

In several experiments, β -peptides each with a distinct chromophore were mixed together to form oligomers with a heterogeneous chromophore composition. The usual procedure^{8,9} was followed with the following modification. The first conjugate was dissolved in hexafluoroacetone-trihydrate (HFA) and treated with an aliquot of 4.5% (w/v) *n*-octyl β -D-glucoside (hereafter referred to as ‘octyl glucoside’) in 50 mM potassium phosphate buffer (pH 7.5). The resulting conjugate solution was then added to the second conjugate to afford a binary mixture, which then was added to the third conjugate. The resulting ternary mixture of conjugates was combined with the α -peptide, and subsequent treatment with BChl *a* formed the corresponding mixture of subunits.

(V) Photophysical and infrared characterization studies

Static and time-resolved optical studies and single-reflection Fourier transform infrared (FTIR) measurements were performed as described previously.⁷⁻⁹ Photophysical measurements were typically made on samples contained in 1 cm path cuvettes held at 10 °C that had absorbance of 0.1–0.3 at 875 nm. Samples for fluorescence studies typically had an

absorbance of ≤ 0.1 at the excitation wavelength. Transient absorption measurements utilized ~ 100 fs, 0.5 μJ excitation flashes (1 mm diameter) in the visible or NIR spectral region. FTIR studies utilized a sample solution deposited on an Au substrate and a spectrometer equipped with a Ge attenuated total reflection (GATRTM) accessory at a spectral resolution of 4 cm^{-1} . Each spectrum was recorded at room temperature with dry N_2 purging and is the average of 256 scans.

Results and discussion

(I) Multiple sites of attachment to the β -peptide

There are many favorable characteristics of the native *Rb. sphaeroides* LH1 α - and β -peptides for preparation of the biohybrid light-harvesting complexes. The peptides are small in size, around 50 amino acids long, and are therefore easy to synthesize and manipulate. The peptides specifically associate with each other and BChl *a* to form well-defined subunits ($\alpha\beta$ -dyads) which in turn associate to form LH1-type oligomers. The extensive structural information available for the subunit and oligomer greatly facilitates molecular design for semisynthesis approaches. Although there is no high-resolution crystal structure for LH1, there are for the related LH2 complexes.^{20,22,23} In addition, solution NMR structures are available of *Rb. sphaeroides* LH1 β -peptide^{35,36} and *Rsp. rubrum* LH1 α - and β -peptides.^{37,38} Together with a host of mutagenesis, chemical synthesis and structural information from resonance Raman and other spectroscopic data^{15,39-46} the structures of the *Rb. sphaeroides* dyad and LH1 oligomers can be readily inferred.

Single-reflection FTIR studies of the new Cys-peptides and chromophore-peptide conjugates employed herein (**Figure 7.3**) and related peptides and conjugates reported

previously (Harris et al. 2013) show that the α -helical structure of the native α - and β -peptides is not compromised by Cys (or PGly) substitution of β at one position (-2 , -6 , -14 , or -34), at two positions (-10 and -21 or -10 and -17), or with chromophore attachment at these positions to form a β -peptide conjugate with any of the three synthetic bacteriochlorins (**BC1**, **BC2**, **BC3**). The helical structure is indicated by the amide-I and amide-II vibrations. Similar results were found previously for truncated 31-mer analogues of the β -peptide, including upon attachment of **OGR**, **BC1** or **BC2** to the β -peptide.^{7,8}

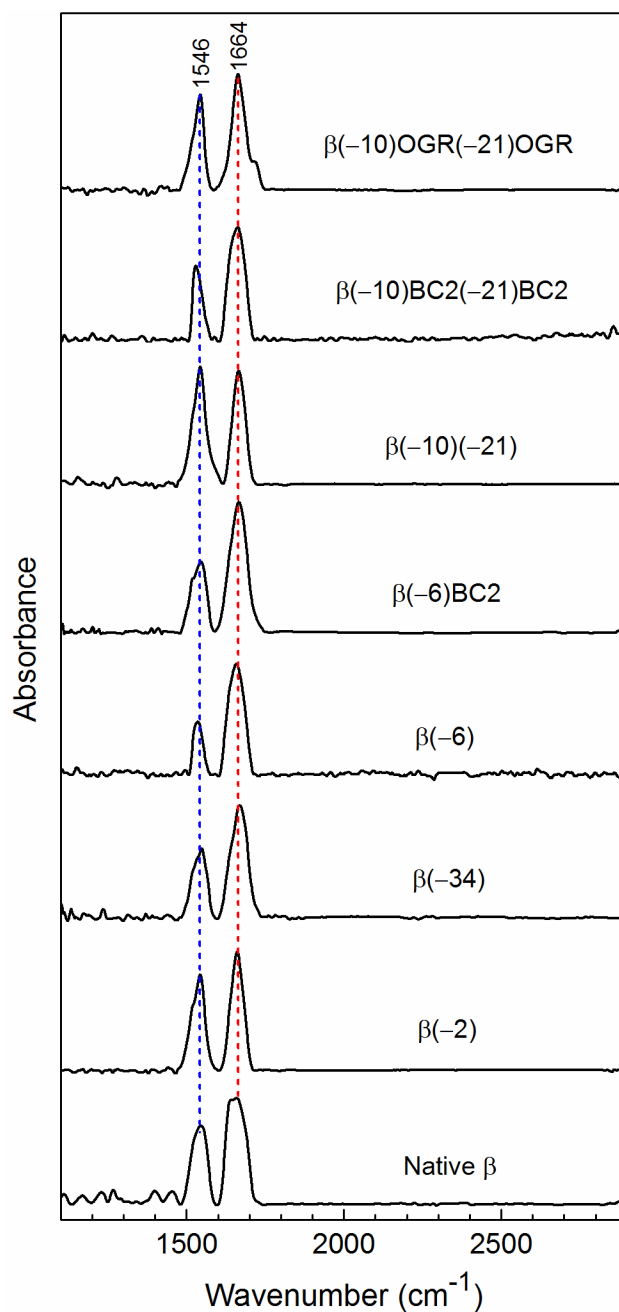


Figure 7.3. Single-reflection FTIR spectra of synthetic native-length peptides, Cys-mutants, and chromophore-peptide conjugates in films on gold. The α -helix signature amide-I and amide-II bands are labeled and the positions indicated by the vertical red and blue dashed lines, respectively. The maximum absorbance is typically in the range 0.001 to 0.01.

On the basis of this knowledge, amino acid sites can be chosen where modifications are unlikely to inhibit the interactions of the peptides and BChl *a* to form subunits and LH1-type oligomers. For our purposes, sites are chosen on the outside-facing parts of the β -peptide α -helix in the subunit so as to not interfere with the interactions between BChl *a* and the peptides. The available sites are -2, -6, -10, -14, -17, -21 or -34 (**Figure 7.4a**). Four peptides contained a single replacement of an amino acid with Cys, one contained two Cys replacements, and one contained one Cys and one PGly. The chromophore **BC2** was covalently attached to a synthetic Cys-containing β -peptide in 1:1 ratio through a maleimide linkage. Other conjugates were prepared with **BC1**, **BC3** or **OGR**. All of the resulting conjugates are listed in Table 7.1. Each conjugate was subsequently reconstituted with the α -peptide and BChl *a* to form subunits and LH1-type oligomers. As an example, **Figure 7.4b** shows the absorption spectrum of the oligomer formed with the the native α -peptide, BChl *a*, and $\beta(-14)BC2$ or $\beta(-14)$ alone (without **BC2** attached). Since the LH1-type oligomer is readily formed in both cases, the attached chromophore does not prevent formation of subunit and oligomer. This was true for all seven peptide conjugates with **BC2** attached.⁶¹

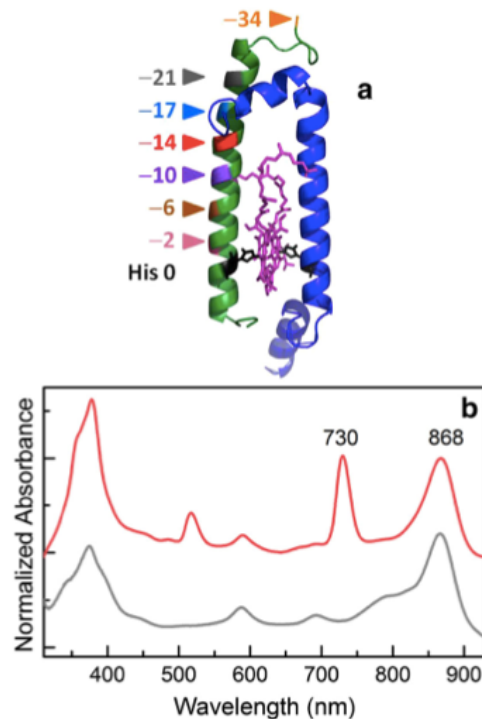


Figure 7.4. (a) $\alpha\beta$ -subunit of the LH2 (B800–850) complex of *Phs. molischianum* showing locations of conjugation of **BC2** to the presumed equivalent structure in the *Rb. sphaeroides* LH1 β -peptide. (b) Absorption spectra of the LH1-type complex prepared from the native α -peptide, BChl *a* and $\beta(-14)$ (grey) or $\beta(-14)$ BC2 (red). Spectra were normalized at the B875 nm peak and offset vertically for clarity.

Sites -2 through -21 are on the α -helical part of the β -peptide with -2 being the closest to the BChl *a* pair of the $\alpha\beta$ -dyad while site -34 is near the *N*-terminus on a more flexible part of the peptide. The association constants for conjugates at sites -14 , -17 and -34 were comparable to that for combining the native α - and β -peptides and BChl *a*.¹⁵ For conjugates at sites -2 , -6 , -10 and -21 , the association constants were about ten-fold smaller. The lower association constants meant that while stable subunits and LH1-type oligomers were formed, more unassociated BChl *a* (absorbing at ~ 780 nm) was present.

The formation of the subunit ($\alpha\beta$ -dyad) and oligomerization to form an LH1-type ($\alpha\beta$)_n-complex can be driven by a temperature-dependent change in medium. The micellar concentration of octyl glucoside in water exhibits a steep and negative temperature dependence over the range 5–40 °C.⁴⁷ As the subunit solution containing octyl glucoside is chilled, the critical micelle concentration of octyl glucoside significantly increases to above that of the octyl glucoside concentration. The diminished stability upon cooling of octyl glucoside micelles, and presumably of subunit–octyl glucoside heteromicelles, forces interaction between the hydrophobic surfaces of the dyads, thereby forming oligomers. Because this change in temperature so strongly favors oligomer formation, the process is essentially quantitative.¹⁵

The efficiency of excitation energy transfer (Φ_{EET}) from the attached chromophore to the BChl *a* component of the LH1 oligomer (B875) was determined for each biohybrid antenna by measuring (1) the fluorescence quantum yield and singlet excited-state lifetime of the donor chromophore in the oligomer versus chromophore–peptide conjugate, (2) the fluorescence quantum yield of B875 in the oligomer using excitation of B875 or the donor chromophore (**OGR** or synthetic bacteriochlorin), (3) fluorescence excitation versus absorbance (1 – transmittance) spectra, and (4) bleaching of the B875 ground state absorption upon excitation of the donor via ultrafast transient absorption spectroscopy. Each of these measurements has pros and cons for determination of Φ_{EET} and the energy-transfer dynamics in these types of self-assembled systems.⁷⁻⁹ Examples of such measurements are shown in **Figure 7.5** for $\beta(-14)\text{BC2}$. Because of the relatively short distance between the

BC2 and B875 in this case, the Φ_{EET} based on the average of the measurements is quite high (0.95). The value of Φ_{EET} for each conjugate is provided in Table 7.2.

Bacteriochlorin **BC2** at the six sites on the α -helical part of the peptide (positions -2 through -21) has an estimated range of distances from B875 that are used to calculate the Förster Φ_{EET} in Table 7.2. The minimum and maximum values were calculated on the basis of the expected range of motion of the attached synthetic chromophore. A fundamental issue is the energy-acceptor molar absorption coefficient to be used, as this value depends on the number of BChl *a* over which an excitation in B875 is initially delocalized, and thus the net absorption dipole moment that is coupled to the emission dipole moment of the attached synthetic chromophore. A value of $236,000 \text{ M}^{-1} \text{ cm}^{-1}$ is appropriate for a BChl *a* pair in an $\alpha\beta$ -dyad subunit of an LH1-type oligomer; the value is twice the molar absorption coefficient per BChl *a* determined for B875 in ref 49.

Table 7.2. Efficiency of excitation-energy transfer in LH1-type complexes.

Chromophore–Peptide Conjugate	Primary Energy- Transfer Path^a	Measured^b Φ_{EET}	Calculated^c Förster Φ_{EET}
<i>Mono-Chromophore Systems</i>			
$\beta(-2)\text{BC2}$	$\text{BC2}(-2)\rightarrow\text{B875}$	0.80	0.93–0.96
$\beta(-6)\text{BC2}$	$\text{BC2}(-6)\rightarrow\text{B875}$	0.85	0.89–0.96
$\beta(-10)\text{BC2}(-21)$	$\text{BC2}(-10)\rightarrow\text{B875}$	0.85	0.73–0.96
$\beta(-14)\text{BC1}$	$\text{BC1}(-14)\rightarrow\text{B875}$	0.85	0.61–0.93
$\beta(-14)\text{BC2}$	$\text{BC2}(-14)\rightarrow\text{B875}$	0.95	0.64–0.93
$\beta(-14)\text{BC3}$	$\text{BC3}(-14)\rightarrow\text{B875}$	0.95	0.80–0.97
$\beta(-10\text{PGly})(-17)\text{BC2}$	$\text{BC2}(-17)\rightarrow\text{B875}$	0.80	0.50–0.89
$\beta(-10)(-21)\text{BC2}$	$\text{BC2}(-21)\rightarrow\text{B875}$	0.50	0.35–0.84
$\beta(-34)\text{BC2}$	$\text{BC2}(-34)\rightarrow\text{B875}$	0.60	0.25–0.64
<i>Di-Chromophore Systems</i>			
$\beta(-10)\text{BC2}(-21)\text{BC2}$	$\text{BC2}(-21)\rightarrow\text{BC2}(-10)\rightarrow\text{B875}$	0.90	$(0.73-0.96)^d$
$\beta(-10)\text{OGR}(-21)\text{OGR}$	$\text{OGR}(-21)\rightarrow\text{OGR}(-10)\rightarrow\text{B875}$	0.40	$(0.60-0.92)^e$
<i>Heterogeneous System</i>			
Mixture of 3 dyads ^f	Multipath $\rightarrow\text{B875}$	$\geq 0.95^g$	

^aIn di-chromophore and heterogeneous systems, energy can also flow directly from the more distant site to B875. ^bTypical error is ± 0.05 . ^cFörster calculations⁴⁸ were performed using parameters given in ref 61; the range of values given reflect an estimated maximum to minimum chromophore–B875 distance. ^dCalculated for the process $\text{BC2}(-10)\rightarrow\text{B875}$. ^eCalculated for the process $\text{OGR}(-10)\rightarrow\text{B875}$. ^fApproximately 1:1:1 ratio of $\beta(-14)\text{BC1}$, $\beta(-14)\text{BC2}$, and $\beta(-14)\text{BC3}$. ^gValue measured for each of the three bacteriochlorins.

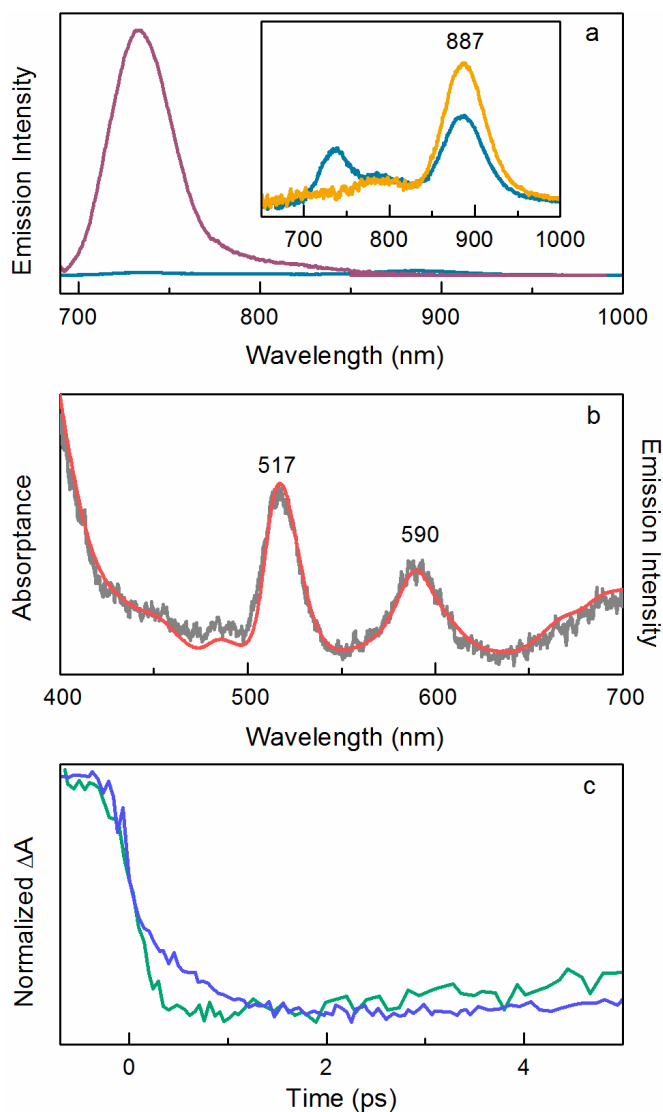


Figure 7.5. (a) Fluorescence emission for $\beta(-14)BC2$ chromophore-peptide conjugate (mauve) and $\beta(-14)BC2$ plus native α -peptide and BChl *a* to form the LH1-type oligomer (blue) showing quenching of **BC2** fluorescence feature at 734 nm. Panel-a inset shows the emission from the LH1-type oligomer based on $\beta(-14)BC2$ when selectively exciting BChl *a* (gold) and **BC2** (blue) both with B875 emission feature at 887 nm. (b) Absorbance (1-T) (coral) versus fluorescence excitation (grey) ($\lambda_{det} = 890$ nm) for LH1-type oligomer containing $\beta(-14)BC2$ normalized at 590 nm (c) Time profiles for combined B875 bleaching and B875* stimulated emission for LH1-type oligomer containing $\beta(-14)$, when exciting BChl *a* array (teal) and for LH1-type oligomer formed from $\beta(-14)BC2$ when exciting **BC2** (blue).

The majority of the experimental Φ_{EET} values (typically ± 0.05) fall within the range of the calculated Förster Φ_{EET} values using the estimated distance span (Table 7.2). This conclusion holds for a substantial (two-fold or more) change in the acceptor molar absorption coefficient, which has only a modest effect at the high Φ_{EET} values typically calculated (and observed). These results show that the measured Φ_{EET} for **BC2** to BChl *a* in the biohybrid antenna are consistent with Förster theory, independent of precise parameter values. Therefore, the desired efficiency of energy transfer can be generally designed into the conjugate-peptide by selecting the location of the chromophore, and thus the approximate distance from the BChl *a* (B875) target.

Because the region of the peptide from position -21 to the *N*-terminus is not α -helical, the distance from the BChl *a* to the **BC2** at position -34 cannot be readily predicted. The oligomer formed from the $\beta(-34)\text{BC2}$ conjugate had an efficiency of 0.60, higher than the 0.50 efficiency at -21. This result suggests that the hydrophobic **BC2** attached at position -34, which is a more flexible region of the peptide (**Figure 5a**), is able to assume either (1) a position near the hydrophobic α -helices and hence closer to B875 than when attached to the -21 site, (2) an orientation that gives a more favorable alignment of its Q_y transition dipole moment with that of B875, or (3) both of the above. Additionally, enhanced energy transfer to B875 would result if (1)–(3) takes place in even a fraction of the $\alpha\beta$ -dyads in an LH1 ring if energy flows between **BC2** attached at the -34 position on adjacent β -peptides, thereby providing a relay effect.

(II) Two chromophores attached to the β -peptide

To test the effects of increased chromophore density, two identical **BC2** chromophores were attached to the $\beta(-10,-21)$ peptide. Three products were isolated from the coupling reaction: $\beta(-10)\text{BC2}(-21)$, $\beta(-10)(-21)\text{BC2}$ and $\beta(-10)\text{BC2}(-21)\text{BC2}$. Each product was separated by HPLC and characterized by mass spectrometry.⁶¹ The conjugate with two **BC2** per β -peptide, $\beta(-10)\text{BC2}(-21)\text{BC2}$, was identified from the absorption spectrum (**Figure 7.6a**) and mass spectral results. According to the absorption spectra (**Figure 7.6a**) and mass spectral results, the other two products each had one **BC2** per peptide, but it could not be distinguished which was $\beta(-10)\text{BC2}(-21)$ and which was $\beta(-10)(-21)\text{BC2}$. Each of these conjugates was separately reconstituted with α -peptide and BChl *a* to form LH1-type oligomers, whereupon values of Φ_{EET} of 0.50 and 0.85 were obtained (Table 7.2). On the basis of Förster calculations (Table 7.2), an efficiency of 0.50 is consistent with the range of 0.50–0.89 for $\beta(-10)(-21)\text{BC2}$, whereas 0.85 is consistent with the range of 0.73–0.96 for $\beta(-10)\text{BC2}(-21)$. The latter value is within the error of the measured efficiency of 0.90 for $\beta(-10)\text{BC2}(-21)\text{BC2}$, which contains two **BC2** chromophores per β -peptide. The high efficiency observed for $\beta(-10)\text{BC2}(-21)\text{BC2}$ suggests relay energy transfer from the **BC2** at the -21 position through **BC2** at the -10 position to B875.

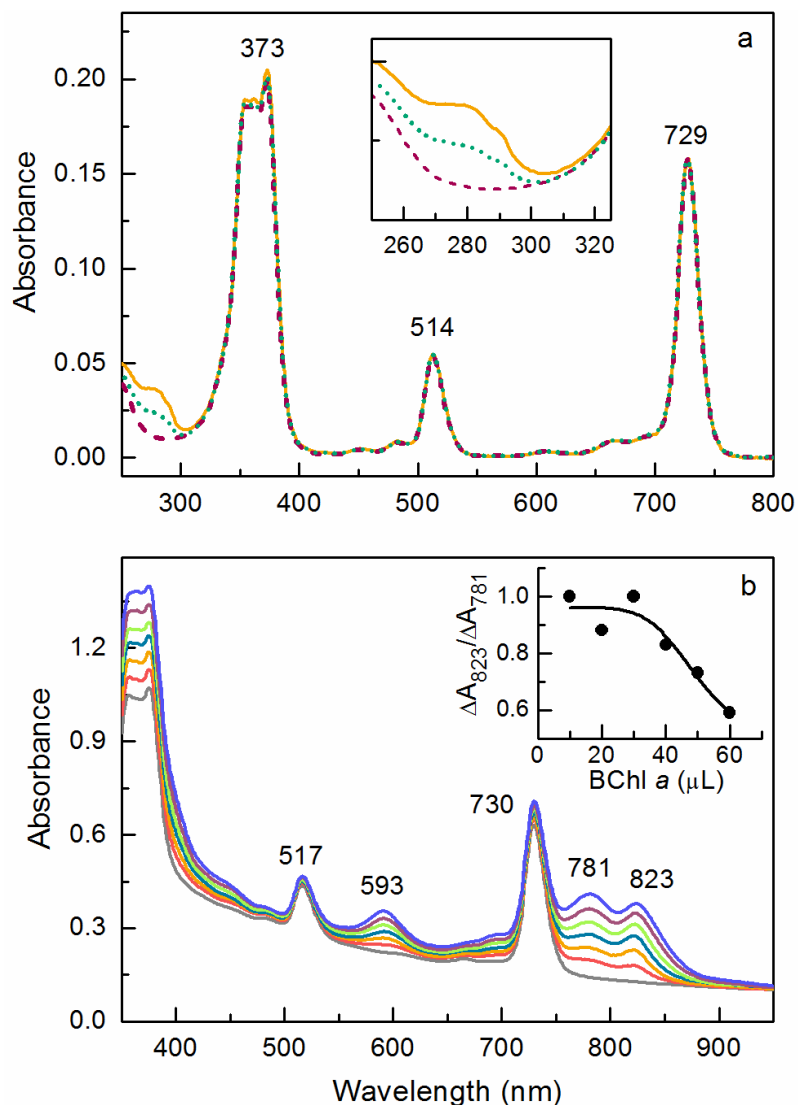


Figure 7.6. (a) Absorption spectra of **BC2** (burgundy), and oligomer antenna formed by combining BChl *a*, native α -peptide, and conjugates $\beta(-10)\text{BC2}(-21)$ or $\beta(-10)(-21)\text{BC2}$ (teal) or $\beta(-10)\text{BC2}(-21)\text{BC2}$ (gold). Spectra were normalized at 729 nm (2 mm cuvette). All samples were in HPLC solvent with composition where they eluted in the gradient. The inset highlights spectral differences in the UV, from which protein concentrations are obtained. (b) Addition of BChl *a* to $\beta(-6)\text{BC2}$ and the native α -peptide at 0.90% octyl glucoside. Curves are for 0 (grey), 10 (coral), 20 (gold), 30 (cyan), 40 (green), 50 (mauve) and 60 (violet) μL of BChl *a*. Inset: ratio of change in absorbance at 823 nm (B820) compared with that at 781 nm (free BChl *a*) as BChl *a* is added.

In a second experiment that increased the density of chromophores per peptide, **OGR** was conjugated to the $\beta(-10,-21)$ peptide and the resulting products purified by HPLC. Two closely overlapping peaks were collected as the earlier half and later half of the peak.⁶¹ According to mass spectrometry results, the material from both halves contained two **OGR** per peptide; each also similarly formed subunits and LH1-type oligomers. The Φ_{EET} was also similar for material from each half so it was concluded that the coupling reaction had gone to completion, which was typical in prior experiments with **OGR**.^{7,8} The mass determined for the first half material was 16 Da greater than that of the second half, consistent with the addition of an oxygen.⁶¹ The extra mass is likely due to oxidation of Met-14 to methionine sulfoxide as is often observed in these peptides.

The Φ_{EET} of $\beta(-10)\text{OGR}(-21)\text{OGR}$ was determined to be 0.40 (Table 7.2). This efficiency is consistent with earlier data where the Φ_{EET} from **OGR** at the -34 position to B875 was 0.15⁹ and from **OGR** at the -14 position to B850 (in an oligomer formed from 31-mer β -peptides) was 0.30.⁷ The poorer overlap between **OGR** emission and the Q_x band of B875 (BChl *a* ring) than between a synthetic bacteriochlorin emission and the Q_y band of B875 would give a lower Φ_{EET} for **OGR** than for a synthetic bacteriochlorins if all other parameters were equal. However, Φ_{EET} also depends on the Φ_f value of the donor chromophore in the absence of the acceptor. The photophysical properties of members of the Oregon Green family of fluorofluoresceins have been extensively studied⁵⁰⁻⁵⁷ and depend markedly on the local environment. For $\Phi_f = 0.30$, Förster calculation affords $\Phi_{\text{EET}} = 0.60$ – 0.92 for **OGR** at the -10 position and 0.22 – 0.74 for **OGR** at the -21 position to B875. The

overall efficiency of 0.40 found with two **OGR**/peptide is consistent with relay energy transfer from the **OGR** at the -21 position through the **OGR** at the -10 position and then to B875 in the biohybrid antenna.

From these experiments, doubling the density of the chromophore per peptide enhances the effectiveness per unit biohybrid antenna and allows for a relay effect to increase energy transfer efficiency from a more distant chromophore. The increased chromophore density does not inhibit association of the biohybrid antenna to form subunits and LH1-type oligomers, nor cause excited-state concentration quenching. Thus, with this biohybrid system, peptides containing two or more covalently attached chromophores may be used to form homogeneous oligomers consisting of a supramolecular ring with ~30 BChl *a* and an equal or greater number of covalently attached chromophores.

(III) Combining three distinct chromophore–peptide conjugates

To further investigate ways to enhance solar coverage, three distinct chromophores were each attached to $\beta(-14)$ to make the chromophore–peptide conjugates $\beta(-14)BC1$, $\beta(-14)BC2$ and $\beta(-14)BC3$. Each was separately reconstituted with the α -peptide and BChl *a* to make LH1-type oligomers (**Figure 7.7a,c**) and the Φ_{EET} for energy transfer to B875 was measured (Table 7.2). For all three bacteriochlorin–peptide conjugates, homogeneous LH1-type oligomers readily form and exhibit highly efficient energy transfer (0.85–0.95).

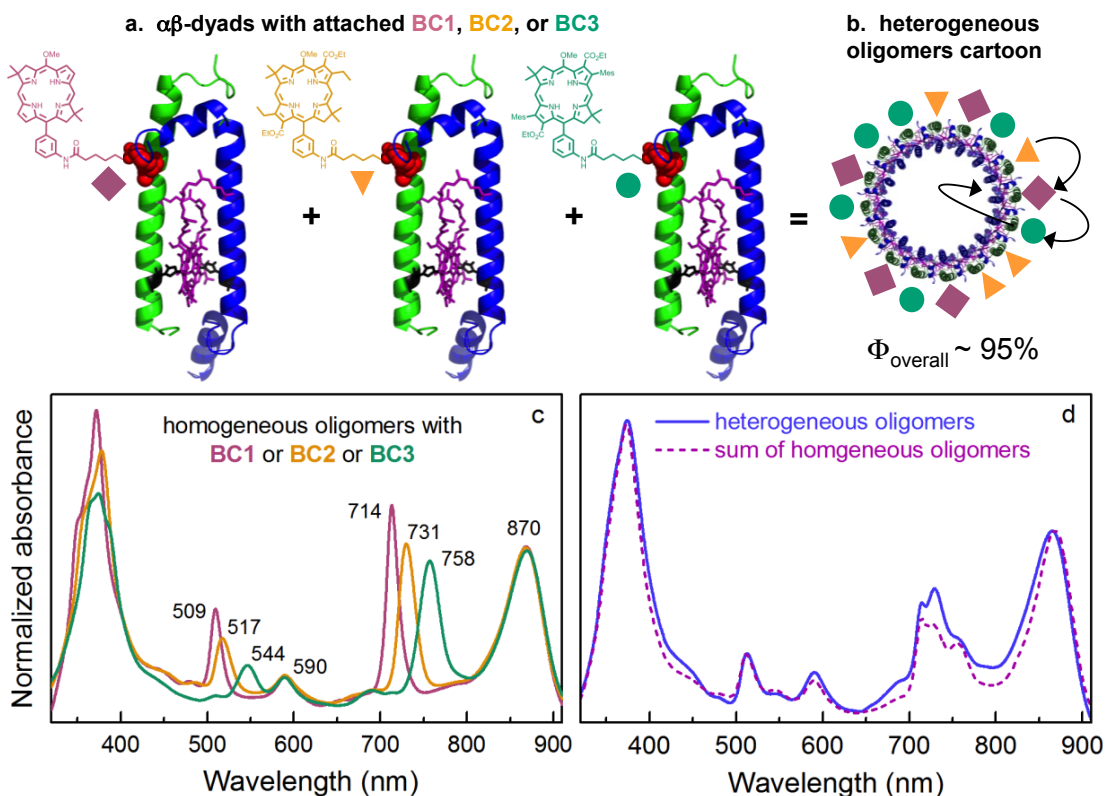


Figure 7.7. (a) Schematic structures of $\alpha\beta$ -dyads with bacteriochlorins BC1 (mauve) or BC2 (gold) or BC3 (teal) attached to the -14 position of the β -peptide. (b) Cartoon showing one of a large number of possible arrangements of BC1 (mauve triangle) and BC2 (gold triangle) and BC3 (teal circle) around an $(\alpha\beta)_n$ cyclic oligomer. (c) Absorption spectra for LH1-type complexes prepared by individually combining chromophore-peptide conjugate $\beta(-14)\text{BC1}$ (mauve), $\beta(-14)\text{BC2}$ (gold), or $\beta(-14)\text{BC3}$ (teal) with the native LH1 α -peptide and BChl *a*. (d) Absorption spectra for heterogeneous LH1-type complexes prepared with native α -peptide, BChl *a* and an approximately 1:1:1 ratio of $\beta(-14)\text{BC1}$, $\beta(-14)\text{BC2}$, and $\beta(-14)\text{BC3}$ (violet), and the calculated sum of the spectra of the three individual (single-chromophore) homogeneous oligomers pictured in panel c (dashed purple).

Each bacteriochlorin-peptide conjugate was then combined together in approximately equal amounts and reconstituted with α -peptide and BChl *a* to form heterogeneous LH1-type oligomers. The resulting oligomers are most likely rings that contain 14, 15 or 16 subunits as was observed previously with LH1 complexes of chromophore-peptide conjugates (Harris et

al. 2013). Because the chromophores are similar in structure and do not differ in hydrophobicity, charge or size, and the conjugated peptides exhibit similar association constants for forming subunits ($\alpha\beta$ -dyads), the chromophores are likely to be randomly distributed in the LH1-type oligomers (**Figure 7.7b, d**).

The question of how many cyclic complexes could theoretically form can be addressed using the program *Cyclaplex*,⁵⁸ which was designed for calculating the virtual library of cyclic products formed upon combinatorial reaction of multiple distinct reactants. The program has been employed to calculate the possible heterogeneity of biohybrid antennas derived from two distinct subunit dyads⁹ as well as native antennas obtained from multiple distinct dyads.⁵⁹ For cyclic n -mers of size $n = 14, 15, \text{ or } 16$, the use of 3 distinct subunit dyads can give up to 341,802, 956,635, or 2,690,844 rings, respectively. Examination of the virtual library shows that the fraction of cyclic oligomers containing at least one copy of each of the three distinct bacteriochlorins is 0.989, 0.993, and 0.995, respectively. In other words, those cyclic oligomers that are homogeneous (one bacteriochlorin type) or contain only two of the bacteriochlorins occupy a tiny fraction of the total. Any more in-depth analysis of the composition of the virtual libraries of such vast diversity appears to be of little import.

The combination of three different chromophores (**BC1, BC2, and BC3**) significantly increases solar coverage in the NIR region (**Figure 7.7d**). An apparent increase in Φ_{EET} from 0.85 to 0.95 was observed for **BC1** in the heterogeneous LH1-type oligomer relative to the homogeneous oligomer with only **BC1** present (Table 7.2). Although the change in efficiency is within the error of these measurements (typically ± 0.05), the results are

consistent with highly efficient paths of (cascade) energy transfer through **BC2** and **BC3** to B875. Regardless, the high efficiency shows the absence of detrimental effects in mixing three different conjugated β -peptides to form a heterogeneous LH1-type biohybrid antenna. This method of incorporating different chromophores into the same LH1 is therefore a simple yet effective way to extend and enhance solar coverage.

Outlook

The development of tailorable antenna complexes has been largely impeded by the dearth of design strategies for organizing a large number of chromophores into a functional whole of nanoscale if not mesoscale dimensions. The biohybrid approach provides an effective blend of the blueprint of the natural photosynthetic systems with the malleability afforded by synthetic chemistry. A key feature of the biohybrid approach that we have been developing is the reliance on synthetic modification of relatively short α - and β -peptides. A subunit dyad forms from an α - and a β -peptide and two BChl *a* molecules; the dyad then self-associates to give oligomers with a supramolecular LH1-type ring containing roughly 30 BChl *a* molecules (for rings with an average of 14–16 dyad subunits). By piggybacking on this two-tiered assembly process, an average of 15 or 30 synthetic chromophores can be incorporated to augment the absorption provided by the native BChl *a* molecules. The biohybrid approach hence provides one solution to the daunting challenges of 3-dimensional organization of large numbers of chromophores as required to create a viable light-harvesting antenna.

The versatility of the biohybrid approach has been extended herein in three ways: (1) Seven distinct sites on the β -peptide (positions -2, -6, -10, -14, -17, -21 and -34)

substituted with Cys were used to covalently attach a single synthetic chromophore without disrupting the subsequent formation of subunit dyads and LH1-type oligomers. (2) Two chromophores were incorporated on a β -peptide and again the corresponding LH1-type oligomers formed, thereby affording a nanoscale assembly containing 30 BChl *a* molecules and 30 synthetic chromophores (assuming an average ring size of 15). (3) A mixture of three β -peptides, each conjugated with a spectrally distinct synthetic chromophore, afforded a heterogeneous mixture of LH1-type oligomers. In both of the latter cases, the efficiency of energy transfer is consistent with relay or cascade processes from distant via proximal chromophores on the path to excitation of the circular array of BChl *a* molecules (B875).

The results obtained from the three designs illustrate the robustness of the self-assembly process and the versatility of the overall biohybrid design. By selecting the chromophore and position for covalent attachment, it is possible to design chromophore-conjugated peptides with unique features such as specific wavelengths of light absorption, increased extent of solar coverage, and a specific level of efficiency of energy capture. The ability to create a high density of absorbing chromophores may be very useful for the design of light-capturing modules where very thin layers of antenna are advantageous. Indeed, a major open question now is how many synthetic chromophores can be loaded on one or both of the peptides while retaining the self-assembly to give cyclic oligomers. The LH1-type oligomers formed are also amenable to incorporation into lipid bilayers or forming monolayers on solid supports.¹⁹ Similarly, the modularity of the semisynthetic light-harvesting complexes suggests the possibility of association to form a planar array analogous to the large photosynthetic units found in many photosynthetic organisms.^{16-18,60}

References

1. N. Aratani and A. Osuka A, In: *Handbook of porphyrin science*, ed. K. M. Kadish, K. M. Smith and R. Guilard R, World Scientific Publishing Co., Singapore, 2010, Vol. 1, pp.1–132.
2. T. S. Balaban, H. Tamiaki and A. R. Holzwarth, *Top Curr. Chem.*, 2005, **258**,1–38.
3. J. Yang, M. C. Yoon, H. Yoo, P. Kim and D. Kim, *Chem. Soc. Rev.*, 2012, **41**, 4808–482.
4. P. D. Harvey, In: *The porphyrin handbook*, ed. K. M. Kadish, K. M. Smith and R. Guilard, Academic Press, San Diego, CA, 2003, Vol. 18, pp. 63–250.
5. J. S. Lindsey, O. Mass and C. Y. Chen, *New J. Chem.*, 2011, **35**, 511–516.
6. P. D. Harvey, C. Stern and R. Guilard, In: *Handbook of porphyrin science*, ed. K. M. Kadish, K. M. Smith and R. Guilard, World Scientific Publishing Co., Singapore, 2011, Vol. 11, pp. 1–179.
7. J. W. Springer, P. S. Parkes-Loach, K. R. Reddy, M. Krayner, J. Jiao, G. M. Lee, D. M. Niedzwiedzki, M. A. Harris, C. Kirmaier, D. F. Bocian, J. S. Lindsey, D. Holten and P. A. Loach, *J. Am. Chem. Soc.*, 2012, **134**, 4589–4599.
8. K. R. Reddy, J. Jiang, M. Krayner, M. A. Harris, J. W. Springer, E. Yang, J. Jiao, D. M. Niedzwiedzki, D. Pandithavidana, P. S. Parkes-Loach, C. Kirmaier, P. A. Loach, D. F. Bocian, D. Holten and J. S. Lindsey, *Chem. Sci.*, 2013, **4**, 2036–2053.

9. M. A. Harris, P. S. Parkes-Loach, J. W. Springer, J. Jiang, E. C. Martin, P. Qian, J. Jiao, D. M. Niedzwiedzki, C. Kirmaier, J. D. Olsen, D. F. Bocian, D. Holten, C. N. Hunter, J. S. Lindsey and P. A. Loach, *Chem. Sci.*, 2013, **4**, 3924–3933.
10. M. Gabrielsen, A. T. Gardiner and R. J. Cogdell, In: *The purple phototropic bacteria*, ed. C. N. Hunter, F. Daldal, M. C. Thurnauer and J. T. Beatty, Springer, Dordrecht, 2009, pp. 135–153.
11. P. A. Bullough, P. Qian and C. N. Hunter, In: *The purple phototropic bacteria*, ed. C. N. Hunter, F. Daldal, M. C. Thurnauer and J. T. Beatty, Springer, Dordrecht, 2010, pp. 155–179.
12. P. S. Parkes-Loach, J. R. Sprinkle and P. A. Loach, *Biochemistry*, 1988, **27**, 2718–2727.
13. J. Kikuchi, T. Asakura, P. A. Loach, P. S. Parkes-Loach, K. Shimada, C. N. Hunter, M. J. Conroy and M. P. Williamson, *Biopolymers*, 1999, **49**, 361–372.
14. P. A. Loach and P. S. Parkes-Loach, In: *Advances in photosynthesis: Anoxygenic photosynthetic bacteria*, ed. R. E. Blankenship, M. T. Madigan, C. E. Bauer CE, Kluwer Academic Publishers, Dordrecht, 1995, pp. 437–471.
15. P. A. Loach and P. S. Parkes-Loach, In: *The purple phototropic bacteria*, C. N. Hunter, F. Daldal, M. C. Thurnauer and J. T. Beatty, 2009, Springer, Dordrecht, pp. 181–198.
16. K. R. Miller, *Proc. Natl. Acad. Sci. USA*, 1979, **76**, 6415–6419.
17. H. Engelhardt, W. Baumeister and W. O. Saxton WO, *Arch. Microbiol.*, 1983, **135**, 169–175.

18. W. Stark, W. Kühlbrandt, I. Wildhaber, E. Wehrli and K. Mühlethaler, *EMBO J.*, 1984, **3**, 777–783.
19. K. Iida, T. Dewa and M. Nango, In: *The purple phototropic bacteria*, ed. C. N. Hunter, F. Daldal and M. C. Thurnauer and J. T. Beatty, 2009, Springer, Dordrecht, pp. 861–875.
20. J. Koepke, X. Hu, C. Muenke, K. Schulten and H. Michel, *Structure*, 1996, **4**, 581–597.
21. X. Hu and K. Schulten, *Biophys. J.*, 1998, **75**, 683–694.
22. G. McDermott, S. M. Prince, A. A. Freer, A. M. Hawthornthwaite-Lawless, M. Z. Papiz, R. J. Cogdell, N. W. Isaacs, *Nature*, 1995, **374**, 517–521.
23. M. Z. Papiz, S. M. Prince, T. Howard, R. J. Cogdell and N. W. Isaacs, *J. Mol. Biol.*, 2003, **326**, 1523–1538.
24. A. W. Roszak, T. D. Howard, J. Southall, A. T. Gardiner, C. J. Law, N. W. Isaacs, R. J. Cogdell, *Science*, 2003, **302**, 1969–1972.
25. P. Qian, C. N. Hunter and P. A. Bullough, *J. Mol. Biol.*, 2005, **349**, 948–960.
26. M. K. Sener and K. Schulten, In: *The purple phototropic bacteria*, ed. C. N. Hunter, F. Daldal, M. C. Thurnauer and J. T. Beatty, Springer, Dordrecht, The Netherlands, 2009, pp. 275–294.
27. P. Qian, M. Z. Papiz, P. J. Jackson, A. A. Brindley, I. W. Ng, J. D. Olsen, M. J. Dickman, P. A. Bullough and C. N. Hunter, *Biochemistry*, 2013, **52**, 7575–7585.
28. C.-Y. Chen, E. Sun, D. Fan, M. Taniguchi, B. E. McDowell, E. Yang, D. F. Diers, D. Bocian, D. Holten and J. S. Lindsey JS, *Inorg. Chem.*, 2012, **51**, 9443–9464.

29. K. A. Meadows, K. Iida, T. Kazuichi, P. A. Recchia, B. A. Heller, B. Antonio, M. Nango P. A. Loach, *Biochemistry*, 1995, **34**, 1559–1574.
30. H. Scheer, In: *Chlorophylls and bacteriochlorophylls: biochemistry, biophysics, functions and applications*, ed. B. Grimm, R. J. Porra, W. Rüdiger and H. Scheer, Springer, Dordrecht, The Netherlands, 2006, pp. 1–26.
31. M. Kobayashi, M. Akiyama, H. Kano and H. Kise, In: *Chlorophylls and bacteriochlorophylls: biochemistry, biophysics, functions and applications*, ed. B. Grimm, R. J. Porra, W. Rüdiger and H. Scheer, Springer, Dordrecht, The Netherlands, 2006, pp. 79–94.
32. K. Biemann, *Annu. Rev. Biochem.*, 1992, **61**, 977–1010.
33. Y.-F. Chen, C. A. Chang, Y.-H. Lin and Y.-G. Tsay, *Anal. Biochem.*, 2013, **440**, 108–113.
34. C.-Y. Chen, D. F. Bocian and J. S. Lindsey JS, *J. Org. Chem.*, 2014, **79**, 1001–1016.
35. M. J. Conroy, W. H. J. Westerhuis, P. S. Parkes-Loach, P. A. Loach, C. N. Hunter and M. P. Williamson, *J. Mol. Biol.*, 2000, **298**, 83–94.
36. P. L. Sorgen, S. M. Cahill, R. D. Krueger-Koplin, S. T. Krueger-Koplin, C. C. Schenck and M. E. Girvin, *Biochemistry*, 2002, **41**, 31–41.
37. Z. Wang, Y. Muraoka, M. Shimonaga, M. Kobayashi and T. Nozawa, *J. Am. Chem. Soc.*, 2002, **124**, 1072–1078.
38. Z.-Y. Wang, K. Gokan, M. Kobayashi and T. Nozawa, *J. Mol. Biol.*, 2005, **347**, 465–477.

39. G. J. S. Fowler, G. D. Sockalingum, B. Robert and C. N. Hunter, *Biochem. J.*, 1994, **299**, 695–700.
40. J. D. Olsen, G. D. Sockalingum, B. Robert and C. N. Hunter, *Proc. Natl. Acad. Sci. USA*, 1994, **91**, 7124–7128.
41. J. D. Olsen, J. N. Sturgis, W. H. J. Westerhuis, G. J. S. Fowler, C. N. Hunter and B. Robert, *Biochemistry*, 1997, **36**, 12625–12632.
42. J. N. Sturgis, J. D. Olsen, B. Robert and C. N. Hunter CN, *Biochemistry*, 1997, **36**, 2772–2778.
43. C. M. Davis, P. L. Bustamante, J. B. Todd, P. S. Parkes-Loach, P. McGlynn, J. D. Olsen, L. McMaster, C. N. Hunter and P. A. Loach PA, *Biochemistry*, 1997, **36**, 3671–3679.
44. J. B. Todd, P. A. Recchia, P. S. Parkes-Loach, J. D. Olsen, G. J. S. Fowler, P. McGlynn, C. N. Hunter and P. A. Loach, *Photosynth. Res.*, 1999, **62**, 85–98.
45. K. A. Meadows, P. S. Parkes-Loach, J. W. Kehoe and P. A. Loach, *Biochemistry*, 1998, **37**, 3411–3417.
46. P. S. Parkes-Loach, A. P. Majeed, C. J. Law and P. A. Loach, *Biochemistry*, 2004, **43**, 7003–7016.
47. M. da Graca Miguel, O. Eidelman, M. Ollivon and A. Walter, *Biochemistry*, 1989, **28**, 8921–8928.
48. H. Du, R. C. A. Fuh, J. Li, L. A. Corkan and J. S. Lindsey, *Photochem. Photobiol.*, 1998, **68**, 141–142.

49. M. C. Chang, P. M. Callahan, P. S. Parkes-Loach, T. M. Cotton and P. A. Loach, *Biochemistry*, 1990, **29**, 421–429.
50. C. Delmotte and A. Delmas, *Bioorg. Med. Chem. Lett.*, 1999, **9**, 2989–2994.
51. H. J. Lin, H. Szmecinski and J. R. Lakowicz, *Anal. Biochem.*, 1999, **269**, 162–167.
52. N. O. Mchedlov-Petrossyan, N. A. Vodolazkaya, Y. A. Gurina, W. C. Sun and K. R. Gee, *J. Phys. Chem. B*, 2010, **114**, 4551–4564.
53. A. Orte, L. Crovetto, E. M. Talavera, N. Boens, J. M. Alvarez-Pez, *J. Phys. Chem. A*, 2005a, **109**, 734–747.
54. A. Orte, R. Bermejo, E. M. Talavera, L. Crovetto and J. M. Alvarez-Pez, *J. Phys. Chem. A*, 2005b, **109**, 2840–2846.
55. A. Orte, E. M. Talavera, A. L. Maçanita, J. C. Orte and J. M. Alvarez-Pez, *J. Phys. Chem. A*, 2005c, **109**, 8705–8718.
56. E. Rusinova, V. Tretyachenko-Ladokhina, O. E. Vele, D. F. Senear and J. B. A. Ross, *Anal. Biochem.*, 2002, **308**, 18–25.
57. W. C. Sun, K. R. Gee, D. H. Klaubert and R. P. Haugland, *J. Org. Chem.*, 1997, **62**, 6469–6475.
58. M. Taniguchi, H. Du and J. S. Lindsey, *J. Chem. Inf. Model*, 2013, **53**, 2203–2216.
59. M. Taniguchi, S. Henry, R. J. Cogdell and J. S. Lindsey, *Photosynth. Res.*, 2014, **121**, 49–60.
60. D. Mauzerall and N. L. Greenbaum, *Biochim. Biophys. Acta.*, 1989, **974**, 119–140.

61. M. A. Harris, J. Jiang, D. M. Niedzwiedzki, J. Jiao, M. Taniguchi, C. Kirmaier, P. A. Loach, D. F. Bocian, J. S. Lindsey, D. Holten, P. S. Parkes-Loach, *Photosynth. Res.*, 2014, **121**, 35–48.